Zentrum für Humangenetik
der
Universität Bremen

Strukturelle und funktionelle Analyse ausgewählter High Mobility Group Gene des Haushundes

Dissertation

Zur Erlangung des Grades eines Doktors der
Naturwissenschaften
- Dr. rer. nat -

Dem Promotionsausschuss Dr. rer. nat
im Fachbereich Biologie / Chemie der Universität Bremen

vorgelegt von Jan Thies Soller

1. Gutachter: Prof. Dr. Jörn Bullerdiek
2. Gutachter: Prof. Dr. Ingo Nolte

Hiermit erkläre ich, Jan Thies Soller, geboren am 04.11.1973, dass für das Verfassen der vorliegenden Dissertation „Strukturelle und funktionelle Analyse ausgewählter High Mobility Group Gene des Haushundes“ folgende drei Aussagen zutreffen:

1. Ich habe die Arbeit ohne unerlaubte fremde Hilfe angefertigt.
2. Ich habe keine anderen als die von mir angegeben Quellen und Hilfsmittel benutzt.
3. Ich habe die den benutzten Werken wörtlich oder inhaltlich entnommenen Stellen als solche kenntlich gemacht.

Bremen, 2010

Jan Thies Soller

"Fast is fine, but accuracy is everything."

Wyatt Earp

Inhalt

Abkürzungsverzeichnis

aa	Aminoacid (Aminosäure)
AAV	Adeno-assoziiertes Virus
AGER	Advanced Glycosylation End Product-specific Receptor
as	Antisense
AuNP	Goldnanopartikel
AX	Ampicillin-X-Gal
BAC	Bacterial Artificial Chromosome
bp	Basenpaare
BrdU	Bromodeoxyuridin
cDNA	Komplementäre DNA
CDS	Kodierende Sequenz
CFA	canines Chromosom (*Canis familiaris*)
Contig	Set von zusammenhängenden DNA Sequenzen in einem Alignment
Da	Dalton (1 Da = 1 u atomare Masseneinheit)
DMEM	Dulbecco's Modified Eagle Medium
DNA	Desoxyribonukleinsäure
DNase	Desoxyribonuklease
dNTP(s)	Desoxyribonukleotidtriphosphat(e)
EB	Elutionspuffer
E. coli	*Escherichia coli*
EDTA	Ethylendiamin-Tetraacetat
et al.	et alia
FKS	Fötales Kälberserum
g	Gramm
h	Stunde
GFP	Grün fluoreszierendes Protein
d_h	Hydrodynamischer Durchmesser
HMG	High mobility group Protein
HMGA	High mobility group Protein A
HMGA1a	High mobility group Protein A1 Isoform a
HMGA1b	High mobility group Protein A1 Isoform b

HMGA1c	High mobility group Protein A1 Isoform c
HMGA2	High mobility group Protein A2
HMGB1	High mobility group Protein B1
HSA	humanes Chromosom (*Homo sapiens*)
IRES	Interne ribosomale Eintrittsstelle
kb	Kilobasenpaare
kDa	Kilodalton
LacZ	β-Galactosidase
LB	Luria Bertami
M	Molar
MAP	Mitogen-activated Protein
MCS	Multiple Cloning Site
min	Minute
miRNA	micro RNA
µCi	Mikrocurie
µl	Mikroliter
ml	Milliliter
mM	Millimolar
M-MLV	Moloney Murine Leukemia Virus
MMU	murines Chromosom (*Mus Musculus*)
mRNA	Messenger Ribonukleinsäure
NCBI	National Center for Biotechnology Information
ng	Nanogramm
nm	Nanometer
NOD-Scid	Non-obese Diabetic – Severe Combined Immunodeficiency
ORF	Open Reading Frame
pAAV	AAV-Genom kodierendes Plasmid
PCR	Polymerasekettenreaktion
PBS	Phosphat Buffered Saline (phosphatgepufferte Salzlösung)
rAAV	rekombinantes Adeno-assoziiertes Virion
RACE	Rapid Amplification of cDNA ends
RAGE	Receptor for Advanced Glycation End Products
RNA	Ribonukleinsäure
RNAi	RNA Interferenz

rpm	Rounds per Minute
RT	Raumtemperatur
RT	Reverse Transkriptase
s	Sekunde
SDS	Natriumdodecylsulfat
siRNA	small interfering RNA
SSC	Standard Saline Citrate Buffer
THADA	Thyroid Adenoma associated
u	Unit
UTR	Nichttranslatierte Region
V	Volt
vg	Virusgenom(e)
v/v	Volumen zu Volumen in Prozent
X-Gal	5-Brom-4-Chloro-3-Indolyl-Beta-D-Galactopyranosid
syn.	Synonym

1. Einleitung

In der Tumorgenetik werden viele Experimente zur Erforschung neuer Medikamente und Therapiekonzepte mit Hilfe von Nagetiermodellen entwickelt.
Allerdings hat die Erforschung des Nagetiermodells seine Grenzen, weil Nagetiere eine Physiologie und einen Zellstoffwechsel besitzen, die nicht ohne weiteres mit denen des Menschen vergleichbar sind. Die dadurch gewonnenen Erkenntnisse lassen sich somit nicht uneingeschränkt auf humane Tumorerkrankungen übertragen.
Der Hund gilt schon seit langem als Tiermodell zur Erforschung und Entwicklung von Medikamenten und Therapien in der Humanmedizin. Das Herzkreislauf-, das Nerven-, das Urogenitalsystem und der Bewegungsapparat beider Spezies sind in großen Teilen in ihrer Anatomie und Physiologie sehr ähnlich (Hongo et al. 1997; McMurray et al. 2006; Shelton & Engvall 2005; Ostrander & Giniger 1997). Bei der Entwicklung neuer therapeutisher Ansätze in der Tumorforschung hat sich der Hund gegenüber anderen Tiermodellen bewährt. Insbesondere die Pathogenese humaner und caniner Tumoren sind vergleichbar (Khanna et al. 2006). Am häufigsten treten bei Hunden verschiedene Tumor-Erkrankungen wie Lymphome und Karzinome auf. Es wird geschätzt, dass einer von drei Hunden ab einem Alter von zwei Jahren tödlich an Krebs erkrankt (Withrow & Vail 2007).
Die Gemeinsamkeiten bei der Pathogenese von Tumorerkrankungen zwischen Mensch und Hund umfassen Resistenzen gegen Therapeutika, das Auftreten von Tumor-Rezidiven und Metastasierungsmuster, die in den herkömmlichen Tiermodellen, wie z.B. bei Nagetieren, nicht vergleichend erforscht werden können (Khanna & Hunter 2005).
Zwischen Hunden und Menschen besteht eine enge Lebensgemeinschaft. In den USA leben in 40 % aller Haushalte Hunde, während in Deutschland in 13 % der Haushalte ein Hund gehalten wird. Die Anzahl der Tiere wird in den USA auf bis zu 72 Millionen geschätzt, in Deutschland leben ca. 5 Millionen Hunde (Olson 2007; Ohr & Zeddies 2006). Die Wahrscheinlichkeit einer spontanen Bildung von Tumorerkrankungen beim Hund in seinem natürlichen Lebensraum, d.h. im Lebensumfeld seines Besitzers, steigt mit dem voranschreitenden Lebensalter. Sie leiden häufig an den gleichen Tumorerkrankungen wie sie auch bei Menschen vorkommen. Hunde haben im Vergleich zum Menschen eine etwa doppelt so hohe

Wahrscheinlichkeit an Krebs zu erkranken. Ihr kürzeres Lebensalter macht klinische Studien im Rahmen eines überschaubaren Zeitraums erst möglich (Knapp & Waters 1997).

Die Bereitschaft der Besitzer ist sehr hoch neue therapeutische Ansätze bei ihren erkrankten Hunden anzuwenden, auch im Vorzug gegenüber bereits etablierten aber wenig aussichtsreichen, konventionellen Therapien.Die Ergebnisse neuer Therapien liefern, im Zusammenhang mit klinischen Studien, wertvolle Erkenntnisse für die Zulassung neuer Medikamente und Therapeutika in der Humanmedizin (Paoloni & Khanna 2007).

Herkunft und die Entstehung (Ätiologie) humaner und caniner Tumoren sind vergleichbar. Faktoren wie z.B. Alter, Geschlecht, Ernährung, Größe und Gewicht, hormonelles Gleichgewicht und Umwelteinflüsse wie Schadstoffbelastungen, werden auch bei Hunden als Ursache von Tumorerkrankungen beschrieben (Paoloni & Khanna 2007). Dabei liegen auch häufig genetische Rassen-Prädispositionen vor. An malignen Lymphomen erkranken vorwiegend Golden Retriever; Berner Sennenhunde weisen eine hohe Inzidenzrate auf an einer besonders schweren Form der malignen Histiozytose oder des disseminierten histiozytischen Sarkoms zu erkranken (Olson 2007; Waters & Wildasin 2006; Nolte & Nolte 2001; Abadie et al. 2009).

Jede Hunderasse repräsentiert einen in sich abgegrenzten Genpool. Die gegenwärtig über 400 verschiedenen Hunderassen besitzen eine relativ hohe phänotypische Uniformität mit einem sehr geringen Grad genetischer Heterogenität und Variabilität (Wayne & Ostrander 1999). Zur selektiven Züchtung einer Hunderasse wurde eine kleine Gründerpopulation nahverwandter Individuen verwendet, in der üblicherweise die Inzucht gezielt eingesetzt wurde. Dies führte zur Ausprägung eines engen und isolierten Genpools. Innerhalb der Hundepopulation sind Kreuzungen der einzelnen Rassen häufig, wodurch genetische Prädispositionen für Tumorerkrankungen an die Nachkommen weitervererbt werden. Für die Humangenetik sind genetische Prädispositionen für bestimmte Tumorarten von besonderem Interesse, da sie die Möglichkeit bieten seltene, vererbbare Tumorerkrankungen zu erforschen (Kuska 1999; Ostrander & Giniger 1997).

Die Sequenzierung des caninen Genoms im Jahr 2005 bietet die Möglichkeit auf molekular-genetischer Ebene die Pathogenese und das Metastasierungs-Muster von Tumoren *in vivo* zu erforschen (Lindblad-Toh et al. 2005). Es stellte sich heraus,

dass die Organisation des caninen Genoms bezüglich der Reihenfolge der Gene auf den verschiedenen Chromosomenabschnitten (Syntenie) von Menschen und Hunden bis zu 95 % identisch sind (Fleischer et al. 2008).

Bereits im Jahre 2000 wurden bei über 370 der beschriebenen caninen Erbkrankheiten genetische Ausprägungen einzelner Genloci oder polygene Faktoren entdeckt, die auch in der menschlichen Population auftreten. Von diesen 370 untersuchten Erbkrankheiten beim Hund zeigen etwa die Hälfte ähnliche klinische Befunde wie sie auch bei humanen Erkrankungen auftreten. Bei über 40 caninen Erkrankungen liegen dieselben homologen Genmutationen vor, die auch bei den humanen Erkrankungen vorliegen (Ostrander et al. 2000; Patterson 2000).

Zuvor etablierte Therapien gegen humane Tumorerkrankungen finden auch in der Veterinärmedizin bei Hunden zahlreiche Anwendungen, wie beispielsweise die Behandlung von malignen Lymphomen mit entsprechenden chemotherapeutischen Protokollen (Withrow & Vail 2007).

Die Erforschung der Tumorbiologie des Prostatakarzinoms bildet in dieser Arbeit einen besonderen Schwerpunkt. In vielen Ländern weltweit ist das Prostatakarzinom bei Männern die häufigste diagnostizierte Tumorerkrankung (Boyle & Levin 2008). Während beim Menschen die Heilungschancen eines nicht-metastasierenden Prostatakarzinoms hoch sind, verläuft die Erkrankung beim Hund in den meisten Fällen tödlich. Außerdem erkranken Rüden eher selten an Prostatakarzinomen. Im Rahmen vergleichender Untersuchungen in der Tumormedizin gehört der Hund, neben den Primaten, zu den wenigen Säugetieren bei denen eine spontane Bildung von Prostatakarzinomen diagnostiziert wird. Eine Ausnahme bilden die spontanen Entwicklungen von Prostata-Tumoren bei speziellen Zuchtstämmen von Ratten beobachtet. Das canine Prostatakarzinom zeigt ein dem Menschen vergleichbares Metastasierungs-Muster. Beide Spezies weisen einen ähnlichen anatomischen Aufbau der Prostata auf (Leroy & Northrup 2009; Waters et al. 1998; Nolte & Nolte 2001).

Genomische Charakterisierungen dienen als Ausgangspunkt für funktionelle Analysen von tumorrelevanten Genen. Unter diesen Aspekten werden in dieser Arbeit die caninen Gene der evolutionär stark konservierten HMGA Familie charakterisiert. Weiterführend wird zur Inhibierung der Expression von HMGA Genen in einer caninen Prostatakarzinomzelllinie ein gentherapeutischer Ansatz entwickelt. Zur Aufklärung weiterer tumorrelevanter Gene, wie z.B. *Interleukin-1*,

TNF-α und *RAGE*, werden canine BAC Klone, genomische DNA, RNA und FISH-Analysen verwendet. Diese sind für zukünftige vergleichende Studien im Rahmen einer vergleichenden Onkologie zwischen Mensch und Hund unerlässlich.

Bei vielen humanen Tumoren beobachtet man eine erhöhte Expression von HMGA Proteinen. Im Gegensatz dazu ist die Expression von HMGA in adulten, bereits ausdifferenzierten Zellen gering. Eine Überexpression von HMGA Proteinen geht oft einher mit einer malignen neoplastischen Transformation mit ungünstigen Prognosen für den weiteren Krankheitsverlauf (Fusco & Fedele 2007). Das humane *HMGA1* Gen ist auf dem Chromosom 6 auf der Bande p21 lokalisiert (Johnson et al. 1989; Friedmann et al. 1993). Das verwandte HMGA2 Protein wird durch ein Gen auf Chromosom 12 auf der Bande q14-15 kodiert (Schoenmakers et al. 1995; Wanschura et al. 1995).

Eine stark erhöhte *HMGA1* mRNA Expression wurde bei einer Vielzahl von menschlichen Tumoren gemessen, wie z.B. Mamma-, Cervix-, Schilddrüsen- und Prostata-Tumoren (Flohr et al. 2003; Bandiera et al. 1998; Bussemakers et al. 1991; Chiappetta et al. 1998). Beobachtet wurde eine erhöhte Transkription von *HMGA2* in Karzinomen der Mamma, der Lunge und des Pankreas (Rogalla et al. 1997; Meyer et al. 2007; Abe et al. 2000).

Ein weiteres Protein der HMG Familie, das mit seiner Funktion als architektonischer Transkriptionsfaktor den HMGA Proteinen ähnelt, ist das High Mobility Protein B1 (HMGB1, syn. Amphoterin) (Reeves & Adair 2005). HMGB1 kann aktiv von Monozyten ausgeschüttet werden und wirkt als proinflammatorisches Zytokin (Andersson et al. 2002). Als extrazelluläres Protein ist HMGB1 ein Ligand des Rezepors RAGE („Receptor for Advanced Glycation Endprodukts“) (Vazzana et al. 2009). RAGE ist auf der Zellmembran lokalisiert und steuert zusammen mit HMGB1 die Aktivierung der Signaltransduktion mit Hilfe von MAP-Kinasen. Es spielt eine wichtige Rolle bei Entzündungsreaktionen, Proliferationen und Metastasierungsprozessen (Rouhiainen et al. 2004). Durch die Applikation von rekombinanten RAGE Proteinen, denen die Cytosol- und Transmembran-Domäne fehlt, konnte die Signaltransduktion inhibiert und das Wachstum von Tumorzellen stark reduziert werden (Taguchi et al. 2000). Dieses RAGE Protein besteht nur aus einer extrazellulären Domäne und wird als trunkierte, lösliche („**s**oluble“) sRAGE Variante bezeichnet. Beim Menschen konnten bereits viele natürlich existierende sRAGE Varianten nachgewiesen werden. Sie agieren als

kompetitive Inhibitoren des membrangebunden Rezeptors. Eine Störung des Gleichgewichts zwischen membrangebundenen und löslichen RAGE Varianten konnte bei Alzheimer Erkrankung oder rheumatischer Arthritis, sowie verschiedenen Tumoren nachgewiesen werden (Lue et al. 2005; Pullerits et al. 2005; Sparvero et al. 2009). Bei Tumoren wird ein Zusammenhang zwischen einer aberranten Expression des sRAGE und des HMGB1 Proteins bei Chondrosarkomen diskutiert (Takeuchi et al. 2007).

Die aberrante Expression von Zytokinen vor allem Interleukin-1 (IL-1α and IL-1β) und des Tumornekrosisfaktor alpha (TNF-α) spielt eine wichtige Rolle bei der Einleitung von Entzündungsreaktionen und der Immunantwort. Basenpaarsubstitutionen innerhalb der Gensequenzen dieser Zytokine wurden bei vielen Krankheiten wie Alzheimer, Parkinson und nicht-kleinzelligen Bronchialkarzinom beschrieben (McGeer & McGeer 2001; Mattila et al. 2002; Zienolddiny et al. 2004). Die humane Langerhans-Zell-Histiozytose zeichnet sich durch eine hohe Produktion von Interleukin-1 und des TNF-α in den Langerhans-Zellen und T-Zellen aus (Arico 2006). Es handelt sich hierbei um eine Autoimmunkrankheit, die durch eine Autophagozytose der Erythrozyten charakterisiert ist. In den betreffenden Organen, wie z.B. Lunge, Leber, Milz und Skelett, treten Neoplasien auf, die in kürzester Zeit in benachbarte Gewebe infiltrieren und metastasieren. Die Krankheit tritt hauptsächlich bei Kindern bis zu einem Alter von drei Jahren, aber auch jungen Erwachsenen auf, und endet meistens tödlich (Egeler et al. 1999; Tazi et al. 1999). Die molekularen Mechanismen der Pathogenese dieser Erkrankung und Therapiekonzepte sind weitestgehend unerforscht (Allen 2008). Die maligne Histiozytose ist bei Berner Sennenhunden eine häufig auftretende Erkrankung. Diese Rasse besitzt eine deutliche Prädisposition zur Ausbildung dieser Tumorerkrankung (Ramsey et al. 1996; Nolte & Nolte 2001). Viele klinische und pathologische Eigenschaften der caninen malignen Histiozytose ähneln der menschlichen Langerhans-Zell-Histiozytose (Affolter & Moore 2002). Zur Aufklärung der molekulargenetischen Pathogenese der humanen Langerhans-Zell-Histiozytose dient somit der Berner Sennenhund als Tiermodell.

Die vorliegende Arbeit gliedert sich in die folgenden inhaltliche Abschnitte:
Der erste Abschnitt behandelt die molekulargenetische Charakterisierung und chromosomale Lokalisation des caninen *HMGA1* Gens, sowie gesamt-genomische und vergleichende Analysen des caninen Gens mit denen anderer Säugetierspezies. Mit Hilfe einer spontan immortalisierten caninen Prostata-Adenokarzinomzelllinie wurde zur Erforschung des caninen Prostatakarzinoms ein Nagetiermodell etabliert. Diese Zelllinie wurde verwendet, um mit deren Hilfe *HMGA* anti-sense kodierende Adeno-assoziierte Viren (AAVs) zu konstruieren Diese stellen einen gentherapeutischen Ansatz zur Inhibierung der nativen *HMGA* Überexpression dar. Desweiteren wird eine alternative Transfektions-Methode beschrieben, bei der DNA Moleküle mit Hilfe von Gold-Nanopartikeln effizient in Zellen eingebracht wurden.

Der zweite Abschnitt befasst sich mit der molekulargenetischen Charakterisierung des caninen *RAGE* Gens. Dazu wurde in ausgewählten gesunden Geweben sowie in Tumorgeweben die *RAGE* Expression untersucht. Das Verhältnis der Expression von membrangebundenen und solublen *RAGE* Varianten wurde analysiert.Zudem wurden weitere canine und humane *RAGE* Varianten molekulargenetisch charakterisiert.
Bei vielen Neoplasien beobachtet man häufig eine Überexpression von Zytokinen, deren Folge wiederum zu aberranten Inflammations- und Immunantworten führen.

Der dritte Abschnitt beinhaltet das Screening nach Basenpaarsubstitutionen, den „Single Nucleotide Polymorphisms“, in den kodierenden Regionen der *IL-1 und TNF-α* cDNA Sequenzen. Es wurden RNAs von verschiedenen Hunderassen isoliert, die unterschiedliche Rassen-Prädispositionen zur Ausprägung der malignen Histiozytose aufweisen. Des Weiteren wurde eine vergleichende Analyse und eine Zusammenstellung der *IL-1*, *TNF-α* Gene und Proteine bei verschiedenen Säugetieren durchgeführt.

2 Material und Methoden

2.1. Entnahme von Gewebeproben

Die canine Gewebebank war die Grundlage für die Isolierung von RNA und DNA des Haushundes. Sie wurde an der Kleintierklinik der Tierärztlichen Hochschule Hannover entwickelt und aufgebaut. Diverse Gewebearten von verschiedenen Hunderassen wurden unmittelbar während Operationen oder Sektionen gesammelt. Je nach Menge des Ausgangsmaterials wurden ca. 0,5 g bis 2 g Frischgewebe in 2 ml Kryogefäße überführt und sofort in flüssigem Stickstoff (-196°C) eingefroren. Die gesammelten Gewebeproben wurden in einem -80°C Gefrierschrank zur späteren Isolierung von Nukleinsäuren überführt und aufbewahrt.

2.2 Zellkultur und Zelllinien

Die folgenden adhärenten Zelllinien wurden vom Zentrum für Humangenetik der Universität Bremen für diese Arbeit zur Verfügung gestellt:
Die Zelllinie ZMTH3 wurde aus einer caninen Gewebeprobe eines pleomorphen Adenoms hergestellt. Die ursprünglichen Gewebe der Zelllinien MTH52c und MTH53a waren ein Klein-Zell Karzinom bzw. Mamma Gewebe ohne Befund. Die Zelllinie CT1258 wurde direkt aus dem Gewebe eines caninen Prostata Adenokarzinoms etabliert. Die aufgeführten Zelllinien sind spontan immortalisiert, dass bedeutet diese Zellen haben die Fähigkeit erlangt sich unendlich zu teilen, ohne dass diese Eigenschaft künstlich induziert wurde. Die Kultivierung der caninen Zellen erfolgte in 25 cm^2 Kulturflaschen mit 5 ml Medium 199 supplementiert mit 20 % (v/v) fötalem Kälberserum (FKS) bei 37°C und 5 % CO_2 Atmosphäre.
Für die Produktion der rekombinanten Adeno-Assoziierten- Viren (AAV) wurde die Zelllinie AAV-(HEK)-293 (Stratagene) aus humanen embryonalen Nierenzellen kultiviert. Die Titrierung der rAAV-LacZ Viren erfolgte mit der humanen Fibrosarkom Zelllinie HT1080 (Stratagene). Die Kultivierung der humanen Zelllinien erfolgte in 75 cm^2 bis 150 cm^2 Kulturflaschen mit 15 ml bzw. 30 ml DMEM mit 10 % (v/v) FKS (37°C, 5 % CO_2).

2.3 DNA Isolierung und Aufreinigung

2.3.1 Plasmid Präparation aus *E.coli*

Die Isolierung der Plasmid-DNA für Bakteriensuspensions-Kulturen erfolgte nach dem „QIAprep Spin Miniprep Kit“ Protokoll (Qiagen, QIAprep Miniprep Handbook, Seiten 22 bis 23). Die Plasmide wurde nach der Aufreinigung mit 50 µl EB Puffer (10 mM Tris-HCl, pH 8,5) aus der Säule eluiert. Für gößere Bakterienkulturen (≥ 250 ml) LB Medium wurde, analog zum „QIAprep Spin Mini Kit“, das Protokoll für „DNA-Purifcation Using Plasmid Midi and Maxi Kits“ (Qiagen) verwendet (QIAGEN Plasmid Purification Handbook, Seiten 19 bis 23). Das DNA Pellet wurde anschließend in 100 µl bis 500 µl EB Puffer gelöst und die Konzentration photometrisch gemessen.

2.3.2 BAC DNA Präparation

BAC DNA Präparationen wurden mit Hilfe des „QIAGEN Plasmid Maxi Kit“ (QIAGEN) durchgeführt. Zuerst wurde eine Vorkultur in 10 ml LB Medium für 8h bei 37°C im Schüttelschrank (300 rpm) inkubiert. Diese Vorkultur wurde in 500 ml LB Medium gegeben und es erfolgte eine Inkubation des Ansatzes über Nacht im Schüttelschrank bei 37°C. Die anschließende BAC DNA Extraktion erfolgte nach Angaben des Herstellers (QIAGEN Plasmid Purification Handbook, Seiten 47-51, Protocol „Very Low-Copy Plasmid/Cosmid Purification“). Das DNA Pellet wurde in EB Puffer gelöst und die Konzentration und Reinheit bestimmt.

2.3.3 AAV Plasmid Präparation

Zur Herstellung rekombinanter AAVs (Stratagene) wurden die Plasmide pAAV-MCS, pAAV-LacZ und die Plasmide pAAV-Helper und pAAV-RC, welche die Gene für die infektiösen Virionen kodieren, mit Hilfe des „QIAGEN EndoFree Maxi Kit“ (Qiagen) isoliert. Eine Vorkultur wurde selektiv in 5 ml Ampicillin-LB Medium angesetzt und für 6-8 h bei 37°C im Schüttelschrank (300rpm) inkubiert. Anschließend wurden 250 ml Ampicillin-LB Medium mit 500 µl Vorkultur inokuliert und nach dem Hersteller-Protokoll aufgearbeitet (QIAGEN Plasmid Purification Handbook, Seiten 20-23, Protocol EndoFreePlasmid Maxi DNA Purification Using QIAGEN Plasmid Midi and Maxi Kits). Das DNA Pellet wurde

anschließend in 100 µl bis 250 µl TE Puffer (10 mM Tris-HCl, 1 mM EDTA, pH 7,5) gelöst und die photometrisch gemessen.

2.3.4 DNA Isolierung aus Blut und Gewebe

Die Isolierung genomischer DNA erfolgte nach den Angaben des Herstellers (Qiagen, QIAamp DNA Mini Kit). Aus 250 µl EDTA-Vollblut wurde die DNA nach dem „Blood and Body Fluid Spin“ Protokoll, Seiten 27-29, isoliert. Für eine DNA-Isolierung aus Gewebeproben wurde 25 mg frisches oder gefrorenes Gewebe abgewogen, mechanisch zerkleinert und in ATL Puffer und Proteinase K lysiert („Tissue Protocol, Seiten 33-35“). Die DNA aus Zellkultur Proben wurde nach dem Protokoll „Protocol for cultured cells, Seite 49“ isoliert. Mundschleimhaut und Speichelproben („Buccal Swabs“) wurden von den Wattestäbchen in PBS Puffer gelöst und anschließend die DNA nach dem Protokoll „DNA Purification from Buccal Swabs, Seiten 37-39“ aufgereinigt.

2.4 Polymerase Chain Reaction (PCR)

Die Amplifikation der DNA Fragmente erfolgte mit Oligonukleotiden (Primer) entsprechend der Protokolle des Herstellers der Firma Invitrogen (Basic Protocol) oder Promega (GoTaq DNA Polymerase). Die Annealing Temperaturen der Primer variierten gemäß der Nukleotidsequenz der Zielgene, (siehe entsprechende Publikationen). Die PCR Reaktionen wurden in dem Thermoblock T-Gradient (Biometra) durchgeführt. Nach den Angaben des Protokolls „QIAquick Spin Handbook, Seite 18, QIAquick PCR Purification Kit Protocol“ (Qiagen) wurden die PCR-Produkte aufgereinigt.

2.5 Agarose-Gelelektrophorese

Zum Auftrennen der DNA Moleküle wurden abhängig von der zu erwartenden Größe des DNA Amplikons, ein 1,5 % oder 4 % (bei DNA-Molekülen < 300 bp) Agarosegel vorbereitet. Dazu wurde die entsprechende Menge Agarose in 100 ml TAE (40 mM Tris-Acetat, 1mM EDTA, pH 8,0) Puffer bei konstanter Temperatur (bis ca. 100°C) gelöst. Zur Detektion der DNA Banden wurden anschließend 1 µl

Ethidiumbromid (10 mg/ml) in das noch flüssige Agarosegel gegeben. Die Proben wurden mit 6x Farbbeladungspuffer gemischt und in das Gel pipettiert. Die Trennung der DNA Fragmente erfolgte im elektrischen Feld (5 V x Länge der Elektrophoresekammer in cm) in 500 ml TAE Puffer.

2.6 PCR Klonierung

Die PCR Fragmente (Amplikon-Bande) wurden mit einem sterilen Skalpell aus dem Agarosegel (1,5 %) herausgeschnitten und in ein 1,5 ml Reaktionsgefäß überführt. Anschließend erfolgte eine Elution der DNA aus dem Agarosegel mit Hilfe des Protokolls „QIAquick Gel Extraction Kit Protocol using a micro centrifuge“ auf den Seiten 23 - 27 des QIAquick Spin Handbook (Qiagen). Die PCR Fragmente wurden mit Hilfe des Enzyms T_4-DNA Ligase (3 U) in den Vektor „pGEM-T Easy“ nach Angaben des Herstellers (Promega) kloniert. Die Ligations-Reaktion erfolgte mit 4 µl PCR-Eluat und 50 ng Vektor DNA (siehe „Technical Manual, pGEM-T and pGEM-T Easy Vector Systems“, Seite 8: „Protocol for Ligations Using the pGEM-T and pGEM-T Easy Vectors and the 2X Rapid Ligation Buffer”). Anschließend erfolgte eine Transformation des Vektorsystems zur Vervielfältigung der Plasmid DNA in thermokompetente *E. coli* DH5α (Invitrogen).

2.7 Klonierung rekombinanter AAV Expressionsplasmide

Eine PCR zur Amplifikation von *HMGA* Genen wurde mit Adapter-Primern durchgeführt, die am 5’ Ende des Oligonukleotids mit einer entsprechenden Erkennungssequenz für eine spezifische Restriktionsendonuklease modifiziert waren. Als Template für die PCR Reaktion diente cDNA. Nach einer Aufreinigung des PCR Produktes (siehe 2.4.) wurden die DNA Fragmente (Inserts) mit den entsprechenden Restriktionsendonukleasen *Bam*HI und *Eco*RI geschnitten. Für das pAAV-MCS Plasmid erfolgte in einem separaten Ansatz eine Restriktionsendonuklease-Reaktion mit den identischen Enzymen. Die gerichtete Ligationsreaktion erfolgte mit Hilfe der T_4-DNA Ligase (Fermentas) nach Angaben des Herstellers: „DNA Insert Ligation into Vector DNA“ (www.fermentas.com/techinfo/). Das molare Verhältnis von Vektor- zu Insert-DNA betrug 1:3. Anschließend wurde eine Transformation der rekombinanten pAAV-*HMGA* antisense Vektoren zur Vervielfältigung der Plasmid DNA in thermokompetente *E. coli* XL10 Gold (Stratagene) durchgeführt.

2.8 Transformation rekombinanter Plasmide in E. coli

Die rekombinanten Plasmide (siehe 2.6) wurden in thermokompetente Bakterienzellen transformiert. Dabei wurden *E. coli* DH5α mit 4 µl Ligationsansatz nach dem Protokoll von Invitrogen „Library Efficiency DH5α Competent Cells, Cat. No. 18263-012“, Seiten 1-4 transformiert. 100 µl bis 250 µl Bakteriensuspension (in SOC Medium) wurden auf LB-AX-Agar ausplattiert (2 % LB-Medium, 100 µg/ml Ampicillin und 50 µg/ml X-Gal) und für 12 h bei 37°C inkubiert. Eine Auswahl geeigneter Klone wurde durch eine „Blue-White“ Kolonie-Selektion ermöglicht. Analog zu dem DH5α Protokoll erfolgte die Transformation der *E. coli* XL10 Gold Zellen (siehe 2.6) mit Hilfe des Protokolls von Stratagene „XL-10 Gold Ultracompetent Cells“, Seiten 1-2. Es wurden 250 µl Bakteriensuspension (in NZY^+ Medium) auf LB-Ampicillin-Agar Platten (2 % LB-Medium, 100 µg/ml Ampicillin) ausgestrichen.

2.9 DNA Restriktionsendonuklease Verdau

Zum Nachweis einer erfolgreichen Insertion eines DNA Fragments in die verschiedenen Expressions- bzw. Sequenzierungsvektoren wurde ein Restriktionsendonuklease Verdau der Plasmid-DNA angesetzt. Dabei wurde 1 µg bis 3 µg photometrisch quantifizierte Plasmid-DNA mit ausgewählten 5 U Enzymen und Puffern nach Protokoll des Herstellers (Invitrogen, Fermentas) über Nacht bei 37°C im Wasserbad inkubiert. Anschließend erfolgte die Auftrennung der geschnittenen Plasmid-DNA in einem 1 %, ethidiumbromidhaltigem Agarosegel (siehe 2.5).

2.10 Sequenzierung und in silico Auswertung

Die verschiedenen PCR Amplikons, Vektor Inserts und rekombinante Plasmide wurden von der Fa. MWG-Biotech sequenziert. Es wurden 1,2 µg DNA-Plasmid oder 20 ng/bp PCR-Fragmente zur Sequenzierung entnommen und versendet. Die *in silico* Auswertung bzw. Sequenzanalyse erfolgte zunächst in den NCBI Datenbänken mit Hilfe des Blast-Programms. Die weitere Analyse und Bearbeitung der DNA Sequenzen, wie z.B. die Generierung von DNA Contigs und von

Homologie-Alignments, erfolgte mit Hilfe der Lasergene-Suite Software 5.0 bis 7.0 (DNAStar).

2.11 RNA Isolierung

Canine Gewebeproben wurden gesammelt und sofort bei -196°C in flüssigem Stickstoff eingefroren (siehe 2.1) und mit einer bestimmten Menge Lysisreagenz (Trizol LS oder RLT Puffer, siehe unten) versetzt und homogenisiert. Für die Isolierung von Gesamt-RNA aus Zellkulturen (z.B. CT1258) wurde das Medium entfernt und mit 1x PBS (ohne Mg^{2+}) gewaschen. Das Lysisreagenz wurde direkt auf den Zellmonolayer gegeben und die Zellen wurden durch mehrmaliges Auf- und Abpipettieren homogenisiert.

2.11.1 RNA Isolierung mit Trizol® LS

Aus den Kryogefäßen wurden ca. 50 mg bis 100 mg Gewebematerial entnommen und mit 750 ml Trizol®-LS-Reagenz (Fa. Invitrogen) versetzt. Im Gegensatz zu Trizol® sind bei Trizol®-LS die chemischen Komponenten wie Phenol und Guaninthiocyanat höher konzentriert. Mit einem Skalpell wurde die Probe zerkleinert und mit einer Pipettenspitze oder Kanüle (0,9 mm Durchmesser, 2,5 ml Einwegspritze) suspensiert, passiert und homogenisiert. Für die Lysierung von Zellen in Kultur wurden direkt 750 ml Trizol®-LS-Reagenz in die Zellkulturflasche gegeben und die Zellen wurden in durch mehrmaliges Auf- und Abpipettieren homogenisiert. Die weitere Aufarbeitung und Isolierung und Aufbereitung der RNA erfolgte nach den Angaben des Herstellers mit Chloroform und Ethanol (Invitrogen, TRIzol® LS Reagent Protocol). Nach der Trocknung des RNA Pellets wurde sie in nukleasefreiem Wasser gelöst, die Konzentration der Gesamt-RNA photometrisch bestimmt und die RNA bei -80°C eingefroren.

2.11.2 RNA Isolierung mit RNeasy

Die Isolierung von Gesamt RNA aus Gewebe und Zellkultur erfolgte mit Hilfe der Protokolle „Purification of RNA from Animal Tissues“ (Seiten 39 bis 44) oder „Purification of Total RNA from Animal Cells Using Spin Technology” (Seiten 25 bis 30) aus dem RNeasy Mini Handbook, 04/2006 (Qiagen). Die Homogenisierung der Gewebeproben (bis zu 30 mg) erfolgte mit Hilfe des Protokolls „Purification of RNA or Multiple Analytes from Animal and Human Tissues“ (Seiten 10 bis 17) aus dem TissueLyser Handbook (Qiagen). Zellen in Monolayer ($\leq 5x10^6$ Zellen)

wurden zunächst mit 1 ml TrypLE (Gibco) versetzt; nach der Inkubation (1 bis 2 min) wurde das TrypLE mit 1 ml Medium (10 bis 20 % v/v FKS) inaktiviert. Die vereinzelten Zellen wurden in ein 1,5 ml Eppendorfreaktionsgefäß überführt und mit 1x PBS gewaschen. Die Homogenisierung der Zellen erfolgte in der entsprechenden Menge RLT Puffer mit Mercaptoethanol durch die Anwendung von QIAshredder Säulen (Qiagen, Schritt 3a, Seite 29 RNeasy Mini Handbook).
Für größere Gewebemengen und Zellkulturmaterial (≤ 250mg bzw. > $5x10^6$ Zellen) wurde die gesamt RNA mit Hilfe des Protokolls „RNeasy Midi/Maxi Protocol for Isolierung of Total RNA from Animal Tissues“ (Seiten 41 bis 44) aus dem RNeasy Midi/Maxi Handbook (Qiagen) durchgeführt.
Nach dem ersten Waschschritt wurde auf die Säule eine DNase I / Puffer Lösung (RNase-Free DNase Set, Qiagen) pipettiert (siehe Appendix RNeasy Protokolle), um eine Kontamination der RNA mit genomischer DNA auszuschließen. Die Gesamt-RNA wurde mit nukleasefreien Wasser eluiert, die Konzentration der RNA photometrisch gemessen und die RNA bei -80°C eingefroren.

2.12 cDNA Synthese

2.12.1 3’RACE cDNA Synthese

Für die Charakterisierung caniner Transkripte wurde für die cDNA Synthese ein 3’RACE Adapter Primer AP2 ($AAGGATCCGTCGACATC(T)_{17}$) verwendet. Die cDNA Synthese wurde gemäß den Angaben des Herstellers (Invitrogen) mit 5 µg Gesamt-RNA und 200 U Superscript RT durchgeführt, siehe „Superscript Reverse Transcriptase Protocol, review 260903“. Die Inkubation, zum Aufschmelzen potentieller Sekundärstrukturen der RNA, erfolgte bei 65°C für 5 min, die eigentliche Synthese der cDNA erfolgte bei 42°C für 50 min. Für die reverse Transkription langer (> 1000 bp) und GC-reicher Sequenzen wurde die Reaktion mit Trehalose (0,6 M) substituiert. Die Synthese der cDNA erfolgte für 2 min bei 60°C und 2 min 50°C in zehn nacheinander abfolgenden Zyklen. Nach der Erststrang-Synthese wurden 2 U RNase H zu der Probe gegeben (Inkubation bei 37°C für 15 min), um die RNA aus dem DNA/RNA Hybridmolekül enzymatisch abzubauen. Insgesamt wurde1 µl cDNA Lösung für spätere PCR Reaktionen (siehe 2.4) eingesetzt.
Für die Real-Time PCR (siehe 2.13) wurden 250 ng Gesamt-RNA zusammen mit genspezifischen Primern für die 3’RACE cDNA Synthese eingesetzt. Die Synthese

erfolgte mit dem M-MLV Enzym (Invitrogen) nach den Angaben des „M-MLV Reverse Transcriptase Protocol, review 091002“. Der Reaktionsansatz wurde für 50 min bei 37°C inkubiert.
Die cDNA wurde bis zur weiteren Verwendung bei -20°C gelagert.

2.12.2 5’RACE cDNA Synthese

Zur Charakterisierung der Nukleotide am 5’Ende der mRNA wurde eine 5’RACE cDNA Synthese nach dem Protokoll “5´ RACE System for Rapid Amplification of cDNA Ends” handbook, 12/2004“ (Invitrogen) durchgeführt. Für die cDNA Synthese wurden genspezifische Primer und das Enzym Superscript RT verwendet.

2.13 Northern Blot

RNA Gelelektrophoresen, der Aufbau der Blotting Apparatur und der Transfer der Gesamt-RNA auf die Hybridisierungsmembran (Nylon TransferMembran HybondTM-N+, Amersham Pharmacia Biotech) wurden nach Angaben des Protokolls von Stratagene des „Northern Transfer Protocol“, Messenger RNA Isolierung Kit, Instruction Manual, Seiten 13 bis 15 durchgeführt. Hybridisierungssonden wurden durch die Amplifikation von cDNA mit genspezifischen Primerpaaren generiert (siehe 2.4 bis 2.6). Anschließend wurden die PCR Produkte in das pGEM-T Easy Vektor System kloniert und sequenziert.
Die aufgereinigte Sonden-DNA (50 ng/µl) wurde mit dem radioktiven Nukleotid dCTP markiert (Amersham Pharmacia Biotech), welches als α-Phosphat ein Isotop ^{32}P trägt. Die folgenden Arbeiten zur radioaktiven Markierung der Sonden-DNA wurden mit Hilfe des Random Primed Labeling Kit (Roche) durchgeführt. Nicht eingefügte dNTPs wurden mit Hilfe von Sephadex G-50 Säulen (Amersham Pharmacia Biotech) entfernt.
Die Prähybridisierung der Northern Blot Membran erfolgte mit Hilfe der PERFECTHYB PLUS (Sigma-Aldrich) Lösung für 30 min. Die Hybridisierung der Membran erfolgte für 2,5 h bei 68°C im Hybridisierungs-Ofen unter konstanten Mischbewegungen. Anschließend wurde die Membran für 5 min bei RT in 2x SCC/0,1 % SDS gewaschen. Anschließend erfolgte ein zweiter Waschschritt für 20 min bei 68°C in 0,5x SCC/0,1 % SDS, der einmal wiederholt wurde. Die Auswertung, d.h. die Visualisierung der Nukleotidbanden des Northern-Blots erfolgte im Storm 860 Phosphorimager (Molecular Dynamics).

2.14 Quantitative Real-Time PCR

Nach der RNA Isolierung mit anschließendem DNaseI Verdau wurden pro Ansatz 250 ng RNA in einer cDNA Synthese mit M-MLV Enzym und genspezifischen Primern eingesetzt (siehe 2.12.1). Parallel erfolgte eine Synthesereaktion unter gleichen Bedingungen an einem Oligonukleotid-Standard in definierter Menge und kovalent gebundenen Fluoreszenzfarbstoffen (5'6-FAM / 3'TAMRA). Die eigentliche absolute Real-Time PCR erfolgte mit dem „Applied Biosystems 7300 Real-Time PCR System" mit „TaqMan Universal PCR Master Mix" (Applied Biosystem) nach den Angaben des Herstellers. Das PCR Programm bestand aus einer initialen Denaturierung für 10 min bei 95°C, anschließend in 50 Zyklen 15 s bei 95°C und 60 s bei 60°C.

2.14.1 Bestimmung des rAAV Titers

Der genomische rAAV Titer (vg/ml) wurde mit Hilfe einer CMV Promoter spezifischen quantitativen Real-Time PCR bestimmt. Für die folgende Real-Time PCR musste das AAV Virion zunächst aufgebrochen bzw. die ssDNA freigesetzt werden. Es wurden 40 µl aufgereinigtes Virus Eluat (siehe 2.17), 160 µl H_2O und 200 µl NaOH für 30 min bei 56°C inkubiert. Anschließend wurde die Lösung mit 190 µl HCl neutralisiert. Die Probe wurde für die Real-Time PCR 1:100 verdünnt und 3 µl Template wurde in die PCR Reaktion eingesetzt. Zehn Verdünnungen (10^1 bis 10^6 Moleküle / 3 µl Template) eines universellen AAV Oligonukleotid-Standards wurden parallel in weiteren PCRs eingesetzt. Mit dem bereits verwendeten PCR-System (siehe 2.14) erfolgte anschließend die eigentliche Real-Time PCR (Applied Biosystems, 7300 Real-Time PCR System). Die Amplifikation erfolgte für 2 min bei 50°C, 10 min bei 95°C und weiter für 45 Zyklen mit 15 s bei 95°C und 60 s bei 60°C.

2.15 BAC Screening

Für das BAC-Screening wurden PCR Sonden auf den caninen RPCI-81 BAC/PAC Filter (BACPAC Resources) hybridisiert. Die Sonden wurden mit genspezifischen Primern an caniner DNA amplifiziert. Der PCR Ansatz wurde auf ein 1,5 % Agarosegel aufgetragen. Nach einer Gelelektrophorese wurden die DNA Fragmente

aus der Agarose eluiert (Qiagen, „QIAquick Gel Extraction Kit Protocol using a micro centrifuge“ auf den Seiten 23 - 27 des QIAquick Spin Handbook). Nach der erfolgreichen Klonierung der PCR-Produkte in das pGEM-T Easy Vektor System wurden sie sequenziert. 250 ng Sonden-DNA wurde gemäß des Hersteller Protokolls mit 250 µCi (α^{32}P)dCTP makiert (Roche, Random Primed Labeling Kit). Die Aufreinigung der Sonden DNA erfolgte mit Sephadex G-50 Säulen (siehe auch 2.13). Zur Hybridisierung der Sonde wurde das Protokoll „Hybridisation of High Density Filters“ nach Angaben des Herstellers (BACPAC Resources) durchgeführt. Die BAC-Filter wurden unter Verwendung des Storm 860 Phosphorimager (Molecular Dynamics) ausgewertet.

Der BAC Klon, mit der Sequenz des *THADA* Gens, wurde mit genspezifischen Primern an der „*Canis familiaris* DogBAC library“ (Institute of Animal Genetics, Nutrition and Housing, Universität Bern, Schweiz) detektiert.

Die PCR gescreenten BAC-Klone wurden für das chromosomale Mapping caniner Gene mit Hilfe der Fluoreszenz-*in-situ*-Hybridisierung (FISH) Methode verwendet (siehe 3. Ergebnisse).

2.16 Transfektion rekombinanter Plasmide in eukaryotische Zellen

2.16.1 Fugene HD Transfektion caniner Zelllinien (transient)

Wie im Abschnitt 2.7 wurden eGFP-C1 (Invitrogen) Expressionsvektoren konstruiert, in deren MCS (Multiple Clonining Site) die kodierenden Sequenzen von HMG-GFP Fusionproteine ligiert wurden. Die Transfektion der rekombinanten eGFP-C1-HMG Plasmide erfolgte mit Hilfe der Reagenz Fugene HD (Roche) in canine Zelllinien (z.B. MTH53a) (Protokoll: „FuGENE HD Transfection Reagent 11/2007“). Dazu wurden 2,5x10^4 Zellen in 1 ml 199er Medium (20 % FKS) ausgesät. Zum Ansetzen der Transfektions-Lösung wurden 2 µg Plasmid und 3µl Fugene HD in 100 µl serumfreiem Medium verdünnt. Nach einer Inkubation für 15 min bei Raumtemperatur wurde die Transfektions-Lösung auf die Zellen gegeben und der Ansatz für 72 h (37°C, 5 % CO_2) inkubiert. Die Auswertungen der Transfektionseffizienz und die Lokalisation des GFP Fusionsproteins in der Zelle erfolgten durch Fluoreszenzmikroskopie (Carl Zeiss MicroImaging).

2.16.2 Herstellung rekombinanter AAVs (Adeno-assoziierte Viren)

Nach der Konstruktion rekombinanter *HMGA* antisense pAAV Vektoren (siehe 2.7.) erfolgte eine Kalziumphosphat Transfektion der AAV-293 Zellen (siehe Anleitung des Handbuchs von Stratagene „AAV Helper-Free System instruction manuals, 2004“. Es wurde jeweils das pAAV-LacZ (10 µg) oder die verschiedenen antisense Vektoren pAAV-asHMGA (pro Variante 10 µg) zusammen mit den beiden Virusproteinen kodierenden Plasmiden (je 10 µg) pAAV-Helper und pAAV-RC transfiziert (Tabelle 1.1). Nach 72 h wurden die Viren nach Angaben des Herstellers geerntet und der primäre Stock aufgereinigt (siehe 2.17).

Tabelle 1.1 Konstruktion rekombinanter AAVs

Insert	**Orientierung**	**Rekombinanter pAAV Vektor**	**pAAV-RC**	**pHelper**	**Rekombinanter rAAV Virus-Vektor**
HMGA2 short	*antisense*	*pAAV-asHMGA2short*	+	+	*rAAV-asHMGA2short*
HMGA2 long	*antisense*	*pAAV-asHMGA2long*	+	+	*rAAV-asHMGA2long*
HMGA1 short	*antisense*	*pAAV-asHMGA1short*	+	+	*rAAV-asHMGA1short*
HMGA1 long	*antisense*	*pAAV-asHMGA1long*	+	+	*rAAV-asHMGA1long*
LacZ ORF	*sense*	*pAAV-LacZ*	+	+	*rAAV-LacZ*

(Modifiziert nach Pöhler 2006; Bünger 2007)

2.17Aufreinigung des primären AAV Stocks

Die AAV-293 Zellen wurden mit pAAV-asHMGA1 short, pAAV-asHMGA2short sowie mit den langen *HMGA* (Insert > 1000 bp) antisense Plasmiden pAAV-asHMGA1long und pAAV-asHMGA2long wie in Abschnitt 1.16.2 transfiziert. Die konstruierten AAVs enthalten *HMGA1* oder *HMGA2* in langer oder kurzer Variante in antisense Orientierung, sowie das *β-Galactosidase* Gen (rAAV-LacZ) in sense Orientierung. Die hergestellten Viren wurden sowohl mit ViraKit (Virapur) Filtrationseinheiten und mit ViraTrap Heparin-Agarose-Säulen (Omega Bio-Tek) aufgereinigt.

2.17.1 ViraKit AAV Aufreinigung

Die transfizierten AAV-293 Zellen wurden nach 72 h Inkubation wie im Abschnitt „Preparing Viral Stocks“ des Handbuchs „AAV Helper-Free System instruction manuals, 2004“ von Stratagene geerntet und aufbereitet. Konfluente Zellen von zwölf 75 cm^2 Kulturflaschen wurden abgeschabt und in 50 ml Zentrifugationsröhrchen überführt. Diese Zellsuspension bildete den primären AAV Stock. Im weiteren Verlauf wurden die Zellen durch mehrmalige Ethanol/Trockeneis- und 37°C Wasserbad-Inkubationen aufgeschlossen („Freeze & Thaw“). Dadurch wurden die rekombinanten AAVs aus den Zellen freigesetzt. Nach einer Zentrifugation (3500 rpm, 30 min) wurde der Überstand mit DNaseI (10 u/ml) bei 37°C, für 30 min inkubiert. Mit Hilfe der Filtrationseinheiten wurde der Überstand aufgereinigt (Protokoll: „ViraKit AAV – Instruction Booklet for Purification Kit, 2005“, Seiten 6 bis 9). Das Virus Eluat konnte für 4 Wochen bei 4°C gelagert werden oder nach Zusatz von Glycerin (10 % v/v) bei -80°C zur permanenten Lagerung eingefroren werden.

2.17.2 ViraTrap Aufreinigung

Nach dem Ablauf der Inkubationszeit zur Herstellung der rekombinanten AAVs wurden die adhärenten Zellen mit 10 ml 1x PBS gewaschen. Anschließend wurden die Zellen von insgesamt 3 bis 4 Zellkulturflaschen abgeschabt und in einem 50 ml Röhrchen gesammelt. Nach einer Zentrifugation (3500 rpm, 15 min) wurde das Pellet in 3 ml ViraTrap-Binding-Puffer resuspensiert und nach Zugabe von 3 µl ViraTrap-Nuclease (Benzoase 25 u/µl) bei 37°C für 1h im Schüttelschrank (≤ 300 rpm) lysiert. Die weitere Aufreinigung erfolgte nach dem Protokoll des Herstellers „ViraTrap AAV (AAV2) Purification Kit“ über vorgefertigte Heparin-Agarose Säulen. Das aufgereinigte Virus-Eluat konnte für längere oder kürzere Zeit gelagert werden (siehe 2.17.1)

2.18 Funktionstest und Titerbestimmung der rAAV-LacZ

Die Funktionalität und Infektiösität der konstruierten rAAVs wurden mit Hilfe des Kontroll- und Titer-Virus rAAV-LacZ getestet. HT1080 Zellen ($3x10^5$ Zellen) wurden in 12well Mikrotiterplatten ausgesät (“AAV Helper-Free System Instruction Manual, 2004” (Stratagene), Seiten 32 bis 34). Sowohl der Titer des LacZ-Virus des Primär-Stocks, als auch des aufgereinigten Virus (siehe 2.17) wurde nach dem Protokoll des AAV Helper-Free System Handbuchs „Viral Titer Meassurement of Recombinant pAAV-LacZ-AAV“, Seiten 36 bis 37 bestimmt. Nach einer Infektion und 24 h langer Inkubation der HT1080 Zellen mit rAAV-LacZ wurden die Zellen wie auf Seite 3 “Staining transfected cells in a tissue culture dish” des “*In Situ* β-Galactosidase Staining Kit Protokolls (Stratagene) beschrieben, behandelt. Die Inkubation der Staining-Solution erfolgte für 12 h bei 37°C und 5 % CO_2. Abschließend erfolgte die Auswertung am Lichtmikroskop.

2.19 Infektion der CT1258 Zellen mit rAAVs und Proliferationstest

Die canine Prostatakarzinom-Zelllinie CT1258 wurde mit rekombinanten AAVs infiziert, die entweder den *β-Galactosidase* ORF in sense oder *HMGA1* und *HMGA2* Transkripte in antisense Orientierung exprimieren. Die Auswirkung einer rAAVs Infektion auf das Proliferationsverhalten der CT1258 Zellen wurde mit dem Kit „Cell Proliferation ELISA, BrdU Kit (colorimetric), Instruction Manual 11/04“ (Roche) gemessen. Es wurden $2{,}5 \times 10^3$ Zellen pro Well in 96-well Mikrotiterplatten ausgesät (200 µl Medium 199, 10 % FKS). Nach 2h wurden rAAV-Lösungen verschiedener Konzentrationen von Virusgenomen pro Zelle (vg/Z) in die einzelnen Wells hinzugegeben. Es wurden acht Wells pro Virus-Art, Kombination und Konzentration pipettiert, auf jeweils zwei unterschiedlichen 96-well Platten. Kreuzkontaminationen konnten vermieden werden, indem alle Experimente auf separaten Platten durchgeführt wurden. Als Kontrolle diente der Lösungspuffer ohne Virus. Nach einer Inkubationszeit von ca. 60 h (37°C, 5 % CO_2) wurden 20 µl BrdU Lösung (Roche) in die jeweiligen Wells hinzu gegeben. Nach einer weiteren 12 h Inkubation erfolgte die Auswertung des Proliferationstests („Cell Proliferation ELISA, BrdU Kit (colorimetric), Instruction Manual 11/04“ (Roche), Seiten 13 bis 14) beschrieben. Die Messung der Absorption erfolgte bei 370 nm / 492 nm im Synergy HT Multiplate Reader (BIO-TEK) alle 5 min, für insgesamt 30 min.

2.20 Statistik

Die statistischen Analysen wurden mit Hilfe eines einfachen ANOVA Test durchgeführt. Dabei wurde die GraphPad Prism Software (GraphPad) verwendet. Zur Darstellung der Signifikanz wurde der p-Wert berechnet. Lagen die Werte
$\leq$ 1 %, wurde die Nullhypothese verworfen und die Ergebnisse wurden als signifikant bewertet.

3. Ergebnisse

3.1 Strukturelle und funktionelle Analyse des caninen HMGA1

Dieser Abschnitt beinhaltet die molekulargenetische Charakterisierung der caninen *HMGA* Gene. Mit Hilfe einer rekombinanten *HMGA* antisense AAV Applikation, an einer spontan immortalisierten, caninen Prostata-Adenokarzinom-Zelllinie, sollen neue therapeutische Ansätze zur Inhibierung der endogenen *HMGA* Expression etabliert werden.

3.1.1 The canine *HMGA1*

I. Murua Escobar et al., Gene 2004

Die humanen mRNA Sequenzen des architektonischen Transkriptionsfaktors *HMGA1* bildeten die Grundlage für die Charakterisierung der orthologen caninen *HMGA1* Transkripte. Es wurden von zwölf verschiedenen Hunderassen die Gesamt-RNA aus Testis-Gewebe Proben isoliert. Die isolierten caninen RNAs wurden als Template (Matrize) für eine 3'RACE cDNA Synthese mit einem poly-T-Adapter Primer eingesetzt. Mit Hilfe der humanen *HMGA1* Sequenz wurden Primer für eine PCR hergestellt, die es ermöglichten den gesamten ORF der caninen Sequenz zu amplifizieren, zu klonieren und zu sequenzieren. Nach der Sequenzierung der caninen HMGA1 Amplikons wurden vergleichende Similaritäts- und Homologie-Studien durchgeführt.

Das gesamte canine *HMGA1* Transkript besteht aus sieben verschiedenen Exons. Im Gegensatz dazu besitzt das humane Transkript acht Exons. Wie auch bei der humanen mRNA sind beide *HMGA1* Spleiß-Varianten vorhanden. Das canine *HMGA1a* besitzt 1836 bp und das *HMGA1b* 1803 bp. Die charakteristischen 33 bp langen „gaps" der *HMGA1* mRNA, die Deletionen darstellen, sind ebenfalls in der *HMGA1b* mRNA des Hundes nachweisbar. In beiden Spezies sind diese stark konserviert. Die Homologie der vollständigen caninen *HMGA1a* und *HMGA1b* mRNAs zu den humanen *HMGA1* Transkripten zeigt einen Homologie SI Wert von 80,6 %. Unterteilt man den gesamten caninen *HMGA1* ORF in die Regionen 5'UTR, CDS und 3'UTR, betragen die Homologie SI Werte 95,6 %, 95,1 % und 74,7 %. Das canine HMGA1a Protein (11,7 kDa) setzt sich aus 107 Aminosäuren

zusammen. Das canine HMGA1b Protein (10,7 kDa) besteht aus 96 Aminosäuren. Die Aminosäure Sequenzen der HMGA1 Proteine beider Spezies sind identisch. Ebenfalls wurden die kodierenden Sequenzen (CDS) von *HMGA1a* und *HMGA1b* von zwölf unterschiedlichen Hunderassen sequenziert und auf mögliche SNPs (Single Nucleotide Polymorphisms) untersucht. In 11 von 12 Rassen sind die HMGA1 Transkripte identisch oder weisen synonyme Basenpaarsubstitutionen auf. Die canine cDNA-Sequenz von *HMGA1b* eines Teckels wies einen SNP auf, der zur Missense-Mutation innerhalb der kodierenden Region im 7. (6.) Exon führte (geänderte Exon-Nummerierung, siehe 3.1.2). Diese Punktmutation wurde exklusiv für die Spleiß-Variante *HMGA1b* beschrieben, denn *HMGA1a* zeigte keine Basenpaarsubstitutionen. Dieses Ergebnis lässt auf eine Heterozygotie beider Allele schließen.

Die HMGA1 Expressionsanalysen an verschieden Gewebeproben zeigten auf, dass das Gen in allen Geweben exprimiert wird. Allerdings zeigten sich im Vergleich zur endogenen Kontrolle *GAPDH* nur schwache Signale.

3.1.2 "Best friends" sharing the *HMGA1* gene: comparison of the human and canine *HMGA1* to orthologous other species.

II. Murua Escobar et al., J Hered. 2005

Die Charakterisierung der caninen HMGA1 Gene und Proteine und ihr Vergleich zu acht weiteren Spezies konnte aufzeigen, dass humane und canine HMGA1 Proteine zu 100 % identisch sind. Es wurden die caninen mRNAs und Protein Sequenzen des Hundes und des Menschen mit denen der anderen Spezies verglichen.

Zudem wurden die verschiedenen *HMGA1* Transkripte aus der NCBI Datenbank in einer Übersichts-Darstellung verglichen. Nur der Hund besitzt eine *HMGA1* Exon Anzahl und Anordnung, die zur humanen Transkript-Organisation identisch ist. Der Mensch besitzt insgesamt sieben verschiedene *HMGA1* Spleißvarianten mit unterschiedlichen Exonkombinationen, die beim Hund fehlen. Die Homologie SIs der caninen *HMGA1* CDS im Vergleich zu den anderen Spezies variiert zwischen 72 % (Huhn) und 95,7 % (Pferd und Schwein). Die abgeleiteten Aminosäure Sequenzen der caninen Proteine variieren zwischen 67,7 % (Huhn) und Rind (99%). Alle untersuchten Spezies weisen die *HMGA1a* und *HMGA1b* Isoformen, den 33 bp Gap und die vier Exons der kodierenden Sequenz auf. Die AT-Hooks von HMGA1 sind bei den untersuchten Spezies hoch konserviert.

3.1.3 Genomic characterisation, chromosomal assignment and in vivo localisation of the canine High Mobility Group A1 (*HMGA1*) gene

III. Beuing et al., BMC Genet. 2008

Das Ziel dieser Arbeit war die vollständige Charakterisierung des caninen *HMGA1* Gens. Dabei konnte die genomische Organisation, einschließlich der Grenzen und Längen der Exons und Introns des caninen *HMGA1,* bestimmt werden. Die genomische Struktur des caninen *HMGA1* Gens kann für vergleichende Analysen homologer *HMGA1* Sequenzen des Menschen herangezogen werden. Vergleichende Gen-Analysen können zu wichtigen Erkenntnissen in der Tumorforschung beitragen, da sie auf evolutionär-konservierte Gen- und Protein-Strukturen bzw. -Funktionen hinweisen.

Der Genort des caninen *HMGA1* konnte mit Hilfe einer BAC Sonde und der FISH Methode auf dem caninen Chromosom (CFA) 12 lokalisiert werden. Zudem konnten umfangreiche *in silico* Analysen mit Hilfe des vollständig sequenzierten Genoms des Hundes große Bereiche des caninem *HMGA1* dem CFA 12 zugeordnet werden. Das canine *HMGA1* Gen besteht insgesamt aus sieben Exons und sechs Introns und umspannt eine Sequenzlänge von 9524 bp. Die vergleichenden Homologie SI Werte und Ähnlichkeiten zwischen den humanen und caninen *HMGA1* Genen betrugen insgesamt 62,8 %. Im Detail lagen die Homologie SI Werte der Exons beider Spezies zwischen 74,6 % und 97,8 % und die der Introns zwischen 58,9 % und 92,4 %. Es konnte bei den vergleichenden *in silico* Analysen des *HMGA1* aufgezeigt werden, dass der Hund und die Maus kein Exon 4 besitzt. Dadurch ist ein Unterschied beider Spezies in Bezug zur Struktur und Funktion der 5'UTR der mRNA erkennbar. Es wurde deshalb in dieser Arbeit empfohlen die Nomenklatur der caninen Exons und Introns, die bereits in einer vorherigen Publikation (siehe 3.1.1) beschrieben wurde, zu ändern bzw. zu ergänzen. Exon 5 wird folglich als Exon 4 bezeichnet. Aufgrund des sehr hohen GC Gehaltes und. einer Vielzahl von „Repeats" konnten nur 311 bp des caninen Introns 2 sequenziert und beschrieben werden.

Die Transfektion eines HMGA1a-GFP Expressionsvektors in canine MTH53a Zellen konnte aufzeigen, dass das Fusionsprotein innerhalb des Zellkerns lokalisiert

ist. Wie auch bei dem humanen HMGA1 Protein, lässt sich daher auch für das canine HMGA1 eine Funktion als architektonischer Transkriptionsfaktor ableiten.
Wie bereits in 3.1 beschrieben, wurde bei einer Teckel Probe eine Transition in Folge einer Punktmutation beschrieben. Diese liegt innerhalb der CDS von *HMGA1* und führt zu einem Aminosäureaustausch im Protein. Diese Punktmutation wurde bei 55 Teckeln mit Hilfe eines PCR-Screenings analysiert, um zu klären, ob sich diese Transition innerhalb einer Population manifestiert hat. Es wurden allerdings keine weiteren Punktmutationen innerhalb dieser Teckel Population gefunden.

3.1.4 Expression of the high mobility group A1 (*HMGA1*) and A2 (*HMGA2*) in canine lymphoma: Analysis of 23 cases and comparison to control cases

VI Joetzke et al., Vet Comp Oncol 2010

Die Expression von *HMGA* Genen in caninen hämatopoetischen Tumoren wurde bisher nicht untersucht. In dieser Studie wurden von 23 an Non-Hodgkin Lymphomen erkrankten Hunden und 4 gesunden Hunden Lymphknoten Gewebe gesammelt. Nach der RNA Isolierung wurde die cDNA synthetisiert. Es wurden 19 multizentrische und 4 intestinale B- und T-Zell-Lymphome auf die Gen-Expression von *HMGA1* und *HMGA2* untersucht. Bei multizentrischen Lymphomen sind unterschiedliche Organe betroffen, wie z.B. Lymphknoten, Leber und Milz.
Im Rahmen dieser Arbeit wurde zur relativen Quantifizierung der HMGA1 und HMGA2 Transkripte eine quantitative Real-time PCR etabliert. Als endogene Amplifikations-Kontrolle diente die Expression des Haushalts-Gen *β-Glucuronidase* (*GUSB*). In 15 caninen B-Zell Lymphom Proben wurde eine 4,79-fache bis 12,14-fache Überexpression für das *HMGA1* Gen im Vergleich zum endogenen *GUSB* Gens gemessen. Dagegen war in 3 caninen T-Zell Lymphomen eine nur gering erhöhte *HMGA1* Expression nachzuweisen (1,09- bis 1,53-fach).
Die relativen Expressionsraten von *HMGA1* Transkripten innerhalb der multizentrischen Lymphome waren, im Vergleich zu der gesunden Kontrollgruppe, nur gering erhöht (0,94- bis 1,0-fach). Im Gegensatz zur *HMGA1* Expression wurde eine 21,98-fache bis 317,66-fache Überexpression in den T-Zell Lymphomen und bei den B-Zell Lyphomen eine geringe *HMGA2* Expression (0,03- bis 5,33-fach) gemessen.

3.1.5 Establishing an *in vivo* model of canine prostate carcinoma using the new cell line CT1258

IV. Fork et al., BMC Cancer. 2008

In vitro Studien an Zelllinien sind unerlässlich zur Untersuchung der Tumorentstehung in der Prostata. Bisher gab es nur wenige geeignete canine Zelllinien von Prostata-Tumoren, die für Fragestellungen in Bezug zur Pathogenese von Prostata-Tumoren genutzt werden konnten. In dieser Arbeit wurde die canine, spontan immortalisierte Zelllinie CT1258 subkutan und intraperitoneal in 19 immundefiziente NOD-Scid Mäusen injiziert. Dieses Experiment sollte aufzeigen, ob die Zelllinie CT1258 *in vivo* die gleichen Charakteristika in Bezug zur Tumorgenese, Histologie und Metastasierung aufweist, wie das ursprüngliche canine maligne Prostata-Adenokarziom.

Die untersuchten Tumoren bestanden aus einer heterogenen Zell-Population. Die Zellen zeichneten sich durch zahlreiche strukturell unterschiedliche Mitosen aus. Dabei variierte die Form und Größe des Zellkerns (Anisokaryose) oder die Anzahl von verschieden großen Zellkernen (Anisozytosen). Ein ähnlicher histologischer Befund wurde auch für die intraperitonal induzierten Tumore aufgezeigt. Insgesamt führte die Injektion von CT1258 zu einer massiven Penetration des entstehenden Tumors innerhalb der Bauchhöhle und des Mesenteriums mit ausgeprägter Aszites. Jedoch konnten keine Metastasierungen in den umliegenden Geweben entdeckt werden. In beiden Gruppen von induzierten Tumoren wurden die gleichen Zytogenetischen Marker detektiert wie im Ursprungs-Tumor. Für die *in vivo* Applikation der Zelllinie CT1258 wurde der gleiche histologische, zytologische und zytogenetische Befund erbracht wie zuvor beim ursprünglichen Adenokarziom. Aufgrund dessen eignet sich die Zelllinie CT1258 als Modell für die Erforschung der molekularen Mechanismen zur Pathogenese caniner Prostata-Karzinome.

3.1.6 Application of antisense *HMGA* AAVs suppresses cell proliferation in a canine carcinoma cell line

V Soller et al., in Vorbereitung 2010; (fertiges Manuskript)

In dieser Arbeit wurde ein gentherapeutischer Ansatz entwickelt, der mit Hilfe von Adenoassoziierten Viren (AAV) Vektorkonstrukte in CT1258 Zellen einbringt, welche verschiedene Konstrukte von HMGA antisense mRNAs transkribieren. Es wurde die canine Prostatakarzinom-Zelllinie CT1258 (siehe 3.3.4) verwendet, die die Gene *HMGA1a/b* und *HMGA2* stark exprimierten. Mit Hilfe der *HMGA* antisense Vektoren sollte eine Überexpression der sense *HMGA* mRNA in den CT1258 Zellen inhibiert werden. Der Effekt auf das Proliferationsverhalten der transduzierten CT1258 Zellen wurde anschließend untersucht. Zwei verschiedene antisense *HMGA1* und antisense *HMGA2* AAV Vektor-Varianten wurden konstruiert. Parallel wurde ein Kontroll-Virus eingesetzt, welches den ORF des *β-Galactosidase* Gens kodiert. Die Genome der verschiedenen AAV Vektoren (siehe Tabelle 1.1) kodieren entweder kurze („short“) Varianten der *HMGA* mRNA (rAAV-asHMGA1short und rAAV-asHMGA2short) oder lange („long“) Varianten der *HMGA* mRNAs (rAAV-asHMGA1long und rAAV-asHMGA2long). Die kurzen Varianten exprimieren die CDS von *HMGA* in antisense Richtung. Die langen Varianten exprimieren zusätzlich zu der kodierenden Sequenz große Teile der 3'UTR der *HMGA* mRNAs in antisense Orientierung. Das Proliferationsverhalten der CT1258 Zellen wurde nach einer Infektion mit den verschiedenen rAAVasHMGA Varianten und Kombinationen (rAAV-asHMGA1 und rAAV-asHMGA2) ausgewertet. Hierzu wurde mit Hilfe eines Immunoassays der Einbau des Basenanalogon BrdU (Bromdesoxyuridin) in die DNA der Zellen während der S-Phase gemessen. Es konnte gezeigt werden, dass Infektionen mit rAAV-asHMGA Vektoren nach 72h, im Vergleich zur nicht behandelten Kontrolle, zur Proliferationabnahme in der CT1258 Zell-Population führen. Mit steigendem Virustiter nimmt die Proliferation im Vergleich zur unbehandelten Kontrolle stetig ab. Diese Abnahme wird besonders bei den antisense HMGA1 AAV Varianten deutlich. Eine Infektion der CT1258 Zellen mit $1x10^4$ vg/Zelle und $1{,}5x10^4$ vg/Zelle rAAV-asHMGA1short Viren, führt zu einer Proliferationabnahme von 21,6 % (von 55,9 % auf 34,3 %). Eine Infektion mit der gleichen Menge von rAAV-asHMGA1long verringerte die Proliferation um 34,6 % (von 35,4 % auf 0,8 %).

Ebenfalls zeigte sich ein deutlicher Effekt auf die Abnahme der Proliferation der CT1258 Zellen durch eine Kombination beider antisense *HMGA1* und *HMGA2* AAV Vektoren. Eine Infektion mit $1{,}5x10^4$ vg/Zelle rAAV-LacZ Viren führte ebenfalls zu einem leichten Proliferationsrückgang von CT1258.
Somit wurde gezeigt, dass eine Applikation von AAV Vektoren, die *HMGA* mRNA in antisense Orientierung exprimieren, zur Verringerung der Proliferation in caninen CT1258 Zellen führt.

3.1.7 Co-transfection of plasmid DNA and laser-generated gold nanoparticles does not disturb the bioactivity of GFP-HMGB1 fusion protein.

XV Petersen et al., J Nanobiotechnology 2009

Lasergenerierte AuNPs (AG „JRG Nanoparticles, Research Cluster of Excellence Rebirth“ vom Laserzentrum Hannover e.V.) besitzen eine große Anzahl an positiven Ladungen bzw. eine hohe Elektronen-Akzeptanz. Aufgrund dieser Eigenschaft wurde die Interaktion von AuNPs mit einem Expressionsvektor analysiert, um festzustellen, ob AuNPs die biochemische Funktionalität von Biomolekülen verändern.
Der canine Expressionsvektor eGFP-C1-HMGB1 kodiert für ein rekombinantes GFP-HMGB1 Fusionsprotein. Es wurden jeweils 250 ng AuNP mit 1 µg eGFP-C1-HMGB1 Vektor-DNA für 24h Raumtemperatur in wässriger Lösung inkubiert. Dabei wurden vier verschiedene AuNPs-Suspensionen eingesetzt, deren Nanopartikel unterschiedliche hydrodynamische Durchmesser besaßen (d_h = 14 bis 89 nm). Nach Ablauf der Inkubationszeit wurden die unterschiedlichen AuNPs/DNA Lösungen, zusammen mit einem Transfektionsreagenz (FugeneHD, Fa Roche), in die canine MTH53a Zelllinie transfiziert. Nach 48h wurden die transfizierten Zellen mit Hilfe eines Fluoreszenz-Mikroskops ausgewertet. In allen untersuchten Ansätzen konnte erfolgreich nachgewiesen werden, dass die biologischen Eigenschaften des GFP-HMGB1 Fusionsproteins nicht durch lasergenerierte AuNPs beeinträchtigt wurden. Zudem wurde beobachtet, dass eine Inkubation mit den mittleren Au-NPs der Größen d_h = 24 nm und 59 nm die

Transfektionseffizienz des eGFP-C1-HMGB1 Vektors, im Vergleich zur Kontrolle ohne AuNPs, um 30 bis 50 % erhöht.

3.2 Die molekulargenetische Charakterisierung des caninen RAGE (Receptor for Advanced Glycation End Products)

Im vorherigen Kapitel wurde ein therapeutischer Ansatz zur Inhibierung der HMGA Expression in Tumorzellen sowie die genomische Charakterisierung des caninen *HMGA1* als Tumormarker vorgestellt. Im Folgenden Abschnitt wurde untersucht, inwiefern sich, ausgehend vom Primärtumor, Rückschlüsse auf die molekularen Mechanismen der Metastasierung gezogen werden können. Dazu wurden die genomische Struktur und die Expression des caninen *RAGE* Gens untersucht.

Der Rezeptor für „Advanced Glycation End Products" RAGE (syn. AGER) ist ein Multiligand-Rezeptor, der auf der Zellmembran lokalisiert ist. Der Rezeptor interagiert unter anderem mit HMGB1. Als Ligand-Rezeptor-Komplex reguliert RAGE/HMGB1 Stoffwechselwege, die in einer Signalkaskade Zell-Wachstum und -Proliferation initiieren. Bei einer Vielzahl von Erkrankungen wird die RAGE-HMGB1 (Rezeptor-Ligand) Interaktion eine Schlüsselrolle in der Pathogenese zugeschrieben, wie z.B. der Alzheimer Krankheit, Diabetes, der Tumorangiogenese und Metastasierung.

3.2.1 Cloning and characterization of the canine receptor for advanced glycation end products

VII Murua Escobar & Soller et al., Gene 2006

Zur Charakterisierung des caninen *RAGE* Gens wurde aus caninem Lungengewebe die Gesamt-RNA isoliert. Diese wurde in eine 5' RACE und 3'RACE cDNA Synthese Reaktion eingesetzt und diente anschließend als Templates in verschiedenen PCRs mit Hilfe genspezifischer Primer. Die anschließend klonierten und sequenzierten PCR-Produkte wurden in einem Alignment zu einem Contig zusammengesetzt. Der gesamte ORF des caninen *RAGE* mit 1384 bp konnte konstruiert werden. Die *RAGE* cDNA Sequenz bildete die Grundlage für weitere PCRs zur Aufklärung der vollständigen Exon/Intron Organisation mit insgesamt 11 Exons und 2835 bp. Die Größe der Exons variiert zwischen 27 bp und 254 bp. Die Introns haben eine Länge von 94 bp bis 268 bp.

Die canine *RAGE* mRNA besitzt eine 5'UTR von 18 bp und eine CDS von 1215 bp. Die 3'UTR hat eine Länge von 151 bp und der Homologie-SI Wert der gesamten cDNA zwischen Mensch und Hund beträgt 80,9 %, während die CDS eine Sequenzhomologie von 82,9 % aufweist. Das abgeleitete canine Protein weist eine Übereinstimmung von 77,6 % zwischen beiden Spezies auf. Im Detail die SI-Werte zwischen Mensch und Hund in den funktionellen Domänen von RAGE: Extrazelluläre Domäne 78,2 %, Transmembran Domäne 78,9 % und die Cytosol Domäne 72,7 %. Im Northern Blot mit Gesamt-RNA aus verschiedenen caninen Geweben (Testis, Herz, Lunge, Muskel, Niere, Pankreas, Milz und Leber) konnte ausschließlich eine 1,4 kb große Bande in der Lungenprobe detektiert werden. Diese Expressionsmuster ist homolog zum humanen *RAGE.* Zur Lokalisation bzw. zum Mapping des *RAGE* Gens im caninen Genom wurde eine DNA Sonde auf den caninen RPCI 81 BAC/PAC Filter hybridsiert. Der BAC 339-J10 Klon wurde identifiziert. Ein Teil der BAC-DNA wurde mit Hilfe einer PCR amplifiziert und anschließend durch eine Sequenzierung verifiziert. Die BAC DNA wurde in einem FISH Experiment verwendet, um das canine *RAGE* Gen auf CFA 12 zu lokalisieren.

3.2.2 Cloning, characterisation and comparative quantitative expression analysis of receptor for advanced glycation end products

VIII Sterenczak et al., Gene. 2009

Beim Menschen konnten bisher 19 verschiedene *RAGE* Spleiß-Varianten charakterisiert werden. Eine charakterisierte Spleißvariante kodiert für die sRAGE Protein Variante („solubles" RAGE), deren carboxy-terminales Ende trunkiert ist und dadurch nicht in der Zellmembran verankert ist. Dennoch kann sie mit extrazellulären Liganden interagieren.

In dieser Arbeit wurde aus 17 caninen Tumoren, 7 verschiedenen gesunden Gewebeproben (u.a. aus Milz, Leber, Pankreas) und aus 4 caninen und 3 humanen Zelllinien die RNA isoliert. Insgesamt wurden 24 canine und 6 humane *RAGE* Transkripte gefunden. Diese kodieren für 16 verschiedene canine und 5 humane Spleiß-Varianten. Von diesen Transkripten wurden 14 verschiedene canine und 4 verschiedene humane *RAGE* Varianten neu beschrieben.

Demnach lassen sich die *RAGE* Transkripte in zwei verschiedene Gruppen aufteilen:

Die erste Gruppe besteht aus *RAGE* Transkripten, die den vollständigen ORF oder die solublen sRAGE Proteine kodieren. Die zweite Gruppe besteht aus Transkripten, die durch alternatives Exons/Intron Spleißen und Intron Insertionen charakterisiert sind und zu „non-sense“ Proteinen translatiert werden. In dieser Gruppe fällt im Besonderen eine *RAGE*-Variante mit einer Intron 1 Insertion (Intron 1 Variante) auf, die sich sowohl in normalen Geweben als auch im Tumoren detektieren lässt.
Real-time PCR Experimente konnten aufgezeigen, dass in gesunden Lungen-, Hoden- und Schilddrüsengeweben überwiegend die komplette oder soluble *RAGE* Varianten exprimiert werden. In Tumoren wird dagegen überwiegend die Intron 1 Variante von *RAGE* exprimiert.

3.3 SNP Screening und Homologie Analysen caniner Zytokine

Ein weiterer Faktor der zur Entstehung invasiver Tumoren führen kann ist die durch die neoplastische Erkrankung bedingte Einleitung einer Inflammation (tumor-induzierte Inflamation) in umliegenden Geweben. Eine unkontrollierte Inflammation kann aber auch selbst der Auslöser einer malignen Transformation sein (inflammations-induzierter Tumor). Ein Mechanismus zur Tumorenstehung, oder Proliferation bereits vorhandener neoplastischer Gewebe, ist eine Überexpression von Zytokinen, die durch Zellen des Immunsystems während der Inflammation sezerniert werden. Die Zytokine fördern weitere Zellteilungen und die Bildung von neuen Blutgefäßen (Neoangiogenese).
Die Zytokine Interleukin-1 (IL-1α und IL-1β) und der Tumor-Nekrose-Faktor-α (TNFα) werden von Monozyten und Makrophagen sezerniert. Sie spielen eine wichtige Rolle in der Signal-Transduktion zur Einleitung von Entzündungsreaktion und Immunantworten des Körpers. Eine erhöhte Sezernierung von IL-1α, IL-1β und TNFα wird bei vielen Krankheiten des Menschen und des Hundes beobachtet, wie z.B. Tumor-, Autoimmun-, Alzheimer- und Parkinson-Erkrankungen sowie Sepsis.

3.3.1 Comparison of the human and canine IL-1 (α/β) and TNFα to orthologous other mammalians

X Soller et al., J Hered. 2007

In dieser Arbeit wurden die humanen und caninen Nukleotid- und Aminosäuresequenzen IL-1 (IL-1α und IL1-β) und TNFα mit den bekannten Sequenzen anderer Säugetieren, wie z.B.mit denen der Maus, der Ratte, der Katze, des Schweins, des Rindes, des Pferdes und des Schafs, verglichen.

Vergleichende Sequenz-Analysen, d.h. die Berechnung der Homologie SIs, wurden erstellt und die Homologien und evolutionär-konservierte Regionen der Zytokine des Hundes, des Menschen und weiterer Säugetiere in einer Gesamtübersicht dargestellt. Die genomische Organisation, d.h. die Länge und die Anzahl der Exons der beschriebenen Zytokine variiert nur bedingt. Während bei allen untersuchten Säugetieren *IL-1* aus sieben Exons besteht, setzt sich das *TNFα* Transkript aus vier Exons zusammen. Es werden Abweichungen in der Anzahl der Nukleotide der einzelnen Exons zwischen den Arten beobachtet, die sich in unterschiedlichen Längen der kodierenden Sequenzen zeigen. Die vergleichenden Homologie SI der beschriebenen Zytokin CDS in Bezug zum Hund liegen zwischen 43,9 % (Maus, *IL-1β*) und 93,43 % (Katze, *TNFα*). Bei den Proteinen liegen die Werte zwischen 57,1 % (Maus, IL-1β) bis 94,4 % (Katze, TNFα). Auf der Ebene der funktionellen Domänen und Regionen der Proteine von IL-1 und TNFα besteht eine evolutionär-konservierte Homologie innerhalb der Säugetier-Ordnungen. So zeigt sich, dass z.B. die Calpain Erkennungssequenz von IL-1α bei allen Säugetieren stark konserviert ist. Des Weiteren wurden in dieser Arbeit die Nukleotid-Sequenzen der caninen Zytokine *IL-1* (*IL-1α* und *IL-1β*) und *TNFα* vollständig charakterisiert. Die Charakterisierung caniner Zytokine und die vergleichenden Homologie-Analysen innerhalb der Säugetiere zur Darstellung evolutionär-konservierter Gen- und Protein-Regionen, ermöglichen neue Strategien für experimentelle und therapeutische Ansätze.

3.3.2 Cytokine Genes Single Nucleotide Polymorphism (SNP) Screening Analyses in Canine Malignant Histiocytosis

IX Soller et al., Anticancer Res. 2006

Der Hund als Modeltier in der Tumorforschung kann hier zur Erforschung der malignen Histiozytose beitragen, weil der Berner Sennenhund (BSH) eine Rassendisposition für diese Erkrankung aufweist. In dieser Arbeit wurden von 17 verschieden Hunden (15 BSHs, ein Collie und ein West Highland Terrier) Gewebeproben der Lunge, Milz, Testis und der Haut gesammelt. Nach der RNA Isolierung folgte die cDNAs Synthese für die Zytokin Transkripte *TNF α*, *Interleukin-1-α (IL-1α)* und *Interleukin-1-β (IL-1)*. Es erfolgte eine PCR, anschließend wurden die Amplikons in pGEM-T Easy Vektoren kloniert, sequenziert und auf Single Nucleotide Polymorphisms (SNPs) untersucht. Von insgesamt 17 untersuchten Hunden zeigten 8 Zytokin Transkripte Basenpaarsubstitutionen. Diese führen zu Missense Mutationen innerhalb der Aminosäuresequenz der abgeleiteten Proteine TNFα, IL-1α und IL-1β. Eine BSH Lungenprobe zeigte eine Punktmutation in *TNFα* Exon 4, Codon 113 die zu einem Aminosäureaustausch führt (GAT → GGT, Asp → Gly). Für das *IL-1α* Gen wurde die vollständig kodierende Sequenz (CDS), sowie die alternative Spleiß-Variante *IL-1α Exon 5 del* amplifiziert. Nach einer Sequenzierung der CDS des *IL-1α* Gens konnte eine Punktmutation in Exon 3 Codon 23 (TTC → TCC, Ser → Pro) und Exon 4 Codon 47 (TGC → CGC, Cys → Arg) nachgewiesen werden.

Innerhalb der Isoform von *IL-1α Exon 5 del* wurde bei einem West Highland Terrier eine Punktmutation im Exon 4 Codon 43 (CTT → CCT, Leu → Pro) gefunden. Bei *IL-1β* Transkripten von drei verschiedenen Leberproben wurden Basenpaarsubstitutionen in den caninen Exons gefunden. In zwei Proben (BSH) wurde je eine Punktmution in der CDS von Exon 5 Codon 113 (GAT → GGT, Asp → Gly) bzw. Codon 124 (CAG → AAG, Gln → Lys) entdeckt. Die dritte Probe (BSH) zeigte zwei Basenpaarsubstitutionen die das Exon 7 betreffen: Codon 228 (TCT → CCT, Ser → Pro) und Codon 234 (TAC → CAC, Tyr → His). *In silico* Analysen ergaben, dass die entdeckten Basenpaarsubstitutionen innerhalb der funktionellen Domänen der Zytokine liegen.

3.4 Charakterisierung weiterer caniner Gene

3.4.1 A domain of thyroid adenoma associated gene (THADA) conserved in vertebrates becomes destroyed by chromosomal rearrangements observed in thyroid adenomas

XIII Drieschner et al., Gene 2007

In benignen menschlichen Schilddrüsenadenomen beobachtet man häufig Translokationen in der chromosomalen Region 2p21. Dort wurde das *THADA* Gen (365 kb) mit Hilfe der FISH Analyse lokalisiert. Der Bruchpunkt liegt im Intron 28.
Die CDS der *THADA* Variante 1 kodiert für eine abgeleitete Sequenz von 1953 Aminosäuren. Bis auf die COG5543 Domäne konnten keine bekannten Homologien menschlicher Protein-Domänen oder -Regionen nachgewiesen werden. Es handelt sich hierbei um ein Protein Cluster, das bereits bei Pilzen beschrieben wurde. Die Funktion der COG5543 Domäne (COG: „Cluster of Orthologous Groups“) wurde bisher noch nicht aufgeklärt.
In dieser Arbeit wurden die cDNA Sequenzen des *THADA* Gens des Hundes, des Huhns, der Grünen Meerkatze (Altweltaffen) und der Maus sequenziert und charakterisiert sowie die Aminosäuresequenzen *in silico* abgeleitet.
In der evolutionär am höchsten konservierten Protein-Region aller Spezies wurde eine Ähnlichkeit von 78,6 % aufgezeigt, die der menschlichen THADA Region von 1033 aa bis 1415 aa entspricht. In dieser Region befindet sich bei allen fünf untersuchten Spezies die hochkonservierte COG5543 Domäne. Weitere Strukturen, die bei allen THADA Proteinen der verschiedenen Spezies gefunden wurden, konnten als ARM- Wiederholungsmotive (Arginine Rich Motifs z.B. „Armadillo- und HEAT-Repeats“) identifiziert werden. Diese werden als eine Familie rechtsdrehender Superhelices zusammengefasst. Funktionelle *in silico* Analysen ergaben, dass das THADA Protein eine hohe Homologie zum CAND1 Protein (Cullin-Associated Neddylation-Dissociated Protein 1) aufweist (E-value: 0,00025). CAND Proteine besitzen ebenfalls Abfolgen von ARM Motiven.

3.4.2 Chromosomal assignment of canine THADA gene to CFA 10q25

XIV Soller et al., Mol Cytogenet 2008

Für die Lokalisation des caninen *THADA* Gens wurden, mit Hilfe der ermittelten („predicted“) caninen *THADA* Sequenz aus der NCBI Datenbank, PCR-Primer hergestellt. Die PCR wurde an caniner DNA etabliert, das PCR Fragment kloniert, sequenziert und verifiziert. Mit Hilfe dieser etablierten PCR wurde die „*Canis familiaris* DogBAC library“ (Institute of Animal Genetics, Nutrition and Housing, Universität Bern, Schweiz) auf das Vorhandensein positiver BAC Klone überprüft. Mit einer zweiten semi-nested PCR wurden diese BAC Klone verifiziert. Der Klon „DogBAC library ID S011P24K05RE“ wurde für ein FISH Mapping verwendet. Das canine *THADA* konnte im Genom des Hundes auf dem Chromosom (CFA) 10 lokalisiert werden. Der canine Genlocus auf Chromosom 10 Bande q25 ist homolog zum menschlichen Chromosom 2 Bande p21.

Der Grund für die Lokalisation des caninen *THADA* war die Fragestellung, ob dieses Gen auch durch homologe Translokations Ereignisse bei Schilddrüsenerkrankungen des Hundes betroffen ist. Diese wurden bereits für die Bruchpunktregion auf Chromosom 2 Bande p21 bei menschlichen Schilddrüsenadenomen beschrieben. In dieser Arbeit wurde nachgewiesen, dass für canine Schilddrüsenadenome das *THADA* Gen nicht durch Translokationen betroffen ist. Abschließend ist darauf hinzuweisen, dass bei Hunden im Vergleich zum Menschen bösartige Erkrankungen der Schilddrüse vorherrschen. Es wird eine wesentlich höhere Anzahl an Karzinomen anstatt Adenomen der Schilddrüse beobachtet. Weitere Analysen könnten aufklären, ob das canine *THADA* als Kandidaten-Gen eine wichtige Rolle bei einer malignen Transformation des caninen Schilddrüsenadenoms spielt.

4. Diskussion

Obwohl die Medizin in den vergangenen Jahrzehnten Fortschritte in der Behandlung und Heilung von Tumorerkrankungen zu verzeichnen hat, ist Krebs nach wie vor die Hauptursache aller Todesfälle. Während in den USA die Todesrate an Herzkreislauferkrankungen von 1950 bis 2002 um ca. 40% zurückging, blieb die Anzahl tödlicher Tumorerkrankungen nahezu unverändert (Olson 2007).

Der Hund als Tiermodell kann die bisherigen Forschungen über die genetischen Ursachen der Tumorgenese beim Menschen ergänzen und vervollständigen.

Das Ziel dieser Arbeit ist die strukturelle Charakterisierung und funktionelle Analyse der caninen *HMGA* und weiterer Gene, die auch bei menschlichen Erkrankungen, vor allem in der Tumorgenese eine große Rolle spielen. Im Rahmen des Tiermodells Hund hilft die molekulargenetische Charakterisierung der caninen Gene und Genprodukte die Grundlagen für neue potentielle Therapieansätze zu entwickeln, die zu nützlichen Erkenntnissen in klinischen Studien und zur Entwicklung neuer Medikamente für die Humanmedizin führen.

Die HMGA Proteine sind kleine, chromatin-assoziierte nicht-Histon Proteine, die bei einer Vielzahl von regulativen Prozessen in der Genexpression eine wichtige Rolle als architektonische Transkriptionsfaktoren spielen. Reeves und Beckerbauer beschrieben bereits 2001, dass HMGA Proteine die Transkription von über 45 eukaryotischen und retroviralen Genen regulieren. Sgarra et al. haben in einer umfangreichen elektronischen Datenbank ein molekulares Proteonom Netzwerk beschrieben, welches die bekannten HMGA Partner auflistet. Neben der Transkriptionsregulation sind die nativen HMGA- und post-transkriptional modifizierten Proteine (Phosphorylierung, Methylierung und Acetylierung) in der Organisation des Chromatins, der DNA Reparatur, der RNA Prozessierung, sowie der Interaktion mit anderen Enzymen, wie z.B. p53 beteiligt (Sgarra et al. 2009).

Die „High Mobility Group A“ (HMGA) Familie besteht aus vier Proteinen HMGA1a (11,7 kDa), HMGA1b (10,6 kDa), HMGA1c (19,7 kDa) und HMGA2 (12 kDa). Diese Proteine werden durch zwei verschiedene Gene kodiert, wobei das *HMGA1* Gen durch alternatives Spleißen drei verschiedene Protein-Isoformen kodiert (Reeves & Beckerbauer 2001).

4.1 Das canine HMGA1

Im Jahr 2004 wurde die canine *HMGA1* mRNA Sequenz vollständig sequenziert, die Exon Organisation aufgeklärt sowie mit den humanen und verschiedenen Nagetier *HMGA1* Sequenzen verglichen (Murua Escobar et al. 2004).

Die kodierende Sequenz (CDS) des caninen *HMGA1* zeigt eine Homologie zu den Exons 5 bis 8 der menschlichen CDS auf. Beide Sequenzen sind auf der Ebene der Nukleotidsequenz zu 95,1 % identisch mit der gleichen Anzahl an Basenpaaren für *HMGA1a* mit 324 bp und *HMGA1b* mit 291 bp. Bei allen untersuchten Hunden konnte die 33 bp Deletion von *HMGA1b* homolog zur humanen *HMGA1b* Sequenz nachgewiesen werden. Damit weisen beide Arten dieselbe *HMGA1b* Spleißvariante auf (Murua Escobar et al. 2004).

Neben der Charakterisierung der caninen mRNA wurden die CDS von *HMGA1a/b* von zwölf verschiedenen Hunderassen auf Punktmutationen untersucht. Eine Teckel-Probe zeigte eine Transition (A→G) in Exon 6, Codon 64.. Diese Punktmutation führt zu einer Missense Mutation (Thr→Ala) außerhalb der AT-Hook Domäne von HMGA1. Zur Evalution des gefundenen SNP wurde aus 55 Teckel-Proben gesammelt die Region des Exon 6 amplifiziert. Die darauffolgenden Sequenzierungen zeigten, dass keiner der untersuchten Teckel ein Träger dieser Missense Mutation war. Die zuvor in einer Teckel Probe gefundene Basenpaarsubstitution spielt keine größere Rolle in der *HMGA1* Pathogenese (Beuing et al. 2008).

Ein Vergleich der caninen *HMGA1(a/b)* CDS mit sieben verschiedenen kodierenden Regionen von *HMGA1* anderer Säugetiere ergibt, dass die Sequenzen des Schweins (*Sus scrofa*) und des Pferdes (*Equus caballus*) eine leicht höhere Ähnlichkeit zur caninen *HMGA1* CDS als zu der des Menschen aufweist (Murua Escobar et al. 2005). Die SI-Homologie Werte von Hund zu Schwein, bzw. zum Pferd, zeigt eine Ähnlichkeit von 95,7 %. Die SI-Homologie der caninen *HMGA1* Sequenzen zu denen der Nagetiere liegen zwischen 90,1 % bis 92,6 %.

Die SI-Homologien der caninen *HMGA1* CDS zu Nicht-Säugetieren, wie dem Krallenfrosch (*Xenopus laevis*), liegen bei 90,4 % für *HMGA1a* bzw. dem Huhn (*Gallus gallus*) bei 72,0 % für *HMGA1b* (Murua Escobar et al. 2005). In allen Spezies besteht die mRNA aus vier proteinkodierenden Exons. Des Weiteren existiert bei allen Spezies im ersten kodierenden Exon die spezifische 33 bp

Deletion der *HMGA1b* Spleiß-Variante. Die abgeleiteten Proteinsequenzen besitzen alle 107 Aminosäuren für HMGA1a und 96 Aminosäuren für HMGA1b.

Die Aminosäuresequenzen des Menschen, des Hundes und des Pferdes sind zu 100 % identisch. Trotz höherer Sequenz-Ähnlichkeit auf Nukleotid-Ebene zeigt die Aminosäuresequenz von HMGA1 des Schweins eine SI-Homologie von 99 % zu den humanen und caninen Proteinen. Insgesamt liegt die Sequenzähnlichkeit der abgeleiteten Aminosäuresequenzen von HMGA1a und HMGA1b zwischen 69,7 % (*Gallus gallus*) und 100 % (*Homo sapiens*, *Canis lupus familiaris* und *Equus caballus*). Die SI-Homologie der caninen HMGA1 Proteine zu denen der Nagetiere, wie Maus, Ratte und Hamster liegen zwischen 95,8 % bis 98,1 %. Es zeigt sich, dass die Aminosäuresequenzen der verschiedenen Säugetiere eine höhere Sequenzähnlichkeit zum Krallenfrosch mit 97,2 % aufweisen, als zum Vertreter der evolutionär näher verwandten Vögel, wie dem Huhn mit 69,7 %. Die funktionellen AT-Hooks der HMGA1 Proteine sind evolutionär konserviert, d.h. in diesen Domänen gibt es nur sehr wenige Aminosäure-Austausche zwischen den verschiedenen Arten.

Das canine *HMGA1* Gen besteht aus 7 Exons und 6 Intronsund hat eine Anzahl von insgesamt 9524 Basenpaaren. Die Sequenzähnlichkeit des caninen *HMGA1* zum menschlichen Gen hat eine SI-Homologie von 62,8 %. Die SI-Homologien der einzelnen Exons liegen zwischen 74,6 % und 97,8 %, während die der Introns beider Arten zwischen 58,9 % und 92,4 % liegen. *In silico* Analysen mit Sequenzen aus der NCBI Datenbank (AY366395, NW_876254) und sequenzierten PCR Amplikons des BAC Klons MGA572P20K12RG zeigten, dass das orthologe humane Exon 4 beim Hund fehlt.

Erst im Rahmen der vollständigen Sequenzierung des caninen *HMGA1* Gens wurde festgestellt, dass die veröffentlichte canine mRNA Sequenz (NM_001003387) einer neuen Exon Nummerierung bedarf. Da die canine mRNA Sequenz kein Exon besitzt, welches homolog zum menschlichen Exon 4 ist, wurde die bekannte Bezeichnung der caninen Exons geändert. Das im Jahr 2004 bezeichnete canine *HMGA1* Exon 5 wird seit der Charakterisierung des vollständigen caninen *HMGA1* Gens im Rahmen der numerischen Reihenfolge als Exon 4 bezeichnet. Diese Exon 4 Deletion beim Hund ist ebenfalls für die *Hmga1* Sequenz der Maus charakteristisch. Dadurch sind die Strukturen der 5'UTRs des Hundes und der Maus im Vergleich zur menschlichen Sequenz betroffen (Beuing et al. 2008; Murua Escobar et al. 2004;

Friedmann et al. 1993). Jedoch zeigen NCBI Datenbank-Analysen, dass der Mensch insgesamt 7 verschiedene *HMGA1* Spleißvarianten (SPV) besitzt, die allerdings nur für die Protein Isoformen HMGA1a und HMGA1b kodieren (NCBI 2010a). Die Maus besitzt insgesamt 14 *Hmga1* Spleißvarianten, die für insgesamt fünf (*a* bis *e*) verschiedene Protein Isoformen kodieren (NCBI 2010b). Beim Hund konnten bisher die zwei *HMGA1* Spleißvarianten *HMGA1a* und *HMGA1b* beschrieben werden, die für die entsprechenden Protein Isoformen kodieren und direkt zu den SPV 1 (NM_145899.2) und SPV 2 (NM_002131.3) des Menschen homolog sind.

Das menschliche *HMGA1* Gen ist auf dem Chromosom 6 Bande p21 lokalisiert (Friedmann et al. 1993). Innerhalb dieser chromosomalen Region wurden überwiegend 3'stromabwärts, seltener 5' stromaufwärts des *HMGA1* Genlocus, Bruchpunkte gefunden. Diese führen bei benignen mesenchymalen Tumoren wie z.B. in chondroiden Lungenhamartomen, Polypen der Gebärmutterschleimhaut, Lipomen, Uterus Leiomyomen (Kazmierczak et al. 1998; Kazmierczak et al. 1999; Williams et al. 1997; Tallini et al. 2000) zu chromosomalen Rearrangierungen. Bei 25 % aller chondroiden Lungenhamartomen findet man innerhalb des *HMGA1* Genlocus (Xiao et al. 1997) aberrante Translokationen. Die chromosomalen Aberrationen innerhalb des *HMGA1* Genlocus gehen einher mit einer Überexpression des HMGA1 Proteins in diesen mesenchymalen Tumoren (Reeves et al. 2001). Das canine *HMGA1* Gen befindet sich auf dem Chromosom 12 (Beuing et al. 2008). Diese Region ist aber nur selten ein Ausgangspunkt für chromosomale Rearrangierungen bei caninen Tumoren (Reimann et al. 1999; Thomas et al. 2007), so dass chromosomale Aberrationen, die den Genlocus des caninen *HMGA1* betreffen, für die Pathogenese caniner Neoplasien nur eine untergeordnete Rolle spielen.

Eine Vielzahl von malignen epithelialen Tumoren ist durch eine Überexpression von *HMGA1* charakterisiert, die nicht als Ursache von chromosomalen Translokationen innerhalb des Gens oder des Promotors erklärt werden können. Eine Überexpression von *HMGA1* wurde in humanen Karzinomen des Pankreas, des Gebärmutterhalses, des Dickdarms, der Schilddrüse, der Leber und der Prostata beobachtet (Abe et al. 2000; Mellone et al. 2008; Huang et al. 2009; Chiappetta et al. 1998; Martinez Hoyos et al. 2009; Chang et al. 2005; Tamimi et al. 1993). Bei Hunden mit B-Zell-Lymphomen konnte eine signifikant erhöhte Expression von *HMGA1* Transkripten beobachtet werden. Dagegen gibt es Hinweise, dass *HMGA1*

bei B-Zell-Lymphomen im Gegensatz zu T-Zell-Lymphomen viel höher exprimiert wird (Joetzke et al. 2010). Lymphome gehören zu den häufigsten Tumoren bei Hunden (MacEwen 1990). Obwohl bereits eine Reihe von prognostischen Markern für maligne Lymphome beim Hund beschrieben wurden wie z.B. histologischer Differenzierungsgrad und Ki-67 Proliferation, stellen sich abschließende Diagnosen zur Einteilung der Schwere bzw. Prognosen über den Verlauf der Erkrankung als weithin ungenau dar. Molekulare Marker wie *HMGA1* könnten zu neuen Erkenntnissen sowohl in der Pathogenese des caninen Lymphoms, als auch in der vergleichenden Onkologie führen.

4.2 Inhibierung der HMGA Transkription

Bereits im Jahr 1995 konnte eine viral induzierte, onkogene Transformation von Ratten Schilddrüsenzellen, mit Hilfe eines *HMGA2* antisense Vektors, unterdrückt werden. Im Vergleich zur unbehandelten Kontrolle wurde die Proliferation der antisense behandelten Tumorzellen stark inhibiert. Nothern- und Western-Blots der behandelten Schilddrüsenzellen zeigten im Vergleich zur Kontrolle neben einer starken Abnahme von HMGA2 Transkripten bzw. Proteinen, auch eine deutliche Reduktion von *HMGA1* Transkripten und Proteinen (Berlingieri et al. 1995).

Fünf Jahre später gelang es der derselben Arbeitsgruppe mit einem adenoviralen HMGA1 antisense Vektor (Ad-Yas), das Wachstum eines artifiziell induzierten Schilddrüsenkarzinoms bei athymischen Mäusen stark zu reduzieren. Zudem konnte die Apoptose mit Hilfe des rekombinanten Ad-Yas Virus bei Lungen-, Schilddrüsen-, Dickdarm- und Brust-Karzinom-Zelllinien eingeleitet werden. Ein Adenovirus, welches ein LacZ Gen transkribierte, diente als Kontrolle und zeigte keine inhibierende Wirkung auf das Wachstum der Tumorzellen (Scala et al. 2000).

In der vorliegenden Arbeit wurden analog zu den oben beschriebenen Ergebnissen canine AAV HMGA antisense Vektoren konstruiert. Die canine Adenokarzinomzelllinie CT1258 wurde mit den rekombinanten antisense *HMGA* Viren infiziert (Soller et al 2010). Die verwendete Zelllinie wurde ursprünglich aus einem stark metastasierenden Adenokarzinom der Prostata etabliert (Winkler et al. 2005). Der originale Tumor und die Zelllinie besitzen eine sehr hohe *HMGA2* Expression. Eine absolute Real-time PCR quantifizierte für das Adenokarzinom $4{,}2 \times 10^6$ und für die Zelllinie CT1258 $11{,}9 \times 10^6$ HMGA2 Transkripte pro 250 ng Gesamt-RNA. Im Vergleich dazu wurden bei nicht-neoplastischen Geweben von

Hunden ca. 1 bis $5x10^2$ Transkripte pro 250 ng Gesamt-RNA gemessen (Winkler et al. 2007). Durch die Infektion der Zelllinie mit einer Kombination aus beiden langen AAV HMGA antisense Vektoren (rAAV-asHMGA1long und rAAV-asHMGA2long) konnte die Proliferation im Vergleich zur Kontrolle (gesetzt auf 100 %) auf 1 % verringert werden. Die Applikation der „langen" AAV HMGA antisense Vektoren führen, im Gegensatz zu den „kurzen" antisense Varianten, zu einer stärkeren Abnahme der Proliferation. Sie tragen Teile der 3'UTR Regionen der *HMGA* Gene. Die rAAV-asHMGA2long Variante kodiert zusätzlich zur CDS ca. 1000 bp oder 32 % der caninen *HMGA2* 3'UTR (insgesamt 3085 bp) in antisense Orientierung. In diesem Anteil der 3'UTR befindet sich die erste *let-7* Bindungsstelle #1169. Luziferase-Reporter Experimente zeigten, dass durch diese einzelne Bindungstelle in der 3'UTR die Expression von *HMGA2* um über 50 % reduziert wurde (Lee & Dutta 2007). Die rAAV-asHMGA1long Variante kodiert die vollständige 3'UTR in antisense Orientierung und beinhaltet sowohl die Bindungsstellen für *let-7* als auch für mir-16 (s.o.). Die Expression der antisense mRNA wird durch die stromaufwärts gelegene CMV Promotor Sequenz des rekombinanten AAV Genoms gesteuert. Die antisense *HMGA* Transkripte lagern sich an den endogenen *HMGA* Transkripten von CT1258 an und formen doppelsträngige RNA Komplexe, wodurch die Translation der nativen HMGA mRNAs blockiert wird. Bei der Genregulation, vor allem bei der genomischen Prägung („Imprinting"), spielt die Expression von endogener antisense mRNA bei höheren Eukaryoten eine wichtige Rolle. Bei Menschen und Mäusen existieren stromabwärts des väterlich vererbten IGF2r Gens nicht methylierte „CpG-Inseln", die als Promotorsequenz für die Expression von antisense IGFr RNA funktionieren (Kumar & Carmichael 1998). Ein weiteres Beispiel zeigt die Transkriptionsregulation der Gene für die Synthese des Myosins in Herzmuskelzellen durch antisense *MyHC* RNA (Haddad et al. 2003; Luther et al. 2005). Die besondere Wirksamkeit der langen antisense AAVs könnte durch die Einleitung des RNA-Interferenz Signalweges erklärt werden. Das Dicer Enzym schneidet die dsRNA HMGA Moleküle in 20 bis 25 bp große siRNAs, die bedingt durch die vorhandene 3'UTR der antisense Konstrukte, *let-7* bzw. *mir-16* miRNA ähnliche Sequenzeigenschaften haben könnten. Die durch das Dicer Enzym entstehenden doppelsträngigen RNA Oligos (dsRNA) sind vollständig revers-komplementär zu den endogenen *HMGA* Transkripten, so dass sie im Rahmen des

RNAi Stoffwechsels abgebaut werden. Dieser Mechanismus ist auch vergleichbar mit der *in vitro* Synthese und *in vivo* Applikation von esiRNA (**e**ndoribonuclease prepared **si**RNA) (Yang et al. 2002). Tatsächlich konnte bei Säuger-Zelllinien, die durch das RNA-Virus Influenza A infiziert wurden, eine Beteiligung des Dicer Enzyms und des RNAi Stoffwechsels bei der anti-viralen unspezifischen Immunantwort nachgewiesen werden (Matskevich & Moelling 2007).

Die Reduzierung der Proliferation ist deutlich abhängig vom infektiösen Titer, d.h. je höher die Konzentration an Virusgenomen pro Zelle (vg/Z), desto stärker ist die Abnahme der Proliferation. Des Weiteren zeigen die *HMGA1* antisense AAVs im Vergleich zu den *HMGA2* antisense Vektoren eine höhere Inhibition des Zellwachstums der CT1258. Der rekombinante AAV-asHMGA1long Vektor führte zu einer Reduktion der Proliferation auf bis zu 0,8 % ($1{,}5x10^4$ vg/Zelle) im Vergleich dazu AAV-asHMGA2long 20,3 % ($1{,}5x10^4$ vg/Zelle).

Eine Überexpression von *HMGA1* wurde zuvor bei menschlichen Prostatatumoren beschrieben und geht einher mit hohem Metastasierungspotentential und steigenden Tumorgrad (Tamimi et al. 1993; Tamimi et al. 1996). Nicht-metastasierende Prostatatumorzellen von Ratten („G Dunning rat prostate cancer cells“), die eine geringe Anzahl an *HMGA1* Transkripten aufwiesen, wurden mit einem *HMGA1a* CDS Expressionsvektoren transfiziert. Dadurch wurde die Proliferation der Zellen *in vitro* und eine Zunahme des Tumorvolumens *in vivo* im Vergleich zu den nicht transfizierten Zellen signifikant erhöht. cDNA Microarray Analysen von *HMGA1* transfizierten Zellen weisen eine 8-fach erhöhte Expression des *MMP-2* (Matrix Metalloproteinase 2) Gens auf (Takaha et al. 2004).

Die CT1258 Zelllinie weist einen stark rearrangierten Karyotyp mit komplexer Chromosomenaberration auf. Intraperitoneale und subkutane Injektion ($1x10^6$ und $1x10^5$ bzw. $5x10^5$ Zellen) von CT1258 in NOD-SCID Mäuse zeigten eine hohe Tumorigenität der Zelllinie (Fork et al. 2008).

Die durch die Zelllinie induzierten Tumore zeigten die gleichen histopathologischen und karyotypischen Veränderungen wie das ursprüngliche Adenokarzinom. Die auffälligsten Translokationen von CT1258 bilden die klonalen Fusionen der akrozentrischen Chromosomen CFA 4 und 5 und CFA 1 und CFA 2 zu dem sogenannten Markerchromosom. Während in 50 % aller Metaphasen das Fusionschromosom 4 und 5 vorhanden war, konnte das Markerchromosom in jeder Metaphase nachgewiesen werden (Winkler et al. 2005). Die Fusion von

akrozentrischen Chromosomen ist ein charakteristisches Merkmal von Karyotypveränderungen in caninen Tumoren (Reimann et al. 1999), wobei neben den Chromosomen 4, 5, 25 und X, die Chromosomen 1 und 2 am häufigsten davon betroffen sind. Entscheidend dabei ist das insgesamt vervielfältigte Chromosomenmaterial der tetraploiden CT1258 Zelllinie (Fork et al. 2008; Winkler et al. 2005).

Auf den ersten Blick ist die Überexpression der *HMGA* Gene bei CT1258 nur bedingt zu erklären. Die Genloci von *HMGA1* und *HMGA2* des Hundes liegen auf CFA 12 und 10 in der Nähe der Zentromere. CT1258 ist charakterisiert durch komplexe Chromosomen-Rearrangierungen. Bei den bisher identifizierten Markerchromosomen sind die Chromosomen 1, 2, 4 und 5 involviert. Jedoch können die Chromosomen 10 und 12 durchaus an der Entstehung der anderen komplex rearrangierten Fusionschromosomen beteiligt gewesen sein. Die Rearrangierungen können einen Einfluss auf die *HMGA* Genloci haben. Auch Mikrodeletionen, die die transkriptionsregulativen Sequenzen innerhalb der 3´UTR betreffen, können nicht ausgeschlossen werden.

Zudem könnte durch das vermehrte Vorhandensein von Chromosom 2 in der Zelllinie das canine Gen *Lin-28a* überexprimiert sein. Das Lin-28a kann als RNA-Bindungs-Protein die Reifung der pre-miRNA von *let-7* blockieren (Viswanathan et al. 2009).

Die Applikation von Adeno-assoziierten Virus HMGA Antisense-Vektoren ist ein geeigneter gentherapeutischer Ansatz zur Inhibierung der Proliferation der caninen Prostataadenokarzinomzellen. Trotzdem ist die Methode sehr aufwendig d.h. Kosten und Zeit intensiv. Die Produktion und Ernte der rekombinanten AAVs kann stark innerhalb der einzelnen Chargen varrieren. Zudem können starke qualitative und quantitative Unterschiede zwischen infektiösen und genomischen Titer entstehen, die die Transfektionseffizienzen beeinflussen (Rohr et al. 2005).

Eine alternative Strategie zur Transfektion von caninen Zellen kann eine Applikation von Gold-Nanopartikeln und rekombinaten caninen Transkriptionsvektoren sein. Gold Nanopartikel spielen bei vielen biomedizinischen Anwendungen eine immer wichtigere Rolle, wie z.B. Cell Imaging Techniken, Diagnostikverfahren und Drug Targeting. In dieser Arbeit wurden Gold Nanopartikel (AuNPs) mit Hilfe einer Femtosekunden Laser-Ablationstechnik ohne die Verwendung von Chemikalien und Vorläufermolekülen hergestellt. Erste

Ergebnisse deuten darauf hin, dass sich Säugetierzellen effizient transformieren lassen (Petersen et al. 2009).

SNPs innerhalb der kodierenden Sequenz sind von *HMGA2* in der menschlichen Population selten. Von 87 verschiedenen, gesunden Individuen konnten zeigte ein Transkript einen Aminosäureaustausch innerhalb der CDS (von Ahsen et al. 2006). In einer genomweiten Assoziationsstudie (GWAS) wurden die Genome erkrankter Individuen mit Prostatatumoren und gesunde Individuen miteinander genotypisiert. Dabei wurden in sieben Loci neun verschiedene SNPs m menschlichen Genom entdeckt, die signifikant im Zusammenhang zur Pathogenese von vererbbaren Prostatakarzinomen stehen. Ein SNP (rs7578597) wurde auf dem HSA 2p21 gefunden, innerhalb des Intron 30 des *THADA* Gens (Eeles et al. 2009). Ein weiterer SNP im Exon 24 von *THADA* ist assoziiert mit Diabetes Typ 2 (Zeggini et al. 2008). Der Genort von *THADA* ist häufig ein Hotspot für chromosomale Rearrangierungen bei Schilddrüsenadenomen (Rippe et al. 2003). Der Genort des caninen *THADA* liegt auf CFA 10 Bande q25. Die abgeleiteten Aminosäuresequenzen und Proteindomänen sind bei Menschen und Hunden stärker konserviert als zwischen Menschen und Nagetieren (Drieschner et al. 2007; Soller et al. 2008). Chromosomale Aberrationen des CFA 10 sind eher selten und bisher sind noch keine chromosomalen Rearrangierungen bei caninen Schilddrüsenadenomen bekannt die den Genort des caninen *THADA* betreffen (Mayr et al. 1991; Reimann et al. 1996).

4.3 Inflammation und Angiogenese bei Tumorerkrankungen

Die vorherigen Abschnitte beinhalteten die molekularen Entstehungsmechanismen von Tumoren ausgehend von der klonalen Aberration und erhöhten Proliferation einer einzelnen Zelle oder einer Zellpopulation in einem Gewebeverband, welche sich zu Tumorzellen entwickeln. HMGA Proteine spielen als architektonische Transkriptionsfaktoren für die maligne Transformation eine entscheidende Rolle, wenn sie in einer gesunden Körperzelle überexprimiert werden. Daneben gibt es aber auch weitere Ereignisse, die es Tumorzellen ermöglichen sich in einem Organismus zu etablieren bzw. zu wachsen und schließlich zur Bildung von Metastasen führen. Im folgenden Abschnitt soll im Rahmen der Inflammation und

Neoangiogenese die Funktion weiterer humaner und caniner Genprodukte während einer Tumorerkrankung untersucht werden.

Der Rezeptor für „Advanced Glycation End Products" RAGE ist ein Mitglied der Immunoglobulin-Familie und ein transmembranes Zelloberflächenprotein, das als Multiligand-Rezeptor nicht-enzymatisch glykolysierte Moleküle wie „Advanced Glycation End Products" (AGE) bindet.Neben den TLR 2 und TLR 4 („Toll-like" Rezeptoren) ist RAGE ein wichtiger Rezeptor für HMGB1 (van Beijnum et al. 2008).

Das RAGE Protein und seine vielfältigen Isoformen sind bei der Pathogenese verschiedener Erkrankungen bedeutend wie z.B. bei Störungen des Immunsystems, bei. Sepsis, Morbus Alzheimer, Diabetes bedingter Arteriosklerose, rheumatoide Arthritis, Multiple Sklerose, Wundheilungsstörungen und Tumorerkrankungen (Schmidt et al. 2001; Liliensiek et al. 2004; Yan et al. 1997; Emanuele et al. 2005; Park et al. 1998; Pullerits et al. 2005; Sternberg et al. 2008; Goova et al. 2001; Bhawal et al. 2005).

Innerhalb der Klasse der Säugetiere sind die genomische Exon/Intron Organisation, die Nukleotidsequenzen der Transkripte und die abgeleiteten Aminosäuresequenzen der Proteine von RAGE und HMGB1 beim Menschen und Hund evolutionär konserviert. Das humane und canine HMGB1 haben eine identische Aminosäuresequenz. Die SI-Homologien zwischen dem humanen und caninen RAGE Proteinen betragen 77,6 %. Die SI-Homologien von RAGE zwischen Hund und Nagetieren bzw. Rindern liegen zwischen 73,5 % bis 77,7 %. Der Rezeptor besteht aus drei verbundenen Immunoglobinen (Ig-Klassen: V-C-C'), der extrazelluären Domäne, einer Transmembran- und einer Cytosol-Domäne. HMGB1 bindet am Rezeptor die Ig-V-Domäne. Diese Domäne ist zwischen Mensch und Hund mit einer SI-Homologie von 85,7 % am stärksten evolutionär konserviert. Die hohe Ähnlichkeit des humanen und caninen RAGE/HMGB1 Komplexes und der beteiligten Ligand/Rezeptor-Domänen lassen Therapieansätze, die für das Tiermodell Hund entwickelt werden, besser auf den Menschen übertragen als experimentelle Erkenntnisse, die mit Hilfe anderer Tiermodelle erlangt werden (Murua Escobar et al. 2003; Murua Escobar et al. 2006).

Eine Vielzahl experimenteller Therapieansätze konnte belegen, dass die von RAGE vermittelte Signaltransduktionskaskade durch trunkierte, soluble RAGE Proteinisoformen kompetitiv inhibiert werden kann. Dieses sRAGE Protein besitzt

nur die extrazelluläre V-C-C'-Domäne, während die Transmembran- und Cytosol-Motive fehlen. Durch die Applikation von sRAGE wird das Wachstum und die Metastasierungen von Tumorzellen deutlich reduziert (Huttunen & Rauvala 2004).
Zurzeit sind beim Menschen 19 verschiedene endogene Spleiß-Varianten bekannt, die entweder N- oder C-terminal trunkierte Proteine kodieren (Malherbe et al. 1999; Schlueter et al. 2003; Yonekura et al. 2003; Park et al. 2004; Ding & Keller 2005; Hudson et al. 2008). Ihre zellbiologischen Funktionen sind bisher wenig charakterisiert worden. Es wird diskutiert, ob die Protein-Isoformen eine Funktion innerhalb eines komplexen Netzwerks der Selbst-Regulation haben sowie für die Besetzung der RAGE Moleküle innerhalb der Zellmembran verantwortlich sind. Eine weitere wichtige Funktion der sRAGE Isoformen liegt in der kompetitiven Inhibition des vollständig, membrangebunden Rezeptors und im Zusammenspiel der Aufrechterhaltung der Homöostasen zwischen Ligand, Rezeptor und solublen Protein Konzentrationen im inter- und intrazellulären Raum. Soluble RAGE Isoformen konnten im Blutplasma und in verschiedenen Geweben nachgewiesen werden. Erkenntnisse, die die Regulation bzw. das Verhältnis der verschiedenen solublen RAGE Isoformen und membrangebundenen RAGE Proteine auf Transkript-Ebene beschreiben, sind selten (Vazzana et al. 2009).
Für den Hund konnte Sterenczak et al. 2009 14 neue RAGE Spleiß-Varianten aus gesunden und neoplastischen Geweben und Zelllinien beschreiben, die bisher noch in keiner Spezies entdeckt wurden. Daneben wurden vier neue Spleiß-Varianten aus humanen Zelllinien entdeckt. Wie in Kapitel 3.3.2 beschrieben, ergaben sich zwei Gruppen von abgeleiteten RAGE Isoformen. Die erste Gruppe kodierte vollständige oder soluble RAGE Proteine, die zweite Gruppe N-terminal trunkierte Proteine mit fehlender Ligand-bindender Ig-V Domäne.
Die CDS der N-terminal trunkierten Protein-Gruppe sind durch Insertionen des Intron 1 gekennzeichnet („*RAGE Intron 1 ins*" Variante). Sie haben ihre Funktion als kompetitive Inhibitoren verloren. Dieses Expressions-Verhältnis zwischen den *RAGE Intron 1 ins* Varianten und den Ligand-bindenden *RAGE* Transkripten ist in gesunden und neoplastischen Geweben und Zelllinien gemessen worden. In den gesunden Geweben der Lunge, des Hodens und der Schilddrüse ist die Menge der Ligand-bindenden Transkripte signifikant höher als die *RAGE Intron 1 ins* Varianten. Im Gegensatz weist die Mehrheit der untersuchten Tumorproben und Zelllinien eine weitaus größere Menge an N-terminal trunkierten *RAGE Intron 1 ins*

Transkripten auf. Diese vergleichende Studie zur Charakterisierung der Transkription einer Vielzahl von verschiedenen *RAGE* Varianten beim Hund und beim Menschen trägt zum Verständnis bei, inwieweit eine Deregulierung bzw. Aberration der Spleiß-Varianten eine Rolle bei der Pathogenese von Tumorerkrankungen, Angiogenese und chronischer Inflammation spielen (Sterenczak et al. 2009). Unter dem Aspekt der Tumorenstehung und Metastasierung zeigt eine Studie, die das Verhältnis zwischen den unterschiedlichen RAGE Isoformen und HMGB1 beschreibt, dass die Expression von endogenen sRAGE (esRAGE) ein geeigneter Tumormarker zur Klassifizierung der Malignität von Chondrosarkomen ist (Takeuchi et al. 2007).

Gerade der Zusammenhang zwischen chronischer Inflammation und die Entstehung von Tumoren lässt sich durch den RAGE/HMGB1 Komplex besonders eingängig darstellen. Bei chronischer Inflammation können absterbende Zellen ein durch einen verminderten Sauerstoffpartialdruck gekennzeichnetes Mikroumfeld entstehen lassen (Hypoxie). Im Gegensatz zur Apoptose können nekrotische Zellen durch passive Diffusion Chromatin-assoziiertes HMGB1 in den extrazellulären Raum abgeben (Scaffidi et al. 2002).

Der RAGE/HMGB1-Komplex vermittelt eine Signaltransduktion über die GTPase CDC42/Rac oder über diverse MAP-Kinasen, die zur NFκB abhängigen Transkription pro-inflammatorischer Gene führt (weiterführende Übersichtsartikel siehe Riehl et al. 2009). Tumorzellen sezenieren in einem hypoxischen Umfeld angiogenetische Faktoren und Zytokine wie z.B. VEGF, TNFα, IL-8, IL-6, und IL-1 (Shweiki et al. 1992; Bates & Mercurio 2003; Sparmann & Bar-Sagi 2004; Germano et al. 2008; Shchors et al. 2006). In einer positiven Rückkopplung exprimieren diese Zellen weitere RAGE-Rezeptoren (van Beijnum et al. 2008). Das proinflammatorische Milieu lockt Makrophagen an, die wiederum HMGB1 in den intrazellulären Raum aktiv sezernieren, dadurch wird in einer sich selbstverstärkenden inflammatorischen Kaskade weitere Zytokine ausgeschüttet (Andersson et al. 2002). Wachstumsfaktoren fördern die vermehrte Bildung von Blutgefäßen (Angiogenese), die den wachsenden Tumor versorgen. Am Anfang dieser aus dem Gleichgewicht geratenen Stoffwechselkaskade stehen der Ligand HMGB1 und sein Rezeptor RAGE (Schlueter et al. 2005).

Während der Einleitung der Inflammation und der Initiierung der Immunabwehr führt eine durch RAGE oder TLR vermittelte Signalkaskade zur Aktivierung von

NFκB (Huttunen et al. 1999; Yang et al. 1999; Kawai & Akira 2007). Dabei spielt NFκB eine wichtige Schlüsselrolle bei der unspezifischen bzw. angeborenen Immunabwehr, da es als Transkriptionsfaktor die Transkription proinflammatorischer Zytokine induziert. Monozyten und Makrophagen erkennen durch einen rezeptorvermittelten Mechanismus pathogen-assoziierte molekulare Muster. Sie aktivieren über den Transkriptionsfaktor NFκB die Sezernierung der Zytokine IL1 und TNFα.

Gerät diese multifaktoriell beeinflusste Immunantwort aus dem Gleichgewicht, kommt es zur Signaltransduktion vermittelter, permanenter Aktivierung des Transkriptionsfaktors NFκB. Die endogene negative Rückkopplung gerät in diesem proinflammatorischen Umfeld außer Kontrolle, so dass dies zu chronischen Veränderungen des Gewebes führt. Eine hohe Konzentration an Zytokinen führt zu einer Aktivierung endothelialer Zellen der Blutgefäße. Über die Wachstumsfaktoren VEGF und TGFβ bilden sich in den Tumoren Einsprossungen neuer Kapillaren in den Tumor (Neoangiogenese). Die gebildeten Blutgefäße versorgen den wachsenden Tumor mit Nährstoffen. Dies gilt als Vorraussetzung für die weitere Tumor-Proliferation und schließlich für die Bildung von Metastasen (McMahon 2000; Pardali & Moustakas 2007).

Vergleichende Analysen der Aminosäuresequenzen der Zytokine IL-1 und TNFα zwischen verschiedenen Säugetierarten zeigen hohe Sequenzhomologien innerhalb der funktionellen Proteindomänen. Die „Calpain Cleavage Site“ bei IL-1α oder das β-Faltblatt-Motiv bei IL-1β sind bei beiden Spezies hoch konserviert (Soller et al. 2007). Die SI- Homologie zwischen humanen und caninen IL-1α beträgt 68,5 %, zwischen Maus, Mensch und Hund liegen die SI-Homologien bei 60,1 % bzw. 57,1 %. Für das IL-1β beträgt die SI-Homologie zwischen der humanen und caninen Aminosäuresequenz 62,8 %. Im Gegensatz zu IL-1α teilen sich Mäuse und Menschen eine leicht höhere SI-Homologie von 66,4 %. Dagegen ist die Aminosäuresequenz von TNFα zwischen Mensch und Hund im Vergleich zu sieben weiteren Säugetieren, mit Ausnahme der Katze, am stärksten evolutionär konserviert. Die SI Homologie von Mensch zu Hund bzw. Katze beträgt 91 %, von Mensch zu Maus 77,8 %. Die genomische Organisation aller drei Zytokine ist zwischen den Säugetieren nahezu identisch. Eine Ausnahme bildet eine Spleiß-Variante von IL-1α, die bisher nur bei Hunden, Katzen und Schweinen entdeckt

wurden. Parallel zu den normal Transkripten fehlt hier die Calpain-cleavage site (Straubinger et al. 1999; Soller et al. 2007).

4.4 Maligne Histiozytose und Langerhans-Zell Histiozytose

Menschen und Hunde teilen sich viele Gemeinsamkeiten in Bezug auf molekular genetische Stoffwechselwege bei inflammatorischen Prozessen. Es gibt bemerkenswerte Ähnlichkeiten bei der Dysfunktion des Immunsystems bei verschiedenen Erkrankungen, wie z.B. die Langerhans' Zell Histiozytose (LCH) und maligne Histiozytose (MH) (Affolter & Moore 2002). In neueren Untersuchungen wird diese Erkrankung als disseminiertes histiozytäres Sarkom bezeichnet (Abadie et al. 2009). Die MH oder LCH Erkrankung bildet sich spontan aus aberrant proliferienden Histiozyten oder Langerhansschen Zellen. Als Folge ändert sich das Verhalten der Zellen, d.h. sie wandern wie Metastasen in umliegende Gewebe und initiieren unter anderem die Phagozytose der Erythrozyten (Kannourakis & Abbas 1994). Die Pathogenese der malignen Histiozytose ist noch weitgehend unerforscht. Während der Erkrankung sezernieren Histiozyten und T-Zellen große Mengen von Zytokinen in die betroffenen Gewebe (Egeler et al. 1999). In einer Studie konnten in einigen Zytokin-Transkripten bei insgesamt 17 untersuchten Hunden Punktmutationen innerhalb der CDS gefunden werden, die zu Aminosäureaustauschen der abgeleiteten Proteine führen (Soller et al. 2006). Die *IL-1α* CDS eines Berner Sennenhundes (BSH Probe Nr. 2) zeigte auf Codon 23 eine Basenpaarsubstitution, dadurch wird im abgeleiteten Protein die native polare Aminosäure Serin zu unpolaren Prolin translatiert. Dieses Transkript zeigte eine zweite Basenpaarsubstitution (ebenfalls Probe Nr.2). Die Aminosäure Cystein auf der Position 47 wurde durch die positiv geladene Aminosäure Arginin substituiert. Cysteine bilden innerhalb der Vorstufe des IL-1α Proteins Disulfidbrücken aus und interagieren mit der DNA des Zellkerns. Bei diesem Individuum konnte auch ein Aminosäureaustausch in der abgeleiteten membrangebunden Domäne des TNFα gefunden werden. Zwei BSHs (Proben Nr. 1 und 4) zeigten Basenpaarsubstitutionen, die zu Aminosäureaustauschen innerhalb der der β-Faltblattmotive von IL-1β führten. Ein weiterer BSH zeigte einen Austausch der Aminosäure Asparagin zu unpolarem Glycin. Dieser Aminosäureaustausch liegt innerhalb der ICE-Domäne des Proteins. Alle *IL-1β* Basenpaarsubstitutionen wurden in Leberproben von drei verschiedenen Berner Sennenhunden detektiert.

SNPs innerhalb der Promotorsequenzen der untersuchten Zytokine sind mit der Pathogenese menschlicher Erkrankungen wie Morbus Alzheimer, Sepsis, rheumatoide Arthritis und Tumoren assoziiert (Dennis et al. 2004; Correa et al. 2005; Zienolddiny et al. 2004). SNP Screenings bei BSHs im Rahmen der Pathogenese der malignen Histiozytose sind bisher selten. Die in dieser Studie gefundenen Basenpaarsubstitutionen innerhalb der CDS von *TNFα* und *IL-1* zeigen erste Hinweise auf einen molekulargenetischen Hintergrund der Pathogenese dieser Erkrankung bei Hunden (Soller et al. 2006).

Die humane LCH wird durch eine unkontrollierte, klonale Proliferation antigen-präsentierender Zellen verursacht, den Histiozyten oder Langhans' Zellen. Die Langerhans' Zellen bilden sich aus myeloiden Vorläuferzellen und sie haben die gleichen Eigenschaften, wie z.B. Zelloberflächenmarkerproteine wie bei unreifen dendritischen Zellen (DC). Sie exprimieren große Mengen an proinflammatorischen Zytokinen und diese Eigenschaft wird durch die Interaktion mit T-Zellen in einer positiven Rückkopplung weiter verstärkt (Egeler et al. 1999). Die canine MH oder das disseminierte histiozytäre Sarkom ist eine aggressive Multisystemerkrankung. Es bilden sich große Tumoren in verschiedenen Organen. Primäre Läsionen treten zunächst in der Milz, der Lunge und im Knochenmark auf, danach bilden sich sekundäre Läsionen in den Lymphknoten, in der Leber und in weiteren Organen (Affolter & Moore 2002).

Wie bei der LCH wird auch bei der MH eine aberrante Proliferation von DCs als die Ursache der Erkrankung angesehen. Die Zellen der humanen LCH als auch die caninen MH Zellen weisen beide die CD1a bis c Marker auf, die charakteristisch für unreife dendritische Zellen sind (Laman et al. 2003; Affolter & Moore 2002; Affolter 2004).

Der RAGE/HMGB1 Komplex spielt über den stromabwärts gelegenen MAPK und NFκB Signaltransduktionsweg eine wichtige Schlüsselrolle bei der Reifung der DCs, in der Interaktion mit T-Zellen und der Fähigkeit zur Mobilität (Manfredi et al. 2008). Die Behandlung mit anti-RAGE Antikörper verhindert die Reifung der DCs der Milz bei Ratten (Zhu et al. 2009). Dendritische Zellen von *RAGE* Knock-out Mäusen verlieren die Fähigkeit zur Mobilität und verbleiben in einem unreifen („immature") Zustand. Zudem verlieren sie die Eigenschaft T-Zellen zu aktivieren. Diese Eigenschaften zeigen auch die humanen LCH Zellen (Laman et al. 2003). Real-time Experimente an verschiedenen Gewebeproben (Lunge, Milz, Leber und

Lymphknoten) von MH erkrankten Hunden zeigten im Vergleich eine geringere *RAGE* Expression hauptsächlich in der Milz, aber auch in der Lunge als bei vergleichbaren nicht-neoplastischen Geweben (Sterenczak et al. 2010, in Vorb.). Interessanterweise zeigen humane Tumoren der Lunge, d.h. nicht-kleinzellige Bronchialkarzinome, ebenfalls eine erniedrigte *RAGE* Expression. Je höher das Grading bzw. die TNM-Klassifikation der malignen Tumoren, desto niedriger ist die mRNA und die Protein Konzentration von RAGE (Bartling et al. 2005).

RAGE wird in der Rhabdomyosarkom Zelllinie TE671/wt nicht transkribiert. NOD-SCID Mäuse, die mit dieser Zelllinie injiziert werden, entwickeln größere Tumore, als eine Vergleichs-Gruppe, die mit Zellen injiziert wurden, die zuvor stabil mit einem rekombinanten *RAGE* Expressionsvektor transfiziert wurde (Riuzzi et al. 2007). Die Autoren der Studie beschrieben eine Signaltransduktionkaskade, die über den RAGE/HMGB1 Komplex die MAP Kinase p38 aktiviert. Dadurch werden wiederum Transkriptionsfaktoren aktiviert, die die Expression von Genen steuern, welche für die Differenzierung von Myoblasten verantwortlich sind. Weiterhin hemmt MAPK p38 die unkontrollierte Proliferation von Myoblasten durch eine Inaktivierung der c-Jun N-terminalen Kinase (JNK). Dadurch wird die Expression von Zyklin D1 gestoppt (Lee et al. 2002). Die Phosphorylierung und Aktivierung von MAPK p38 und anderer Signaltransduktoren haben ebenfalls eine Bedeutung in der Reifung humaner dendritischer Zellen (Nakahara et al. 2006).

Abschließend betrachtet, bietet die molekularbiologische Erforschung der Pathogenese der humanen LCH und der caninen MH Einsichten in dem Gesamtkomplex chronischer Inflammation, durch die aberrante Expression von Zytokinen, der Tumorgenese und einer aberranten Immunantwort.

5. Zusammenfassung

Der „World Cancer Report 2008“ der Weltgesundheitsorganisation (WHO) berichtet von über 12,4 Millionen neuen Krebserkrankungen jährlich mit 7,6 Millionen Toten weltweit. In den vergangenen Jahrzehnten sind durch die moderne Medizin Fortschritte in der Behandlung und Heilung von Krebs erzielt worden, trotzdem gilt diese Krankheit nach wie vor als Hauptursache aller Todesfälle.

Das Tiermodell Hund kann für die Erforschung der Entstehung von Krebs beim Menschen zu neuen Ansätzen in der Therapie von Tumorerkrankungen und Entwicklung neuer Diagnose-Verfahren verhelfen sowie die bisherigen Nager-Tiermodelle für die Untersuchung der genetischen Ursachen von Krebs ergänzen. Die spontane Tumorenstehung, der gemeinsame Lebensraum von Hunden und Menschen unter denselben Umweltfaktoren, zeigen eine vielversprechende Übertragbarkeit der experimentellen Ergebnisse für die Humanmedizin. Die Anamnese und die Histologie von Tumoren beider Spezies sind einander sehr ähnlich. Tumorgenese und Tumorprogression verlaufen beim Hund in kürzester Zeit, so dass sich eine Vielzahl von übertragbaren Daten in einem überschaubareren Zeitrahmen sammeln lassen.

Einen besondereren Schwerpunkt der vorliegenden Arbeit bildet die Erforschung und vergleichende Tumorbiologie der caninen und humanen Prostatatumoren und weiterer Tumorerkrankungen, unter dem Aspekt der genomischen Charakterisierung der caninen Gene und Proteine HMGA1, HMGA2, THADA, RAGE, TNFα und IL-1α/β.

Genomische Charakterisierungen stark evolutionär konservierter Gene sind die grundlegenden Maßnahmen für funktionelle und strukturelle Analysen tumorrelevanter Gene und Proteine. Darauf aufbauend ist ein gentherapeutischer Ansatz zur Inhibierung der Expression von *HMGA* Genen in einer caninen Prostatakarzinomzelllinie mit Hilfe von antisense Adeno-assoziierten Viren entwickelt worden. Zusätzlich konnte eine alternative Transfektionsmethode aufzeigen, dass sich eukaryotische Zellen besonders effizient mit Goldnanopartikeln transfizieren lassen.

Im Rahmen der Inflammation und Angiogenese während einer Tumorerkrankung wurde der canine Rezeptor für „Advanced Glycation End Products” RAGE untersucht. Dabei zeigte sich eine hohe molekulargenetische Ähnlichkeit zwischen

dem humanen und caninen RAGE und den verschiedenen RAGE Isoformen und den beteiligten Ligand/Rezeptor-Domänen.

Eine aberrante Expression von Zytokinen, vor allem Interleukin-1 (IL-1α and IL-1β) und der Tumornekrosisfaktor alpha (TNF-α), spielen bei beiden Spezies eine wichtige Rolle bei der Einleitung von Entzündungsreaktionen und der Immunantwort.

Viele klinische und pathologische Eigenschaften, wie beispielsweise die Überexpression von Zytokinen bei der caninen malignen Histiozytose (MH), ähneln der humanen Langerhans-Zell-Histiozytose (LCH).

Die molekularbiologische Erforschung der Pathogenese der humanen LCH und der caninen MH bieten neue Einsichten im Zusammenhang zwischen Überexpression von Zytokinen, chronischer Inflammation, einer aberranten Immunantwort und der Tumorgenese. In diesem Zusammenhang wurden Basenpaarsubstitutionen und evolutionär konservierte Gensequenzen und Proteindomänen in caninen und humanen Zytokinen erforscht.

5. Summary

Medical advances due to scientific research made remarkable progress in the past decades fighting cancer. Nevertheless according to the United Nation's World Cancer Report 2008 tumour diseases are the leading cause of death with 7.6 million deaths and 12.4 million the new cancer cases a year.

According to cancer the dog as an animal model joins the popular rodent model in order to study and understand the molecular genetics of tumour diseases and to develop new therapeutic strategies against cancer. Canine tumour diseases are distinguished by spontaneous development and dogs and humans share striking similarities in the case of oncology.

The main part of this thesis comprises the comparative genomics and tumour biology of the human and canine tumour diseases focusing in particular prostate carcinomas by molecular characterisation of the genes and proteins HMGA1, HMGA2, THADA, RAGE, TNFα and IL-1α/β.

Genomic characterisations of high evolutionary conserved genes are the fundamentals for functional and structural analysis of tumour relevant genes. According to this principle a gene therapeutic approach was developed in order inhibit the *HMGA* expression of a canine prostate carcinoma cell line with the help of an adeno-associated virus vector. Furthermore and alternative method with gold nanoparticles was established for efficient transfection of eukaryotic cells.

In the context of inflammation and angiogenesis during a tumour disease the canine receptor for advanced glycation end products (RAGE) was analysed. The results showed highly conserved molecular similarities (N.B. ligand-receptor domains) between the human and canine RAGE and its isoforms.

In both species an aberrant Expression of cytokines e.g. interleukin-1 (IL-1α/β) and the tumour necrosis factor alpha (TNFα) plays an important role during the initiation of immune response and inflammation. In particular during the course of the Langerhans cell histiocytosis (LCH) large quantities of cytokines are produced. Interestingly most clinical and pathological features of the canine malignant histiocytosis resemble those of LCH in humans. Finally dogs could be used as an animal model to elucidate the molecular genetics of malignant histiocytosis as well as LCH. In this connection nucleic base pair substitution within evolutionary

conserved gene and amino acid sequences of canine and human cytokines were investigated.

6 Literatur

Abadie J., Hedan B., Cadieu E., De Brito C., Devauchelle P., Bourgain C., Parker H.G., Vaysse A., Margaritte-Jeannin P., Galibert F., Ostrander E.A., Andre C. (2009) Epidemiology, pathology, and genetics of histiocytic sarcoma in the Bernese mountain dog breed. J Hered 100 Suppl 1:S19-27

Abe N., Watanabe T., Masaki T., Mori T., Sugiyama M., Uchimura H., Fujioka Y., Chiappetta G., Fusco A., Atomi Y. (2000) Pancreatic duct cell carcinomas express high levels of high mobility group I(Y) proteins. Cancer Res 60:3117-3122

Affolter V.K. Histiocytic Proliferative Diseases in Dogs and Cats. 29th World Congress of the WSAVA. Rhodes, Greece. Oktober 6-9. (2004) http://www.vin.com/proceedings/Proceedings.plx?CID=WSAVA2004&PID=8600&O=Generic,

Affolter V.K., Moore P.F. (2002) Localized and disseminated histiocytic sarcoma of dendritic cell origin in dogs. Vet Pathol 39:74-83

Allen T.C. (2008) Pulmonary Langerhans cell histiocytosis and other pulmonary histiocytic diseases: a review. Arch Pathol Lab Med 132:1171-1181

Andersson U., Erlandsson-Harris H., Yang H., Tracey K.J. (2002) HMGB1 as a DNA-binding cytokine. J Leukoc Biol 72:1084-1091

Arico M. (2006) Langerhans cell histiocytosis: too many cytokines, not enough gene regulation? Pediatr Blood Cancer 47:118-119

Bandiera A., Bonifacio D., Manfioletti G., Mantovani F., Rustighi A., Zanconati F., Fusco A., Di Bonito L., Giancotti V. (1998) Expression of HMGI(Y) proteins in squamous intraepithelial and invasive lesions of the uterine cervix. Cancer Res 58:426-431

Bartling B., Hofmann H.S., Weigle B., Silber R.E., Simm A. (2005) Down-regulation of the receptor for advanced glycation end-products (RAGE) supports non-small cell lung carcinoma. Carcinogenesis 26:293-301

Bates R.C., Mercurio A.M. (2003) Tumor necrosis factor-alpha stimulates the epithelial-to-mesenchymal transition of human colonic organoids. Mol Biol Cell 14:1790-1800

Berlingieri M.T., Manfioletti G., Santoro M., Bandiera A., Visconti R., Giancotti V., Fusco A. (1995) Inhibition of HMGI-C protein synthesis suppresses retrovirally induced neoplastic transformation of rat thyroid cells. Mol Cell Biol 15:1545-1553

Beuing C., Soller J.T., Muth M., Wagner S., Dolf G., Schelling C., Richter A., Willenbrock S., Reimann-Berg N., Winkler S., Nolte I., Bullerdiek J., Murua Escobar H. (2008) Genomic characterisation, chromosomal assignment and in vivo localisation of the canine high mobility group A1 (HMGA1) gene. BMC Genet 9:49

Bhawal U.K., Ozaki Y., Nishimura M., Sugiyama M., Sasahira T., Nomura Y., Sato F., Fujimoto K., Sasaki N., Ikeda M.A., Tsuji K., Kuniyasu H., Kato Y. (2005) Association of expression of receptor for advanced glycation end products and invasive activity of oral squamous cell carcinoma. Oncology 69:246-255

Boyle P., Levin B. (2008) World cancer report 2008. International Agency for Research on Cancer; Distributed by WHO Press, Lyon, Geneva

Bünger S. (2007) Herstellung von HMGA-rekombinanten adeno-assoziierten antisense-Viren und deren Applikation an caninen Zelllinien. Diplomarbeit,

FB 2 Biologie/Chemie, Zentrum für Humangenetik, Universität Bremen, Bremen

Bussemakers M.J., van de Ven W.J., Debruyne F.M., Schalken J.A. (1991) Identification of high mobility group protein I(Y) as potential progression marker for prostate cancer by differential hybridization analysis. Cancer Res 51:606-611

Chang Z.G., Yang L.Y., Wang W., Peng J.X., Huang G.W., Tao Y.M., Ding X. (2005) Determination of high mobility group A1 (HMGA1) expression in hepatocellular carcinoma: a potential prognostic marker. Dig Dis Sci 50:1764-1770

Chiappetta G., Tallini G., De Biasio M.C., Manfioletti G., Martinez-Tello F.J., Pentimalli F., de Nigris F., Mastro A., Botti G., Fedele M., Berger N., Santoro M., Giancotti V., Fusco A. (1998) Detection of high mobility group I HMGI(Y) protein in the diagnosis of thyroid tumors: HMGI(Y) expression represents a potential diagnostic indicator of carcinoma. Cancer Res 58:4193-4198

Correa P.A., Gomez L.M., Cadena J., Anaya J.M. (2005) Autoimmunity and tuberculosis. Opposite association with TNF polymorphism. J Rheumatol 32:219-224

Dennis R.A., Trappe T.A., Simpson P., Carroll C., Huang B.E., Nagarajan R., Bearden E., Gurley C., Duff G.W., Evans W.J., Kornman K., Peterson C.A. (2004) Interleukin-1 polymorphisms are associated with the inflammatory response in human muscle to acute resistance exercise. J Physiol 560:617-626

Ding Q., Keller J.N. (2005) Splice variants of the receptor for advanced glycosylation end products (RAGE) in human brain. Neurosci Lett 373:67-72

Drieschner N., Kerschling S., Soller J.T., Rippe V., Belge G., Bullerdiek J., Nimzyk R. (2007) A domain of the thyroid adenoma associated gene (THADA) conserved in vertebrates becomes destroyed by chromosomal rearrangements observed in thyroid adenomas. Gene 403:110-117

Eeles R.A., Kote-Jarai Z., Al Olama A.A., Giles G.G., Guy M., Severi G., Muir K., et al. (2009) Identification of seven new prostate cancer susceptibility loci through a genome-wide association study. Nat Genet 41:1116-1121

Egeler R.M., Favara B.E., van Meurs M., Laman J.D., Claassen E. (1999) Differential In situ cytokine profiles of Langerhans-like cells and T cells in Langerhans cell histiocytosis: abundant expression of cytokines relevant to disease and treatment. Blood 94:4195-4201

Emanuele E., D'Angelo A., Tomaino C., Binetti G., Ghidoni R., Politi P., Bernardi L., Maletta R., Bruni A.C., Geroldi D. (2005) Circulating levels of soluble receptor for advanced glycation end products in Alzheimer disease and vascular dementia. Arch Neurol 62:1734-1736

Fleischer S., Sharkey M., Mealey K., Ostrander E.A., Martinez M. (2008) Pharmacogenetic and metabolic differences between dog breeds: their impact on canine medicine and the use of the dog as a preclinical animal model. AAPS J 10:110-119

Flohr A.M., Rogalla P., Bonk U., Puettmann B., Buerger H., Gohla G., Packeisen J., Wosniok W., Loeschke S., Bullerdiek J. (2003) High mobility group protein HMGA1 expression in breast cancer reveals a positive correlation with tumour grade. Histol Histopathol 18:999-1004

Fork M.A., Murua Escobar H., Soller J.T., Sterenczak K.A., Willenbrock S., Winkler S., Dorsch M., Reimann-Berg N., Hedrich H.J., Bullerdiek J., Nolte I. (2008) Establishing an in vivo model of canine prostate carcinoma using the new cell line CT1258. BMC Cancer 8:240

Friedmann M., Holth L.T., Zoghbi H.Y., Reeves R. (1993) Organization, inducible-expression and chromosome localization of the human HMG-I(Y) nonhistone protein gene. Nucleic Acids Res 21:4259-4267

Fusco A., Fedele M. (2007) Roles of HMGA proteins in cancer. Nat Rev Cancer 7:899-910

Germano G., Allavena P., Mantovani A. (2008) Cytokines as a key component of cancer-related inflammation. Cytokine 43:374-379

Goova M.T., Li J., Kislinger T., Qu W., Lu Y., Bucciarelli L.G., Nowygrod S., Wolf B.M., Caliste X., Yan S.F., Stern D.M., Schmidt A.M. (2001) Blockade of receptor for advanced glycation end-products restores effective wound healing in diabetic mice. Am J Pathol 159:513-525

Haddad F., Bodell P.W., Qin A.X., Giger J.M., Baldwin K.M. (2003) Role of antisense RNA in coordinating cardiac myosin heavy chain gene switching. J Biol Chem 278:37132-37138

Hongo M., Ryoke T., Ross J. (1997) Animal Models of Heart Failure - Recent Developments and Perspectives Trends in Cardiovascular Medicine 7:161-167

Huang M.L., Chen C.C., Chang L.C. (2009) Gene expressions of HMGI-C and HMGI(Y) are associated with stage and metastasis in colorectal cancer. Int J Colorectal Dis 24:1281-1286

Hudson B.I., Carter A.M., Harja E., Kalea A.Z., Arriero M., Yang H., Grant P.J., Schmidt A.M. (2008) Identification, classification, and expression of RAGE gene splice variants. Faseb J 22:1572-1580

Huttunen H.J., Fages C., Rauvala H. (1999) Receptor for advanced glycation end products (RAGE)-mediated neurite outgrowth and activation of NF-kappaB require the cytoplasmic domain of the receptor but different downstream signaling pathways. J Biol Chem 274:19919-19924

Huttunen H.J., Rauvala H. (2004) Amphoterin as an extracellular regulator of cell motility: from discovery to disease. J Intern Med 255:351-366

Joetzke A., Sterenczak K.A., Eberle N., Wagner S., Soller J.T., Nolte I., Bullerdiek J., Murua Escobar H., Simon D. (2010) Expression of the high mobility group A1 (HMGA1) and A2 (HMGA2) in canine lymphoma: Analysis of 23 cases and comparison to control cases. Vet Comp Oncol 8:87-95

Johnson K.R., Lehn D.A., Reeves R. (1989) Alternative processing of mRNAs encoding mammalian chromosomal high-mobility-group proteins HMG-I and HMG-Y. Mol Cell Biol 9:2114-2123

Kannourakis G., Abbas A. (1994) The role of cytokines in the pathogenesis of Langerhans cell histiocytosis. Br J Cancer Suppl 23:S37-40

Kawai T., Akira S. (2007) Signaling to NF-kappaB by Toll-like receptors. Trends Mol Med 13:460-469

Kazmierczak B., Dal Cin P., Wanschura S., Borrmann L., Fusco A., Van den Berghe H., Bullerdiek J. (1998) HMGIY is the target of 6p21.3 rearrangements in various benign mesenchymal tumors. Genes Chromosomes Cancer 23:279-285

Kazmierczak B., Meyer-Bolte K., Tran K.H., Wockel W., Breightman I., Rosigkeit J., Bartnitzke S., Bullerdiek J. (1999) A high frequency of tumors with

rearrangements of genes of the HMGI(Y) family in a series of 191 pulmonary chondroid hamartomas. Genes Chromosomes Cancer 26:125-133
Khanna C., Hunter K. (2005) Modeling metastasis in vivo. Carcinogenesis 26:513-523
Khanna C., Lindblad-Toh K., Vail D., London C., Bergman P., Barber L., Breen M., Kitchell B., McNeil E., Modiano J.F., Niemi S., Comstock K.E., Ostrander E., Westmoreland S., Withrow S. (2006) The dog as a cancer model. Nat Biotechnol 24:1065-1066
Knapp D.W., Waters D.J. (1997) Naturally occurring cancer in pet dogs: important models for developing improved cancer therapy for humans. Mol Med Today 3:8-11
Kumar M., Carmichael G.G. (1998) Antisense RNA: function and fate of duplex RNA in cells of higher eukaryotes. Microbiol Mol Biol Rev 62:1415-1434
Kuska B. (1999) Sit, DNA, sit: cancer genetics going to the dogs. J Natl Cancer Inst 91:204-206
Laman J.D., Leenen P.J., Annels N.E., Hogendoorn P.C., Egeler R.M. (2003) Langerhans-cell histiocytosis 'insight into DC biology'. Trends Immunol 24:190-196
Lee J., Hong F., Kwon S., Kim S.S., Kim D.O., Kang H.S., Lee S.J., Ha J. (2002) Activation of p38 MAPK induces cell cycle arrest via inhibition of Raf/ERK pathway during muscle differentiation. Biochem Biophys Res Commun 298:765-771
Lee Y.S., Dutta A. (2007) The tumor suppressor microRNA let-7 represses the HMGA2 oncogene. Genes Dev 21:1025-1030
Leroy B.E., Northrup N. (2009) Prostate cancer in dogs: comparative and clinical aspects. Vet J 180:149-162
Liliensiek B., Weigand M.A., Bierhaus A., Nicklas W., Kasper M., Hofer S., Plachky J., Grone H.J., Kurschus F.C., Schmidt A.M., Yan S.D., Martin E., Schleicher E., Stern D.M., Hammerling G.G., Nawroth P.P., Arnold B. (2004) Receptor for advanced glycation end products (RAGE) regulates sepsis but not the adaptive immune response. J Clin Invest 113:1641-1650
Lue L.F., Yan S.D., Stern D.M., Walker D.G. (2005) Preventing activation of receptor for advanced glycation endproducts in Alzheimer's disease. Curr Drug Targets CNS Neurol Disord 4:249-266
Luther H.P., Bartsch H., Morano I., Podlowski S., Baumann G. (2005) Regulation of naturally occurring antisense RNA of myosin heavy chain (MyHC) in neonatal cardiomyocytes. J Cell Biochem 94:848-855
MacEwen E.G. (1990) Spontaneous tumors in dogs and cats: models for the study of cancer biology and treatment. Cancer Metastasis Rev 9:125-136
Malherbe P., Richards J.G., Gaillard H., Thompson A., Diener C., Schuler A., Huber G. (1999) cDNA cloning of a novel secreted isoform of the human receptor for advanced glycation end products and characterization of cells co-expressing cell-surface scavenger receptors and Swedish mutant amyloid precursor protein. Brain Res Mol Brain Res 71:159-170
Manfredi A.A., Capobianco A., Esposito A., De Cobelli F., Canu T., Monno A., Raucci A., Sanvito F., Doglioni C., Nawroth P.P., Bierhaus A., Bianchi M.E., Rovere-Querini P., Del Maschio A. (2008) Maturing dendritic cells depend on RAGE for in vivo homing to lymph nodes. J Immunol 180:2270-2275
Martinez Hoyos J., Ferraro A., Sacchetti S., Keller S., De Martino I., Borbone E., Pallante P., Fedele M., Montanaro D., Esposito F., Cserjesi P., Chiariotti L.,

Troncone G., Fusco A. (2009) HAND1 gene expression is negatively regulated by the High Mobility Group A1 proteins and is drastically reduced in human thyroid carcinomas. Oncogene 28:876-885
Matskevich A.A., Moelling K. (2007) Dicer is involved in protection against influenza A virus infection. J Gen Virol 88:2627-2635
Mattila K.M., Rinne J.O., Lehtimaki T., Roytta M., Ahonen J.P., Hurme M. (2002) Association of an interleukin 1B gene polymorphism (-511) with Parkinson's disease in Finnish patients. J Med Genet 39:400-402
Mayr B., Schleger W., Loupal G., Burtscher H. (1991) Characterisation of complex karyotype changes in a canine thyroid adenoma. Res Vet Sci 50:298-300
McGeer P.L., McGeer E.G. (2001) Polymorphisms in inflammatory genes and the risk of Alzheimer disease. Arch Neurol 58:1790-1792
McMahon G. (2000) VEGF receptor signaling in tumor angiogenesis. Oncologist 5 Suppl 1:3-10
McMurray G., Casey J.H., Naylor A.M. (2006) Animal models in urological disease and sexual dysfunction. Br J Pharmacol 147 Suppl 2:S62-79
Mellone M., Rinaldi C., Massimi I., Petroni M., Veschi V., Talora C., Truffa S., Stabile H., Frati L., Screpanti I., Gulino A., Giannini G. (2008) Human papilloma virus-dependent HMGA1 expression is a relevant step in cervical carcinogenesis. Neoplasia 10:773-781
Meyer B., Loeschke S., Schultze A., Weigel T., Sandkamp M., Goldmann T., Vollmer E., Bullerdiek J. (2007) HMGA2 overexpression in non-small cell lung cancer. Mol Carcinog
Murua Escobar H., Meyer B., Richter A., Becker K., Flohr A.M., Bullerdiek J., Nolte I. (2003) Molecular characterization of the canine HMGB1. Cytogenet Genome Res 101:33-38
Murua Escobar H., Soller J.T., Richter A., Meyer B., Winkler S., Bullerdiek J., Nolte I. (2005) "Best friends" sharing the HMGA1 gene: comparison of the human and canine HMGA1 to orthologous other species. J Hered 96:777-781
Murua Escobar H., Soller J.T., Richter A., Meyer B., Winkler S., Flohr A.M., Nolte I., Bullerdiek J. (2004) The canine HMGA1. Gene 330:93-99
Murua Escobar H., Soller J.T., Sterenczak K.A., Sperveslage J.D., Schlueter C., Burchardt B., Eberle N., Fork M., Nimzyk R., Winkler S., Nolte I., Bullerdiek J. (2006) Cloning and characterization of the canine receptor for advanced glycation end products. Gene 369:45-52
Nakahara T., Moroi Y., Uchi H., Furue M. (2006) Differential role of MAPK signaling in human dendritic cell maturation and Th1/Th2 engagement. J Dermatol Sci 42:1-11
NCBI. NCBI Entrez Gene: HMGA1 [*Homo sapiens*]. (2010a) http://www.ncbi.nlm.nih.gov/gene/3159?ordinalpos=1&itool=EntrezSystem2.PEntrez.Gene.Gene_ResultsPanel.Gene_RVDocSum,
NCBI. NCBI Entrez Gene: Hmga1 [*Mus Musculus*]. (2010b) http://www.ncbi.nlm.nih.gov/gene/15361?ordinalpos=2&itool=EntrezSystem2.PEntrez.Gene.Gene_ResultsPanel.Gene_RVDocSum,
Nolte I., Nolte M. (2001) Praxis der Onkologie bei Hund und Katze. Enke Verlag,Stuttgart
Ohr R., Zeddies G. (2006) Ökonomische Gesamtbetrachtung der Hundehaltung in Deutschland. http://wwwuser.gwdg.de/~lstohr/Aktuelles/BetrachtungHundehaltung.pdf, Lehrstuhl für Wirtschaftspolitik, Georg-August-Universität Göttingen

Olson P.N. (2007) Using the canine genome to cure cancer and other diseases. Theriogenology 68:378-381

Ostrander E.A., Galibert F., Patterson D.F. (2000) Canine genetics comes of age. Trends Genet 16:117-124

Ostrander E.A., Giniger E. (1997) Semper fidelis: what man's best friend can teach us about human biology and disease. Am J Hum Genet 61:475-480

Paoloni M.C., Khanna C. (2007) Comparative oncology today. Vet Clin North Am Small Anim Pract 37:1023-1032; v

Pardali K., Moustakas A. (2007) Actions of TGF-beta as tumor suppressor and pro-metastatic factor in human cancer. Biochim Biophys Acta 1775:21-62

Park I.H., Yeon S.I., Youn J.H., Choi J.E., Sasaki N., Choi I.H., Shin J.S. (2004) Expression of a novel secreted splice variant of the receptor for advanced glycation end products (RAGE) in human brain astrocytes and peripheral blood mononuclear cells. Mol Immunol 40:1203-1211

Park L., Raman K.G., Lee K.J., Lu Y., Ferran L.J., Jr., Chow W.S., Stern D., Schmidt A.M. (1998) Suppression of accelerated diabetic atherosclerosis by the soluble receptor for advanced glycation endproducts. Nat Med 4:1025-1031

Patterson D.F. (2000) Companion animal medicine in the age of medical genetics. J Vet Intern Med 14:1-9

Petersen S., Soller J.T., Wagner S., Richter A., Bullerdiek J., Nolte I., Barcikowski S., Murua Escobar H. (2009) Co-transfection of plasmid DNA and laser-generated gold nanoparticles does not disturb the bioactivity of GFP-HMGB1 fusion protein. J Nanobiotechnology 7:6

Pöhler C. (2006) Construction of adeno-associated viruses for gene therapy and characterisation of cancer-related HMGA2 gene. Master Thesis, FB 2 Biology/Chemistry; MSc programme in Biochemistry & Molecular Biology, Centre for Humangenetics, University of Bremen, Bremen

Pullerits R., Bokarewa M., Dahlberg L., Tarkowski A. (2005) Decreased levels of soluble receptor for advanced glycation end products in patients with rheumatoid arthritis indicating deficient inflammatory control. Arthritis Res Ther 7:R817-824

Ramsey I.K., McKay J.S., Rudorf H., Dobson J.M. (1996) Malignant histiocytosis in three Bernese mountain dogs. Vet Rec 138:440-444

Reeves R., Adair J.E. (2005) Role of high mobility group (HMG) chromatin proteins in DNA repair. DNA Repair (Amst) 4:926-938

Reeves R., Beckerbauer L. (2001) HMGI/Y proteins: flexible regulators of transcription and chromatin structure. Biochim Biophys Acta 1519:13-29

Reeves R., Edberg D.D., Li Y. (2001) Architectural Transcription Factor HMGI(Y) Promotes Tumor Progression and Mesenchymal Transition of Human Epithelial Cells. Mol Cell Biol 21:575-594

Reimann N., Nolte I., Bartnitzke S., Bullerdiek J. (1999) Re: Sit, DNA, sit: cancer genetics going to the dogs. J Natl Cancer Inst 91:1688-1689.

Reimann N., Nolte I., Bonk U., Werner M., Bullerdiek J., Bartnitzke S. (1996) Trisomy 18 in a canine thyroid adenoma. Cancer Genet Cytogenet 90:154-156

Riehl A., Nemeth J., Angel P., Hess J. (2009) The receptor RAGE: Bridging inflammation and cancer. Cell Commun Signal 7:12

Rippe V., Drieschner N., Meiboom M., Murua Escobar H., Bonk U., Belge G., Bullerdiek J. (2003) Identification of a gene rearranged by 2p21 aberrations in thyroid adenomas. Oncogene 22:6111-6114

Riuzzi F., Sorci G., Donato R. (2007) RAGE expression in rhabdomyosarcoma cells results in myogenic differentiation and reduced proliferation, migration, invasiveness, and tumor growth. Am J Pathol 171:947-961

Rogalla P., Drechsler K., Kazmierczak B., Rippe V., Bonk U., Bullerdiek J. (1997) Expression of HMGI-C, a member of the high mobility group protein family, in a subset of breast cancers: relationship to histologic grade. Mol Carcinog 19:153-156

Rohr U.P., Heyd F., Neukirchen J., Wulf M.A., Queitsch I., Kroener-Lux G., Steidl U., Fenk R., Haas R., Kronenwett R. (2005) Quantitative real-time PCR for titration of infectious recombinant AAV-2 particles. J Virol Methods 127:40-45

Rouhiainen A., Kuja-Panula J., Wilkman E., Pakkanen J., Stenfors J., Tuominen R.K., Lepantalo M., Carpen O., Parkkinen J., Rauvala H. (2004) Regulation of monocyte migration by amphoterin (HMGB1). Blood 104:1174-1182

Scaffidi P., Misteli T., Bianchi M.E. (2002) Release of chromatin protein HMGB1 by necrotic cells triggers inflammation. Nature 418:191-195

Scala S., Portella G., Fedele M., Chiappetta G., Fusco A. (2000) Adenovirus-mediated suppression of HMGI(Y) protein synthesis as potential therapy of human malignant neoplasias. Proc Natl Acad Sci U S A 97:4256-4261

Schlueter C., Hauke S., Flohr A.M., Rogalla P., Bullerdiek J. (2003) Tissue-specific expression patterns of the RAGE receptor and its soluble forms--a result of regulated alternative splicing? Biochim Biophys Acta 1630:1-6

Schlueter C., Weber H., Meyer B., Rogalla P., Roser K., Hauke S., Bullerdiek J. (2005) Angiogenetic Signaling through Hypoxia: HMGB1: An Angiogenetic Switch Molecule. Am J Pathol 166:1259-1263

Schmidt A.M., Yan S.D., Yan S.F., Stern D.M. (2001) The multiligand receptor RAGE as a progression factor amplifying immune and inflammatory responses. J Clin Invest 108:949-955

Schoenmakers E.F., Wanschura S., Mols R., Bullerdiek J., Van den Berghe H., Van de Ven W.J. (1995) Recurrent rearrangements in the high mobility group protein gene, HMGI-C, in benign mesenchymal tumours. Nat Genet 10:436-444

Sgarra R., Zammitti S., Lo Sardo A., Maurizio E., Arnoldo L., Pegoraro S., Giancotti V., Manfioletti G. (2009) HMGA molecular network: From transcriptional regulation to chromatin remodeling. Biochim Biophys Acta 1799:37-47

Shchors K., Shchors E., Rostker F., Lawlor E.R., Brown-Swigart L., Evan G.I. (2006) The Myc-dependent angiogenic switch in tumors is mediated by interleukin 1beta. Genes Dev 20:2527-2538

Shelton G.D., Engvall E. (2005) Canine and feline models of human inherited muscle diseases. Neuromuscul Disord 15:127-138

Shweiki D., Itin A., Soffer D., Keshet E. (1992) Vascular endothelial growth factor induced by hypoxia may mediate hypoxia-initiated angiogenesis. Nature 359:843-845

Soller J.T., Beuing C., Escobar H.M., Winkler S., Reimann-Berg N., Drieschner N., Dolf G., Schelling C., Nolte I., Bullerdiek J. (2008) Chromosomal assignment of canine THADA gene to CFA 10q25. Mol Cytogenet 1:11

Soller J.T., Murua-Escobar H., Willenbrock S., Janssen M., Eberle N., Bullerdiek J., Nolte I. (2007) Comparison of the human and canine cytokines IL-1(alpha/beta) and TNF-alpha to orthologous other mammalians. J Hered 98:485-490

Soller J.T., Murua Escobar H., Janssen M., Fork M., Bullerdiek J., Nolte I. (2006) Cytokine genes single nucleotide polymorphism (SNP) screening analyses in canine malignant histiocytosis. Anticancer Res 26:3417-3420

Sparmann A., Bar-Sagi D. (2004) Ras-induced interleukin-8 expression plays a critical role in tumor growth and angiogenesis. Cancer Cell 6:447-458

Sparvero L.J., Asafu-Adjei D., Kang R., Tang D., Amin N., Im J., Rutledge R., Lin B., Amoscato A.A., Zeh H.J., Lotze M.T. (2009) RAGE (Receptor for Advanced Glycation Endproducts), RAGE ligands, and their role in cancer and inflammation. J Transl Med 7:17

Sterenczak K.A., Willenbrock S., Barann M., Klemke M., Soller J.T., Eberle N., Nolte I., Bullerdiek J., Murua Escobar H. (2009) Cloning, characterisation, and comparative quantitative expression analyses of receptor for advanced glycation end products (RAGE) transcript forms. Gene 434:35-42

Sternberg Z., Weinstock-Guttman B., Hojnacki D., Zamboni P., Zivadinov R., Chadha K., Lieberman A., Kazim L., Drake A., Rocco P., Grazioli E., Munschauer F. (2008) Soluble receptor for advanced glycation end products in multiple sclerosis: a potential marker of disease severity. Mult Scler 14:759-763

Straubinger A.F., Viveiros M.M., Straubinger R.K. (1999) Identification of two transcripts of canine, feline, and porcine interleukin-1 alpha. Gene 236:273-280

Taguchi A., Blood D.C., del Toro G., Canet A., Lee D.C., Qu W., Tanji N., Lu Y., Lalla E., Fu C., Hofmann M.A., Kislinger T., Ingram M., Lu A., Tanaka H., Hori O., Ogawa S., Stern D.M., Schmidt A.M. (2000) Blockade of RAGE-amphoterin signalling suppresses tumour growth and metastases. Nature 405:354-360

Takaha N., Resar L.M., Vindivich D., Coffey D.S. (2004) High mobility group protein HMGI(Y) enhances tumor cell growth, invasion, and matrix metalloproteinase-2 expression in prostate cancer cells. Prostate 60:160-167

Takeuchi A., Yamamoto Y., Tsuneyama K., Cheng C., Yonekura H., Watanabe T., Shimizu K., Tomita K., Yamamoto H., Tsuchiya H. (2007) Endogenous secretory receptor for advanced glycation endproducts as a novel prognostic marker in chondrosarcoma. Cancer 109:2532-2540

Tallini G., Vanni R., Manfioletti G., Kazmierczak B., Faa G., Pauwels P., Bullerdiek J., Giancotti V., Van Den Berghe H., Dal Cin P. (2000) HMGI-C and HMGI(Y) immunoreactivity correlates with cytogenetic abnormalities in lipomas, pulmonary chondroid hamartomas, endometrial polyps, and uterine leiomyomas and is compatible with rearrangement of the HMGI-C and HMGI(Y) genes. Lab Invest 80:359-369

Tamimi Y., van der Poel H.G., Denyn M.M., Umbas R., Karthaus H.F., Debruyne F.M., Schalken J.A. (1993) Increased expression of high mobility group protein I(Y) in high grade prostatic cancer determined by in situ hybridization. Cancer Res 53:5512-5516

Tamimi Y., van der Poel H.G., Karthaus H.F., Debruyne F.M., Schalken J.A. (1996) A retrospective study of high mobility group protein I(Y) as progression marker for prostate cancer determined by in situ hybridization. Br J Cancer 74:573-578

Tazi A., Moreau J., Bergeron A., Dominique S., Hance A.J., Soler P. (1999) Evidence that Langerhans cells in adult pulmonary Langerhans cell histiocytosis are mature dendritic cells: importance of the cytokine microenvironment. J Immunol 163:3511-3515

Thomas R., Duke S.E., Bloom S.K., Breen T.E., Young A.C., Feiste E., Seiser E.L., Tsai P.C., Langford C.F., Ellis P., Karlsson E.K., Lindblad-Toh K., Breen M. (2007) A cytogenetically characterized, genome-anchored 10-Mb BAC set and CGH array for the domestic dog. J Hered 98:474-484

van Beijnum J.R., Buurman W.A., Griffioen A.W. (2008) Convergence and amplification of toll-like receptor (TLR) and receptor for advanced glycation end products (RAGE) signaling pathways via high mobility group B1 (HMGB1). Angiogenesis 11:91-99

Vazzana N., Santilli F., Cuccurullo C., Davi G. (2009) Soluble forms of RAGE in internal medicine. Intern Emerg Med

Viswanathan S.R., Powers J.T., Einhorn W., Hoshida Y., Ng T.L., Toffanin S., O'Sullivan M., Lu J., Phillips L.A., Lockhart V.L., Shah S.P., Tanwar P.S., Mermel C.H., Beroukhim R., Azam M., Teixeira J., Meyerson M., Hughes T.P., Llovet J.M., Radich J., Mullighan C.G., Golub T.R., Sorensen P.H., Daley G.Q. (2009) Lin28 promotes transformation and is associated with advanced human malignancies. Nat Genet 41:843-848

von Ahsen I., Rogalla P., Bullerdiek J. (2006) Germ line mutations of the HMGA2 gene are rare among the general population. Anticancer Res 26:3289-3291

Wanschura S., Hennig Y., Deichert U., Schoenmakers E.F., Van de Ven W.J., Bartnitzke S., Bullerdiek J. (1995) Molecular-cytogenetic refinement of the 12q14-->q15 breakpoint region affected in uterine leiomyomas. Cytogenet Cell Genet 71:131-135

Waters D.J., Sakr W.A., Hayden D.W., Lang C.M., McKinney L., Murphy G.P., Radinsky R., Ramoner R., Richardson R.C., Tindall D.J. (1998) Workgroup 4: spontaneous prostate carcinoma in dogs and nonhuman primates. Prostate 36:64-67

Waters D.J., Wildasin K. (2006) Cancer clues from pet dogs. Sci Am 295:94-101

Wayne R.K., Ostrander E.A. (1999) Origin, genetic diversity, and genome structure of the domestic dog. Bioessays 21:247-257

Williams A.J., Powell W.L., Collins T., Morton C.C. (1997) HMGI(Y) expression in human uterine leiomyomata. Involvement of another high-mobility group architectural factor in a benign neoplasm. Am J Pathol 150:911-918

Winkler S., Murua Escobar H., Eberle N., Reimann-Berg N., Nolte I., Bullerdiek J. (2005) Establishment of a cell line derived from a canine prostate carcinoma with a highly rearranged karyotype. J Hered 96:782-785

Winkler S., Murua Escobar H., Meyer B., Simon D., Eberle N., Baumgartner W., Loeschke S., Nolte I., Bullerdiek J. (2007) HMGA2 expression in a canine model of prostate cancer. Cancer Genet Cytogenet 177:98-102

Withrow S.J., Vail D.M. (2007) Withrow & MacEwen's small animal clinical oncology. Saunders Elsevier,St. Louis, Mo.

Xiao S., Lux M.L., Reeves R., Hudson T.J., Fletcher J.A. (1997) HMGI(Y) activation by chromosome 6p21 rearrangements in multilineage mesenchymal cells from pulmonary hamartoma. Am J Pathol 150:901-910

Yan S.D., Fu J., Soto C., Chen X., Zhu H., Al-Mohanna F., Collison K., Zhu A., Stern E., Saido T., Tohyama M., Ogawa S., Roher A., Stern D. (1997) An intracellular protein that binds amyloid-beta peptide and mediates neurotoxicity in Alzheimer's disease. Nature 389:689-695

Yang D., Buchholz F., Huang Z., Goga A., Chen C.Y., Brodsky F.M., Bishop J.M. (2002) Short RNA duplexes produced by hydrolysis with Escherichia coli RNase III mediate effective RNA interference in mammalian cells. Proc Natl Acad Sci U S A 99:9942-9947

Yang R.B., Mark M.R., Gurney A.L., Godowski P.J. (1999) Signaling events induced by lipopolysaccharide-activated toll-like receptor 2. J Immunol 163:639-643

Yonekura H., Yamamoto Y., Sakurai S., Petrova R.G., Abedin M.J., Li H., Yasui K., Takeuchi M., Makita Z., Takasawa S., Okamoto H., Watanabe T., Yamamoto H. (2003) Novel splice variants of the receptor for advanced glycation end-products expressed in human vascular endothelial cells and pericytes, and their putative roles in diabetes-induced vascular injury. Biochem J 370:1097-1109

Zeggini E., Scott L.J., Saxena R., Voight B.F., Marchini J.L., Hu T., de Bakker P.I., et al. (2008) Meta-analysis of genome-wide association data and large-scale replication identifies additional susceptibility loci for type 2 diabetes. Nat Genet 40:638-645

Zhu X.M., Yao Y.M., Liang H.P., Xu S., Dong N., Yu Y., Sheng Z.Y. (2009) The effect of high mobility group box-1 protein on splenic dendritic cell maturation in rats. J Interferon Cytokine Res 29:677-686

Zienolddiny S., Ryberg D., Maggini V., Skaug V., Canzian F., Haugen A. (2004) Polymorphisms of the interleukin-1 beta gene are associated with increased risk of non-small cell lung cancer. Int J Cancer 109:353-356

7. Danksagung

Herrn Professor Dr. J. Bullerdiek danke ich für die Überlassung des Themas und die Diskussion dieser Arbeit. Ich danke ihm, dass ich diese Arbeit in dem Zentrum für Humangenetik in Bremen durchführen konnte sowie die damit verbundene wissenschaftliche Betreuung.

Herrn Professor Dr. I. Nolte danke für die vielen lehrreichen Jahre an der Klinik für Kleintiere in Hannover und für die Übernahme des Koreferats. Ich danke ihm besonders für die vielen Chancen, die er mir ermöglicht hat.

Herrn Dr. Hugo Murua Escobar danke ich für die geduldige Betreuung und zahlreichen wissenschaftlichen Gespräche und Anregungen.

Bedanken möchte ich mich auch bei Katharina „Kati“ Sterenczak und Saskia „Sassi“ Willenbrock, die mir mit ihren Erfahrungen immer tatkräftig zur Seite standen.

Mein besonderer Dank gilt auch den zahlreichen Kolleginnen und Kollegen, die mir mit ihrem Fachwissen, ihrer konstruktiven Kritik geholfen habe. Ich bedanke mich bei:
Dr. Nicola Reimann-Berg, PD Dr. Gazanfer Belge, Dr. Susanne Winkler, Andreas Richter, Siegfried Wagner, Merle Skischus und Norbert Drieschner.

Den Hannoveraner Kollegen vielen Dank für Verständnis und Unterstützung in der Klinik!

Schließlich möchte ich mich von ganzen Herzen bei meinen Eltern, meinem Bruder Sören Sönke und Senta Lück dafür bedanken, dass sie immer an das Zustandekommen dieser Arbeit geglaubt haben.

Mein Dank geht an meine liebe Freundin Sabine „Binchen“ Klein, die mich stets bestärkt hat. Sie hat mir die ganze Zeit den Rücken frei gehalten und daher widme ich ihr diese Arbeit.

8. Veröffentlichungen

Die folgenden Arbeiten sind in der Reihenfolge aufgezählt, wie sie auch im Ergebnisteil aufgelistet wurden.

I Murua Escobar H, Soller JT, Richter A, Meyer B, Winkler S, Flohr AM, Nolte I, Bullerdiek J.

The canine *HMGA1*.

Gene. 2004; 330: 93-9.

II Murua Escobar H, Soller JT, Richter A, Meyer B, Winkler S, Bullerdiek J, Nolte I.

"Best friends" sharing the *HMGA1* gene: comparison of the human and canine *HMGA1* to orthologous other species.

J Hered. 2005; 96: 777-81.

III Beuing C, Soller JT, Muth M, Wagner S, Dolf G, Schelling C, Richter A, Willenbrock S, Reimann-Berg N, Winkler S, Nolte I, Bullerdiek J, Murua Escobar H.

Genomic characterisation, chromosomal assignment and in vivo localisation of the canine high mobility group A1 (HMGA1) gene.

BMC Genet. 2008; 9: 49..

IV Joetzke A, Sterenczak KA, Eberle N, Wagner S, Soller JT, Nolte I, Bullerdiek J, Murua Escobar H, Simon D.

Expression of the high mobility group A1 (*HMGA1*) and A2 (*HMGA2*) in canine lymphoma: Analysis of 23 cases and comparison to control cases.

Vet Comp Oncol 2010; 8: 87-95.

V Fork MA, Murua Escobar H, Soller JT, Sterenczak KA, Willenbrock S, Winkler S, Dorsch M, Reimann-Berg N, Hedrich HJ, Bullerdiek J, Nolte I.

Establishing an *in vivo* model of canine prostate carcinoma using the new cell line CT1258.

BMC Cancer. 2008; 8: 240.

VI Soller JT, Murua Escobar H, Sterenczak KA, Willenbrock S, Fork MA, Bünger S, Pöhler C, Nolte, I., Bullerdiek, J.

Application of antisense *HMGA* AAVs suppresses cell proliferation in a canine carcinoma cell line.

in Vorbereitung 2010.

VII Petersen S, Soller JT, Wagner S, Richter A, Bullerdiek J, Nolte I, Barcikowski S, Murua Escobar H.

Co-transfection of plasmid DNA and laser-generated gold nanoparticles does not disturb the bioactivity of GFP-HMGB1 fusion protein.

Nanobiotechnology. 2009; 7: 6.

VIII Murua Escobar H, Soller JT, Sterenczak KA, Sperveslage JD, Schlueter C, Burchardt B, Eberle N, Fork M, Nimzyk R, Winkler S, Nolte I, Bullerdiek J.

Cloning and characterization of the canine receptor for advanced glycation end products.

Gene. 2006 369: 45-52.

IX Sterenczak KA, Willenbrock S, Barann M, Klemke M, Soller JT, Eberle N, Nolte I, Bullerdiek J, Murua Escobar H.

Cloning, characterisation, and comparative quantitative expression analyses of receptor for advanced glycation end products (*RAGE*) transcript forms.

Gene. 2009; 434: 35-42.

X Soller JT, Murua Escobar H, Janssen M, Fork M, Bullerdiek J, Nolte I.

Cytokine genes single nucleotide polymorphism (SNP) screening analyses in canine malignant histiocytosis.

Anticancer Res. 2006; 26: 3417-20.

XI Soller JT, Murua-Escobar H, Willenbrock S, Janssen M, Eberle N, Bullerdiek J, Nolte I.

Comparison of the human and canine cytokines IL-1 (α/β) and TNF-α to orthologous other mammalians.

J Hered. 2007; 98: 485-90.

XII Drieschner N, Kerschling S, Soller JT, Rippe V, Belge G, Bullerdiek J, Nimzyk R.

A domain of the thyroid adenoma associated gene (THADA) conserved invertebrates becomes destroyed by chromosomal rearrangements observed in thyroid adenomas.

Gene. 2007; 403: 110-7.

XIII Soller JT, Beuing C, Murua Escobar H, Winkler S, Reimann-Berg N, Drieschner N, Dolf G, Schelling C, Nolte I, Bullerdiek J.

Chromosomal assignment of canine *THADA* gene to CFA 10q25.

Mol Cytogenet. 2008; 1: 11.

.

I

The canine *HMGA1*.

Murua Escobar H, Soller JT, Richter A, Meyer B, Winkler S, Flohr AM, Nolte I, Bullerdiek J.

Gene. 2004 Apr 14; 330: 93-9.

Eigenleistung:

- Probensammlung und RNA Isolierung
- Durchführung der PCR
- SNP-Screening und *in silico* Analysen

Available online at www.sciencedirect.com
SCIENCE DIRECT®
Gene 330 (2004) 93–99
GENE
AN INTERNATIONAL JOURNAL ON GENES AND GENOMES
www.elsevier.com/locate/gene

The canine *HMGA1*

Hugo Murua Escobar[a,b], Jan T. Soller[a], Andreas Richter[a], Britta Meyer[a], Susanne Winkler[a], Aljoscha M. Flohr[a], Ingo Nolte[b], Jörn Bullerdiek[a,*]

[a] *Centre for Human Genetics, University of Bremen, Leobener Strasse ZHG, D-28359 Bremen, Germany*
[b] *Small Animal Clinic, School of Veterinary Medicine, Bischofsholer Damm 15, D-30173 Hanover, Germany*

Received 28 October 2003; received in revised form 19 December 2003; accepted 15 January 2004

Received by D.A. Tagle

Abstract

Due to the emerging advantages of numerous canine diseases as a genetic model for their human orthologs, the dog could join the mouse as the species of choice to unravel genetic mechanisms, e.g. of cancer predisposition, development and progression. However, precondition for such studies is the characterisation of the corresponding canine genes.

Human and murine HMGA1 non-histone proteins participate in a wide variety of cellular processes including regulation of inducible gene transcription, integration of retroviruses into chromosomes, and the induction of neoplastic transformation and promotion of metastatic progression of cancer cells.

Chromosomal aberrations affecting the human *HMGA1* gene at 6p21 were described in several tumours like pulmonary chondroid hamartomas, uterine leiomyomas, follicular thyroid adenomas and others. Over-expression of the proteins of *HMGA1* is characteristic for various malignant tumours suggesting a relation between high titer of the protein and the neoplastic phenotype.

In this study, we characterised the molecular structure of the canine *HMGA1* cDNA, its splice variants and predicted proteins HMGA1a and HMGA1b. Furthermore, we compared the coding sequence(s) (CDS) of both splice variants for 12 different breeds, screened them for single nucleotide polymorphisms (SNPs) and characterised a basic expression pattern.

Keywords: High mobility group proteins; *HMGA1*; *HMGA1a*; *HMGA1b*; Comparative genomics

1. Introduction

As witnessed by a number of recent articles (Kuska, 1996; Kingman, 2000; Ostrander et al., 2000; Vail and MacEwen, 2000), a growing number of scientists predict that human genetics will focus on the dog in this century (Kuska, 1996). Due to the emerging advantages of numerous canine diseases as a genetic model for their human counterparts, the dog could join the mouse as the species of choice to unravel genetic mechanisms, e.g. of cancer predisposition, development and progression.

The proteins of the human *HMGA1* gene HMGA1a and HMGA1b are associated with various human diseases including cancer. Due to the similarities of various human and canine cancer entities, the characterisation of the canine *HMGA1* gene could open new fields for experimental and therapeutic approaches.

Four human members of the HMGA protein family are presently known: the HMGA1a, HMGA1b, HMGA1c and HMGA2 proteins, which can modify chromatin structure by bending DNA, thus influencing the transcription of a number of target genes. The human *HMGA1* gene on 6p21 encodes the well characterised

Abbreviations: A, adenosine; aa, amino acid(s); BAC, bacterial artificial chromosome; bp, base pair(s); cDNA, DNA complementary to RNA; CDS, coding sequence(s); CFA, Canis familiaris; Ci, Curie; D, Dalton; dCTP, deoxycytidine 5′-triphosphate; DNA, deoxy-ribonucleic acid; DNase, deoxyribonuclease; G, guanosine; GAPDH, glyceraldehyde-3-phosphate dehydrogenase; HMG, high mobility group; HMGA1, high mobility group protein A1; HMGA2, high mobility group protein A2; HSA, *Homo sapiens*; M-MLV, Moloney murine leukemia virus; mRNA, messenger ribonucleic acid; NCBI, National Center for Biotechnology Information; ORF, open reading frame; PCR, polymerase chain reaction; RACE, rapid amplification of cDNA ends; RNA, ribonucleic acid; SDS, sodium dodecyl sulfate; SNP, single nucleotide polymorphism; UTR, untranslated region.

* Corresponding author. Tel.: +49-421-2184239; fax: +49-421-2184239.
E-mail address: bullerdiek@uni-bremen.de (J. Bullerdiek).

0378-1119/$ - see front matter © 2004 Elsevier B.V. All rights reserved.
doi:10.1016/j.gene.2004.01.009

HMGA1a and HMGA1b proteins (formerly known as HMGI and HMGY) derived by alternative splicing and the barely characterised HMGA1c variant, while the HMGA2 protein is encoded by a separate gene on chromosome 12 (12q14–15) (for review, Reeves and Beckerbauer, 2001).

Expression of HMGA1 is detectable only at very low levels or is even absent in adult tissues, whereas it is abundantly expressed in embryonic cells (Chiappetta et al., 1996). In humans, 6p21 is often affected by aberrations leading to an up-regulation of *HMGA1* in benign mesenchymal tumours, e.g. lipomas, uterine leiomyomas, pulmonary chondroid hamartomas and endometrial polyps (Williams et al., 1997; Kazmierczak et al., 1998; Tallini et al., 2000). Transcriptional activation due to a chromosomal alteration of *HMGA1* is probably an early and often even primary event of cancer development. In contrast, *HMGA1* expression in malignant epithelial tumours seems to be a rather late event associated with an aggressive behaviour of the tumours. Thus, an overexpression of *HMGA1* was reported for a number of malignancies including thyroid, prostatic, pancreatic, cervical and colorectal cancer (Tamimi et al., 1993; Chiappetta et al., 1995, 1998; Fedele et al., 1996; Bandiera et al., 1998; Abe et al., 1999, 2000). The correlation between *HMGA* expression and tumour aggressiveness in these malignancies has led to the conclusion that *HMGA* expression may present a powerful prognostic molecular marker. The causal role of *HMGA1* expression in the progression of carcinomas has been elucidated by a set of *in vitro* experiments involving *HMGA1* sense and antisense transfection assays (Reeves et al., 2001). An experimental approach aimed at the down-regulation of HMGA protein in tumours has been presented by Scala et al. (2000) who were able to show that an *HMGA1* antisense strategy using an adenoviral vector treatment of tumours induced in athymic mice caused a drastic reduction in tumour size.

Recently, the canine *HMGA1* gene has been mapped to CFA 23. This cytogenetic assignment indicates that the canine *HMGA1* gene does not map to a hotspot of chromosomal breakpoints seen in canine tumours (Becker et al., 2003). However, despite the emerging role of *HMGA1* gene expression in malignancies, the molecular characterisation of the canine *HMGA1* gene had not been carried out before. The characterisation of the molecular structure could permit new therapeutic approaches using the dog as model organism.

In this study, we characterised the molecular structure of the canine *HMGA1* gene on cDNA level, its splice variants and proteins HMGA1a and HMGA1b, and a basic expression pattern. Furthermore, for 12 different canine breeds the coding sequence(s) (CDS) of both splice variants were characterised and screened for SNPs to find out if changes at protein level exist between the different breeds.

2. Materials and methods

2.1. Tissues

The tissues used in this study were provided by the Small Animal Clinic, Veterinary School, Hanover, Germany. The breeds represented were Alsatian, Bull Terrier, Collie, Dachshund, Doberman Pinscher, German Shorthaired Pointer, Golden Retriever, Jack Russell Terrier, Kangal, Munsterland, West Highland Terrier and Yorkshire Terrier. From each breed up to three samples of testis tissue were taken and used for analyses.

2.2. cDNA characterisation

Total RNA was isolated from 150 mg canine testis tissue using TRIZOL LS (Invitrogen, Karlsruhe, Germany) following the manufacturer's protocol. To avoid genomic DNA contamination a DNase digest of each sample was performed using DNA-*free* (Ambion, Huntingdon, Cambridgeshire, UK). cDNA was synthesised using 3′-RACE adaptor primer AP2 (AAGGATCCGTCGACATC(17)T), 5 μg total RNA and M-MLV (Invitrogen) reverse transcriptase according to the manufacturer's instructions. The polymerase chain reactions (PCRs) for the molecular cloning of the cDNA were done using the primer pairs Ex1up and Ex8lo (5′ GCTCTTTTTAAGCTCCCCTGA 3′/5′ CTGTCCAGTCCCAGAAGGAA 3′) and primer pair Ex8up and 3′UTRlo (5′ AGGGCATCTCGCAGGAGTC 3′/5′ ATTCAAGTAACTGCAAATAGGA 3′) which were derived from human cDNA sequences (accession no. X14957). The PCR products were separated on a 1.5% agarose gel, recovered with QIAEX II (QIAGEN, Hilden, Germany), cloned in pGEM-T Easy vector system (Promega, Madison, USA) and sequenced. The cDNA contig and the homology alignments were created with Lasergene software (DNAStar, Madison, USA) and various sequences from the NCBI database (GenBank accession nos. X14957, X14958, NM_002131, NM_145899, NM_145900, NM_145901, NM_145902, NM_145903, NM_145904, NM_145905).

2.3. Characterisation of splice variants

The splice variants *HMGA1a* and *HMGA1b* were detected by amplifying a fragment spanning the CDS with primer pair Up (5′ CATCCCAGCCATCACTC 3′) and Lo (5′ GCGGCTGGTGTGCTGTGTAGTGTG 3′) using the canine testis cDNA samples as template. The primer pair was designed using the cDNA cloned as described in Section 2.2. The obtained PCR products were separated on a 4.0% agarose gel, recovered with QIAEX II (QIAGEN), cloned in pGEM-T Easy vector system (Promega) and sequenced. The contigs and the homology alignments were created with two sequences from the NCBI database (GenBank accession nos. X14957, X14958).

2.4. CDS comparison between breeds

The CDS of both splice variants were characterised for all breeds as described previously in Section 2.3. The contigs and the homology alignments were created using two sequences from the NCBI database (GenBank accession nos. X14957, X14958). In case of single nucleotide exchanges, the samples were sequenced again in both forward and reverse direction. Exchanges causing no amino acid (aa) substitution were not taken into account for further analyses. For all samples with aa substitutions the initial PCR was repeated and the exchange verified by sequencing the product in both forward and reverse direction. If possible, a restriction enzyme digestion was performed additionally.

2.5. Protein sequences

The canine HMGA1a and HMGA1b protein sequences were derived from the open reading frames (ORFs) of the characterised cDNA sequences described previously in Section 2.2. The protein homology alignments were created with two sequences from the NCBI database (GenBank accession nos. X14957, X14958).

2.6. Northern blot

Total RNAs were isolated from canine heart, lung, muscle, kidney and spleen tissue using RNeasy system (QIAGEN). An additional sample of total RNA was isolated from canine heart tissue by TRIZOL LS acid guanidine isothiocyanate–chloroform method (Invitrogen) in order to figure out whether this isolation method would lead to any difference in hybridisation. Further on poly A RNA was purified from canine spleen total RNA with OLIGOTEX (QIAGEN) and total RNA was prepared from human cultured fibroblasts by RNeasy system (QIAGEN). Spleen poly A RNA was placed on the blot in case that *HMGA1* was not detectable in the total RNA samples.

For Northern Blot hybridisation, 20 μg of total RNA from each sample with the exception of 10 μg of muscle and 3.6 μg of spleen poly A RNA were separated on a 1.2% denaturing agarose gel containing 0.65% formaldehyde. RNAs were transferred onto Hybond-N+ positive nylon membrane (Amersham Pharmacia Biotech, Freiburg, Germany) by capillary blot.

A 489-bp cDNA fragment derived from the canine HMGA1a sequence (exon 5/exon 8) served as a molecular probe for hybridisation. The probe was generated by PCR with the primer set Up and Lo (5′ CATCCCAGCCATCACTC 3′/5′ GCGGCTGGTGTGCTGTGTAGTGTG 3′) using the cloned cDNA described in Section 2.2. Probe labelling was performed by random primed labelling (Amersham Pharmacia Biotech) as described in the manufacturer's protocol with 50 μCi(α^{32}P)dCTP (Amersham Pharmacia Biotech). Purification of the labelled probe was performed using Sephadex G-50 Nick Columns (Amersham Pharmacia Biotech) and the probe was stored at −20 °C before use.

Using the PERFECTHYB PLUS hybridisation solution (Sigma-Aldrich, Saint Louis, MO, USA) prehybridisation was carried out for 30 min and hybridisation for 2.5 h at 68 °C. The membrane was washed for 5 min at room temperature in 2×SSC/0.1% SDS, and twice for 20 min at 68 °C in 0.5×SSC/0.1% SDS. Signals were visualised using a STORM phosphorimager (Molecular Dynamics, Sunnyvale, USA).

3. Results and discussion

3.1. The canine HMGA1 cDNA transcripts

For the human *HMGA1* gene various transcripts were described for both splicing variants (*HMGA1a* and *HMGA1b*) that differ in their 5′-UTR. The characterisation of the canine *HMGA1* cDNAs revealed that the complete canine *HMGA1* cDNA spans six exons and codes for two splicing variants *HMGA1a* with 1836 bp and *HMGA1b* with 1803 bp which are similar to the human transcripts (*HMGA1a* GenBank accession no. AY366390 and *HMGA1b* GenBank accession no. AY366392). The exon structure, the UTRs and the ORFs of both splice variants were defined and their homologies to their human counterparts analysed (Fig. 1, Table 1). The splicing variants showed the "typical" 33 bp gap which is conserved across various species such as human, mouse, hamster and rat (GenBank accession nos. BC013455, NM_016660, A7193763, NM_139327, A7511040). The homology of the canine cDNAs to their human counterparts is 80.6% for both splice variants. The 5′-UTR, CDS and the 3′-UTR showed homologies of 95.6%, 95.1% and 74,7%, respectively (Table 1). Homologies of the canine CDS with the CDS from mouse, hamster and rat on nucleotide level vary from 90.4% to 93.1%. The cDNA sequences were submitted to the NCBI database: *HMGA1a*, GenBank accession no. AY366390 and *HMGA1b,* GenBank accession no. AY366392.

3.2. The canine HMGA1a and HMGA1b proteins

The canine HMGA1a and HMGA1b protein sequences were deduced from the respective cDNA sequences. The canine HMGA1a protein is a 107-amino acid molecule with a calculated weight of 11,674.97 D and HMGA1b a 96-amino acid molecule with a calculated weight of 10,677.85 D (Fig. 2). Homology comparison to the human counterparts (GenBank accession nos. P17096, X14957) showed 100% homology of the molecules including the three "AT-hooks" and the acidic carboxy-terminal domain.

Comparison of the canine and human HMGA1a and HMGA1b proteins with the described mouse, rat and hamster molecules showed aa changes in positions 5, 34,

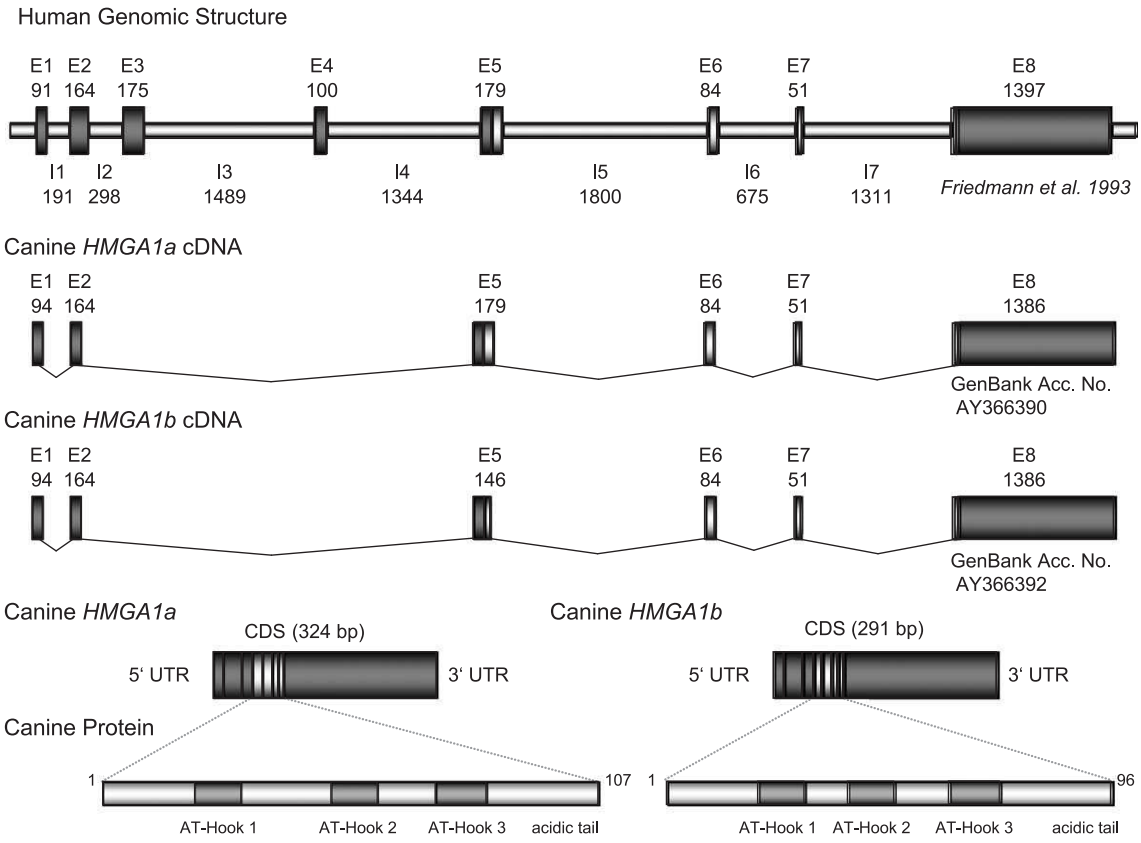

Fig. 1. Structure of the canine *HMGA1a* and *HMGA1b* transcripts and partial genomic structure.

69, 75 and 78 of HMGA1a and positions 5, 34, 58, 64 and 67 of HMGA1b, respectively (Fig. 2) (Johnson et al., 1988, 1989; Friedmann et al., 1993; Aldrich et al., 1999; Sgarra et al., 2000; Strausberg et al., 2002; Sgarra et al., 2003).

According to the definition of the AT-hooks (HMGA1a: I aa 21–31, II aa 53–63, III aa 78–89; HMGA1b: I aa 21–31, II aa 42–52, III aa 67–78) by Reeves and Nissen (1990) and Reeves (2000), none but the aa exchange at position 78 (HMGA1a) or 67 (HMGA1b), respectively, do affect the AT-hooks in either species. The exchange at position 78 leads to a difference in the third AT-hook of mouse and hamster when compared to the other species. According to the definition of the AT-hooks (HMGA1a: I aa 23–31, II aa 55–70, III aa 81–89; HMGA1b: I aa 23–31, II aa 44–59, III aa 70–78) by Huth et al. (1997), this aa exchange does not affect the third AT-hook. Following this definition, the second AT-hook is affected by the aa exchange at position 69 (HMGA1a) or 58 (HMGA1b), respectively.

Table 1
Detailed analysis of the canine *HMGA1a* and *HMGA1b* cDNA

Element of canine *HMGA1* cDNAs	Size in bp	Homology to human counterpart in %
Total cDNA *HMGA1a*	1836	80.6
Total cDNA *HMGA1b*	1803	80.6
5′-UTR	231	95.6
CDS *HMGA1a*	324	95.1
CDS *HMGA1b*	291	95.1
3′-UTR	1332	74.7
Exon 1	94	97.8
Exon 2	114	96.5
Exon 5 *HMGA1a*	179	93.9
Exon 5 *HMGA1b*	146	93.9
Exon 6	84	96.4
Exon 7	51	94.1
Exon 8	1386	75.4

Homology comparison of the cDNA elements of the canine *HMGA1* to its human counterpart (characterisation of the UTRs, the ORF and the exon sizes).

The canine protein sequences were submitted to the NCBI database with GenBank accession nos. HMGA1a AY366390 and HMGA1b AY366392.

Due to the identical structure of the canine HMGA proteins to the respective human molecule, therapeutic approaches applied in dogs could be more suitable in terms of transferability for the development of human therapies than to approaches tested in other organisms.

3.3. HMGA1a and HMGA1b CDS comparison between canine breeds

For twelve different canine breeds the splicing variants *HMGA1a* and *HMGA1b* were detected by amplification of a fragment spanning the CDS using the canine testis cDNA samples as template. The comparison of the characterised protein coding sequences for these twelve canine breeds

```
                                  ---------+---------+---------+---------+---------+----------

C. familiaris HMGA1a (AY366390)   1  MSESSSKSSQPLASKQEKDGTEKRGRGRPRKQPPVSPGTALVGSQKEPSEVPTPKRPRGR  60
C. familiaris HMGA1b (AY366392)   1  MSESSSKSSQPLASKQEKDGTEKRGRGRPRKQPP-----------KEPSEVPTPKRPRGR  49
H. sapiens HMGA1a (AAH08832)      1  MSESSSKSSQPLASKQEKDGTEKRGRGRPRKQPPVSPGTALVGSQKEPSEVPTPKRPRGR  60
H. sapiens HMGA1b (AAH04924)      1  MSESSSKSSQPLASKQEKDGTEKRGRGRPRKQPP-----------KEPSEVPTPKRPRGR  49
M. musculus HMGA1a (AAK66159)     1  MSESGSKSSQPLASKQEKDGTEKRGRGRPRKQPPVSPGTALVGSQKEPSEVPTPKRPRGR  60
M. musculus HMGA1b (AAK66158)     1  MSESGSKSSQPLASKQEKDGTEKRGRGRPRKQPP-----------KEPSEVPTPKRPRGR  49
R. norvegicus HMGA1a (NP_647543)  1  MSESGSKSSQPLASKQEKDGTEKRGRGRPRKQPSVSPGTALVGSQKEPSEVPTPKRPRGR  60
R. norvegicus HMGA1b (AAM74157)   1  MSESVSKSSQPLASKQEKDGTEKRGRGRPRKQPS-----------KEPSEVPTPKRPRGR  49
C. griseus HMGA1a (AAF06666)      1  MSESSSKSSQPLASKQEKDGTEKRGRGRPRKQPPVSPGTALVGSQKEPSEVPTPKRPRGR  60
C. griseus HMGA1b (AAF06667)      1  MSESSSKSSQPLASKQEKDGTEKRGRGRPRKQPP-----------KEPSEVPTPKRPRGR  49

                                  ---------+---------+---------+---------+-------

C. familiaris HMGA1a (AY366390)  61 PKGSKNKGAAKTRKTTTTPGRKPRGRPKKLEKEEEEGISQESSEEEQ 107
C. familiaris HMGA1b (AY366392)  50 PKGSKNKGAAKTRKTTTTPGRKPRGRPKKLEKEEEEGISQESSEEEQ  96
H. sapiens HMGA1a (AAH08832)     61 PKGSKNKGAAKTRKTTTTPGRKPRGRPKKLEKEEEEGISQESSEEEQ 107
H. sapiens HMGA1b (AAH04924)     50 PKGSKNKGAAKTRKTTTTPGRKPRGRPKKLEKEEEEGISQESSEEEQ  96
M. musculus HMGA1a (AAK66159)    61 PKGSKNKGAAKTRKVTTAPGRKPRGRPKKLEKEEEEGISQESSEEGQ 107
M. musculus HMGA1b (AAK66158)    50 PKGSKNKGAAKTRKVTTAPGRKPRGRPKKLEKEEEEGISQESSEEGQ  96
R. norvegicus HMGA1a (NP_647543) 61 PKGSKNKGTAKTRKVTTTPGRKPRGRPKKLEKEEEEGISQESSEEEQ 107
R. norvegicus HMGA1b (AAM74157)  50 PKGSKNKGTAKTRKVTTTPGRKPRGRPKKLEKEEEEGISQESSEEEQ  96
C. griseus HMGA1a (AAF06666)     61 PKGSKNKGAAKTRKATTAPGRKPRGRPKKLEKEEEEGISQESSEEEQ 107
C. griseus HMGA1b (AAF06667)     50 PKGSKNKGAAKTRKATTAPGRKPRGRPKKLEKEEEEGISQESSEEEQ  96
```

Fig. 2. Comparison of the canine, human, mouse, rat and hamster HMGA1a and HMGA1b proteins.

revealed one amino acid change in a single breed. Nucleotide exchanges causing no amino acid substitution were not taken into account in further analyses. Sample 2 (Teckel) showed in its *HMGA1b* transcript a nucleotide transition from A to G at the first base of codon 64 leading to an aa replacement from threonine to alanine and a new restriction recognition site for *Alu*I causing four (58, 100, 158 and 176 bp) instead of three fragments (58, 100 and 334 bp) to appear in an *Alu*I digest. (data not shown). The substitution was missing in the corresponding *HMGA1a* transcript of the dog suggesting a heterozygous genotype. A possible PCR artifact seems rather unlikely since the nucleotide transition was verified as described in Section 2.4. The CDS cDNA sequences of the twelve breeds were submitted to the NCBI database with GenBank accession nos. AY363606, AY363605, AY363607, AY363604, AY363608, AY363610, AY363609, AY363600, AY363603, AY363599, AY363601, AY363602, AY363994, AY363995, AY363611, AY363999, AY364000, AY364002, AY364001, AY363998, AY363996, AY363997, AY364003.

3.4. Canine HMGA1 expression analysis

Expression of human *HMGA1* is detectable at very low levels or is even absent in adult tissues whereas it is abundantly expressed in embryonic cells (Chiappetta et al., 1996). To elucidate a basic *HMGA1* gene expression pattern in dogs, a canine Northern blot was generated containing total RNA from canine spleen, heart, lung, muscle and kidney tissue samples. In order to detect a possible low level expression of *HMGA1* as reported in adult human tissues, a poly A RNA sample from canine spleen was additionally added to the blot. Hybridisation was performed with a α^{32}P-labelled canine *HMGA1a* cDNA probe. Except for the kidney total RNA and one of two heart samples (Trizol method) all total RNA samples showed a weak signal of approximately 1.8 kb (Fig. 3, Trizol sample not shown), while the poly A RNA spleen sample revealed a distinct signal. After stripping, rehybridisation with a canine *GAPDH* probe showed signals corresponding to approximately 1.3 kb in all but the Trizol method (data not shown) samples, indicating a degradation of the Trizol-prepared RNA.

In humans, *HMGA1* expression in malignant epithelial tumours seems to be associated with an aggressive behaviour of the tumours. Over-expression of *HMGA1* was reported for a number of malignancies including thyroid, prostatic, pancreatic, uterus cervical and colorectal cancer (Tamimi et al., 1993; Chiappetta et al., 1995, 1998; Fedele et al., 1996; Bandiera et al., 1998; Abe et al., 1999, 2000). The correlation between *HMGA* expression and tumour

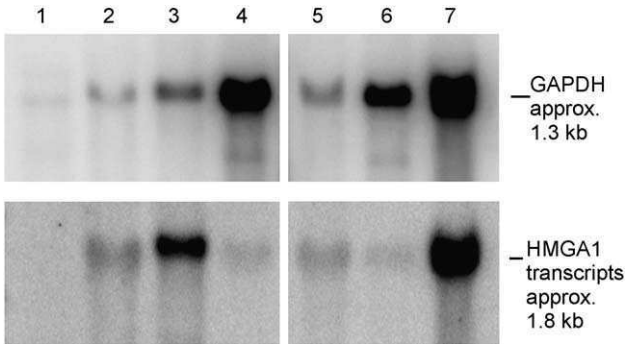

Fig. 3. Northern blot showing 1.8-kb *HMGA1* and 1.3-kb *GAPDH* transcripts. Lanes: (1) canine kidney total RNA, (2) canine spleen total RNA, (3) canine spleen poly A RNA, (4) canine heart total RNA, (5) canine lung total RNA, (6) canine muscle total RNA and (7) human fibroblasts total RNA.

aggressiveness in some of these malignancies has led to the conclusion that *HMGA* expression may present a powerful prognostic molecular marker.

So far no studies analysing the *HMGA1* expression pattern in canine tumours have been carried out. Since these tumours occur spontaneously in dogs as well as in humans a canine *in vivo* analysing system could have significant value for research and drug development.

The causal role of *HMGA1* expression in the progression of carcinomas has been elucidated by a set of *in vitro* experiments involving *HMGA1* sense and antisense transfection assays (Wood et al., 2000a,b; Reeves et al., 2001). A proof of concept for a therapy aimed at the down-regulation of HMGA protein in tumours has been presented by Scala et al. (2000) who were able to show that an *HMGA1* antisense strategy using an adenoviral vector treatment of tumours induced in athymic mice caused a drastic reduction in tumour size.

Due to the similarities of human and canine tumours, the transfer of such experimental approaches could benefit cancer research in either species.

The comprehension of the canine *HMGA1* gene and its gene products could be the precondition for future new experimental approaches and for evaluating the canine gene product as potential target for therapeutic strategies using the dog as model system.

References

Abe, N., Watanabe, T., Sugiyama, M., Uchimura, H., Chiappetta, G., Fusco, A., Atomi, Y., 1999. Determination of high mobility group I(Y) expression level in colorectal neoplasias: a potential diagnostic marker. Cancer Res. 59, 1169–1174.

Abe, N., Watanabe, T., Masaki, T., Mori, T., Sugiyama, M., Uchimura, H., Fujioka, Y., Chiappetta, G., Fusco, A., Atomi, Y., 2000. Pancreatic duct cell carcinomas express high levels of high mobility group I(Y) proteins. Cancer Res. 60, 3117–3122.

Aldrich, T.L., Reeves, R., Lee, C.C., Thomas, J.N., Morris, A.E., 1999. HMG-I (Y) proteins implicated in amplification of CHO cell DNA. Unpublished, GenBank Accession No. AF193763.

Bandiera, A., Bonifacio, D., Manfioletti, G., Mantovani, F., Rustighi, A., Zanconati, F., Fusco, A., Di Bonito, L., Giancotti, V., 1998. Expression of HMGI (Y) proteins in squamous intraepithelial and invasive lesions of the uterine cervix. Cancer Res. 58, 426–431.

Becker, K., Escobar, H.M., Richter, A., Meyer, B., Nolte, I., Bullerdiek, J., 2003. The canine *HMGA1* gene maps to CFA 23. Anim. Genet. 34, 68–69.

Chiappetta, G., Bandiera, A., Berlingieri, M.T., Visconti, R., Manfioletti, G., Battista, S., Martinez-Tello, F.J., Santoro, M., Giancotti, V., Fusco, A., 1995. The expression of the high mobility group HMGI (Y) proteins correlates with the malignant phenotype of human thyroid neoplasias. Oncogene 10, 1307–1314.

Chiappetta, G., Avantaggiato, V., Visconti, R., Fedele, M., Battista, S., Trapasso, F., Merciai, B.M., Fidanza, V., Giancotti, V., Santoro, M., Simeone, A., Fusco, A., 1996. High level expression of the HMGI (Y) gene during embryonic development. Oncogene 13, 2439–2446.

Chiappetta, G., Tallini, G., De Biasio, M.C., Manfioletti, G., Martinez-Tello, F.J., Pentimalli, F., de Nigris, F., Mastro, A., Botti, G., Fedele, M., Berger, N., Santoro, M., Giancotti, V., Fusco, A., 1998. Detection of high mobility group I HMGI (Y) protein in the diagnosis of thyroid tumors: HMGI (Y) expression represents a potential diagnostic indicator of carcinoma. Cancer Res. 58, 4193–4198.

Fedele, M., Bandiera, A., Chiappetta, G., Battista, S., Viglietto, G., Manfioletti, G., Casamassimi, A., Santoro, M., Giancotti, V., Fusco, A., 1996. Human colorectal carcinomas express high levels of high mobility group HMGI (Y) proteins. Cancer Res. 56, 1896–1901.

Friedmann, M., Holth, L.T., Zoghbi, H.Y., Reeves, R., 1993. Organization, inducible-expression and chromosome localization of the human HMG-I (Y) nonhistone protein gene. Nucleic Acids Res. 21, 4259–4267.

Huth, J.R., Bewley, C.A., Nissen, M.S., Evans, J.N., Reeves, R., Gronenborn, A.M., Clore, G.M., 1997. The solution structure of an HMG-I (Y)-DNA complex defines a new architectural minor groove binding motif. Nat. Struct. Biol. 4, 657–665.

Johnson, K.R., Lehn, D.A., Elton, T.S., Barr, P.J., Reeves, R., 1988. Complete murine cDNA sequence, genomic structure, and tissue expression of the high mobility group protein HMG-I (Y). J. Biol. Chem. 263, 18338–18342.

Johnson, K.R., Lehn, D.A., Reeves, R., 1989. Alternative processing of mRNAs encoding mammalian chromosomal high-mobility-group proteins HMG-I and HMG-Y. Mol. Cell. Biol. 9, 2114–2123.

Kazmierczak, B., Dal Cin, P., Wanschura, S., Borrmann, L., Fusco, A., Van den Berghe, H., Bullerdiek, J., 1998. HMGIY is the target of 6p21.3 rearrangements in various benign mesenchymal tumors. Genes Chromosomes Cancer 23, 279–285.

Kingman, S., 2000. Painting a brighter future for dogs and humans. Drug Discov. Today 5, 127–128.

Kuska, B., 1996. Sit, DNA, sit: cancer genetics going to the dogs. J. Natl. Cancer Inst. 91, 204–206.

Ostrander, E.A., Galibert, F., Patterson, D.F., 2000. Canine genetics comes of age. Trends Genet. 16, 117–124.

Reeves, R., 2000. Structure and function of the HMGI (Y) family of architectural transcription factors. Environ. Health Perspect. 108 (Suppl. 5), 803–809.

Reeves, R., Beckerbauer, L., 2001. HMGI (Y) proteins: flexible regulators of transcription and chromatin structure. Biochim. Biophys. Acta 1519, 13–29.

Reeves, R., Nissen, M.S., 1990. The A.T-DNA-binding domain of mammalian high mobility group I chromosomal proteins. A novel peptide motif for recognizing DNA structure. J. Biol. Chem. 265, 8573–8582.

Reeves, R., Edberg, D.D., Li, Y., 2001. Architectural transcription factor HMGI (Y) promotes tumor progression and mesenchymal transition of human epithelial cells. Mol. Cell. Biol. 21, 575–594.

Scala, S., Portella, G., Fedele, M., Chiappetta, G., Fusco, A., 2000. Adenovirus-mediated suppression of HMGI (Y) protein synthesis as potential therapy of human malignant neoplasias. Proc. Natl. Acad. Sci. U. S. A. 97, 4256–4261.

Sgarra, R., Diana, F., Bellarosa, C., Rustighi, A., Toller, M., Manfioletti, G., Giancotti, V., 2000: Increase of HMGA1a protein methylation is a distinctive characteristic of tumor cells induced to apoptosis. Unpublished, GenBank Accession No. AF511040.

Sgarra, R., Diana, F., Bellarosa, C., Dekleva, V., Rustighi, A., Toller, M., Manfioletti, G., Giancotti, V., 2003. During apoptosis of tumor cells HMGA1a protein undergoes methylation: identification of the modification site by mass spectrometry. Biochemistry 42, 3575–3585.

Strausberg, R.L., et al., 2002. Generation and initial analysis of more than 15,000 full-length human and mouse cDNA sequences. Proc. Natl. Acad. Sci. U. S. A. 99, 16899–16903.

Tallini, G., Vanni, R., Manfioletti, G., Kazmierczak, B., Faa, G., Pauwels, P., Bullerdiek, J., Giancotti, V., Van Den Berghe, H., Dal Cin, P., 2000. HMGI-C and HMGI (Y) immunoreactivity correlates with cytogenetic abnormalities in lipomas, pulmonary chondroid hamartomas, endometrial polyps, and uterine leiomyomas and is compatible with rearrangement of the HMGI-C and HMGI (Y) genes. Lab. Invest. 80, 359–369.

Tamimi, Y., van der Poel, H.G., Denyn, M.M., Umbas, R., Karthaus, H.F., Debruyne, F.M., Schalken, J.A., 1993. Increased expression of high

mobility group protein I(Y) in high grade prostatic cancer determined by in situ hybridization. Cancer Res. 53, 5512–5516.

Vail, D.M., MacEwen, E.G., 2000. Spontaneously occurring tumors of companion animals as models for human cancer. Cancer Invest. 18, 781–792.

Williams, A.J., Powell, W.L., Collins, T., Morton, C.C., 1997. HMGI (Y) expression in human uterine leiomyomata. Involvement of another high-mobility group architectural factor in a benign neoplasm. Am. J. Pathol. 150, 911–918.

Wood, L.J., Maher, J.F., Bunton, T.E., Resar, L.M., 2000a. The oncogenic properties of the HMG-I gene family. Cancer Res. 60, 4256–4261.

Wood, L.J., Mukherjee, M., Dolde, C.E., Xu, Y., Maher, J.F., Bunton, T.E., Williams, J.B., Resar, L.M., 2000b. HMG-I/Y, a new c-Myc target gene and potential oncogene. Mol. Cell. Biol. 20, 5490–5502.

II

“Best friends” sharing the *HMGA1* gene: comparison of the human and canine *HMGA1* to orthologous other species.

Murua Escobar H, Soller JT, Richter A, Meyer B, Winkler S, Bullerdiek J, Nolte I.

J Hered. 2005; 96(7): 777-81.

Eigenleistung:

- *in silico* Analysen und Interspezies-Alignments
- grafische Auswertung

Journal of Heredity 2005:96(7):777–781
doi:10.1093/jhered/esi083
Advance Access publication June 15, 2005

"Best Friends" Sharing the *HMGA1* Gene: Comparison of the Human and Canine HMGA1 to Orthologous Other Species

H. Murua Escobar, J. T. Soller, A. Richter, B. Meyer, S. Winkler, J. Bullerdiek, and I. Nolte

From the Small Animal Clinic, School of Veterinary Medicine, Bischofsholer Damm 15, 30137 Hanover, Germany (Murua Escobar, Soller, and Nolte), and Center for Human Genetics, University of Bremen, Leobener Str ZHG, 28359 Bremen, Germany (Meyer, Winkler, Richter, and Bullerdiek).

Address correspondence to Ingo Nolte at the address above, or e-mail: inolte@klt.tiho-hannover.de.

Abstract

HMGA1 nonhistone proteins are reported to participate in various cellular processes including regulation of inducible gene transcription, integration of retroviruses into chromosomes, and the induction of neoplastic transformation and promotion of metastatic progression of cancer cells. Overexpression of *HMGA1* was shown to be characteristic for various malignant tumors, suggesting a relation between the neoplastic phenotype and a high titer of the protein. Also chromosomal aberrations affecting the human *HMGA1* gene at 6p21 were described in several tumors, e.g., uterine leiomyomas, pulmonary chondroid hamartomas, and follicular thyroid adenomas. We characterize the molecular structure of the canine *HMGA1* cDNA, its splice variants, and predicted proteins HMGA1a and HMGA1b. Furthermore, we compared the CDS of both splice variants for 12 different breeds, screened them for SNPs, characterised a basic expression pattern, and mapped the gene via FISH. Additionally, we compared the known human, canine, murine, rat, hamster, bovine, pig, *Xenopus*, and chicken *HMGA1* transcripts.

High mobility group proteins named according to their characteristic mobility in gel electrophoresis are small chromatin-associated nonhistone proteins, which can be subdivided into three families because of their functional sequence motives: the HMGA (functional motive "AT-hook"), HMGB (functional motive "HMG-box"), and HMGN (functional motive "nucleosomal binding domain") protein families (for review see Bustin 2001). By binding DNA with their functional motives, the HMG proteins induce DNA conformation changes influencing the binding of various transcription factors and thus taking indirect influence on transcription regulation as so-called architectural transcription factors (for detail see Bustin and Reeves 1996).

The proteins HMGA1a, HMGA1b, and HMGA2 of the human *HMGA* genes are associated with various human diseases, including cancer. Members of the human HMGA1 protein family presently known are HMGA1a and HMGA1b, which by modifying chromatin structure take influence on transcription and up- and down-regulation of a number of target genes, for example, *ATF2*, *IFN-β*, *NF-κB*, *Interleukin-2 receptor*, *E-Selektin, Interleukin-4*, *Interfeone-A*, *ERCC1*, and *Cyclin A* (Chuvpilo et al. 1993; Du and Maniatis 1994; Thanos and Maniatis 1992; Lewis et al. 1994; John et al. 1995, 1996; Klein-Hessling et al. 1996; Yie et al. 1997; Borrmann et al. 2003).

The expression pattern of the *HMGA* genes in human adult tissues shows only very low levels or even absent expression, whereas it is abundantly expressed in embryonic cells (Rogalla et al. 1996; Chiappetta et al. 1996). In humans the *HMGA1* gene is located on HSA 6p21, a region often affected by aberrations leading to an up-regulation of this gene in various benign mesenchymal tumors, for example, endometrial polyps, lipomas, pulmonary chondroid hamartomas, and uterine leiomyomas (Williams et al. 1997; Kazmierczak et al. 1998; Tallini et al. 2000). This suggests that transcriptional activation due to these chromosomal alterations is probably an early and often even primary event of cancer development. Recently, the canine *HMGA1* gene has been mapped to CFA 23. This cytogenetic assignment

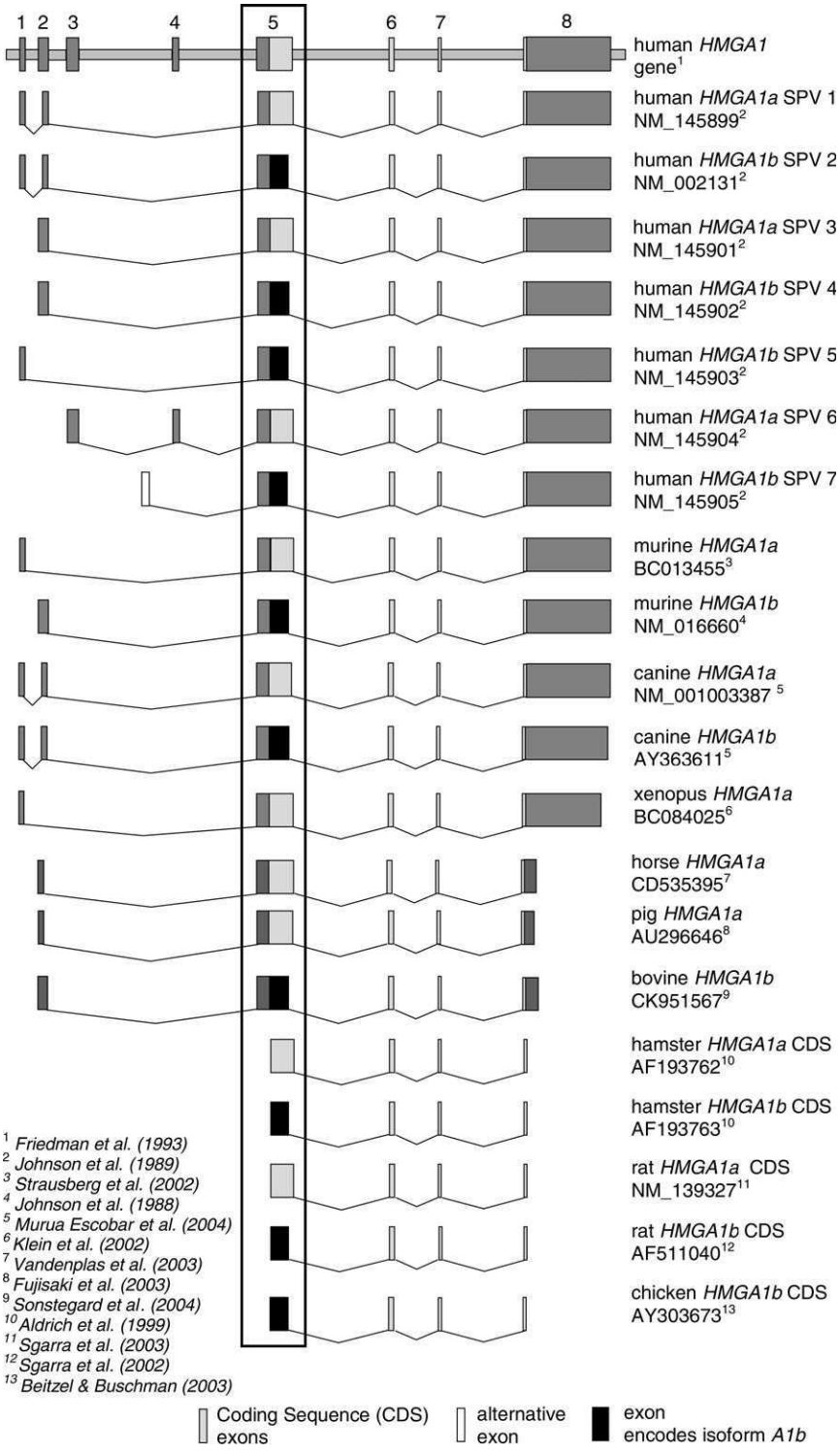

Figure 1. Species comparison of *HMGA1a* and *HMGA1b* transcripts. Exon 5 is enlarged by factor fife for better visualization.

indicates that the canine *HMGA1* gene does not map to a hotspot of chromosomal breakpoints seen in canine tumours (Becker et al. 2003).

HMGA1 expression in human malignant epithelial tumors is reported to be associated with an aggressive behavior of the tumors. Overexpression of *HMGA1* was

detected in a number of malignancies, including thyroid, prostatic, pancreatic, uterine cervical, and colorectal cancer (Tamimi et al. 1993; Chiappetta et al. 1995; Fedele et al. 1996; Bandiera et al. 1998; Abe et al. 1999, 2000; Czyz et al. 2004; Takaha et al. 2004). The correlation between *HMGA* expression and tumor aggressiveness in some of these malignancies has led to the conclusion that *HMGA* expression may present a powerful diagnostic and prognostic molecular marker.

Due to the similarities of various human and canine cancer entities, the characterization of the canine *HMGA* genes could open new fields for experimental and therapeutic approaches. We recently characterized the canine *HMGA1a* and *HMGA1b* transcripts, deduced their proteins, evaluated them as targets for therapeutic approaches, and characterized a basic expression pattern in healthy tissues (Murua Escobar et al. 2004). Sequence comparison showed a 100% identity between the human and canine protein molecules. Although both species showed the identical two proteins, the number of found cDNA transcripts varies. For the human *HMGA1* seven different cDNA transcripts (Figure 1: SPV1–SPV7) were described (Johnson et al. 1988) of which SPV1 and SPV2 are the commonly found variants. The characterized dog variants showed the same composition structure as the mentioned human variants SPV1 and SPV2. Canine counterparts of the human transcript variants SPV3–SPV7 could not be detected using polymerase chain reaction (PCR) amplification approaches. Comparison of the human cDNAs to the known transcripts of other species shows that the dog is the only species showing similar transcripts to those commonly found in humans referring to exon structure and distribution. In detail, human and dog are the only known species showing the presence of exon one and two in both *HMGA1a* or *HMGA1b* transcripts, respectively (Figure 1). Both isoforms (*HMGA1a* and *HMGA1b)* were found in mouse (BC013455, NM_016660), hamster (AF1893762, AF193763), and rat (NM_139327, AF511040), of which for the last two species the described transcripts are limited to the protein coding sequences and the mouse transcripts show either exon one (*HMGA1a*) or exon two (*HMGA1b*) in the respective transcripts (Figure 1).

For the *HMGA1* transcripts of horse (CD535395), pig (AU296646), chicken (AY303673), bovine (CK951567), and *Xenopus* (BC084025), either the *HMGA1a* or the *HMGA1b* isoform are currently (2004) present at the NCBI database. For CDS (coding sequence) and protein identity analysis, we used the described sequences and deduced, if necessary, the corresponding parts for analyses. The in silico analyses were done using Lasergene software programs (DNASTAR, Madison). The coding sequence identities of the canine *HMGA1* transcripts to the sequences from other species vary between 72.0% (chicken AY303673) and 95.7% (pig AU296646, horse CD535395) (Table 1). Identity comparison of the deduced proteins revealed similarities between 69.7% (chicken AY303673) and 100.0% (human: P17096, X14957, horse CD535395) (Table 1). The proteins of all species showed strong conservation in the functional AT-Hook DNA binding domains. Common for all species analysed is that the protein coding sequences are composed of four exons (Figure 1). The described proteins of the different species are composed of 107 amino acids and 96 amino acids, respectively, for HMGA1a and HMGA1b. Also common for those species where both protein isoforms were described is that the difference between the splicing variants is the "typical" 33-bp deletion in the *HMGA1b* transcripts resulting in the lack of 11 amino acids.

Table 1. *HMGA1* identity comparison (CDS and protein) of various species to the canine transcripts and proteins

Species	Isoform	Identity (%) to *C. familiaris*	
		CDS	Protein
Human (*H. sapiens*)	*HMGA1a*	95.1	100.0
Human (*H. sapiens*)	*HMGA1b*	95.1	100.0
Mouse (*M. musculus*)	*HMGA1a*	90.1	96.3
Mouse (*M. musculus*)	*HMGA1b*	90.1	96.9
Rat (*R. norvegicus*)	*HMGA1a*	90.4	96.3
Rat (*R. norvegicus*)	*HMGA1b*	90.4	95.8
Hamster (*C. griseus*)	*HMGA1a*	92.6	98.1
Hamster (*C. griseus*)	*HMGA1b*	92.6	97.9
Pig (*S. scrofa*)	*HMGA1a*	95.7	99.1
Horse (*E. caballus*)	*HMGA1b*	95.7	100.0
Cattle (*B. taurus*)	*HMGA1b*	94.4	99.0
Chicken (*G. gallus*)	*HMGA1b*	72.0	69.7
African clawed frog (*X. laevis*)	*HMGA1a*	90.4	97.2

Previous results describing the comparison of the protein coding sequences in 12 canine breeds revealed that the mentioned deletion is also conserved in the analyzed breeds. SNP screening in these breeds resulted in detection of one-amino-acid change in a single breed. A Teckel showed a nucleotide transition from A to G at the first base of codon 64 in its *HMGA1b* transcript leading to an amino acid replacement from threonine to alanine (Murua Escobar et al. 2004). As far as we know, no other canine *HMGA1* polymorphisms have been described. Summarizing the *HMGA1* transcript and protein comparison data emphasizes the relevance of the canine species as a model organism for the research and development of therapeutic approaches for human disorders.

Due to the mentioned properties of the *HMGA1* gene, its proteins HMGA1a/HMGA1b, and its reported role in development of cancer, future studies targeting HMGA1 proteins could be of significant value.

Acknowledgments

This paper was delivered at the 2nd International Conference on the "Advances in Canine and Feline Genomics: Comparative Genome Anatomy and Genetic Disease," Universiteit Utrecht, Utrecht, The Netherlands, October 14–16, 2004.

References

Abe N, Watanabe T, Masaki T, Mori T, Sugiyama M, Uchimura H, Fujioka Y, Chiappetta G, Fusco A, and Atomi Y, 2000. Pancreatic duct cell carcinomas express high levels of high mobility group I(Y) proteins. Cancer Res 60: 3117–3122.

Abe N, Watanabe T, Sugiyama M, Uchimura H, Chiappetta G, Fusco A, and Atomi Y, 1999. Determination of high mobility group I(Y) expression level in colorectal neoplasias: a potential diagnostic marker. Cancer Res 59:1169–1174.

Aldrich TL, Reeves R, Lee CC, Thomas JN, and Morris AE, 1999. HMG-I(Y) proteins implicated in amplification of CHO cell DNA. Sequence at NCBI AF193763. Unpublished manuscript.

Bandiera A, Bonifacio D, Manfioletti G, Mantovani F, Rustighi A, Zanconati F, Fusco A, Di Bonito L, and Giancotti V, 1998. Expression of HMGI(Y) proteins in squamous intraepithelial and invasive lesions of the uterine cervix. Cancer Res 58:426–431.

Becker K, Murua Escobar H, Richter A, Meyer B, Nolte I, and Bullerdiek J, 2003. The canine HMGA1 gene maps to CFA 23. Anim Genet 34(1): 68–69.

Beitzel B and Bushman F, 2003. Construction and analysis of cells lacking the HMGA gene family. Nucleic Acids Res 31(17):5025–5032.

Borrmann L, Schwanbeck R, Heyduk T, Seebeck B, Rogalla P, Bullerdiek J, and Wisniewski JR, 2003. High mobility group A2 protein and its derivatives bind a specific region of the promoter of DNA repair gene ERCC1 and modulate its activity. Nucleic Acids Res 31:6841–6851.

Bustin M, 2001. Revised nomenclature for high mobility group (HMG) chromosomal proteins. Trends Biochem Sci 26(3):152–153.

Bustin M and Reeves R, 1996. High-mobility-group chromosomal proteins: architectural components that facilitate chromatin function. Prog Nucleic Acid Res Mol Biol 54:35–100.

Chiappetta G, Bandiera A, Berlingieri MT, Visconti R, Manfioletti G, Battista S, Martinez-Tello FJ, Santoro M, Giancotti V, and Fusco A, 1995. The expression of the high mobility group HMGI (Y) proteins correlates with the malignant phenotype of human thyroid neoplasias. Oncogene 10:1307–1314.

Chiappetta G, Avantaggiato V, Visconti R, Fedele M, Battista S, Trapasso F, Merciai BM, Fidanza V, Giancotti V, Santoro M, Simeone A, and Fusco A, 1996. High level expression of the HMGI (Y) gene during embryonic development. Oncogene 13:2439–2446.

Chuvpilo S, Schomberg C, Gerwig R, Heinfling A, Reeves R, Grummt F, and Serfling E, 1993. Multiple closely-linked NFAT/octamer and HMG I(Y) binding sites are part of the interleukin-4 promoter. Nucleic Acids Res 21(24):5694–5704.

Czyz W, Balcerczak E, Jakubiak M, Pasieka Z, Kuzdak K, and Mirowski M, 2004. HMGI(Y) gene expression as a potential marker of thyroid follicular carcinoma. Langenbecks Arch Surg 389(3):193–197.

Du W and Maniatis T, 1994. The high mobility group protein HMG I(Y) can stimulate or inhibit DNA binding of distinct transcription factor ATF-2 isoforms. Proc Natl Acad Sci USA 91:11318–11322.

Fedele M, Bandiera A, Chiappetta G, Battista S, Viglietto G, Manfioletti G, Casamassimi A, Santoro M, Giancotti V, and Fusco A, 1996. Human colorectal carcinomas express high levels of high mobility group HMGI(Y) proteins. Cancer Res 56:1896–1901.

Friedmann M, Holth LT, Zoghbi HY, and Reeves R, 1993. Organization, inducible-expression and chromosome localization of the human HMG-I(Y) nonhistone protein gene. Nucleic Acids Res 21(18):4259–4267.

Fujisaki S, Hiraiwa H, Eguchi T, Watanabe Y, Honma D, Saitou T, and Yasue H, 2003. Construction of a full-length library of swine olfactory bulb and its preliminary characterization. Sequence at NCBI AU296646. Unpublished manuscript.

John S, Reeves RB, Lin JX, Child R, Leiden JM, Thompson CB, and Leonard WJ, 1995. Regulation of cell-type-specific interleukin-2 receptor alpha-chain gene expression: potential role of physical interactions between Elf-1, HMG-I(Y), and NF-kappa B family proteins. Mol Cell Biol 15: 1786–1796.

John S, Robbins CM, and Leonard WJ, 1996. An IL-2 response element in the human IL-2 receptor alpha chain promoter is a composite element that binds Stat5, Elf-1, HMG-I(Y) and a GATA family protein. EMBO J 15:5627–5635.

Johnson KR, Lehn DA, Elton TS, Barr PJ, and Reeves R, 1988. Complete murine cDNA sequence, genomic structure, and tissue expression of the high mobility group protein HMG-I(Y). J Biol Chem 263(34): 18338–18342.

Johnson KR, Lehn DA, and Reeves R, 1989. Alternative processing of mRNAs encoding mammalian chromosomal high-mobility-group proteins HMG-I and HMG-Y. Mol Cell Biol 9(5):2114–2123.

Kazmierczak B, Dal Cin P, Wanschura S, Borrmann L, Fusco A, Van den Berghe H, and Bullerdiek J, 1998. HMGIY is the target of 6p21.3 rearrangements in various benign mesenchymal tumors. Genes Chromosomes Cancer 23:279–285.

Klein SL, Strausberg RL, Wagner L, Pontius J, Clifton SW, and Richardson P, 2002. Genetic and genomic tools for *Xenopus* research: the NIH *Xenopus* initiative. Dev Dyn 225(4):384–391.

Klein-Hessling S, Schneider G, Heinfling A, Chuvpilo S, and Serfling E, 1996. HMG I(Y) interferes with the DNA binding of NF-AT factors and the induction of the interleukin 4 promoter in T cells. Proc Natl Acad Sci USA 93:15311–15316.

Lewis H, Kaszubska W, DeLamarter JF, and Whelan J, 1994. Cooperativity between two NF-kappa B complexes, mediated by high-mobility-group protein I(Y), is essential for cytokine-induced expression of the E-selectin promoter. Mol Cell Biol 14:5701–5709.

Murua Escobar H, Soller JT, Richter A, Meyer B, Winkler S, Flohr AM, Nolte I, and Bullerdiek J, 2004. The canine HMGA1. Gene 14(330): 93–99.

Reeves R, Edberg DD, and Li Y, 2001. Architectural transcription factor HMGI(Y) promotes tumor progression and mesenchymal transition of human epithelial cells. Mol Cell Biol 21:575–594.

Rogalla P, Drechsler K, Frey G, Hennig Y, Helmke B, Bonk U, and Bullerdiek J, 1996. HMGI-C expression patterns in human tissues. Implications for the genesis of frequent mesenchymal tumors. Am J Pathol 149(3):775–779.

Sgarra R, Diana F, Bellarosa C, Rustighi A, Toller M, Manfioletti G, and Giancotti V, 2002. Increase of HMGA1a protein methylation is a distinctive characteristic of tumor cells induced to apoptosis. Sequence at NCBI AF511040. Unpublished manuscript.

Sgarra R, Diana F, Bellarosa C, Dekleva V, Rustighi A, Toller M, Manfioletti G, and Giancotti V, 2003. During apoptosis of tumor cells HMGA1a protein undergoes methylation: identification of the modification site by mass spectrometry. Biochemistry 42(12):3575–3585.

Sonstegard TS, Van Tassell CP, Matukumalli LK, Harhay GP, Bosak S, Rubenfield M, and Gasbarre LC, 2004. Production of EST from cDNA libraries derived from immunologically activated bovine gut. Sequence at NCBI CK951567. Unpublished manuscript.

Strausberg RL, Feingold EA, Grouse LH, Derge JG, Klausner RD, Collins FS, Wagner L, Shenmen CM, Schuler GD, and others, 2002. Generation and initial analysis of more than 15,000 full-length human and mouse cDNA sequences. Proc Natl Acad Sci USA 99(26): 16899–16903.

Takaha N, Resar LM, Vindivich D, and Coffey DS, 2004. High mobility group protein HMGI(Y) enhances tumor cell growth, invasion, and matrix metalloproteinase-2 expression in prostate cancer cells. Prostate 60(2): 160–167.

Tallini G, Vanni R, Manfioletti G, Kazmierczak B, Faa G, Pauwels P, Bullerdiek J, Giancotti V, Van Den Berghe H, and Dal Cin P, 2000. HMGI-C and HMGI(Y) immunoreactivity correlates with cytogenetic abnormalities in lipomas, pulmonary chondroid hamartomas, endometrial polyps, and uterine leiomyomas and is compatible with

rearrangement of the HMGI-C and HMGI(Y) genes. Lab Invest 80: 359–369.

Tamimi Y, van der Poel HG, Denyn MM, Umbas R, Karthaus HF, Debruyne FM, and Schalken JA, 1993. Increased expression of high mobility group protein I(Y) in high grade prostatic cancer determined by in situ hybridization. Cancer Res 53:5512–5516.

Thanos D and Maniatis T, 1992. The high mobility group protein HMG I(Y) is required for NF-kappa B-dependent virus induction of the human IFN-beta gene. Cell 71:777–789.

Vandenplas M, Cordonnier-Pratt MM, Suzuki Y, Sugano S, Moore JN, Liang C, Sun F, Sullivan R, Shah M, and Pratt LH, 2003. An EST database from equine (*Equus caballus*) unstimulated peripheral blood leukocytes. Sequence at NCBI CD535395. Unpublished manuscript.

Williams AJ, Powell WL, Collins T, and Morton CC, 1997. HMGI(Y) expression in human uterine leiomyomata. Involvement of another high-mobility group architectural factor in a benign neoplasm. Am J Pathol 150:911–918.

Yie J, Liang S, Merika M, and Thanos D, 1997. Intra- and intermolecular cooperative binding of high-mobility-group protein I(Y) to the beta-interferon promoter. Mol Cell Biol 17:3649–3662.

Corresponding Editor: Francis Galibert

III

Genomic characterisation, chromosomal assignment and in vivo localisation of the canine high mobility group A1 (*HMGA1*) gene.

Beuing C, Soller JT, Muth M, Wagner S, Dolf G, Schelling C, Richter A, Willenbrock S, Reimann-Berg N, Winkler S, Nolte I, Bullerdiek J, Murua Escobar H.

BMC Genet. 2008 Jul 23; 9: 49

Eigenleistung:

- Probensammlung und RNA/DNA Isolierung
- SNP-Screening und *in silico* Analysen
- GFP Vektorkonstruktion & *in vivo* Auswertung
- Verfassen des Manuskripts zusammen mit C. Beuing und H. Murua Escobar

BMC Genetics

BioMed Central

Research article

Genomic characterisation, chromosomal assignment and *in vivo* localisation of the canine High Mobility Group A1 (HMGA1) gene

Claudia Beuing[†1], Jan T Soller[†1,2], Michaela Muth[2], Sigfried Wagner[2], Gaudenz Dolf[3], Claude Schelling[4], Andreas Richter[2], Saskia Willenbrock[1,2], Nicola Reimann-Berg[1,2], Susanne Winkler[2], Ingo Nolte[1], Jorn Bullerdiek[1,2] and Hugo Murua Escobar*[1,2]

Address: [1]Clinic for Small Animals and Research Cluster of Excellence "REBIRTH", University of Veterinary Medicine Hanover, Bischofsholer Damm 15, 30173 Hanover, Germany, [2]Centre for Human Genetics, University of Bremen, Leobener Str ZHG, 28359 Bremen, Germany, [3]Institute of Animal Genetics, Nutrition and Housing, University of Berne, Berne, Switzerland and [4]Department of Animal Sciences, Swiss Federal Institute of Technology Zurich and Vetsuisse Faculty Zurich, University of Zurich, Zurich, Switzerland

Email: Claudia Beuing - claudia.beuing@tiho-hannover.de; Jan T Soller - soller@uni-bremen.de; Michaela Muth - mmuth@uni-bremen.de; Sigfried Wagner - siegfried.wagner@mail.uni-oldenburg.de; Gaudenz Dolf - dolf.gaudenz@itz.unibe.ch; Claude Schelling - claude.schelling@inw.agrl.ethz.ch; Andreas Richter - arichter@uni-bremen.de; Saskia Willenbrock - swillenbrock@uni-bremen.de; Nicola Reimann-Berg - nicola.reimann-berg@uni-bremen.de; Susanne Winkler - susewinkler@web.de; Ingo Nolte - inolte@klt.tiho-hannover.de; Jorn Bullerdiek - bullerd@uni-bremen.de; Hugo Murua Escobar* - escobar@uni-bremen.de

* Corresponding author †Equal contributors

Published: 23 July 2008

BMC Genetics 2008, **9**:49 doi:10.1186/1471-2156-9-49

Received: 1 April 2008
Accepted: 23 July 2008

This article is available from: http://www.biomedcentral.com/1471-2156/9/49

Abstract

Background: The high mobility group A1 proteins (HMGA1a/HMGA1b) are highly conserved between mammalian species and widely described as participating in various cellular processes. By inducing DNA conformation changes the HMGA1 proteins indirectly influence the binding of various transcription factors and therefore effect the transcription regulation. In humans chromosomal aberrations affecting the *HMGA1* gene locus on HSA 6p21 were described to be the cause for various benign mesenchymal tumours while high titres of HMGA1 proteins were shown to be associated with the neoplastic potential of various types of cancer. Interestingly, the absence of HMGA1 proteins was shown to cause insulin resistance and diabetes in humans and mice.

Due to the various similarities in biology and presentation of human and canine cancers the dog has joined the common rodent animal model for therapeutic and preclinical studies. Accordingly, the canine genome was sequenced completely twice but unfortunately this could not solve the structure of canine *HMGA1* gene.

Results: Herein we report the characterisation of the genomic structure of the canine *HMGA1* gene consisting of 7 exons and 6 introns spanning in total 9524 bp, the *in vivo* localisation of the HMGA1 protein to the nucleus, and a chromosomal assignment of the gene by FISH to CFA12q11. Additionally, we evaluated a described canine *HMGA1* exon 6 SNP in 55 Dachshunds.

Conclusion: The performed characterisations will make comparative analyses of aberrations affecting the human and canine gene and proteins possible, thereby providing a basis for revealing mechanisms involved in HMGA1 related pathogenesis in both species.

Background

The high mobility group A (HMGA) proteins are small chromatin associated non-histone proteins named according to their characteristic motility in acid-urea polyacrylamide gel electrophoresis. The protein family consists of the three proteins HMGA1a, HMGA1b and HMGA2 which are encoded for by two different genes (HMGA1 and HMGA2). The functional motifs of these proteins, named AT-hooks, bind to the minor groove of DNA causing conformational changes of the DNA molecule. On genomic level these structural changes influence the binding of various transcription factors and thus indirectly influence the transcription regulation, which classifies the HMGA proteins as so called architectural transcription factors (for detail see [1]).

In previous studies we characterised the canine HMGA1 cDNAs and proteins and in comparative analyses of these molecules showed that they are highly conserved between different mammalian species. The observed number of amino acid changes seen across mammalian species (cattle, dog, hamster, horse, mouse, pig, and rat) vary between 0 to 3 when compared to the human molecules [2-10]. Interestingly, only the canine HMGA1 proteins are 100% identical to their respective human counterparts [11].

The HMGA1 proteins are well known to play a significant role in the pathogenesis of various diseases including cancer. In humans, chromosomal aberrations affecting the HMGA1 gene locus on HSA 6p21 were described for various benign mesenchymal tumours, e.g. endometrial polyps, lipomas, pulmonary chondroid hamartomas, and uterine leiomyomas [12-14]. The observed aberrations are supposed to lead to an up-regulation of the *HMGA1* gene in the affected tumours, as opposed to adult healthy tissues where *HMGA* gene expression is low or hardly measurable [9,15,16]. In malignant neoplasias *HMGA1* expression is reported to be associated with an aggressive behaviour of tumours. Accordingly, *HMGA1* overexpression was detected in various malignancies including thyroid, lung, prostatic, pancreatic, uterine cervical, and colorectal carcinoma [17-22]. Thus *HMGA* expression is supposed to present a powerful diagnostic and prognostic molecular marker due to the described correlation between *HMGA* expression and tumour aggressiveness.

Whilst overexpression of *HMGA1* is clearly associated with cancerogenesis the disruption of the *HMGA1* gene and thus induced loss of *HMGA1* expression shows significant pathogenic effects. Heterozygous and homozygous Hmga1 knock-out mice develop cardiac hypertrophy combined with hematologic malignancies e.g. B cell lymphoma and myeloid granuloerythroblastic leukemia [23]. Additional research with Hmga1 knock-out mice targeting diabetes presented by Foti et al. (2005) showed that loss of Hmga1 expression is clearly associated with significantly decreased insulin receptor expression and thus causes a characteristic diabetes type 2 phenotype in mice [24].

The various similarities in presentation and biology of numerous canine and human diseases including cancer suggest similar mechanisms to be involved in the respective pathogenic events. Accordingly, at least a dozen distinct canine cancers are hypothesized to be appropriate models for their human counterparts, among those osteosarcoma, breast carcinoma, oral melanomas, lung carcinomas and malignant non-Hodgkin's lymphomas [25].

The characterization of disease related genes and their protein biology will allow for comparative studies to reveal the molecular mechanisms involved therein and serve as a basis for future clinical studies.

Results and discussion

The *HMGA1* gene and its proteins HMGA1a and HMGA1b are described as regulating multiple cellular processes and are widely reported to be associated with various diseases including diabetes and cancer. In previous studies we characterised the canine *HMGA1* cDNAs and proteins completely and did comparative analyses of these molecules to the respective counterparts of different species and showed high evolutionary conservation. The fact that several canine and human cancer types show striking similarities in presentation and biological behaviour, e.g. spontaneous occurrence and metastasis patterns, strongly suggests similar mechanisms to be involved in the respective pathogenic events of both species. Thus, various canine tumours are currently used as models for several human cancer types. Accordingly, comprehension of the canine gene and its gene products is precondition for comparative analyses, allowing the revelation of molecular effects involved in these pathogenic presentations. Understanding and comparison of the respective genes will thus benefit both species. The exact mechanism for the emergence of the pathogenic effects caused by chromosomal aberrations affecting the human *HMGA1* gene in benign mesenchymal tumours, e.g. endometrial polyps, lipomas, pulmonary chondroid hamartomas, and uterine leiomyomas [12-14] are not completely understood. However, it is currently supposed that the aberration causes up-regulation of the *HMGA1* gene in the affected neoplasias. The principal aim of the study was to characterize the genomic structure of the canine *HMGA1* gene allowing the comparison of its genomic structure to the counterparts of other mammals and thus allowing a further evaluation of evolutionary conservation of the gene and a comparative analysis of chromosomal aberrations in both species. Additional aims were the *in vivo* localization of the canine HMGA1 protein and the evalu-

ation of a previously described point mutation which causes a disrupted protein.

Genomic structure, BAC Screening and FISH

A canine *HMGA1* genomic PCR reaction was established and used for screening of a canine BAC for identification of the canine HMGA1 gene locus by FISH. The verified BAC 572 P20 K12 RC was used for FISH experiments. Ten well spread metaphases were analysed and showed signals on both chromatides of both chromosomes CFA 12q11 (Figure 1). The chromosomal localisation was done following the nomenclature established by Reimann et al. [26]. Existing painting probe based synteny studies and RH analyses [27] indicated that the canine CFA 12 shares homology with the human chromosome 6 on which the *HMGA1* gene is located at HSA 6p21. Chromosomal aberrations affecting CFA 12 are not or barely reported to be significantly associated with canine neoplasias [28,29]. While previous studies reported the localization of a HMGA1 gene positive BAC to CFA 23 [30], the performed *in silico* analyses and the recently published canine genome assembly [31] support the herein described assignment of the canine *HMGA1* gene to CFA 12q11 by FISH described in this study. Comparative chromosomal *in silico* analyses using the "Evolutionary Highway" http://evolutionhighway.ncsa.uiuc.edu/results.html showed similar results.

The genomic structure of the canine *HMGA1* gene consists in total of the 7 exons and 6 introns. Overall the canine *HMGA1* gene spans 9524 bp. The exon/intron structure, size and the homologies to their human counterparts were analysed and defined (Figure 2, Table 1). The total identity to the corresponding human region is 62.8%. In detail, the identities of the exons vary between 74.6% and 97.8% to their human counterpart, while the introns show identities between 58.9% and 92.4% (for details see Table 1). The newly characterized sequences combined with the analyses performed *in silico* revealed that the exon 4, which exists in humans, is missing on genomic level in the canine genome. This exon 4 deletion also exists in the mouse genome and affects the respective mRNAs of both species in their 5' UTR. As the genomic characterization of the canine HMGA1 gene was not available when the exons were named previously, the numbering at that time was based on the respective human exon numbers as defined by Friedmann et al. [32]. Consequently, as it is now known that the canine genomic sequence is lacking an equivalent to human exon 4, the previously used canine exon numbering should be revised with the then named canine exon 5 now being canine exon 4 and so on (Figure 2, Table 1). However, a part of intron 2 remains unsequenced due to an extensive CG repeat which also exists in the human counterpart (90%CG), and only the number of nucleotides (311 bp) could be identified. The genomic sequences were submit-

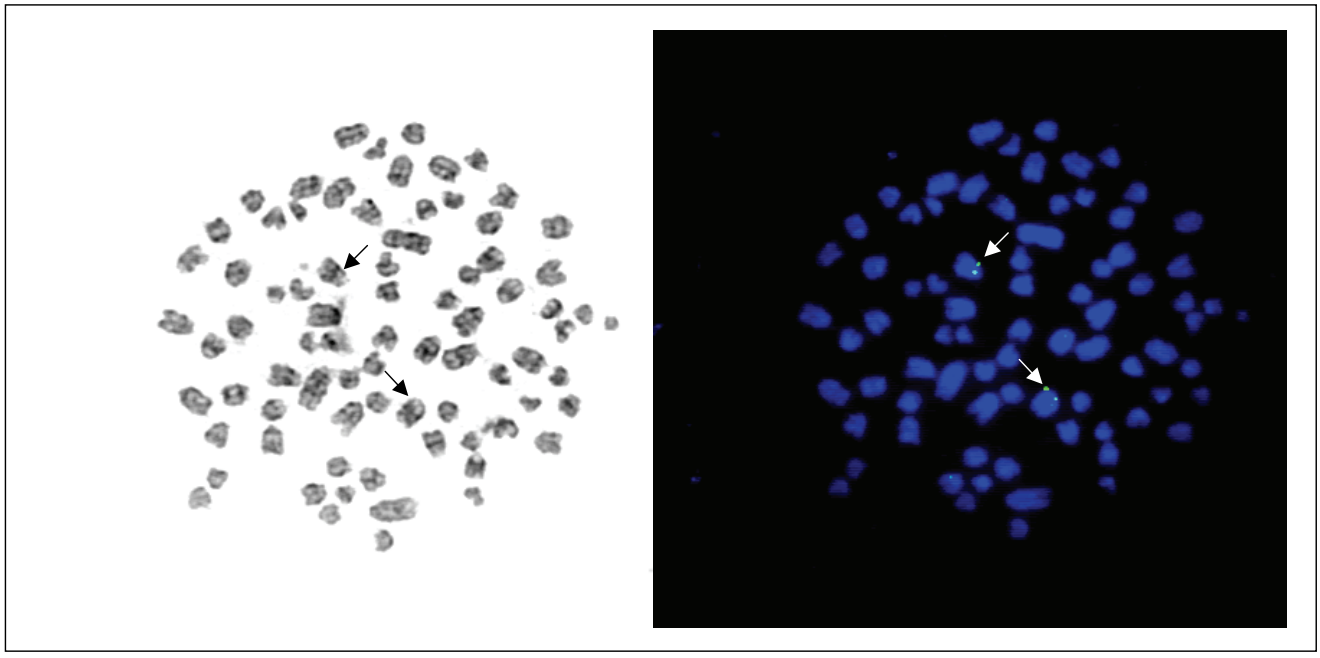

Figure 1
FISH-Mapping of the canine *HMGA1*. Canine metaphase spread after GTG-banding (left) and the same metaphase after fluorescence *in situ* hybridisation with BAC MGA 572 P20 K12 RC showing signals on both chromosomes 12 (right).

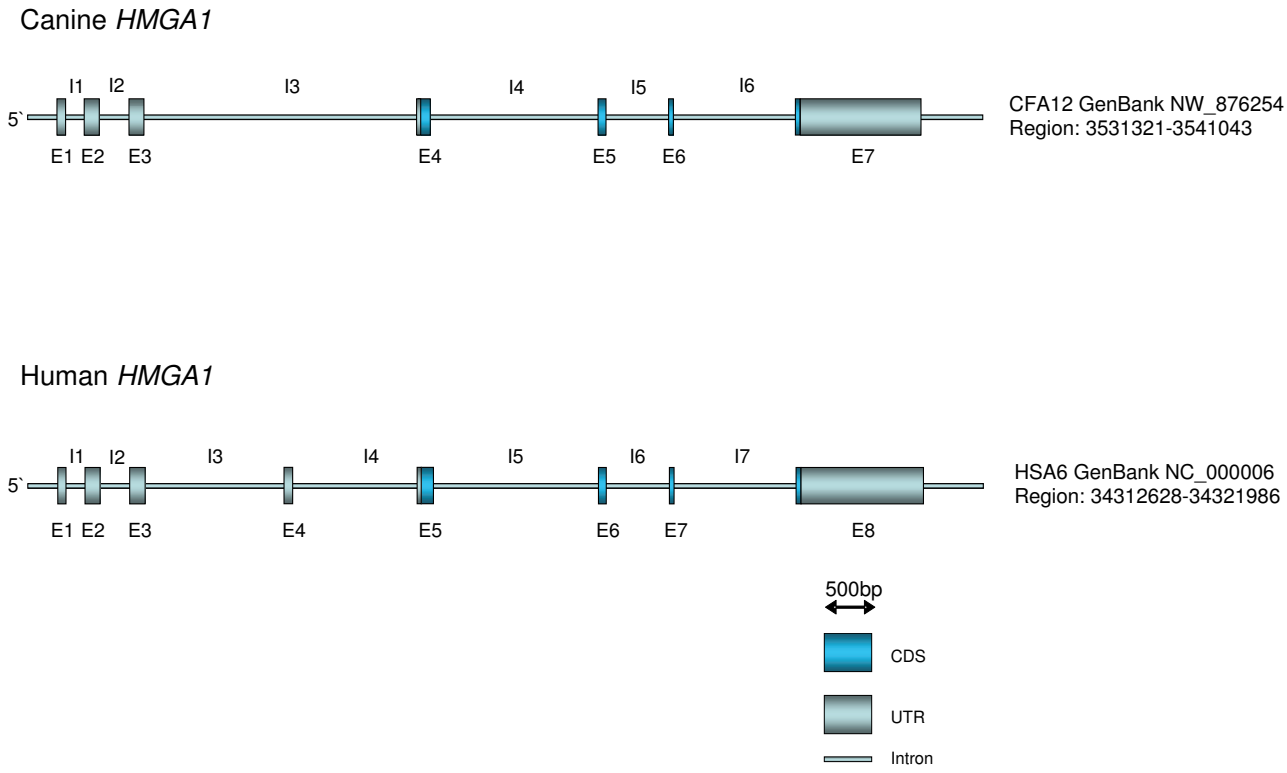

Figure 2
Genomic structure of the canine *HMGA1* gene. Detailed structure of the genomic organisation of the canine *HMGA1* gene.

ted to the NCBI database (bankit1078465, bankit1078536, bankit1078968).

Exon 6 SNP evaluation

While characterising the canine *HMGA1* gene we screened twelve different canine breeds for point mutations affect-

Table 1: Detailed analysis of the canine *HMGA1* gene genomic elements

Element of canine *HMGA1* gene	Size in bp	Identity to human counterpart in % (GenBank NC_000006))
Total gene	9524	62.8
Detail exons/introns (revised numbering)*		
Exon 1	94	97.8
Intron 1	196	92.4
Exon 2	164	95.8
Intron 2	311	-
Exon 3	162	74.6
Intron 3	3096	58.9
Exon 4 (5)	179	93.9
Intron 4 (5)	1761	51.1
Exon 5 (6)	84	96.4
Intron 5 (6)	584	57.5
Exon 6 (7)	51	94.1
Intron 6 (7)	1459	58.1
Exon 7 (8)	1386	75.4

Identity comparison of the genomic elements of the canine *HMGA1* gene with its respective human counterparts.

ing the protein coding region. A Dachshund sample showed a transition from A to G in exon 6 (according to revised exon numeration) leading to an amino acid exchange from threonine to alanine causing a mutated HMGA1 protein [9]. To elucidate if the observed exchange is frequently existent in the Dachshund population we screened 55 Dachshunds for the respective mutation (Figure 3). The results obtained by sequencing and restriction fragment analysis clearly showed that the previously found mutation is a rare event, as none of the screened 55 Dachshunds showed the mutation. Thus our findings suggest that the previously found aberrant *HMGA1* allele leading to a mutated protein form is unlikely to play a major role in HMGA1 pathogenesis in Dachshunds.

In general, different species show significant differences considering the number and probability of described SNPs. This fact surely is directly dependent on total numbers of studies and sequencing reactions performed for the different species. While in 2001 Sachidanandam et al. [33] detected 1.42 million SNPs in the human genome with one SNP per 1.9 kb the currently estimated total number reported SNPs in the public databases is approx. 9 million for the human genome [34]. For the dog Lindblad-Toh et al. reported 2.5 million SNPs, whereas the probability differs depending on the breed between one SNP per 1500 bp and 900 bp [31]. Comparable to the human genome the total numbers of reported SNPs in the other different species is expected to increase significantly according to the performed research efforts, leading to increased knowledge of effects caused by SNPs in general.

HMGA1 in vivo *localization*

The *in vivo* localization of the canine HMGA1 proteins via expression of a canine HMGA1a-GFP fusion protein showed that equivalently to its human counterpart the protein is located in the nucleus (Figure 4). Proteins of the HMGA family are described to be architectural transcription factors, and thus a localisation in the nucleus seems obvious. However, further localisation and function of these proteins seem to be very likely, due to the fact that application of recombinant HMGA1 proteins to porcine cartilage cells *in vitro* showed significant increase of cell proliferation (Richter et al. accepted for publication). For a further member of the HMG proteins called HMGB1 the existence of an extracelluar function was recognised only a long time after its initial characterisation as an architectural transcription factor, revealing a direct influence of

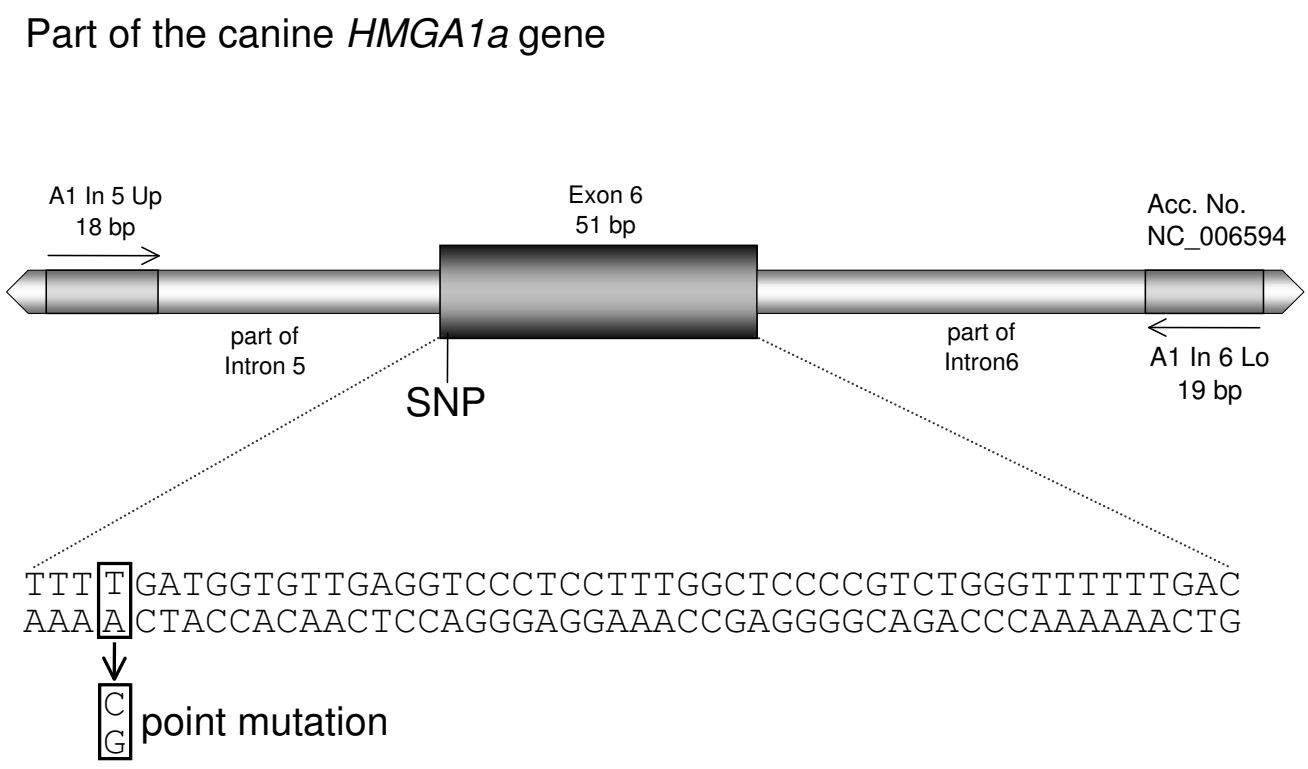

Figure 3
Position of the evaluated Dachshund point mutation. Strategic position of the evaluated point mutation screened in 55 Dachshunds.

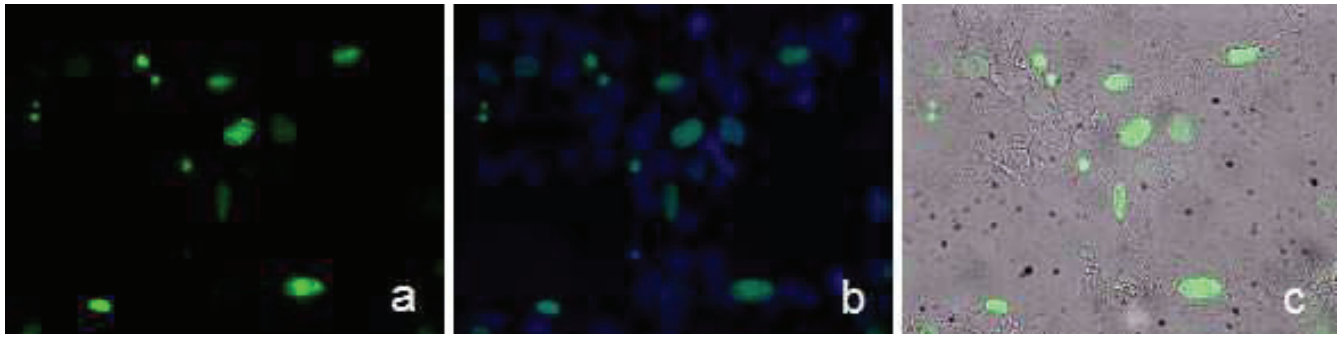

Figure 4
***In vivo* localisation of the canine HMGA1 protein.** *In vivo* localization of a canine HMGA1a-GFP fusion protein in culture canine MTH53A cells, 24 h posttranslational. a) GFP expression in canine mammary cell line MTH53A, b) DAPI fluorescent staining of cell nuclei, merged GFP and DAPI image, c) merged GFP and transmitted light image (magnification ×400).

extracellular HMGB1 on metastatic events [35-37]. Thus, we suppose that a similar mechanism could also exist for HMGA proteins and are currently working towards its identification.

Conclusion

Knowledge about the structure of genes and proteins is precondition to use them as potential therapeutic targets, markers or for revealing mechanisms involved in relevant pathogenic events. The canine and human HMGA genes and proteins have widely been shown to be involved in various diseases especially in cancer. Due to the numerous reasons for using the dog as a model system for human cancer research the characterisation of canine genes and proteins is of special interest. The performed characterisations of the canine HMGA1 gene and proteins will allow performing comparative analyses of aberrations affecting the human and canine genes and proteins as basis for revealing mechanisms involved in HMGA1 related pathogenesis in both species.

Methods

BAC library screening

A PCR reaction for the use in PCR-based screening of the *Canis familiaris* DogBAC library (Schelling et al., 2002) (Institute of Animal Genetics, Nutrition and Housing, University of Berne, Berne, Switzerland) for a BAC clone containing *HMGA1* was established using canine genomic DNA derived from blood. The primers A1In5up (5' GGCATCCGGTGAGCAGTG 3') and A1In6lo (5' CAGGCAGAGCACGCAGGAC 3') were designed using GeneBank sequences AY366395 &NW_876254. PCR parameters were: 95°C for 5 min, followed by 30 cycles of 95°C 30 sec, 59.3°C 30 sec, 72°C 30 sec, and a final elongation of 72°C for 10 min. The corresponding 201 bp PCR product was cloned into the pGEM-T Easy vector system (Promega, Mannheim, Germany) and verified by sequencing. The DNA contigs and alignments were done with Lasergene software (DNAstar, Madison, USA) and various sequences from the NCBI database (AY366395, NW_876254). The verified BAC clone MGA 572 P20 K12 RC was used as probe for the following FISH experiments.

Slide Preparation

1 ml of canine whole blood was incubated for 72 h in Chromosome Medium B (Biochrom, Berlin, Germany). Subsequently, colcemide (0.1 μg/ml) (Biochrom, Berlin, Germany) was added for 2 hours. The cells were centrifuged at 135 × g for 10 min and incubated for 20 min in 0.05 M KCl. Finally the cells were fixed with methanol/glacial acetic acid. This suspension was dropped on ice-cold slides and dried for at least 7 days at 37°C. The chromosomes were stained by GTG banding for karyotype description. Prior to use in FISH investigations, the slides were destained with 70% ethanol.

Fluorescence in situ *Hybridization*

MGA 572 P20 K12 RC BAC-DNA was digoxigenin labelled (Dig-Nick-Translation-Kit, Roche, Mannheim, Germany). The hybridization mixture contained 200 ng probe, 40 ng ssDNA, 600 ng sonicated dog DNA, 2 × SSC, 2 × SSPE, 50% formamide and 10% dextran sulfate. 50 μl of this mixture were applied to each slide and the cover slips were sealed with rubber cement. Probe and chromosomes were denatured at 75°C on an Eppendorf Thermocycler gradient, using the *in situ* adapter. Afterwards, the slides were incubated in a moist chamber at 37°C over night. Cover slips were carefully removed and the slides were incubated in 0.1 × SSC at 61°C and 1 × PBS at RT. Slides were then covered with 100 μl non fat dry milk (NFDM) for 20 min. at 37°C in a moist chamber. For signal detection 100 μl NFDM containing 3 μg of Anti-Digoxigenin-Rhodamine, Fab fragments (Roche, Mannheim, Germany), were added to each slide and again incubated for 20 min at 37°C in a moist chamber, followed by washes with 1 × PBS, 3 × 3 min. at RT. Slides were air dried

before chromosomes staining was performed with 25 μl of Vectashield Mounting Medium with DAPI (Vector Laboratories, Burlingame, CA, USA)

Ten well spread metaphases were examined indicating a signal on CFA 12q11 on both chromatids of both chromosomes CFA 12q11 (Fig. 1). The determination of chromosomes follows the nomenclature of the canine karyotype as described previously [26].

Genomic characterisation

For genomic characterisation of the canine *HMGA1* gene the missing parts were amplified by PCR on the screened BAC clone MGA 572 P20 K12 RC. For the missing part 1 a 858 bp fragment (bankit 1078968) was generated with primer pair A1_6640-6997_upa (5'-GGCGCGGCTCCAAGAA-3'), A1_6_lo_2 (5'-CCAACAGAGCCCTGCAAA-3'), a 1879 bp fragment (bankit 1078465 for the missing part 2 was generated by the primer pair A1_8864-10549_upa (5'-GTCTCACCGTCTGGAGAAT-3'), A1_8864-10549_loa (5'-TCACCGGAGGCTGCTT-3') and for the third missing part a 979 bp fragment (bankit 1078536) was generated with primer pair A1_11223-11834_upa (5'-CTGAGCCCATGCCAGATAA-3'), A1_11223-11834_loa (5'-AGAGATCCCTGCCGTAGT-3'). The obtained PCR products were separated on a 1.5% agarose gel, recovered with QIAquick Gel Extraction Kit (QIAGEN, Hilden, Germany), cloned in pGEM-T Easy vector system (Promega, Mannheim, Germany) and sequenced for verification. The final genomic canine *HMGA1* contig and the identity alignments were created with Lasergene software (DNASTar, Madison, USA) with the generated sequences from the cloned cDNAs described previously and various sequences from the NCBI database derived from the canine genome sequencing (AY366394, AY366395, AY366396, NM_001003387, NW_876254).

SNP screening

Genomic DNA was isolated from the collected 55 Dachshunds samples using the QiaAmp kit (QIAGEN, Hilden, Germany). A specific genomic PCR using the primer pair A1In5up (5' GGCATCCGGTGAGCAGTG 3') and A1In6lo (5' CAGGCAGAGCACGCAGGAC 3') was established allowing the amplification of the complete exon 6 and flanking regions of intron 5 and 6, respectively (Figure 3). In detail the PCRs were performed in a 25 μl volume containing 0.5 μM of both primers (MWG Biotech, Martinsried, Germany), 0.1 mM of each dNTP (Invitrogen, Karlsruhe, Germany) 0.6 units Taq-DNA polymerase (Promega, Mannheim, Germany), 1.5 mM $MgCl_2$ (Promega, Mannheim, Germany), PCR buffer (Promega, Mannheim, Germany) and 2.5 μl template DNA, containing averaged 26.5 ng/μl.

After an initial denaturation step of 5 min at 95°C, the amplification followed in 30 cycles (30 sec. at 95°C, 30 sec at 59.3°C and 30 sec at 72°C). To complete, a final elongation step for 10 min. at 72°C completed the process. The obtained PCR products were purified using the QIAquick PCR Purification Kit (Qiagen, Hilden, Germany), directly sequenced by MWG Biotech (Martinsried, Germany), and additionally digested enzymatically with AluI (Fermentas, St. Leon-Rot, Germany). The occurrence of the described SNP creates a new restriction site for the enzyme AluI (5' AG▼CT 3'). Thus, a digestion with AluI cuts the 201 bp PCR product in two fragments of 69 bp and 132 bp, respectively allowing a verification of the sequencing results.

HMGA1 in vivo *localisation*

For the HMGA1 *in vivo* localisation the protein coding sequence of the canine HMGA1a was amplified by PCR using primer pair EcoR1_IY-upATG (5'-CGGAATTCCACCATGAGCGAGTCGAGCTCGA-3'), BamH1_IY-loSTOP (5'-CGGGATCCTCACTGCTCCTCTTCGGAGGACT-3'). The obtained PCR products were separated on a 1.5% agarose gel, recovered with QIAquick Gel Extraction Kit (QIAGEN, Hilden, Germany), ligated into the pEGFP-C1 vector plasmid (BD Bioscience Clontech) and sequenced for verification.

Cells from canine mammary tumour cell line MTH53a were cultivated using medium 199 (Invitrogen, Karlsruhe, Germany) supplemented with 20% FCS, penicillin, and streptomycin. The transfection was performed according to the manufacturer's instructions using 3 μl FugeneHD reagent (Roche, Mannheim, Germany) in 100 μl PBS (without Mg^{2+}) containing 2 μg of recombinant pEGFP-C1-HMGA1a. After treatment, the cells were incubated for 48 hours in the culture media. The uptake and expression of DNA was verified by fluorescence microscopy.

Authors' contributions

CB: collected the Dachshund samples and performed the point mutation screening, JB: head of the centre for human genetics, took part in the conception design of the study, GD: constructed the screened BAC library, JTS: *in silico* analyses and construction of the *HMGA1* gene structure, MM: construction of expression vectors for the *in vivo* localisation, HME: principal study design, IN: head of the small animal clinic, took part in the conception design of the study, NR-B: karyotyping, AR: transfection of cells for in vivo localisation, CS: screening of the canine BAC library, SiW: molecular cloning of the newly characterised HMGA1 fragments, SaW: supervision point mutation screening, SuW: performed the FISH experiments.

Acknowledgements

We would like to thank Melissa Domel and Merle Skischus for technical assistance.

This work was supported in part by the German Excellence Cluster "REBIRTH" (From Regenerative Biology to Reconstructive Therapy, Hanover) within the Excellence Initiative of the German Federal Ministry of Education and Research and the German Research Foundation.

References

1. Bustin M, Reeves R: **High-mobility-group chromosomal proteins: architectural components that facilitate chromatin function.** *Prog Nucleic Acid Res Mol Biol* 1996, **54:**35-100.
2. Fujisaki S HH Eguchi T, Watanabe Y, Honma D, Saitou T, and Yasue H: **Construction of a full-length library of swine olfactory bulb and its preliminary characterization.** *Unpublished manuscript* 2003.
3. Johnson KR, Lehn DA, Elton TS, Barr PJ, Reeves R: **Complete murine cDNA sequence, genomic structure, and tissue expression of the high mobility group protein HMG-I(Y).** *The Journal of biological chemistry* 1988, **263(34):**18338-18342.
4. Aldrich TL RR Lee CC, Thomas JN, and Morris AE: **HMG-I(Y) proteins implicated in amplification of CHO cell DNA.** *Unpublished manuscript* 1999.
5. Strausberg RL, Feingold EA, Grouse LH, Derge JG, Klausner RD, Collins FS, Wagner L, Shenmen CM, Schuler GD, Altschul SF, Zeeberg B, Buetow KH, Schaefer CF, Bhat NK, Hopkins RF, Jordan H, Moore T, Max SI, Wang J, Hsieh F, Diatchenko L, Marusina K, Farmer AA, Rubin GM, Hong L, Stapleton M, Soares MB, Bonaldo MF, Casavant TL, Scheetz TE, Brownstein MJ, Usdin TB, Toshiyuki S, Carninci P, Prange C, Raha SS, Loquellano NA, Peters GJ, Abramson RD, Mullahy SJ, Bosak SA, McEwan PJ, McKernan KJ, Malek JA, Gunaratne PH, Richards S, Worley KC, Hale S, Garcia AM, Gay LJ, Hulyk SW, Villalon DK, Muzny DM, Sodergren EJ, Lu X, Gibbs RA, Fahey J, Helton E, Ketteman M, Madan A, Rodrigues S, Sanchez A, Whiting M, Madan A, Young AC, Shevchenko Y, Bouffard GG, Blakesley RW, Touchman JW, Green ED, Dickson MC, Rodriguez AC, Grimwood J, Schmutz J, Myers RM, Butterfield YS, Krzywinski MI, Skalska U, Smailus DE, Schnerch A, Schein JE, Jones SJ, Marra MA: **Generation and initial analysis of more than 15,000 full-length human and mouse cDNA sequences.** *Proceedings of the National Academy of Sciences of the United States of America* 2002, **99(26):**16899-16903.
6. Sgarra R, Diana F, Bellarosa C, Dekleva V, Rustighi A, Toller M, Manfioletti G, Giancotti V: **During apoptosis of tumor cells HMGA1a protein undergoes methylation: identification of the modification site by mass spectrometry.** *Biochemistry* 2003, **42(12):**3575-3585.
7. Sgarra R DF Bellarosa C, Rustighi A, Toller M, Manfioletti G, and Giancotti V: **Increase of HMGA1a protein methylation is a distinctive characteristic of tumor cells induced to apoptosis.** *Unpublished manuscript* 2002.
8. Vandenplas M CPMM Suzuki Y, Sugano S, Moore JN, Liang C, Sun F, Sullivan R, Shah M, and Pratt LH: **An EST database from equine (Equus caballus) unstimulated peripheral blood leukocytes.** *Unpublished manuscript* 2003.
9. Murua Escobar H, Soller JT, Richter A, Meyer B, Winkler S, Flohr AM, Nolte I, Bullerdiek J: **The canine HMGA1.** *Gene* 2004, **330:**93-99.
10. Sonstegard TS VTCP Matukumalli LK, Harhay GP, Bosak S, Rubenfield M, and Gasbarre LC: **Production of EST from cDNA libraries derived from immunologically activated bovine gut.** *Unpublished manuscript* 2004.
11. Murua Escobar H, Soller JT, Richter A, Meyer B, Winkler S, Bullerdiek J, Nolte I: **"Best friends" sharing the HMGA1 gene: comparison of the human and canine HMGA1 to orthologous other species.** *The Journal of heredity* 2005, **96(7):**777-781.
12. Kazmierczak B, Dal Cin P, Wanschura S, Borrmann L, Fusco A, Van den Berghe H, Bullerdiek J: **HMGIY is the target of 6p21.3 rearrangements in various benign mesenchymal tumors.** *Genes Chromosomes Cancer* 1998, **23(4):**279-285.
13. Tallini G, Vanni R, Manfioletti G, Kazmierczak B, Faa G, Pauwels P, Bullerdiek J, Giancotti V, Van Den Berghe H, Dal Cin P: **HMGI-C and HMGI(Y) immunoreactivity correlates with cytogenetic abnormalities in lipomas, pulmonary chondroid hamartomas, endometrial polyps, and uterine leiomyomas and is compatible with rearrangement of the HMGI-C and HMGI(Y) genes.** *Lab Invest* 2000, **80(3):**359-369.
14. Williams AJ, Powell WL, Collins T, Morton CC: **HMGI(Y) expression in human uterine leiomyomata. Involvement of another high-mobility group architectural factor in a benign neoplasm.** *Am J Pathol* 1997, **150(3):**911-918.
15. Chiappetta G, Avantaggiato V, Visconti R, Fedele M, Battista S, Trapasso F, Merciai BM, Fidanza V, Giancotti V, Santoro M, Simeone A, Fusco A: **High level expression of the HMGI (Y) gene during embryonic development.** *Oncogene* 1996, **13(11):**2439-2446.
16. Rogalla P, Drechsler K, Frey G, Hennig Y, Helmke B, Bonk U, Bullerdiek J: **HMGI-C expression patterns in human tissues. Implications for the genesis of frequent mesenchymal tumors.** *The American journal of pathology* 1996, **149(3):**775-779.
17. Fedele M, Bandiera A, Chiappetta G, Battista S, Viglietto G, Manfioletti G, Casamassimi A, Santoro M, Giancotti V, Fusco A: **Human colorectal carcinomas express high levels of high mobility group HMGI(Y) proteins.** *Cancer research* 1996, **56(8):**1896-1901.
18. Bandiera A, Bonifacio D, Manfioletti G, Mantovani F, Rustighi A, Zanconati F, Fusco A, Di Bonito L, Giancotti V: **Expression of HMGI(Y) proteins in squamous intraepithelial and invasive lesions of the uterine cervix.** *Cancer research* 1998, **58(3):**426-431.
19. Abe N, Watanabe T, Masaki T, Mori T, Sugiyama M, Uchimura H, Fujioka Y, Chiappetta G, Fusco A, Atomi Y: **Pancreatic duct cell carcinomas express high levels of high mobility group I(Y) proteins.** *Cancer research* 2000, **60(12):**3117-3122.
20. Diana F, Di Bernardo J, Sgarra R, Tessari MA, Rustighi A, Fusco A, Giancotti V, Manfioletti G: **Differential HMGA expression and post-translational modifications in prostatic tumor cells.** *International journal of oncology* 2005, **26(2):**515-520.
21. Frasca F, Rustighi A, Malaguarnera R, Altamura S, Vigneri P, Del Sal G, Giancotti V, Pezzino V, Vigneri R, Manfioletti G: **HMGA1 inhibits the function of p53 family members in thyroid cancer cells.** *Cancer research* 2006, **66(6):**2980-2989.
22. Sarhadi VK, Wikman H, Salmenkivi K, Kuosma E, Sioris T, Salo J, Karjalainen A, Knuutila S, Anttila S: **Increased expression of high mobility group A proteins in lung cancer.** *The Journal of pathology* 2006, **209(2):**206-212.
23. Fedele M, Fidanza V, Battista S, Pentimalli F, Klein-Szanto AJ, Visone R, De Martino I, Curcio A, Morisco C, Del Vecchio L, Baldassarre G, Arra C, Viglietto G, Indolfi C, Croce CM, Fusco A: **Haploinsufficiency of the Hmga1 gene causes cardiac hypertrophy and myelo-lymphoproliferative disorders in mice.** *Cancer research* 2006, **66(5):**2536-2543.
24. Foti D, Chiefari E, Fedele M, Iuliano R, Brunetti L, Paonessa F, Manfioletti G, Barbetti F, Brunetti A, Croce CM, Fusco A, Brunetti A: **Lack of the architectural factor HMGA1 causes insulin resistance and diabetes in humans and mice.** *Nature medicine* 2005, **11(7):**765-773.
25. MacEwen EG: **Spontaneous tumors in dogs and cats: models for the study of cancer biology and treatment.** *Cancer metastasis reviews* 1990, **9(2):**125-136.
26. Reimann N, Bartnitzke S, Bullerdiek J, Schmitz U, Rogalla P, Nolte I, Ronne M: **An extended nomenclature of the canine karyotype.** *Cytogenetics and cell genetics* 1996, **73(1-2):**140-144.
27. Breen M, Bullerdiek J, Langford CF: **The DAPI banded karyotype of the domestic dog (Canis familiaris) generated using chromosome-specific paint probes.** *Chromosome Res* 1999, **7(5):**401-406.
28. Reimann N, Bartnitzke S, Nolte I, Bullerdiek J: **Working with canine chromosomes: current recommendations for karyotype description.** *The Journal of heredity* 1999, **90(1):**31-34.
29. Reimann N, Nolte I, Bartnitzke S, Bullerdiek J: **Re: Sit, DNA, sit: cancer genetics going to the dogs.** *Journal of the National Cancer Institute* 1999, **91(19):**1688-1689.
30. Becker K, Murua Escobar H, Richter A, Meyer B, Nolte I, Bullerdiek J: **The canine HMGA1 gene maps to CFA 23.** *Animal genetics* 2003, **34(1):**68-69.
31. Lindblad-Toh K, Wade CM, Mikkelsen TS, Karlsson EK, Jaffe DB, Kamal M, Clamp M, Chang JL, Kulbokas EJ 3rd, Zody MC, Mauceli E, Xie X, Breen M, Wayne RK, Ostrander EA, Ponting CP, Galibert F, Smith DR, DeJong PJ, Kirkness E, Alvarez P, Biagi T, Brockman W, Butler J, Chin CW, Cook A, Cuff J, Daly MJ, DeCaprio D, Gnerre S, Grabherr M, Kellis M, Kleber M, Bardeleben C, Goodstadt L, Heger A, Hitte C, Kim L, Koepfli KP, Parker HG, Pollinger JP, Searle SM, Sutter NB, Thomas R, Webber C, Baldwin J, Abebe A, Abouelleil A, Aftuck L, Ait-Zahra M, Aldredge T, Allen N, An P, Anderson S, Antoine C, Arachchi H, Aslam A, Ayotte L, Bachantsang P, Barry A, Bayul T, Benamara M, Berlin A, Bessette D, Blitshteyn B, Bloom T, Blye J,

Boguslavskiy L, Bonnet C, Boukhgalter B, Brown A, Cahill P, Calixte N, Camarata J, Cheshatsang Y, Chu J, Citroen M, Collymore A, Cooke P, Dawoe T, Daza R, Decktor K, DeGray S, Dhargay N, Dooley K, Dooley K, Dorje P, Dorjee K, Dorris L, Duffey N, Dupes A, Egbiremolen O, Elong R, Falk J, Farina A, Faro S, Ferguson D, Ferreira P, Fisher S, FitzGerald M, Foley K, Foley C, Franke A, Friedrich D, Gage D, Garber M, Gearin G, Giannoukos G, Goode T, Goyette A, Graham J, Grandbois E, Gyaltsen K, Hafez N, Hagopian D, Hagos B, Hall J, Healy C, Hegarty R, Honan T, Horn A, Houde N, Hughes L, Hunnicutt L, Husby M, Jester B, Jones C, Kamat A, Kanga B, Kells C, Khazanovich D, Kieu AC, Kisner P, Kumar M, Lance K, Landers T, Lara M, Lee W, Leger JP, Lennon N, Leuper L, LeVine S, Liu J, Liu X, Lokyitsang Y, Lokyitsang T, Lui A, Macdonald J, Major J, Marabella R, Maru K, Matthews C, McDonough S, Mehta T, Meldrim J, Melnikov A, Meneus L, Mihalev A, Mihova T, Miller K, Mittelman R, Mlenga V, Mulrain L, Munson G, Navidi A, Naylor J, Nguyen T, Nguyen N, Nguyen C, Nguyen T, Nicol R, Norbu N, Norbu C, Novod N, Nyima T, Olandt P, O'Neill B, O'Neill K, Osman S, Oyono L, Patti C, Perrin D, Phunkhang P, Pierre F, Priest M, Rachupka A, Raghuraman S, Rameau R, Ray V, Raymond C, Rege F, Rise C, Rogers J, Rogov P, Sahalie J, Settipalli S, Sharpe T, Shea T, Sheehan M, Sherpa N, Shi J, Shih D, Sloan J, Smith C, Sparrow T, Stalker J, Stange-Thomann N, Stavropoulos S, Stone C, Stone S, Sykes S, Tchuinga P, Tenzing P, Tesfaye S, Thoulutsang D, Thoulutsang Y, Topham K, Topping I, Tsamla T, Vassiliev H, Venkataraman V, Vo A, Wangchuk T, Wangdi T, Weiand M, Wilkinson J, Wilson A, Yadav S, Yang S, Yang X, Young G, Yu Q, Zainoun J, Zembek L, Zimmer A, Lander ES: **Genome sequence, comparative analysis and haplotype structure of the domestic dog.** *Nature* 2005, **438(7069):**803-819.

32. Friedmann M, Holth LT, Zoghbi HY, Reeves R: **Organization, inducible-expression and chromosome localization of the human HMG-I(Y) nonhistone protein gene.** *Nucleic acids research* 1993, **21(18):**4259-4267.
33. Sachidanandam R, Weissman D, Schmidt SC, Kakol JM, Stein LD, Marth G, Sherry S, Mullikin JC, Mortimore BJ, Willey DL, Hunt SE, Cole CG, Coggill PC, Rice CM, Ning Z, Rogers J, Bentley DR, Kwok PY, Mardis ER, Yeh RT, Schultz B, Cook L, Davenport R, Dante M, Fulton L, Hillier L, Waterston RH, McPherson JD, Gilman B, Schaffner S, Van Etten WJ, Reich D, Higgins J, Daly MJ, Blumenstiel B, Baldwin J, Stange-Thomann N, Zody MC, Linton L, Lander ES, Altshuler D: **A map of human genome sequence variation containing 1.42 million single nucleotide polymorphisms.** *Nature* 2001, **409(6822):**928-933.
34. Kim S, Misra A: **SNP genotyping: technologies and biomedical applications.** *Annual review of biomedical engineering* 2007, **9:**289-320.
35. Muller S, Scaffidi P, Degryse B, Bonaldi T, Ronfani L, Agresti A, Beltrame M, Bianchi ME: **New EMBO members' review: the double life of HMGB1 chromatin protein: architectural factor and extracellular signal.** *The EMBO journal* 2001, **20(16):**4337-4340.
36. Huttunen HJ, Fages C, Kuja-Panula J, Ridley AJ, Rauvala H: **Receptor for advanced glycation end products-binding COOH-terminal motif of amphoterin inhibits invasive migration and metastasis.** *Cancer research* 2002, **62(16):**4805-4811.
37. Taguchi A, Blood DC, del Toro G, Canet A, Lee DC, Qu W, Tanji N, Lu Y, Lalla E, Fu C, Hofmann MA, Kislinger T, Ingram M, Lu A, Tanaka H, Hori O, Ogawa S, Stern DM, Schmidt AM: **Blockade of RAGE-amphoterin signalling suppresses tumour growth and metastases.** *Nature* 2000, **405(6784):**354-360.

IV

Expression of the high mobility group A1 (*HMGA1*) and A2 (*HMGA2*) in canine lymphoma: Analysis of 23 cases and comparison to control cases.

Joetzke A, Sterenczak KA, Eberle N, Wagner S, Soller JT, Nolte I, Bullerdiek J, Murua Escobar H, Simon D.

Vet Comp Oncol 2010 Feb 28, 8(2): 87-95.

Eigenleistung:

- Vorarbeiten zur Bestimmung der Genexpression
- *In silico* Analysen und Auswertung

Veterinary and Comparative Oncology

Original Article

DOI: 10.1111/j.1476-5829.2010.00207.x

Expression of the high mobility group A1 (*HMGA1*) and A2 (*HMGA2*) genes in canine lymphoma: analysis of 23 cases and comparison to control cases

A. E. Joetzke[1], K. A. Sterenczak[1,2], N. Eberle[1], S. Wagner[1,2], J. T. Soller[1,2], I. Nolte[1], J. Bullerdiek[1,2], H. Murua Escobar[1,2] and D. Simon[1]

[1]Small Animal Clinic and Research Cluster of Excellence 'REBIRTH', University of Veterinary Medicine Hannover, Hannover, Germany
[2]Centre for Human Genetics, University of Bremen, Bremen, Germany

Abstract

Overexpression of high mobility group A (*HMGA*) genes was described as a prognostic marker in different human malignancies, but its role in canine haematopoietic malignancies was unknown so far. The objective of this study was to analyse *HMGA1* and *HMGA2* gene expression in lymph nodes of canine lymphoma patients. The expression of *HMGA1* and *HMGA2* was analysed in lymph node samples of 23 dogs with lymphoma and three control dogs using relative quantitative real-time RT-PCR. Relative quantity of *HMGA1* was significantly higher in dogs with lymphoma compared with reference samples. *HMGA2* expression did not differ between lymphoma and control dogs. With the exception of immunophenotype, comparison of disease parameters did not display any differences in *HMGA1* and *HMGA2* expression. The present findings indicate a role of *HMGA* genes in canine lymphoma. This study represents the basis for future veterinary and comparative studies dealing with their diagnostic, prognostic and therapeutic values.

Keywords
dogs, gene expression, HMGA, lymphoma, relative quantitative real-time RT-PCR

Correspondence address:
Alexa E. Joetzke
Small Animal Clinic and Research Cluster of Excellence 'REBIRTH'
University of Veterinary Medicine Hannover
Bischofsholer Damm 15
30173 Hannover, Germany
e-mail: alexa.joetzke@tiho-hannover.de

Introduction

The high mobility group A (HMGA) protein family consists of three members: HMGA1a, HMGA1b and HMGA2. These highly conserved,[1] small, chromatin associated non-histone proteins are encoded for by two different genes (*HMGA1* and *HMGA2*) and regulate gene expression by inducing genomic DNA conformation changes. These changes indirectly take effect on transcription regulation by influencing the binding of various transcription factors.[2] Although *HMGA* genes are abundantly expressed in embryonic cells, their expression in most human adult healthy tissues is low or even absent.[3]

The HMGA proteins are known to play a significant role in the pathogenesis of various diseases including cancer. Re-expression of *HMGA1* was detected in various human malignancies including thyroid, lung, prostatic and colorectal carcinoma, as well as leukaemia and lymphoma,[4–11] whereas *HMGA2* re-expression was described, for example, in leukaemia, mammary, non-small cell lung, oral squamous cell and thyroid carcinoma.[12–16] In several of these malignancies *HMGA* overexpression has been reported to be associated with aggressive biologic behaviour.[4,7,9–11,13,15] Furthermore, HMGA1 and HMGA2 have attracted interest as potential therapeutic targets and future influencers on the choice of therapy.[17] Demonstration of *HMGA2* expression in canine prostate carcinoma tissue provided evidence that *HMGA* expression may also play a role in malignant tumours of dogs.[18]

The various similarities in biologic behaviour of many canine and human neoplastic diseases suggest similar mechanisms to be involved in the respective pathogenic events. Numerous canine malignancies are considered to be appropriate models for human oncology: among these, osteosarcoma, mammary carcinoma, oral melanoma, pulmonary carcinoma and non-Hodgkin's lymphoma.[19]

Lymphoma is one of the most common neoplastic diseases in the dog with an estimated annual incidence of 24–114 per 100 000 dogs.[20,21] Furthermore, it belongs to the most chemoresponsive malignancies in dogs.[19] Therefore, factors involved in the pathogenesis of canine lymphoma are of great interest for veterinarians as well as for comparative oncology. A wide variety of factors, for example, has been investigated for prognostic relevance,[22–27] but there are still strong variations in outcome of canine lymphoma that cannot be completely predicted. Molecular markers may provide new insight into the pathogenesis of canine lymphoma and therefore might help in predicting outcome.

As a result of the reported role of *HMGA* re-expression in malignant tumours and its association with tumour aggressiveness in humans, the expression of the corresponding proteins is presumed to represent a powerful diagnostic and prognostic molecular marker. Therefore, it was the aim of the present study to analyse the *HMGA1* and *HMGA2* gene expression in canine lymphomas and to compare it with findings in a group of control cases.

Materials and methods

Patients

Dogs with cytologically or histologically confirmed lymphoma were included in the analysis. Dogs that had received chemotherapy prior to sampling were excluded, whereas those pretreated only with glucocorticoids were included. Control lymph node samples were acquired from dogs with clinically unaltered peripheral lymph nodes diagnosed with diseases other than haematopoietic neoplasia. Signed owner consent was obtained for every patient and the study design was reviewed and approved by the governmental animal care committee.

Staging and immunophenotyping

Clinical staging in dogs with lymphoma was performed according to the WHO clinical staging system[28] based on physical examination, complete blood count, serum biochemistry, thoracic and abdominal radiographs and bone marrow aspiration cytology. Flow cytometry was used to determine the immunophenotype of multicentric lymphoma cases as previously described.[29]

Samples

Enlarged peripheral (multicentric lymphoma) or abdominal (intestinal lymphoma) lymph nodes were sampled via fine needle aspiration. Control samples were obtained from excised peripheral popliteal or superficial cervical lymph nodes within 20 min following euthanasia. All samples were immediately frozen in liquid nitrogen and stored at −80 °C until RNA isolation.

RNA isolation and complementary DNA synthesis for transcript characterization

The samples were homogenized using the iron-beads QIAshredder homogenizer method (Qiagen, Hilden, Germany). Following, total RNA was isolated using the RNeasy Mini Kit according to the manufacturer's instructions (Qiagen, Hilden, Germany). In order to avoid genomic DNA contaminations, on-column DNase digestion with the RNase-Free DNase set (Qiagen, Hilden, Germany) was performed.

The respective complementary DNA (cDNA) syntheses were performed using 250 ng total RNA of each sample, the adaptor primer AP2: AAG GAT CCG TCG ACA TC(17)T and Quantiscript Reverse Transcriptase following the manufacturer's protocol (Qiagen, Hilden, Germany) with an integrated removal of genomic DNA contamination.

Quantitative real-time RT-PCR

For relative quantification of the *HMGA1* and *HMGA2* transcript levels, reverse transcription PCR (RT-PCR) amplifications were carried out using the Applied Biosystems 7300 real-time PCR System (Applied Biosystems, Darmstadt, Germany). Two

Table 1. Sequences of the primers and fluorogenic probes used in the RT-PCR procedures

Gene	Forward primer 5′ → 3′	Reverse primer 5′ → 3′	Fluorogenic probe 5′ → 3′
HMGA1	ACCCAGTGAAGTGCCAACA CCTAA	CCTCCTTCTCCAGTTT TTTGGGTCT	6-FAM-AGGGTGCTGCCAA GACCCGGAAAACTACC A-TAMRA
HMGA2	AGTCCCTCCAAAGC AGCTCA AAAG	GCCATTTCCTAGGTCT GCCTC	6-FAM-AGAAGCCACTGGAGAAAAACG GCCA-TAMRA
GUSB	TGGTGCTGAGGATTGGCA	CTGCCACATGGACCCC ATTC	6-FAM-CGCCCACTACTATGCCATCGT GTG-TAMRA

GUSB, glucuronidase beta.

microlitres of each cDNA corresponding to 25 ng of total RNA was amplified in a total volume of 25 μL using universal PCR Mastermix (Applied Biosystems, Darmstadt, Germany) with 600 nM each of the respective forward and reverse primer (Table 1) and 200 nM of the respective fluorogenic probe (Table 1). PCR conditions were as follows: 2 min at 50 °C and 10 min at 95 °C, followed by 45 cycles with 15 s at 95 °C and 1 min at 60 °C.

For relative quantification based on the comparison of the *HMGA* expression with the expression of a housekeeping gene the canine glucuronidase beta transcript was chosen as endogenous control.[30] Two microlitres of each cDNA corresponding to 25 ng of total RNA was amplified with 600 nM of each primer (Table 1) and 200 nM fluorogenic probe (Table 1). The PCR was performed under the same conditions as the PCR reactions of the target genes.

All samples were measured in triplicate and for each run, non-template controls and no reverse transcriptase control reactions were included. Before performing the relative real-time quantifications, an absolute real-time PCR reaction was performed with all assays (results not shown), in order to ensure the comparability between the endogenous control and the respective target PCR reactions. All PCR reactions showed similar amplification efficiencies. To compare the gene expression levels based on the delta-delta-CT method, the expression in the control lymph node sample with the lowest variations between the three measurements of both *HMGA1* and *HMGA2* was used as a calibrator (expression level = 1).[31]

Statistical analysis

Expression levels of *HMGA1* and *HMGA2* were evaluated for statistically significant differences between anatomic type (multicentric versus intestinal lymphoma, Mann–Whitney test), immunophenotype (B-cell versus T-cell, Mann–Whitney test), WHO-substage (substage a versus substage b, Mann–Whitney test) and WHO-stage (clinical stage 3 versus 4 versus 5, Kruskal–Wallis test and clinical stage 3 and 4 versus 5, Mann–Whitney test). A Mann–Whitney test was also used to compare expression levels in lymphomas with those in control dogs.

A P-value of <0.05 was considered to be statistically significant. Statistical analysis was performed using SPSS 15.0 statistics software (SPSS, Chicago, IL, USA).

Results

Patient population

Twenty-three dogs with lymphoma were included in the study. Control lymph node samples were obtained from three dogs that were euthanized because of a sarcoma of the liver, pneumonia and a mediastinal sarcoma, respectively. Patient characteristics are summarized in Table 2.

HMGA1 and *HMGA2* expression analyses

Lymph node expression of *HMGA1* was measured in all 23 dogs with lymphoma, whereas *HMGA2* expression was determined in 22 of the 23 lymphoma patients. Expression of both genes was analysed in three control lymph node samples.

HMGA expression in lymphoma samples and comparison to control

The median expression level of *HMGA1* in lymphoma samples ($n = 23$) was 6.88 (range

Table 2. Patient characteristics of the lymphoma-affected and the control dogs

	Lymphoma Patients ($n = 23$)	Control Dogs ($n = 3$)
Breeds		
Mixed-breed	$n = 6$	$n = 1$
Rottweiler	$n = 3$	
Beagle	$n = 2$	
Small Munsterlander	$n = 2$	
Jagdterrier	$n = 2$	
Pitbull Terrier	$n = 2$	
Dachshund	$n = 1$	
German Shepherd	$n = 1$	$n = 1$
White Shepherd	$n = 1$	
Hovawart	$n = 1$	
Golden Retriever	$n = 1$	
Dogo Argentino	$n = 1$	
Jack Russel Terrier		$n = 1$
Age (years)		
Median	9	
Range	4–13	7–12
Body weight (kg)		
Median	26.5	
Range	8.8–52	6–40
Gender		
Female (spayed)	$n = 9$ ($n = 4$)	$n = 2$ ($n = 2$)
Male (castrated)	$n = 14$ ($n = 7$)	$n = 1$ ($n = 0$)
Anatomic form		
Multicentric	$n = 19$ (83%)	
Intestinal	$n = 4$ (17%)	
WHO-stage		
3	$n = 3$ (13%)	
4	$n = 5$ (22%)	
5	$n = 15$ (65%)	
WHO-substage		
a	$n = 7$ (30%)	
b	$n = 16$ (70%)	
Immunophenotype		
B	$n = 15$	
T	$n = 3$	
Not determined	$n = 5$	

1.09–12.14), which was significantly higher than the expression measured in control samples (median 0.95, range 0.94–1.00, $P = 0.006$). *HMGA2* expression showed no significant difference between lymphoma-affected ($n = 22$; median 0.32, range 0.03–317.66) and control lymph nodes (median 0.52, range 0.33–1.00, $P = 0.738$).

HMGA expression in multicentric lymphoma

In a separate evaluation including only the dogs with multicentric lymphoma ($n = 19$), *HMGA1* was detected with a median relative quantity of 7.20 (range 1.09–12.14). The median relative quantity of *HMGA2* in these dogs ($n = 18$) was 0.28 (range 0.03–317.66). The expression levels of *HMGA1* in the multicentric lymphoma cases were higher than in the control samples (median 0.95, range 0.94–1.00, $P = 0.001$, Fig. 1A). Expression of *HMGA2* did not differ significantly between multicentric lymphoma and control samples (median 0.52, range 0.33–1.00, $P = 0.534$, Fig. 1B).

HMGA1 and *HMGA2* expression levels in the dogs with multicentric lymphoma did not differ from those in dogs with intestinal lymphoma ($n = 4$ *HMGA1*: median 4.59, range 1.63–10.04, $P = 0.505$; *HMGA2*: median 7.02, range 0.14–138.69, $P = 0.118$).

In the dogs with multicentric lymphoma, clinical stage and clinical substage were not significantly associated with different *HMGA1* ($P = 0.340$ and $P = 0.482$, respectively) and *HMGA2* ($P = 0.964$ and $P = 0.126$, respectively) expression values. Comparison of a combined group of dogs in stages 3 and 4 with dogs in stage 5 also did not display any differences in *HMGA1* and *HMGA2* expression ($P = 0.940$ and $P = 0.965$, respectively).

Median relative *HMGA1* expression level in the multicentric lymphoma dogs with B-cell subtype ($n = 15$) was 7.42 (range 4.79–12.14). This was significantly higher than the respective relative quantity in the T-cell lymphoma cases ($n = 3$; 1.09, 1.50 and 1.53, respectively, $P = 0.002$, Fig. 2A). The relative quantity of *HMGA2* expression was on the other hand significantly higher in the T-cell subtype ($n = 3$; 21.98, 93.48 and 317.66, respectively) than in the B-cell lymphoma dogs ($n = 14$; median 0.17, range 0.03–5.33, $P = 0.003$, Fig. 2B).

Discussion

The present study aimed at the quantification of *HMGA1* and *HMGA2* expression in canine lymphoma and a comparison to control cases. It is the first report of *HMGA* expression analysis in canine haematopoietic malignancy. In the present population of dogs with lymphoma, *HMGA1* was overexpressed when compared with control dogs. In certain subtypes of human non-Hodgkin's lymphoma an alternative methodical approach using microarray technology indicated differences in

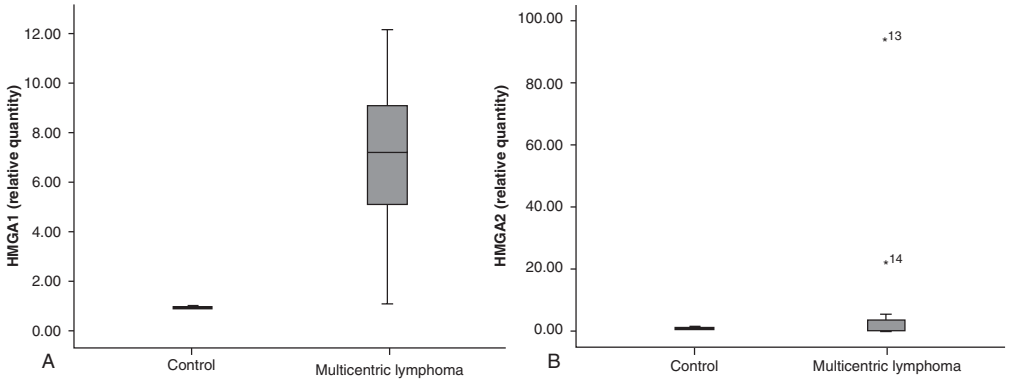

Figure 1. Relative quantity of *HMGA1* (A) and *HMGA2* (B) in dogs with multicentric lymphoma and control dogs. Boxplots graphs comparing multicentric lymphoma to control lymph nodes. (A) Median relative *HMGA1* quantity in multicentric lymphoma ($n = 19$): 7.20 (range 1.09–12.14), control samples ($n = 3$): 0.95 (range 0.94–1.00; $P = 0.001$); (B) median relative *HMGA2* quantity in multicentric lymphoma ($n = 18$): 0.28 (range 0.03–317.66), control samples ($n = 3$): 0.52 (range 0.33–1.00; $P = 0.534$).

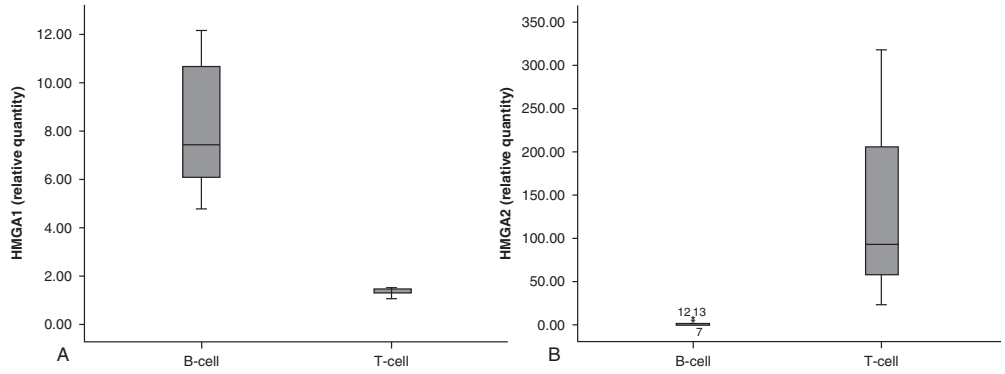

Figure 2. Relative quantity of *HMGA1* (A) and *HMGA2* (B) in multicentric lymphoma with different immunophenotype. Boxplots graphs comparing B-cell and T-cell lymphoma. (A) Median relative *HMGA1* quantity in B-cell lymphoma ($n = 15$): 7.42 (range 4.79–12.14), in T-cell lymphoma ($n = 3$): 1.50 (range 1.09–1.53; $P = 0.002$); (B) median relative *HMGA2* quantity in B-cell lymphoma ($n = 14$): 0.17 (range 0.03–5.33), in T-cell lymphoma ($n = 3$): 93.48 (range 21.98–317.66; $P = 0.003$).

HMGA1 expression levels as well. The expression was found to be significantly upregulated in the aggressive phase of follicular lymphoma compared with the indolent phase.[10] Human mantle cell lymphomas with a high proliferative index as determined immunohistochemically via Ki-67 expression showed a 3.3-fold higher *HMGA1* expression than those with a low proliferative index.[11] Increased levels of HMGA1 proteins were also described in Burkitt's lymphoma cell lines with increased c-Myc protein.[32] Furthermore, *HMGA1* overexpression has been shown in human leukaemias both of lymphoid and myeloid origin.[6,8] In addition, findings in mice emphasize the importance of *HMGA1* in haematopoietic malignancies. Induction of *HMGA1* overexpression in transgenic mice was found to be associated with the development of NK-cell lymphomas.[33] Interestingly, the loss of function of the *HMGA1* gene shows significant pathogenic effects, as well. Heterozygous and homozygous *HMGA1* knock-out mice develop cardiac hypertrophy combined with haematopoietic malignancies, for example, B-cell lymphoma and myeloid granuloerythroblastic leukaemia.[34]

No significant difference in *HMGA2* expression levels between canine lymphoma and control lymph

node samples was detected in the study population. In human haematopoietic malignancies, both of lymphoid and myeloid origin, aberrant expression and/or chromosomal rearrangements affecting *HMGA2* have been described.[35–38] Transgenic mice carrying a truncated *HMGA2* gene develop NK-cell lymphomas with a high frequency and thus show an association of *HMGA2* expression with haematopoietic neoplasia, as well.[39] Although increased *HMGA2* expression levels seem to play a role in several human myeloid neoplasias,[14,38,40] findings in lymphoid malignancies are more heterogeneous. Significantly lower expression levels of *HMGA2* were found in the bone marrow of human acute lymphoblastic leukaemia (ALL) patients when compared with healthy bone marrow.[35] In contrast, there is a report of *HMGA2* locus rearrangement with overexpression of a *HMGA2* mRNA lacking a carboxy-terminal tail in a case of ALL.[37] Another paper showed HMGA2 protein expression in bone marrow blasts associated with chromosomal translocation involving *HMGA2* in Richter transformation of a chronic lymphocytic leukaemia.[36]

Despite the lack of significant differences in *HMGA2* expression between canine lymphoma and control lymph nodes in the present study, the *HMGA2* expression in canine lymphomas varied widely. This indicates that aberrant *HMGA2* expression may play a role in canine lymphoma but that its overexpression is not a consistent finding. The role of these expression differences in the respective pathogenesis remains to be investigated in future studies incorporating a larger study population. Interestingly, *HMGA2* expression levels were found to be significantly higher in T-cell than in B-cell lymphomas. The T-cell immunophenotype is observed less frequently in canine lymphoma, comprising approximately 19–33% of lymphoma cases.[22,24,29] Consistent with these findings, T-cell lymphomas accounted for 17% of phenotyped lymphoma cases in the present study. A higher proportion of T-cell lymphomas may have resulted in a significant difference in *HMGA2* expression between multicentric lymphomas and control samples. Expression of *HMGA1* as well was significantly different between T-cell and B-cell lymphomas. In contrast to *HMGA2*, *HMGA1* was expressed significantly higher in B-cell lymphomas. The known association of immunophenotype with prognosis of canine lymphoma[22,24,25] in addition to the proven prognostic significance of *HMGA* expression in several human malignancies[4,7,9,13,15] gives rise to the assumption that *HMGA* expression levels and especially the different expression of *HMGA1* and *HMGA2* may be associated with prognosis in canine lymphoma, as well. Further studies are needed to verify the present findings and to prove an association with prognosis. It is interesting, that there seems to be a low expression of *HMGA1* especially in the subgroup (T-cell lymphomas) with a significantly higher expression of *HMGA2*. When reviewing other studies about *HMGA* expression in different human tumours concurrent overexpression of HMGA1 and HMGA2 is found in some tumour types[7] and overexpression of either HMGA1 or HMGA2 in others.[41,42] In some human tumour entities, the expression profile of HMGA seems to be useful as a diagnostic tool to differentiate between histologically similar tumours.[41,42] It is possible, that differential expression of *HMGA1* and *HMGA2* may be attributed to different roles they play in tissue differentiation and tumour pathogenesis. Whether it possesses diagnostic or prognostic importance in canine tumours and especially in canine lymphomas may become subject of future studies.

The present study has some limitations that need to be considered. Some subgroups within the study population were relatively small, which decreases the statistical significance of the results but reflects the epidemiological situation in the canine lymphoma population. The low number of control cases must be regarded as a limitation, as well. This group consisted of euthanized dogs with clinically unaltered peripheral lymph nodes and without haematopoietic neoplasia. Other neoplastic or non-neoplastic diseases were not excluded. It cannot be ruled out that the *HMGA* gene expression levels measured in the apparently unaltered peripheral lymph nodes of these dogs has been influenced by their respective disease or the postmortem sampling.

In the present study, overexpression of *HMGA* genes was demonstrated in dogs with lymphoma. The findings indicate that *HMGA* gene expression

may possess a role in the pathogenesis of canine lymphoma. Hence, the results of the present study may provide the basis for future veterinary and comparative studies on the diagnostic, prognostic and therapeutic use of *HMGA1* and *HMGA2*.

Acknowledgments

This study was supported in part by the German Excellence Cluster 'REBIRTH' (From Regenerative Biology to Reconstructive Therapy, Hannover) within the Excellence Initiative of the German Federal Ministry of Education and Research and the German Research Foundation. Additionally, this study was supported in part by the SFB Transregio 37 (Micro- and Nanosystems in Medicine). A. E. J. was sponsored by the German National Academic Foundation.

References

1. Murua Escobar H, Soller JT, Richter A, Meyer B, Winkler S, Bullerdiek J and Nolte I. 'Best friends' sharing the HMGA1 gene: comparison of the human and canine HMGA1 to orthologous other species. *Journal of Heredity* 2005; **96**: 777–781.
2. Bustin M and Reeves R. High-mobility-group chromosomal proteins: architectural components that facilitate chromatin function. *Progress in Nucleic Acid Research and Molecular Biology* 1996; **54**: 35–100.
3. Rogalla P, Drechsler K, Frey G, Hennig Y, Helmke B, Bonk U and Bullerdiek J. HMGI-C expression patterns in human tissues. Implications for the genesis of frequent mesenchymal tumors. *American Journal of Pathology* 1996; **149**: 775–779.
4. Bussemakers MJ, van de Ven WJ, Debruyne FM and Schalken JA. Identification of high mobility group protein I(Y) as potential progression marker for prostate cancer by differential hybridization analysis. *Cancer Research* 1991; **51**: 606–611.
5. Chiappetta G, Tallini G, De Biasio MC, Manfioletti G, Martinez-Tello FJ, Pentimalli F, de Nigris F, Mastro A, Botti G, Fedele M, Berger N, Santoro M, Giancotti V and Fusco A. Detection of high mobility group I HMGI(Y) protein in the diagnosis of thyroid tumors: HMGI(Y) expression represents a potential diagnostic indicator of carcinoma. *Cancer Research* 1998; **58**: 4193–4198.
6. Xu Y, Sumter TF, Bhattacharya R, Tesfaye A, Fuchs EJ, Wood LJ, Huso DL and Resar LM. The HMG-I oncogene causes highly penetrant, aggressive lymphoid malignancy in transgenic mice and is overexpressed in human leukemia. *Cancer Research* 2004; **64**: 3371–3375.
7. Sarhadi VK, Wikman H, Salmenkivi K, Kuosma E, Sioris T, Salo J, Karjalainen A, Knuutila S and Anttila S. Increased expression of high mobility group A proteins in lung cancer. *Journal of Pathology* 2006; **209**: 206–212.
8. Pierantoni GM, Agosti V, Fedele M, Bond H, Caliendo I, Chiappetta G, Lo Coco F, Pane F, Turco MC, Morrone G, Venuta S and Fusco A. High-mobility group A1 proteins are overexpressed in human leukaemias. *Biochemical Journal* 2003; **372**: 145–150.
9. Abe N, Watanabe T, Sugiyama M, Uchimura H, Chiappetta G, Fusco A and Atomi Y. Determination of high mobility group I(Y) expression level in colorectal neoplasias: a potential diagnostic marker. *Cancer Research* 1999; **59**: 1169–1174.
10. Glas AM, Kersten MJ, Delahaye LJ, Witteveen AT, Kibbelaar RE, Velds A, Wessels LF, Joosten P, Kerkhoven RM, Bernards R, van Krieken JH, Kluin PM, van't Veer LJ and de Jong D. Gene expression profiling in follicular lymphoma to assess clinical aggressiveness and to guide the choice of treatment. *Blood* 2005; **105**: 301–307.
11. Ek S, Bjorck E, Porwit-MacDonald A, Nordenskjold M and Borrebaeck CA. Increased expression of Ki-67 in mantle cell lymphoma is associated with de-regulation of several cell cycle regulatory components, as identified by global gene expression analysis. *Haematologica* 2004; **89**: 686–695.
12. Meyer B, Loeschke S, Schultze A, Weigel T, Sandkamp M, Goldmann T, Vollmer E and Bullerdiek J. HMGA2 overexpression in non-small cell lung cancer. *Molecular Carcinogenesis* 2007; **46**: 503–511.
13. Rogalla P, Drechsler K, Kazmierczak B, Rippe V, Bonk U and Bullerdiek J. Expression of HMGI-C, a member of the high mobility group protein family, in a subset of breast cancers: relationship to histologic grade. *Molecular Carcinogenesis* 1997; **19**: 153–156.
14. Rommel B, Rogalla P, Jox A, Kalle CV, Kazmierczak B, Wolf J and Bullerdiek J. HMGI-C, a member of the high mobility group family of proteins, is expressed in hematopoietic stem cells and in leukemic cells. *Leukemia and Lymphoma* 1997; **26**: 603–607.
15. Miyazawa J, Mitoro A, Kawashiri S, Chada KK and Imai K. Expression of mesenchyme-specific gene

HMGA2 in squamous cell carcinomas of the oral cavity. *Cancer Research* 2004; **64**: 2024–2029.
16. Belge G, Meyer A, Klemke M, Burchardt K, Stern C, Wosniok W, Loeschke S and Bullerdiek J. Upregulation of HMGA2 in thyroid carcinomas: a novel molecular marker to distinguish between benign and malignant follicular neoplasias. *Genes, Chromosomes and Cancer* 2008; **47**: 56–63.
17. Fusco A and Fedele M. Roles of HMGA proteins in cancer. *Nature Reviews Cancer* 2007; **7**: 899–910.
18. Winkler S, Escobar HM, Meyer B, Simon D, Eberle N, Baumgartner W, Loeschke S, Nolte I and Bullerdiek J. HMGA2 expression in a canine model of prostate cancer. *Cancer Genetics and Cytogenetics* 2007; **177**: 98–102.
19. MacEwen EG. Spontaneous tumors in dogs and cats: models for the study of cancer biology and treatment. *Cancer and Metastasis Reviews* 1990; **9**: 125–136.
20. Dorn CR, Taylor DO and Schneider R. The epidemiology of canine leukemia and lymphoma. *Bibliotheca haematologica* 1970; **36**: 403–415.
21. Dobson JM, Samuel S, Milstein H, Rogers K and Wood JL. Canine neoplasia in the UK: estimates of incidence rates from a population of insured dogs. *Journal of Small Animal Practice* 2002; **43**: 240–246.
22. Greenlee PG, Filippa DA, Quimby FW, Patnaik AK, Calvano SE, Matus RE, Kimmel M, Hurvitz AI and Lieberman PH. Lymphomas in dogs. A morphologic, immunologic, and clinical study. *Cancer* 1990; **66**: 480–490.
23. Simon D, Nolte I, Eberle N, Abbrederis N, Killich M and Hirschberger J. Treatment of dogs with lymphoma using a 12-week, maintenance-free combination chemotherapy protocol. *Journal of Veterinary Internal Medicine* 2006; **20**: 948–954.
24. Teske E, van Heerde P, Rutteman GR, Kurzman ID, Moore PF and MacEwen EG. Prognostic factors for treatment of malignant lymphoma in dogs. *Journal of the American Veterinary Medical Association* 1994; **205**: 1722–1728.
25. Vail DM, Kisseberth WC, Obradovich JE, Moore FM, London CA, MacEwen EG and Ritter MA. Assessment of potential doubling time (Tpot), argyrophilic nucleolar organizer regions (AgNOR), and proliferating cell nuclear antigen (PCNA) as predictors of therapy response in canine non-Hodgkin's lymphoma. *Experimental Hematology* 1996; **24**: 807–815.
26. Bergman PJ, Ogilvie GK and Powers BE. Monoclonal antibody C219 immunohistochemistry against P-glycoprotein: sequential analysis and predictive ability in dogs with lymphoma. *Journal of Veterinary Internal Medicine* 1996; **10**: 354–359.
27. Gentilini F, Calzolari C, Turba ME, Agnoli C, Fava D, Forni M and Bergamini PF. Prognostic value of serum vascular endothelial growth factor (VEGF) and plasma activity of matrix metalloproteinase (MMP) 2 and 9 in lymphoma-affected dogs. *Leukemia Research* 2005; **29**: 1263–1269.
28. Owen LN. TNM Classification of tumours in domestic animals. *World Health Organization, Geneva* 1980: 46–47.
29. Culmsee K, Simon D, Mischke R and Nolte I. Possibilities of flow cytometric analysis for immunophenotypic characterization of canine lymphoma. *Journal of Veterinary Medicine, Series A: Physiology, Pathology, Clinical Medicine* 2001; **48**: 199–206.
30. Brinkhof B, Spee B, Rothuizen J and Penning LC. Development and evaluation of canine reference genes for accurate quantification of gene expression. *Analytical Biochemistry* 2006; **356**: 36–43.
31. Schmittgen TD and Livak KJ. Analyzing real-time PCR data by the comparative C(T) method. *Nature Protocols* 2008; **3**: 1101–1108.
32. Wood LJ, Mukherjee M, Dolde CE, Xu Y, Maher JF, Bunton TE, Williams JB and Resar LM. HMG-I/Y, a new c-Myc target gene and potential oncogene. *Molecular and Cellular Biology* 2000; **20**: 5490–5502.
33. Fedele M, Pentimalli F, Baldassarre G, Battista S, Klein-Szanto AJ, Kenyon L, Visone R, De Martino I, Ciarmiello A, Arra C, Viglietto G, Croce CM and Fusco A. Transgenic mice overexpressing the wild-type form of the HMGA1 gene develop mixed growth hormone/prolactin cell pituitary adenomas and natural killer cell lymphomas. *Oncogene* 2005; **24**: 3427–3435.
34. Fedele M, Fidanza V, Battista S, Pentimalli F, Klein-Szanto AJ, Visone R, De Martino I, Curcio A, Morisco C, Del Vecchio L, Baldassarre G, Arra C, Viglietto G, Indolfi C, Croce CM and Fusco A. Haploinsufficiency of the Hmga1 gene causes cardiac hypertrophy and myelo-lymphoproliferative disorders in mice. *Cancer Research* 2006; **66**: 2536–2543.
35. Patel HS, Kantarjian HM, Bueso-Ramos CE, Medeiros LJ and Haidar MA. Frequent deletions at 12q14.3 chromosomal locus in adult acute lymphoblastic leukemia. *Genes, Chromosomes and Cancer* 2005; **42**: 87–94.
36. Santulli B, Kazmierczak B, Napolitano R, Caliendo I, Chiappetta G, Rippe V, Bullerdiek J and Fusco A. A 12q13 translocation involving the HMGI-C gene in richter transformation of a chronic lymphocytic leukemia. *Cancer Genetics and Cytogenetics* 2000; **119**: 70–73.

37. Pierantoni GM, Santulli B, Caliendo I, Pentimalli F, Chiappetta G, Zanesi N, Santoro M, Bulrich F and Fusco A. HMGA2 locus rearrangement in a case of acute lymphoblastic leukemia. *International Journal of Oncology* 2003; **23**: 363–367.
38. Odero MD, Grand FH, Iqbal S, Ross F, Roman JP, Vizmanos JL, Andrieux J, Lai JL, Calasanz MJ and Cross NC. Disruption and aberrant expression of HMGA2 as a consequence of diverse chromosomal translocations in myeloid malignancies. *Leukemia* 2005; **19**: 245–252.
39. Baldassarre G, Fedele M, Battista S, Vecchione A, Klein-Szanto AJ, Santoro M, Waldmann TA, Azimi N, Croce CM and Fusco A. Onset of natural killer cell lymphomas in transgenic mice carrying a truncated HMGI-C gene by the chronic stimulation of the IL-2 and IL-15 pathway. *Proceedings of the National Academy of Sciences of the United States of America* 2001; **98**: 7970–7675.
40. Meyer B, Krisponeit D, Junghanss C, Escobar HM and Bullerdiek J. Quantitative expression analysis in peripheral blood of patients with chronic myeloid leukaemia: Correlation between HMGA2 expression and white blood cell count. *Leukemia and Lymphoma* 2007; **48**: 2008–2013.
41. Franco R, Esposito F, Fedele M, Liguori G, Pierantoni GM, Botti G, Tramontano D, Fusco A and Chieffi P. Detection of high-mobility group proteins A1 and A2 represents a valid diagnostic marker in post-pubertal testicular germ cell tumours. *The Journal of Pathology* 2008; **214**: 58–64.
42. Hui P, Li N, Johnson C, De Wever I, Sciot R, Manfioletti G and Tallini G. HMGA proteins in malignant peripheral nerve sheath tumor and synovial sarcoma: preferential expression of HMGA2 in malignant peripheral nerve sheath tumor. *Modern Pathology* 2005; **18**: 1519–1526.

V

Establishing an in vivo model of canine prostate carcinoma using the new cell line CT1258.

Fork MA, Murua Escobar H, Soller JT, Sterenczak KA, Willenbrock S, Winkler S, Dorsch M, Reimann-Berg N, Hedrich HJ, Bullerdiek J, Nolte I.

BMC Cancer. 2008 Aug 15; 8 :240.

Eigenleistung:

- Probensammlung
- Tierexperimentelle Arbeiten

BMC Cancer

BioMed Central

Research article

Establishing an *in vivo* model of canine prostate carcinoma using the new cell line CT1258

Melani AM Fork*[1], Hugo Murua Escobar[1,2], Jan T Soller[1,2], Katharina A Sterenczak[1,2], Saskia Willenbrock[1,2], Susanne Winkler[2], Martina Dorsch[3], Nicola Reimann-Berg[1,2], Hans J Hedrich[3], Jörn Bullerdiek[1,2] and Ingo Nolte[1]

Address: [1]Small Animal Clinic, University of Veterinary Medicine Hanover, Hanover, Germany, [2]Center for Human Genetics, University of Bremen, Bremen, Germany and [3]Institute of Laboratory Animal Science, Hanover Medical School, Hanover, Germany

Email: Melani AM Fork* - melani.fork@tiho-hannover.de; Hugo Murua Escobar - hescobar@tiho-hannover.de; Jan T Soller - jasoller@tiho-hannover.de; Katharina A Sterenczak - Katharina.Sterenczak@gmx.de; Saskia Willenbrock - swillen@tiho-hannover.de; Susanne Winkler - Susewinkler@web.de; Martina Dorsch - martina.dorsch@mh-hannover.de; Nicola Reimann-Berg - nicola.reimann-berg@uni-bremen.de; Hans J Hedrich - hedrich.hans@mh-hannover.de; Jörn Bullerdiek - jbullerd@tiho-hannover.de; Ingo Nolte - ingo.nolte@tiho-hannover.de

* Corresponding author

Published: 15 August 2008

BMC Cancer 2008, **8**:240 doi:10.1186/1471-2407-8-240

Received: 1 April 2008
Accepted: 15 August 2008

This article is available from: http://www.biomedcentral.com/1471-2407/8/240

Abstract

Background: Prostate cancer is a frequent finding in man. In dogs, malignant disease of the prostate is also of clinical relevance, although it is a less common diagnosis. Even though there are numerous differences in origin and development of the disease, man and dog share many similarities in the pathological presentation. For this reason, the dog might be a useful animal model for prostate malignancies in man.

Although prostate cancer is of great importance in veterinary medicine as well as in comparative medicine, there are only few cell lines available. Thus, it was the aim of the present study to determine whether the formerly established prostate carcinoma cell line CT1258 is a suitable tool for *in vivo* testing, and to distinguish the growth pattern of the induced tumours.

Methods: For characterisation of the *in vivo* behaviour of the *in vitro* established canine prostate carcinoma cell line CT1258, cells were inoculated in 19 NOD.CB17-*Prkdc*^{Scid}/J (in the following: NOD-Scid) mice, either subcutaneously or intraperitoneally. After sacrifice, the obtained specimens were examined histologically and compared to the pattern of the original tumour in the donor.

Cytogenetic investigation was performed.

Results: The cell line CT 1258 not only showed to be highly tumourigenic after subcutaneous as well as intraperitoneal inoculation, but also mimicked the behaviour of the original tumour.

Conclusion: Tumours induced by inoculation of the cell line CT1258 resemble the situation in naturally occurring prostate carcinoma in the dog, and thus could be used as *in vivo* model for future studies.

Background

Only few species are known to spontaneously develop prostatic neoplasia; therefore the search for a suitable animal model for this disease is difficult. Currently, the dog is used as *in vivo* model for prostate malignancies in man, since it shows a similar metastatic pattern as well as age dependent development of malignant prostatic lesions [1-3]. Whereas prostate cancer is a frequent finding in man and even one of the leading causes of death in the Western world, it is less common in the dog. The prevalence is only 0. 2%–0. 6% [20]. Since this number is based on necropsy findings, the true number might be higher [4,5]. Although the relative number appears to be quite low, it results in an absolute count of estimated 60,000–180,000 affected dogs in the USA, 6,000–18,000 dogs in the UK, and 5,300–15,900 dogs in Germany, based on population.

Although there are some reports observing a permissive or protective effect of androgens [6-10], androgens do not seem to have an influence on development, growth, or metastasis in prostate carcinoma in dogs. Other than in human medicine, the diagnosis is usually made at a very late state of the disease, since for dogs no screening tests are available as there are for man [13]. Therefore treatment options for prostate cancer in the dog are limited and mostly remain to be palliative.

Despite the rather high incidence of prostate carcinoma in man, there are only three cell lines of human prostate carcinoma and their sub lines available. Thus, it is not surprising that there are only occasional reports about cell lines of canine prostatic carcinoma [11-13]. Hence the purpose of the present study was to establish an animal model, using the recently described cell line CT1258, which has been derived from a spontaneous canine prostate carcinoma [14,15]. Special attention was directed towards comparison of the clinical behaviour of the induced tumour in mice to the spontaneous tumour in the donor, as well as histological comparison. A comparison of the Ki67 index was performed in order to be able to address a potential change in proliferation. The Ki67 Index has been described to be associated with a poor outcome in human prostate cancer [18].

Methods

Donor

The cell line was derived from a prostatic tumour of a Briard, 10 years, male intact, which had been presented at the Small Animal Clinic of the University of Veterinary Medicine Hanover, Germany. The dog had a two week history of dyschezia, gain of abdominal girth, polydipsia, and loss of appetite. Clinical examination revealed an undulating and strained abdomen. Abdominal radiographs showed a highly reduced perceptibility of detail. On abdominal ultrasound an enlarged prostate could be detected, which contained several cysts.

Explorative laparatomy was performed and about 3000 ml abdominal fluid were obtained; the prostate itself was highly enlarged and several miliary masses were found in the mesentery. There was no evidence of contact metastases to abdominal organs or distant metastases to the lung. Biopsies have been taken under general anaesthesia; the cytological diagnosis of a highly malignant adenocarcinoma of the prostate resulted in euthanasia ad tabulam. Prior to euthanasia, biopsies have been taken for further histological examination and for cell culture. Histological staining and immunohistochemical staining as well as cytogenetic analysis was performed as described below.

Cell line

The cell culture conditions, as well as the characteristics of the canine prostate carcinoma cell line CT1258 have been described previously [15].

Animals

This study involved 19 NOD-Scid mice (10 male, 9 female). All animals were bred and maintained in a protected environment at the Institute of Laboratory Animal Science of the Hanover Medical School. The mice were fed autoclaved food and water *ad libitum*, any manipulation was performed in a laminar flow hood. The animals were observed on a daily basis and sacrificed depending on the clinical condition and the size of detectable tumour, respectively. The tumours were allowed to grow up to a diameter of 10 mm. Additional criteria for euthanasia were ulceration of subcutaneous masses, a reduced level of activity of the mice, and the loss of appetite. The animals were humanely sacrificed by cervical dislocation after inhalation of > 70% carbon dioxide. The study was approved by the Lower Saxony State Office of Consumer Security and Food Safety (33-42502-05/950), the ethical approval was sought from the University of Veterinary Medicine Hanover.

Inoculation of Cells

The cells were harvested from the culture flasks with 1 ml of TrypLE Express (Invitrogen, Karlsruhe, Germany) and incubated at room temperature for 1 minute. L-199 medium (Invitrogen, Karlsruhe, Germany) supplemented with 20% FCS was added and the cells were centrifuged at 350 g for 15 minutes. The cell pellet was washed twice with PBS. The cells were resuspended in 200 μl PBS; immediately before application the suspension was aspirated into Insulin-Syringes (BD Micro-Fine, BD, Heidelberg, Germany) and inoculated either subcutaneously into the left flank of the animals or intraperitoneally.

For subcutaneous inoculation, the animals received 1 × 10^6 cells. For intraperitoneal application, mice received either 1 × 10^5 or 5 × 10^5 cells. The 19 NOD-Scid mice were subdivided into two groups: One group consisted of four female and five male mice, the animals received 1 × 10^6cells subcutaneously each. The second group consisted of five male and five female animals, cells were inoculated intraperitoneally. Four of them (2 male, 2 female) received 1 × 10^5 cells; six animals (3 male, 3 female) received 5 × 10^5 cells, respectively.

Necropsy and histological staining

Necropsy was performed immediately after death had occurred. Lung, liver, spleen, kidneys, gonads, bowel, and detected masses were removed, fixed in 10% buffered formalin, paraffin embedded, sectioned, and stained with hematoxylin and eosin; immunohistochemical staining for Ki67 was performed, using the monoclonal antibody MIB-1 (Dianova, Hamburg, Germany) in a dilution of 1:100. The paraffin sections were pretreated in a microwave oven for 20 minutes in citrate buffer solution, pH 6. The secondary antibody was a biotinylated goat-α-mouse antibody, for detection, the Vectastain ABC-Kit (Vector Laboratories, Burlingame, USA) has been used. The Ki67 Index was determined by detecting the fraction of Ki67 positive stained cells in total 500 cells. This was performed in the original tumour, as well as in the induced tumours. Intestinal mucosa served as positive control. In addition, tumour samples of each mouse were obtained in liquid nitrogen for real time RT-PCR and in Hank's Medium for further *in vitro* culturing and Cytogenetic analysis. In order to address the growth pattern, the original canine tumour and the murine tumours have been classified based upon the presence of glandular, urothelial, squamoid, or sarcomatoid differentiation.

Cytogenetic analysis

For cytogenetic investigation, cells have been processed as described previously [15]. Tissue was transferred to liquid nitrogen immediately after dissection and stored at -70°C until examination.

Statistics

This study was intended to be descriptive rather than statistically significant. However, a paired student's t-test was performed. A P-value < 0.05 was considered to be significant.

Results

Pathological and histological examination

Original canine tumour

On histological examination the tumour showed to be consisting of poorly differentiated cells with numerous signs of malignancy. A strong anisocytosis, numerous cells with multiple nuclei, anisokaryosis, multiple mitotic figures, to some extent atypical mitotic figures, and a varying nucleus: plasma ratio could be detected. The tumour showed a compact growth with glandular differentiation. The Ki67 index was 43%.

Subcutaneous tumours

For analysis of duration until sacrifice of the mice, only those individuals were considered that were sacrificed due to tumour burden. All female mice and four of five male mice developed a detectable tumour mass after subcutaneous inoculation of 1 × 10^6 cells of the canine prostate carcinoma cell line CT1258 (Table 1). One mouse without detectable tumour growth was sacrificed due to bad clinical condition; necropsy revealed a mass of the thymus, histologically addressed as thymoma. In the remaining mice tumours were allowed to grow up to a size of 5–8 mm, which lasted 20 to 42 days (mean 25.37 days, median 22 days). Gender distribution showed a mean value of 28.75, median 26.5 days for female mice, and a mean and a median of 22 days for the males. None of the mice showed any signs of metastasis or of invasive growth pathologically or histologically; except for the mouse that did not develop any tumour mass, all animals remained in good clinical and nutritional condition.

Histology revealed a highly heterogeneous population of cells, numerous mitotic figures, anisokaryosis, anisocytosis, and several cells containing more than one nucleus; there was a variable nucleus: plasma ratio (Figures 1, 2). The centre of the obtained masses showed to be highly necrotic. Glandular differentiation was present. Immunohistochemistry revealed a strong positivity for the Ki67-antigen (Figure 3); the Ki67 index was between 41% and 48%, respectively

Intraperitoneal Tumours

The group was subdivided in two categories: Animals receiving 1 × 10^5 cells, consisting of two males and two females each, and animals receiving 5 × 10^5 cells, consisting of three males and three females each. The criteria for sacrification were impairment of the general condition, worsening of the nutritional condition, and/or reduction of activity level. Weight gain was not a reliable factor due to the development of massive peritoneal effusion.

Table 1: Tumour growth after subcutaneous injection of 1 × 10^6 cells of CT1258.

	Mean [days]	No growth [No of animals]	Range [days]	SD
Male	22	1	20–24	1.63
Female	28.75	0	20–42	10.05
Total	25.38	1	20–42	7.58

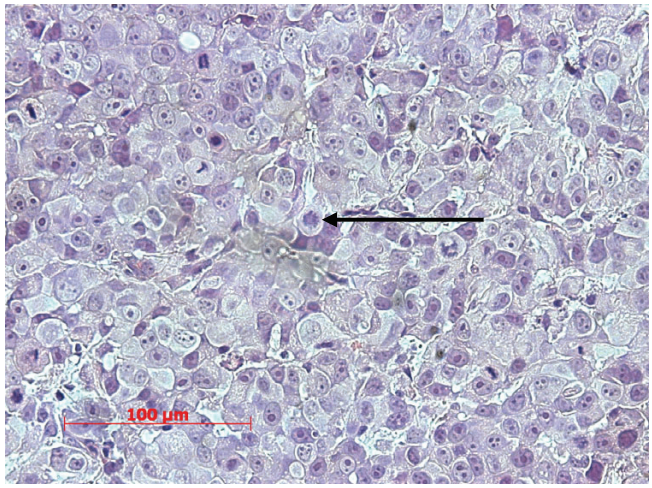

Figure 1
Subcutaneous mass with a high mitotic index. The arrow indicates an atypical mitotic figure.

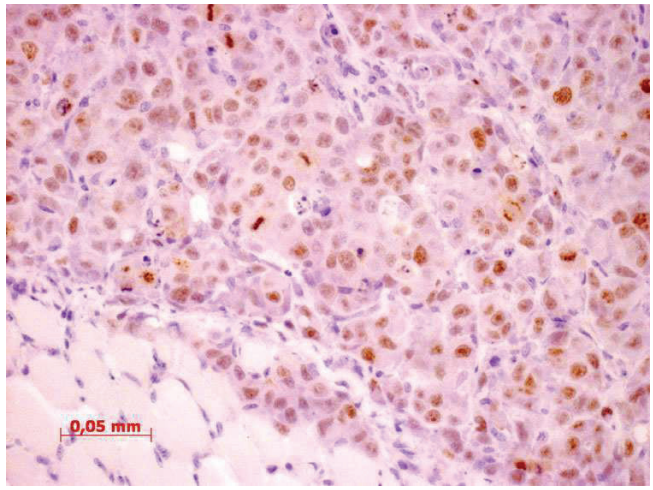

Figure 3
Ki67 staining of subcutaneous mass with a high amount of cells staining positively for Ki67.

In all mice receiving 1 × 10^5 cells tumour growth could be detected. The mean duration until sacrifice was 28 days. In one of three females and two of three males inoculated with 5 × 10^5 cells tumour growth could be detected, in this group the mean duration until sacrifice was 26 days (Table 2). Overall seven out of ten mice intraperitoneally inoculated with CT1258 developed tumour growth. Of those animals all but one male, which had received 5 × 10^5 cells, had an extended abdomen and proved to have peritoneal effusion. The male without obvious tumour growth had developed a thymoma, which was the cause for the bad clinical condition. Six of these ten mice developed a mass at the injection site, although at inoculation a proper amount of time had elapsed until withdrawal of the needle. Necropsy showed a moderate to high tumour burden at the peritoneum and no visible signs of metastasis to the lungs (Figure 4). Histological examination of the obtained masses showed a similar pattern as the subcutaneous masses with a glandular differentiation (Figure 5); staining for Ki67 was strongly positive with a Ki67 index between 45% and 47%. Isolated populations of tumour cells could be detected in the lungs, but there was no sign

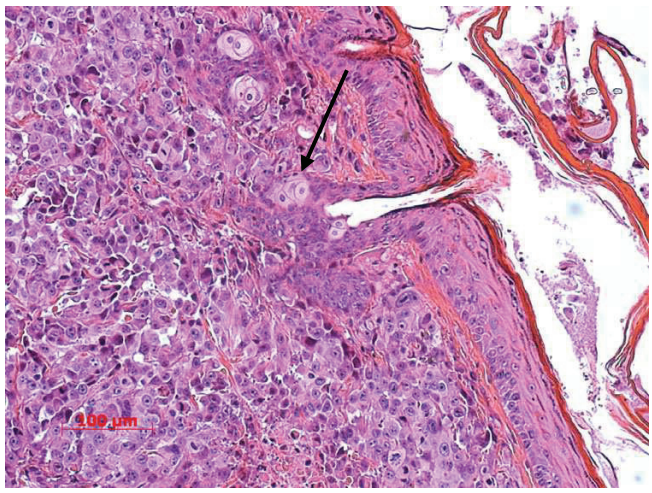

Figure 2
Subcutaneous mass with multiple mitotic figures and necrotic area; the large pale cells surrounding the hair follicle are part of the sebaceous gland and should not be mistaken as tumour cells (arrow).

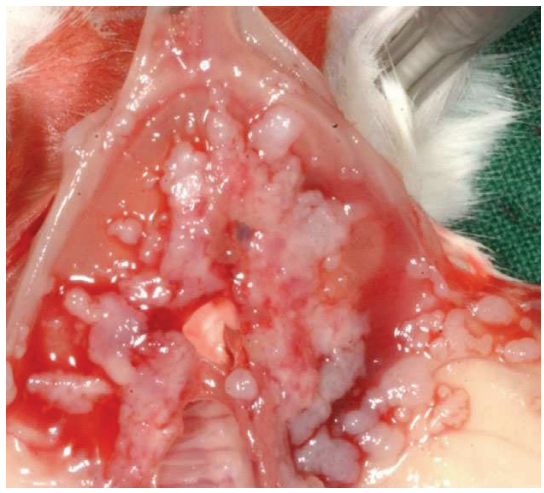

Figure 4
Diaphragm after i.p. injection of 5 × 10^5 cells with a high tumour burden; see Figure 5 for histology; the thoracic aspect of the diaphragm is not affected.

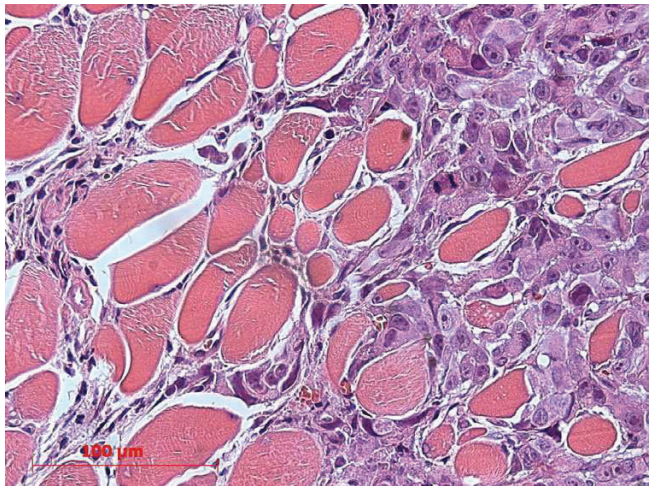

Figure 5
Diaphragmatic mass (see figure 4 for macroscopic appearance).

of vascularisation (Figure 6). In abdominal organs only peripheral tumour growth could be observed.

Cytogenetic Analysis

The cytogenetic investigation of intraperitoneal and subcutaneous tumours revealed the same markers that have been shown in analysis of the original tumour and of the cell line [15]. A hyperdiploid karyotype was present. Centromeric fusion between chromosomes 1 and 5 (der (1; 5)) and chromosomes 4 and 5 (der (4; 5)) were detected. A large biarmed marker (mar) was found (Figure 7, 8).

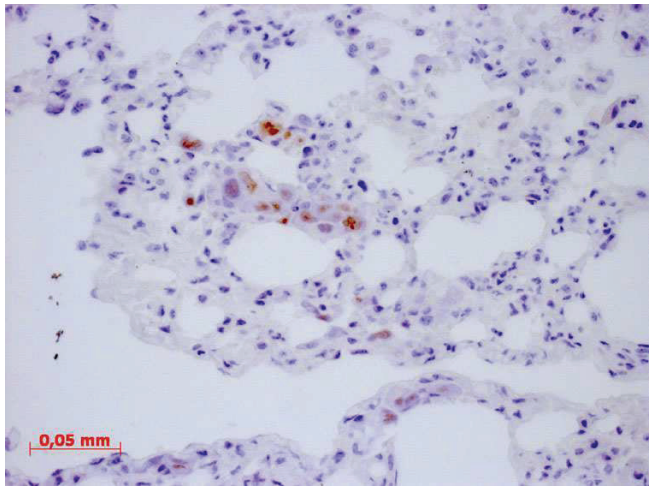

Figure 6
Ki67-staining of tumour cells in the lung; there is no evidence of vascularisation, therefore these cells are tumour emboli rather than metastasis.

Table 2: Tumour growth after intraperitoneal injection of 1×10^5 and 5×10^5 cells.

	Mean [days]	No growth [No of animals]	Range [days]	SD
Male	26.75	1	24–30	3.2
Female	27.67	2	24–30	3.21
1×10^5 cells	28	0	24–30	2.71
5×10^5cells	26	3	24–30	3.46
Total	27.14	3	24–30	1.12

Discussion

Ideally a cell line should not only be immortalized spontaneously but also be tumourigenic in experimental animals. Another claim may be the mimicking of the original natural behaviour of the tumour in the host. This condition promotes the predictability of any results obtained with that very cell line. This is true especially for cell lines derived from nonhuman tumours if the origin may serve as a model itself.

This study reveals that the cell line CT1258 is highly tumourigenic in NOD-Scid mice. Local tumour growth occurred in 89% of the animals that had received cells subcutaneously; 86% of the animals that had been inoculated intraperitoneally and that had developed tumour growth also developed local tumour growth at the injection site. The latter was not desired, and since it is not known how many cells remained in the branch canal, the size of those accidental masses cannot be compared accurately. Focussing on the mice with cells inoculated i.p., 86% developed peritoneal effusion just as the donor did and all of them had multiple small nodules within the serous membranes of the peritoneum rather than one large mass. The excellent local tumour growth on one hand and the rapid development of pleural effusion on the other hand indicates that in studies to come the use of the cell line might be of a greater value in local administration rather than in systemic inoculation. Orthotopic implantation might be of great value, since this could enable the assessment of local growth and invasion as well as potential metastasis. Due to the lack of vascularisation, the tumour cells found in the lungs of the mice must be addressed as tumour cell embolism rather than metastasis. Since neither the mice nor the donor had evidence of lymphogenic or hematogenic metastasis, we conclude that time for metastasis exceeds the time limitation owed to local tumour growth. Whether this is due to the rapid growth rate or due to potentially little disposition of the cells to degrade extracellular matrix and therefore has a generally low tendency to metastasise remains unclear. The absence of bone metastasis is a remarkable fact, which is contrary to the high incidence of bone metastasis in

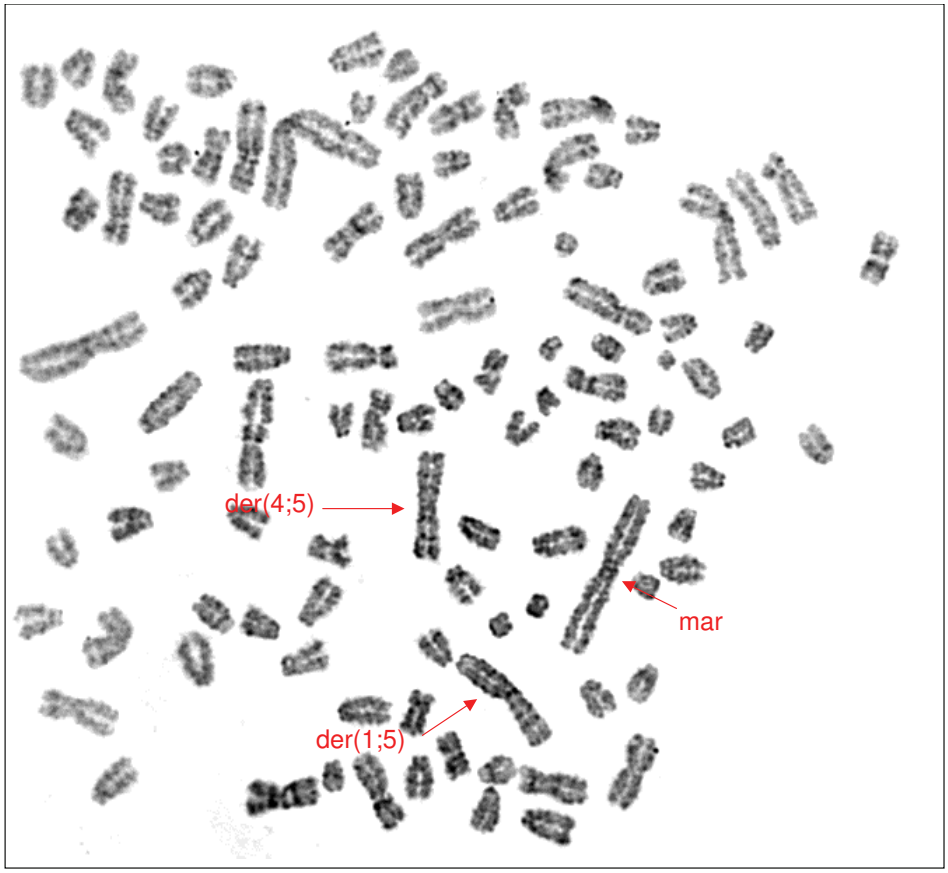

Figure 7
Metaphase spread from cells derived from the original canine tumour. The arrows indicate the derivative chromosomes der (1; 5), der (4; 5) and the marker chromosome mar, which consists of chromosome 1 and chromosome 2 material.

canine and human patients [5,19]. Potentially there was not enough time for bone metastasis to develop due to rapid local tumour growth, on the other hand, this particular tumour might have a reduced tendency for skeletal metastasis. At first glance this reduces the value of the present tumour model for comparative oncology, but this interesting feature might be used for further studies focussing on skeletal metastasis in particular, if the cause for the absence of metastasis to the skeleton in this otherwise highly malignant prostate carcinoma is detected. The tendency to show necrotic areas in the centre might be due to rapid tumour growth.

The number of cells obviously did not seem not to have a direct impact on tumour growth, since all mice that had been inoculated with 1×10^5 cells developed tumours, but 50% of the animals that received 5×10^5 cells did not; although this is not considered to be statistically significant, it suggests that an even lower number of cells might have been sufficient to induce a tumour. The difference between male and female animals is not statistically significant.

The Ki67 indices in both, the original tumour and the experimentally induced tumours, were considered to be high. The difference between the original tumour on one hand and the subcutaneous and intraperitoneal masses on the other hand were statistically not significant. In human medicine a high Ki67 index has shown to be associated with a poor prognosis [20]. Considering the histological characteristics of the described tumour, the high Ki67 index is not a surprising finding. Comparison of the Ki67 index of the original tumour to the xenograft revealed no change in proliferation.

One limiting factor is that two of the nineteen mice in the study developed thymoma within the course of the study. This is a frequent finding in older NOD-Scid mice [16,17]. Therefore the animals must not be considered to be healthy.

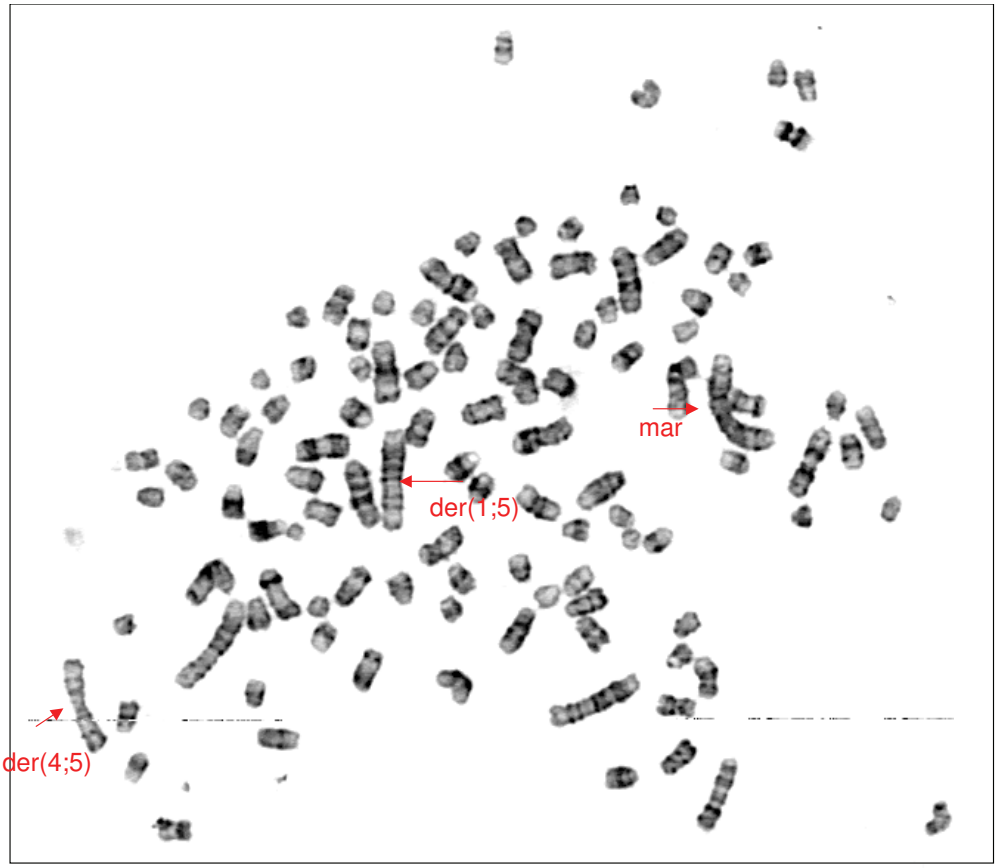

Figure 8
Metaphase spread from cells derived from a CT1258 induced tumour. The arrows indicate the derivative chromosomes der (1; 5), der (4; 5) and the marker chromosome mar, which consists of chromosome 1 and chromosome 2 material.

Conclusion

The canine prostate carcinoma cell line CT1258 demonstrated to be tumourigenic in the NOD-Scid mouse. Tumours induced in mice resembled the biological behaviour of the tumour from which the cell line was originally derived regarding growth pattern and histological appearance. Therefore we conclude that the use of this animal model will provide results with a high predictability towards clinical use in veterinary medicine and due to the correlation between canine and human prostate carcinoma in humans as well. The lack of skeletal metastasis is a potential field for further studies.

Competing interests

The authors declare that they have no competing interests.

Authors' contributions

MAMF was involved in study-design, implemented the in vivo tasks and the histopathology, and wrote the paper, HME was involved in study-design and coordination of in vitro work up, JTS and KAS assisted with dissection of the animals and in vitro work up, SaW prepared the cells for inoculation, SuW was involved in study-design, NR–B was involved in chromosomal preparation, cytogenetic analyses and karyotyping, MD and HHJH were involved in study-design and supervising the *in vivo* work up, JB and IN incited the study and coordinated the operational procedure. All authors read and approved the final manuscript.

Acknowledgements

We like to thank Matthias Meyer (Institute of Laboratory Animal Science, Hanover Medical School, Hanover, Germany) for assistance in monitoring and handling of the

References

1. Waters DJ, Sakr WA, Hayden DW, Lang CM, McKinney L, Murphy GP, Radinsky R, Ramoner R, Richardson RC, Tindall DJ: **Workgroup 4: Spontaneous prostate carcinoma in dogs and nonhuman primates.** *Prostate* 1998, **36:**64-67.
2. Maini A, Archer C, Wang CY, Haas GP: **Comparative pathology of benign prostatic hyperplasia and prostate cancer.** In *Vivo* 1997, **11(49):**293-299.
3. Cornell KK, Bostwick DG, Cooley DM, Hall G, Harvey HJ, Hendrick MJ, Pauli BU, Render JA, Stoica G, Sweet DC, Waters DJ: **Clinical**

and pathological aspects of spontaneous canine prostate carcinoma: a retrospective analysis of 76 cases. *Prostate* 2000, **45:**173-183.
4. **Projections of global mortality and burden of disease from 2002 to 2030** [http://www.who.int/healthinfo/statistics/bod_projections2030_paper.pdf]
5. Fan TM, de Lorimier LP: **Tumors of the male reproductive System.** In *Small Animal Clinical Oncology* 4th edition. Edited by: Withrow SJ, Vail DM. St. Louis, Saunders; 2007:637-648.
6. Obradovich J, Walshaw R, Goullaud E: **The influence of castration on the development of prostatic carcinoma in the dog: 43 cases (1978–1985).** *J Vet Intern Med* 1987, **1(4):**183-187.
7. Sorenmo KU, Goldschmidt M, Shofer F, Goldkamp C, Ferracone J: **Immunhistochemical characterization of canine prostatic carcinoma and correlation with castration status and castration time.** *Vet Comp Oncol* 2003, **1:**48-56.
8. Bell FW, Klausner JS, Hayden DW, Feeney DA, Johnston SD: **Clinical and pathological features of prostatic adenocarcinoma in sexual intact and castrated dogs: 31 cases (1970–1987).** *J Am Vet Med Assoc* 1991, **199:**1623-1630.
9. Leav I, Schelling KH, Adams JY, Merk FB, Alroy J: **Role of canine basal cells in postnatal prostatic development, induction of hyperplasia, and sex hormone-stimulated growth, and the ductal origin of carcinoma.** *Prostate* 2001, **48:**210-224.
10. Johnston SD, Kamolpatana K, Root-Kustritz MV, Johnston GR: **Prostatic disorders in the dog.** *Anim Reprod Sci* 2001, **60–61:**405-415.
11. LeRoy BE, Thudi NK, Nadella MV, Toribio RE, Tannehill-Gregg SH, van Bokhoven A, Davis D, Corn S, Rosol TJ: **New bone formation and osteolysis by a metastatic, highly invasive canine prostate carcinoma xenograft.** *Prostate* 2006, **66:**1213-1222.
12. L'Eplattenier HF, Chen Li Lai, van den Ham R, Mol J, van Sluijs F, Teske E: **Regulation of COX-2 expression in canine prostate carcinoma: increased COX-2 expression is not related to inflammation.** *JVIM* 2007, **21:**776-782.
13. Bell FW, Klausner JS, Hayden DW, Lund EM, Liebenstein BB, Feeney DA, Johnston SD, Shivers JL, Ewing CM, Isaacs WB: **Evaluation of serum and seminal plasma markers in the diagnosis of canine prostatic disorders.** *J Vet Intern Med* 1995, **9(3):**149-153.
14. Anidjar M, Vilette JM, Devauchelle P, Delisle F, Cotard JP, Billotey C, Cochand-Priollet B, Copin H, Barnoux M, Triballeau S, Rain JD, Fiet J, Teillac P, Berthon P, Cussenot O: ***In vivo* model mimicking natural history of dog prostate cancer using DPC-1, a new prostate carcinoma cell line.** *Prostate* 2001, **46:**2-10.
15. Winkler S, Murua Escobar H, Eberle N, Reimann-Berg N, Nolte I, Bullerdiek J: **Establishment of a cell line derived from a canine prostate carcinoma with highly rearranged karyotype.** *J Hered* 2005, **96(7):**782-785.
16. Murphy WJ, Durum SK, Anver MR, Ferris DK, McViar DW, O'Shea JJ, Ruscetti SK, Smith MR, Young HA, Longo DL: **Induction of T cell differentiation and lymphomagenesis in the thymus of mice with severe combined immune deficiency (SCID).** *J Immunol* 1994, **1;153(3):**1004-14.
17. Prochazka M, Gaskins HR, Schultz LD, Leiter EH: **The non obese diabetic Scid mouse: Model for spontaneous thymomagenesis associated with Immunodeficiency.** *Proc Natl Acad Sci USA* 1992, **89:**3290-3294.
18. Buhmeida A, Pyrhönen S, Laato M, Collan Y: **Prognostic factors in prostate Cancer.** *Diagn Pathol* 2006, **1:**4.
19. Lage MJ, Barber BL, Harrison DJ, Jun S: **The Cost of treating Skeletal- Related Events in Patients With Prostate Cancer.** *Am J Manag Care* 2008, **14(5):**317-22.
20. [http://www.who.int/infobase/report.aspx?rid=126].

Pre-publication history

The pre-publication history for this paper can be accessed here:

http://www.biomedcentral.com/1471-2407/8/240/prepub

VI

Application of antisense HMGA AAVs suppresses cell proliferation in a canine carcinoma cell line.

Soller JT, Murua Escobar H, Sterenczak KA, Willenbrock S, Fork MA, Bünger S, Pöhler C, Nolte, I., Bullerdiek, J

in Vorbereitung 2010.

Eigenleistung:

- Koordinierung und Planung aller Arbeiten
- *In silico* Analysen und Vektorkonstruktion
- Verfassen des Manuskripts zusammen mit J. Bullerdiek

Application of antisense *HMGA* AAVs suppress cell proliferation in a canine carcinoma cell line

Jan Thies SOLLER[1,2], Dr. Hugo MURUA ESCOBAR[1,3], Sefanie BÜNGER[1], Dr. Susanne WINKLER[1], Melani FORK[2], Christina PÖHLER[1], Katharina Anna STERENCZAK[1,2], Saskia WILLENBROCK[1,2], Prof. Ingo NOLTE[2,3] and Prof. Jörn BULLERDIEK[1,3]

[1]Centre for Human Genetics, University of Bremen, Leobener Strasse ZHG, 28359 Bremen, Germany

[2]Small Animal Clinic, University of Veterinary Medicine Hannover, Bischofsholer Damm 15, 30173 Hannover, Germany

[3]Small Animal Clinic and Research Cluster of Excellence "REBIRTH", University of Veterinary Medicine Hannover, Bischofsholer Damm 15, 30173 Hannover, Germany

Correspondence to:
Jan T. Soller
Centre for Human Genetics
University of Bremen,
Leobener Strasse ZHG
D-28359 Bremen, Germany,
Phone: +49-(0)421-218-2925,
Fax: +49-(0)421-218-4239,
Email: soller@uni-bremen.de

Abstract

Carcinomas of the prostate count to the most common neoplasms in men being one of the leading causes of cancer-related death. Besides men the dog is the only know species developing spontaneously carcinoma of the prostate. These in both species spontaneously appearing neoplasms show significant similarities in their biologic behavior e.g. their metastatic pattern and the expression of cancer related tumor markers. Proteins of the high mobility group A family (HMGA1 and HMGA2) were identified as tumor markers in both species. Accordingly their overexpression has been reported for a variety of cancers in both species showing a correlation of their overexpression and the malignant phenotype of the respective tumors. Herein we report that adeno-associated viruses (AAV)-2 carrying the mRNA of *HMGA1* or *HMGA2* in antisense orientation can significantly inhibit the proliferation of canine CT1258 prostate carcinoma cells *in vitro*, thus a suppression of HMGA expression represents a potential method for treatment of prostate carcinomas.

Introduction

In Europe prostate cancer is a leading cause of cancer related death among men with over 56,000 deaths per year in the European Union.[1] The worldwide incidence of registered prostate cancer accounts for 543,000 new cases each year, which is strongly related to Western lifestyle and an increasing risk of developing the disease at middle age (> 50 years). For men, the lifetime risk is about 10 % with a mortality rate of 3 %.[2, 3]

Dogs are an animal model suited to elucidate the mechanisms of pathogenesis of human prostate carcinomas. First of all, except for humans dogs are the only known mammalian species that spontaneously develop carcinomas of the prostate with a considerably high frequency.[4] As intensively outlined in the recent literature, dogs and humans share striking similarities in the field of oncology.[5, 6] Also, canine cancer diseases are characterized by spontaneous development of neoplasias without the need for experimental induction or transplantation and artificially acquired immunodeficiency, respectively.[7] Interestingly for cancer research, dogs are reported to develop cancer approximately twice as frequent as humans. Additionally the canine neoplasms show a faster progression of the tumors and their development when compared to their human counterparts and thus allow a better monitoring of the tumor related processes.[8]

Akin to human prostate adenocarcinomas their canine counterparts show local invasiveness and metastasize to the same organs, e.g. lungs and bones by bloodstream or lymph.[4] As to age distribution, older individuals are prevalently affected by developing prostate cancer in both species, with an average age of 65 years in men[9] which means a comparable age of 10 years in dogs.[10]

The high mobility AT-hook group of proteins (HMGA) consists of three members: HMGA1a, HMGA1b and HMGA2. HMGA proteins are characterized by three highly conserved DNA binding domains called the "AT-hooks".[11] The proteins HMGA1a and HMGA1b are isoforms coded by the same gene for alternative splicing variants. *HMGA1* is located on human chromosomal band 6p21.[12, 13] The closely related HMGA2 protein is encoded by a different gene, which is located on 12q14-15[14, 15]. These non-histone proteins are small secondary structured polypeptides which preferably bind to the minor groove of AT-rich B-form DNA and are defined as architectural nuclear factors, which are involved in chromatin dynamics. HMGA proteins influence the expression of a large number of genes by modifying chromatin structure.[16-18].

HMGA proteins are abundantly expressed during embryonic and fetal life. It has been proposed that HMGA2 mediates an embryonic chromatin conformation[19] and accordingly HMGA2 has been implicated in the regulation of key developmental genes in pluripotent embryonic stem cells.[20]

Overexpression of HMGA1 is reported in a diversity of human cancers, as for example cancers of breast, cervix, colon, thyroid, and prostate[21-24], whereas high levels of HMGA2 expression are observed in breast cancer, leukemia, non-small cell lung cancer, pancreatic cancer and squamous cell carcinomas of the oral cavity.[25-29] In the latter cancer entity increased HMGA2 expression is correlated with epithelial-mesenchymal transitions and there is evidence that in case of malignant epithelial tumors HMGA proteins act by increasing tumor stemness of cancer cell populations, which is correlated with adverse prognosis.[30]

As to comparative genomics we recently characterized the canine *HMGA1a* and *HMGA1b* transcripts and deduced their protein sequence, which showed a 100 % identity to its human counterpart whereas the coding sequence shows a 95 % identity in both splice variants.[31, 32] To the best of our knowledge the complete canine *HMGA2* transcript was not characterized so far. In order to construct antisense *HMGA2* AAV vectors for the experimental

studies presented herein we have characterized the coding sequence.

Recently a new cell line was established from a canine prostate carcinoma.[33] Due to the similarities between human and canine prostate cancer, this new canine cell line provides a valuable tool in experimental cancer gene therapeutic approaches. Thereby an important aspect is that the original tumor as well as the derived cell line show high levels of *HMGA2* expression. The overexpression of *HMGA* genes in the canine cell line strongly correlates to the described malignancy of the carcinoma.[34]

The aim of this study was to construct recombinant adeno-associated viruses encoding *HMGA1* and *HMGA2* antisense RNA and to analyze their effects on the proliferative behavior of canine carcinoma cells infected with the virus. AAV mediated gene therapy experiments show many advantages compared to the widely used adenoviral vectors, which induce host immune response to the target cells. Recombinant AAVs demonstrate long-term transgene expression and a minimal immune response.[35] Previous studies have shown that AAV vectors can be used successfully for the delivery of gene expression in sense and antisense orientation for up- and down regulation of target genes.[36-39] In terms of suppression of HMGA expression, other studies conducted in athymic mice used adenoviral virus systems to deliver anti-sense *HMGA* cDNA to inhibit cell proliferation, malignant transformation and size of engrafted tumor.[40, 41] In our study, we demonstrate the inhibition of cell proliferation in a canine prostate carcinoma cell line mediated by antisense *HMGA* mRNA recombinant AAVs (rAAV-asHMGA1, rAAV-asHMGA2).

Material and methods

Cell lines

The canine carcinoma cell line CT1258 [33] was cultured in sterile flasks containing 5 ml of medium 199 with Earle's salts (Gibco, Invitrogen, Karlsruhe, Germany) with 20% heat inactivated and filtrated fetal bovine serum (FBS). 12 hours prior to infection with recombinant AAVs, 2500 CT1258 cells per well were seeded into 96 multiwell dishes and cultivated in 10 % FBS 199 medium.

For AAV production HEK-293 cells (AAV-293) were obtained from Stratagene's AAV-Helper-Free System. According to the manufacturer's protocol the cells were cultured in 10 % FBS D-MEM Medium (Biochrom AG, Berlin, Germany). All cell lines were cultivated in a 37°C incubator with 5 % CO_2 saturation.

AAV plasmids

The vector plasmid for generating the recombinant AAVs was obtained from Stratagene's AAV-Helper-Free System (Stratagene, La Jolla, USA). The kit includes the pAAV-MCS (AF396260) plasmid containing the ITR sequences, multiple cloning site (MCS), the CMV promoter and *hGH* poly A tail. The system also includes the pAAV-RC (AF369963) for AAV replication and the capsid genes, the pHelper (AF396965) which provides adenoviral helper function by coding for *E2A*, *E4*, and *VA* RNA genes; the pAAV-LacZ (AF369964) contains the CMV promoter, the ORF for the reporter gene *lacZ* and ITR sequences (Figure 1). Ultra competent the XL-10-Gold *E. coli* (Stratagene, La Jolla, USA) were used to amplify the AAV Helper-Free plasmids and recombinant AAV vectors. The AAV plasmids were harvested and purified with the EndoFree Plasmid Purification Kit (Qiagen, Hilden Germany).

Cloning of canine HMGA cDNA and construction of antisense RNA plasmid vectors

Total RNA was isolated from CT1258 canine carcinoma cell line using RNeasy Mini Kit (Qiagen, Hilden, Germany) following the manufacturer's protocol. In order to prevent genomic DNA contamination DNAse I digestion was performed using RNase-Free DNase Set (Qiagen, Hilden, Germany). cDNA was synthesized using 3'RACE adapter primer AP2 (seq), 5µg of total RNA, and SuperScript II reverse transcriptase (Invitogen, Karlsruhe, Germany) according to the manufacturer's instructions. The RT-PCRs for the molecular cloning the canine for the short cDNA fragments of *HMGA1a* (484 bp) and *HMGA2* (312 bp) were done using BamHI and EcoRI adapter primer pairs. For *HMGA1*, BamHI-IYup (enzyme recognition sites in minuscule) (5'-CGggatccCTCGCGGCATCCCAGCCATCACT C-3'), EcoRI-IYlo (5'-CGgaattcGCGGCTGGTGTGCTGTGTAGTGTG -3') and for *HMGA2*, BamHI-ICup (5'-CGggatccGTGAGGGCGCGGGGCAGCCGTCC ACTTC-3'), EcoRI-IClo (5'-CGgaattcCTCTTCGGCAGACTCTTGTGAGGA TGTCT-3') were used. The primer for generating the long cDNA fragments of *HMGA1b* (1677 bp) were BamHI-IYup and EcoRI-A1-3'UTR (5'-CGgaattcATTCAAGTAACTGCAAATAGGA-3') and for *HMGA2* (1363 bp), BamHI-ICup and EcoRI-A2Ex5lo (5'-CGgaattcTTTCGCTCCTCTCACCTAAT-3').

A 1.5 % agarose gel electrophoresis was performed to separate the PCR products, the fragments were recovered with QIAquick Gel Extraction Kit (Qiagen, Hilden, Germany). The PCR products were cloned in the pGEM-T Easy Vector and sequenced in forward and reverse direction (MWG-Biotech AG, Ebersberg, Germany). The vector plasmid containing the *HMGA* (*HMGA1a* or *HMGA2*) cDNA was afterwards double-digested with *Bam*HI and *Eco*RI (Fermentas GmbH, St.Leon-Rot, Germany), and separated in a 1.5 % agarose gel, and the *HMGA* fragment was purified with QIAquick Gel Extraction Kit. In a

separate preparation the pAAV-MCS plasmid correspondently was digested with *Bam*HI and *Eco*RI and the assay was purified with QIAquick Nucleotide Removal Kit (Qiagen, Hilden, Germany). The *HMGA* fragment was ligated with T4-DNA Ligase (Fermentas GmbH, St Leon-Rot, Germany) at 25°C for 12 h into the *Eco*RI/*Bam*HI sites of the linearized pAAV-MCS (Stratagene, La Jolla, USA) plasmid to generate pAAV-HMGA in anti sense orientation relative to the CMV promoter (Figure 1). For validation the constructed pAAV-asHMGA vectors were confirmed by sequencing and restriction enzyme digestion.

rAAV vector construction, purification and titer measurement

Recombinant AAVs serotype 2 (AAV-2) were generated by transient transfection with $CaCl_2$/HBS buffer of AAV-293 cells with 10 µg of each of the three plasmids (pAAV-RC, pAAV-Helper, pAAV-asHMGA or pAAV-LacZ, respectively) according to the manufacturer's protocol (Stratagene, AAV-Helper-Free System). The AAV-2 primary stocks were purified using ViraTrap preequilibrated heparin agarose columns (Omega Bio-Tek, Doraville, USA) and stored in aliquots at -20°C. The virus genome titer (vg/ml) was determined by CMV promoter sequence specific quantitative RT-PCR (qRT-PCR) according to previously described methods[42, 43]. For absolute quantification of vg/ml the qRT-PCR amplification was carried out using the Applied Biosystem 7300 Real-Time PCR System (Applied Biosystem, Darmstadt, Germany). The following primers were used in the qRT-PCR reactions: forward pAAV (5' GAGGTCTATATAAGCAGAGCTCGTTTAGT 3'), reverse pAAV (5' GGTGTCTTCTATGGAGGTCAAAACA 3') and the fluorogenic probe pAAV (5' 6-FAM-CAGATCGCCTGGAGACGCCATCC-TAMRA).

For each rAAV-asHMGA vector a simultaneous production of rAAV-LacZ vectors was performed in order to evaluate the quality and functionality of rAAV particles. Infections of HT1080 cells were performed followed by counting the induced X-Gal stained LacZ-forming units (Stratagene, AAV-Helper-Free-System and In Situ β-Galactosidase Staining Kit). Furthermore, additional quantitative real-time PCRs for titration of infectious rAAV-2 particles[44] were established using primers and probes mentioned above (data not shown).

Cell proliferation assay

2500 CT1258 cells per well were seeded into a 96 multi well plate in eight different wells in medium 199 (10 % FBS) at 37°C and 5 % CO_2. After 90 min the cells were infected with different quantities of AAV particles. Subsequently, the CT1258 cells were divided into different groups: group LacZ with 350, 1,000, 10,000, 15,000 vg/cell of rAAV-LacZ infected cells and an untreated control. Group asHMGA with 350, 1,000, 10,000, 15,000 rAAV-asHMGA virus genomes per cell (vg/cell) or a combination of both rAAV-asHMGA1 and asHMGA2 (175/175, 500/500, 5,000/5,000 and 7,500/7,500 vg/cell of rAAV-asHMGA1a/rAAV-asHMGA2) and an untreated control. In order to prevent cross-contamination each assay was performed on a separate multi well plate. BrdU was added after 60 h for an incubation time of 12 h. After 72 h of rAAV infection the incubation was stopped and prepared for cell proliferation assay as noted in the manufacturer's instruction. Quantification of the cell proliferation was performed by ELISA, BrdU colorimetric assay (Roche Diagnostics, Penzberg, Germany). The measurement of absorbance of the samples was done with the Synergy HT multititer plate reader (Biotek Inc., Winooski, USA) at 370 nm (reference wavelength 492 nm).

Statistical analysis

Statistical significance between the groups was tested using a one-way ANOVA using GraphPad Prism Software (GraphPad Software, La Jolla, USA). A *P*-value less than 0.01 was considered to be statistically significant. In Figure 2 the standard deviations of all assay controls were summarized for better presentation.

Results

The incorporation of BrdU as a synthetic analog of thymidine into newly synthesized DNA of replicating cells of the S-phase is used for the measurement of proliferation. The cells either served as a control or were treated with 350, 1,000, 10,000 or 15,000 vg/cell of rAAV-LacZ (Figure 2). For antisense *HMGA* AAV treatment the cells were also infected with 350, 1,000, 10,000 and 15,000 vg/cell of rAAV-asHMGA. A double virus infection using *HMGA1* and *HMGA2* anti-sense transcripts was done in a combination (50:50 ratios) of 350, 1,000, 10,000 and 15,000 vg/cell (Figure 2).

For comparability the absorbance were presented as percentage of proliferation. The proliferation rate of untreated cells was presumed to be 100 %, meaning that the quotient of the mean values from treated and untreated cells are expressed as the percentage of proliferation rates of cells exposed to rAAV vectors.

Both rAAV-LacZ and rAAV-asHMGA vectors showed a decrease in proliferation of the CT1285 cells (Figure 2). The effect of 15,000 rAAV-LacZ vg/cells is a decrease of 10.9 % compared to the untreated control, the *P*-value is <0.01.

A decrease in proliferation is shown for the CT1258 cells treated with the rAAV-asHMGA vectors. In detail the rAAV-asHMGA1short showed a 44.1 % decrease in proliferation at a titer of 10,000 vg/cell and respectively a 65.7 % decrease at a titer of 15,000 vg/cell. Whereas the rAAV-asHMGA2short showed a 36.1 % decrease of proliferation at titer of 15,000 vg/cell, the *P*-value are <0.01. The percentage of the decrease of CT1258 cell proliferation induced by the vector combination of rAAV-asHMGA1 short and rAAV-asHMGA2 short is 61.7 % at a titer of 15,000 vg/cell in comparison to the untreated control, with a *P*-value of <0.01.

The inhibitory effect of proliferation is greater for the rAAV-asHMGA containing the CDS and parts of the 3'UTR sequence. For the rAAV-asHMGA1long virus vector the measured decrease of cell proliferation is 64.6 % at a titer of 10,000 vg/cell and 99.2 % at 15,000 vg/cell compared to the control, the *P*-values are <0.01.

The rAAV-asHMGA2long showed a 56.0 % decrease at a titer10,000 vg/cell and 79.7 % decrease at 15,000 vg/cell, whereas in contrast a combination of both rAAV-asHMGA1long and rAAV-asHMGA2long showed a 96.8 % at titer 10,000 vg/cell and a 99.0 % decrease of proliferation compared to the untreated control. Statistical analyses using a one-way ANOVA revealed a highly significant decrease of cell proliferation (*P*<0.0001).

Discussion

In many benign mesemchymal tumors as for example uterine leiomyomas, lipomas, and pulmonary chrondroid hamartomas[14, 45-47], a transcriptional reactivation of *HMGA* genes because of chromosomal rearrangements has been noted.

As to malignant tumors upregulation of *HMGA* protein expression seems to correlate to aggressiveness and severe prognosis of the disease, as has been shown e.g. for thyroid, breast, lung and prostate cancer. Previous *in-vitro* and *in-vivo* studies have shown that antisense *HMGA* vector transcripts induced by adenoviral vectors were able to reduce significantly protein synthesis of HMGA which in turn led to decreasing tumor growth and proliferation in transfected cancer cells and tissues of the thyroid.[40]

In the present study the *in-vitro* infection of canine prostate carcinoma cells by combination of recombinant antisense *HMGA1* and *HMGA2* AAV-vectors also showed an inhibition of cell proliferation.

Recently several studies on *HMGA2* transcription suppression were published concerning the regulation of *HMGA2* by microRNAs of the *let-7* family. In non-small cell lung cancer cell lines the inhibition of cell proliferation was achieved with the transfection of siRNA similar in sequence to the naturally occurring *let-7b*, *let-7e* and *let-7g* miRNAs.[48] The suppressive effect of *let-7* miRNAs on *HMGA2* expression is mediated through its capacity to bind to specific partial match sides within the 3'UTR of *HMGA2*. This effect would explain that in benign mesenchymal tumor entities translocations within the *HMGA2* gene locus can remove the recognition sites for miRNA *let-7*.[49] These studies strongly encourage the potential gene therapeutic approach of inducing antisense *HMGA* transcription for treating cancer because in many tumor entities e.g. lung cancers the transcription of *HMGA2* is up-regulated while the let-7 expression is down-regulated.[48, 50, 51]

Pancreatic adenocarcinomas showing an elevated expression of HMGA1 protein have a significantly decreased median survival compared to patients without HMGA1 expression.

Additionally, application of *HMGA1* silencing siRNA in vivo led to the reduction of pancreatic adenocarcinoma cell line induced tumor volume in nude mice[52].

In summary the infection of canine prostate carcinoma cells with the long rAAVasHMGA virus variants, encoding the CDS and 3'UTR in antisense orientation has led to the most promising effect of decreasing the cell proliferation to 4.5% compared to the untreated control. In mammals, insects, and fungi the existence of natural gene antisense transcripts has been reported to play an important role in gene regulation, e.g. circadian clockwork configuration, RNA processing and imprinting, most of all the regulation of the insulin like growth factor 2 receptor due to the transcription of antisense RNA from upstream control regions.[53, 54] In this study a strong expression of anti-sense *HMGA* transcripts was mediated by the eukaryotic CMV promoter encoded by the AAV genome. These anti-sense *HMGA* transcripts are complementary to endogenous *HMGA* mRNA forming RNA duplexes. These double stranded RNAs are the key targets of the post transcriptional gene silencing machinery of the cell or RNA interference respectively.

In conclusion the repression of HMGA translation mediated by recombinant AAV carrying large *HMGA* RNA in antisense orientation could be a promising target for a gene therapeutic approach for treating prostate cancer.

References

1. Davidson P, Gabbay J. Should mass screening for prostate cancer be introduced at the national level? *WHO Regional Office for Europe's Health Evidence Network (HEN).* 2004:1-12.
2. Brundtland G. *Men, ageing and health - achieving health across the life span.* Geneva: World Health Organisation; 2001.
3. Stewart BW, Kleinhues P (eds). *World cancer report.* 2003.
4. Boutemmine D, Bouchard N, Boerboom D, Jones HE, Goff AK, Dore M *et al.* Molecular characterization of canine prostaglandin G/H synthase-2 and regulation in prostatic adenocarcinoma cells in vitro. *Endocrinology* 2002; **143**(3)**:** 1134-1143.
5. Khanna C, Hunter K. Modeling metastasis in vivo. *Carcinogenesis* 2005; **26**(3)**:** 513-523.
6. Ostrander EA, Wayne RK. The canine genome. *Genome Res* 2005; **15**(12)**:** 1706-1716.
7. Vail DM, MacEwen EG. Spontaneously occurring tumors of companion animals as models for human cancer. *Cancer Invest* 2000; **18**(8)**:** 781-792.
8. MacEwen EG. Spontaneous tumors in dogs and cats: models for the study of cancer biology and treatment. *Cancer metastasis reviews* 1990; **9**(2)**:** 125-136.
9. Detailed Guide: Prostate Cancer. *American Cancer Society*. 08/25/2008. Available at: http://www.cancer.org. Accessed 01/16/2009, 2009.
10. Withrow SJ, MacEwen EG (eds). *Small Animal Clinical Oncology.* 2001.
11. Reeves R, Nissen MS. The A.T-DNA-binding domain of mammalian high mobility group I chromosomal proteins. A novel peptide motif for recognizing DNA structure. *J Biol Chem* 1990; **265**(15)**:** 573-8582.
12. Johnson KR, Lehn DA, Reeves R. Alternative processing of mRNAs encoding mammalian chromosomal high-mobility-group proteins HMG-I and HMG-Y. *Mol Cell Biol* 1989; **9**(5)**:** 2114-2123.
13. Friedmann M, Holth LT, Zoghbi HY, Reeves R. Organization, inducible-expression and chromosome localization of the human HMG-I(Y) nonhistone protein gene. *Nucleic Acids Res* 1993; **21**(18)**:** 4259-4267.
14. Schoenmakers EF, Wanschura S, Mols R, Bullerdiek J, Van den Berghe H, Van de Ven WJ. Recurrent rearrangements in the high mobility group protein gene, HMGI-C, in benign mesenchymal tumours. *Nat Genet* 1995; **10**(4)**:** 436-444.
15. Wanschura S, Kazmierczak B, Schoenmakers E, Meyen E, Bartnitzke S, Van de Ven W *et al.* Regional fine mapping of the multiple-aberration region involved in uterine leiomyoma, lipoma, and pleomorphic adenoma of the salivary gland to 12q15. *Genes Chromosomes Cancer* 1995; **14**(1)**:** 68-70.
16. Bustin M. Regulation of DNA-dependent activities by the functional motifs of the high-mobility-group chromosomal proteins. *Mol Cell Biol* 1999; **19**(8)**:** 5237-5246.
17. Bustin M, Reeves R. High-mobility-group chromosomal proteins: architectural components that facilitate chromatin function. *Progress in nucleic acid research and molecular biology* 1996; **54:** 35-100.
18. Reeves R. Molecular biology of HMGA proteins: hubs of nuclear function. *Gene* 2001; **277**(1-2)**:** 63-81.
19. Bullerdiek J. The molecular target of 12q14-15 aberrations in benign solid tumors. HMGIC rearrangements and beyond. *Fourth International Workshop in Human Chromosome 12 Mapping.* 1997.
20. Li O, Li J, Droge P. DNA architectural factor and proto-oncogene HMGA2 regulates key developmental genes in pluripotent human embryonic stem cells. *FEBS Lett* 2007; **581**(18)**:** 3533-3537.
21. Flohr AM, Rogalla P, Bonk U, Puettmann B, Buerger H, Gohla G *et al.* High mobility group protein HMGA1 expression in breast cancer reveals a positive correlation with tumour grade. *Histology and histopathology* 2003; **18**(4)**:** 999-1004.
22. Bandiera A, Bonifacio D, Manfioletti G, Mantovani F, Rustighi A, Zanconati F *et al.* Expression of HMGI(Y) proteins in squamous intraepithelial and invasive lesions of the uterine cervix. *Cancer Res* 1998; **58**(3)**:** 426-431.
23. Bussemakers MJ, van de Ven WJ, Debruyne FM, Schalken JA. Identification of high mobility group protein I(Y) as potential progression marker for prostate cancer by differential hybridization analysis. *Cancer Res* 1991; **51**(2)**:** 606-611.

24. Chiappetta G, Tallini G, De Biasio MC, Manfioletti G, Martinez-Tello FJ, Pentimalli F *et al.* Detection of high mobility group I HMGI(Y) protein in the diagnosis of thyroid tumors: HMGI(Y) expression represents a potential diagnostic indicator of carcinoma. *Cancer Res* 1998; **58**(18)**:** 4193-4198.
25. Meyer B, Loeschke S, Schultze A, Weigel T, Sandkamp M, Goldmann T *et al.* HMGA2 overexpression in non-small cell lung cancer. *Mol Carcinog* 2007; **46**(7)**:** 503-511.
26. Rogalla P, Drechsler K, Kazmierczak B, Rippe V, Bonk U, Bullerdiek J. Expression of HMGI-C, a member of the high mobility group protein family, in a subset of breast cancers: relationship to histologic grade. *Mol Carcinog* 1997; **19**(3)**:** 153-156.
27. Rommel B, Rogalla P, Jox A, von Kalle CV, Kazmierczak B, Wolf J *et al.* HMGI-C, a member of the high mobility group family of proteins, is expressed in hematopoietic stem cells and in leukemic cells. *Leuk Lymphoma* 1997; **26**(5-6)**:** 603-607.
28. Rogalla P, Drechsler K, Schroder-Babo W, Eberhardt K, Bullerdiek J. HMGIC expression patterns in non-small lung cancer and surrounding tissue. *Anticancer Res* 1998; **18**(5A)**:** 3327-3330.
29. Abe N, Watanabe T, Masaki T, Mori T, Sugiyama M, Uchimura H *et al.* Pancreatic duct cell carcinomas express high levels of high mobility group I(Y) proteins. *Cancer Res* 2000; **60**(12)**:** 3117-3122.
30. Miyazawa J, Mitoro A, Kawashiri S, Chada KK, Imai K. Expression of mesenchyme-specific gene HMGA2 in squamous cell carcinomas of the oral cavity. *Cancer Res* 2004; **64**(6)**:** 2024-2029.
31. Murua Escobar H, Soller JT, Richter A, Meyer B, Winkler S, Flohr AM *et al.* The canine HMGA1. *Gene* 2004; **330:** 93-99.
32. Beuing C, Soller JT, Muth M, Wagner S, Dolf G, Schelling C *et al.* Genomic characterisation, chromosomal assignment and in vivo localisation of the canine high mobility group A1 (HMGA1) gene. *BMC Genet* 2008; **9:** 49.
33. Winkler S, Murua Escobar H, Eberle N, Reimann-Berg N, Nolte I, Bullerdiek J. Establishment of a cell line derived from a canine prostate carcinoma with a highly rearranged karyotype. *J Hered* 2005; **96**(7)**:** 782-785.
34. Winkler S, Murua Escobar H, Meyer B, Simon D, Eberle N, Baumgartner W *et al.* HMGA2 expression in a canine model of prostate cancer. *Cancer Genet Cytogenet* 2007; **177**(2)**:** 98-102.
35. Kaplitt MG, Leone P, Samulski RJ, Xiao X, Pfaff DW, O'Malley KL *et al.* Long-term gene expression and phenotypic correction using adeno-associated virus vectors in the mammalian brain. *Nat Genet* 1994; **8**(2)**:** 148-154.
36. Scallan CD, Lillicrap D, Jiang H, Qian X, Patarroyo-White SL, Parker AE *et al.* Sustained phenotypic correction of canine hemophilia A using an adeno-associated viral vector. *Blood* 2003; **102**(6)**:** 2031-2037.
37. Streck CJ, Dickson PV, Ng CY, Zhou J, Hall MM, Gray JT *et al.* Antitumor efficacy of AAV-mediated systemic delivery of interferon-beta. *Cancer gene therapy* 2006; **13**(1)**:** 99-106.
38. Ponnazhagan S, Nallari ML, Srivastava A. Suppression of human alpha-globin gene expression mediated by the recombinant adeno-associated virus 2-based antisense vectors. *J Exp Med* 1994; **179**(2)**:** 733-738.
39. Li J, Hu SJ, Sun J, Zhu ZH, Zheng X, Wang GZ *et al.* Construction of phospholamban antisense RNA recombinant adeno-associated virus vector and its effects in rat cardiomyocytes. *Acta pharmacologica Sinica* 2005; **26**(1)**:** 51-55.
40. Berlingieri MT, Manfioletti G, Santoro M, Bandiera A, Visconti R, Giancotti V *et al.* Inhibition of HMGI-C protein synthesis suppresses retrovirally induced neoplastic transformation of rat thyroid cells. *Mol Cell Biol* 1995; **15**(3)**:** 1545-1553.
41. Scala S, Portella G, Fedele M, Chiappetta G, Fusco A. Adenovirus-mediated suppression of HMGI(Y) protein synthesis as potential therapy of human malignant neoplasias. *Proc Natl Acad Sci U S A* 2000; **97**(8)**:** 4256-4261.
42. Rohr UP, Wulf MA, Stahn S, Steidl U, Haas R, Kronenwett R. Fast and reliable titration of recombinant adeno-associated virus type-2 using quantitative real-time PCR. *Journal of virological methods* 2002; **106**(1)**:** 81-88.
43. Veldwijk MR, Topaly J, Laufs S, Hengge UR, Wenz F, Zeller WJ *et al.* Development and optimization of a real-time quantitative PCR-based method for the titration of AAV-2 vector stocks. *Mol Ther* 2002; **6**(2)**:** 272-278.
44. Rohr UP, Heyd F, Neukirchen J, Wulf MA, Queitsch I, Kroener-Lux G *et al.* Quantitative real-time PCR for titration of infectious recombinant AAV-2 particles. *Journal of virological methods* 2005; **127**(1)**:** 40-45.
45. Gattas GJ, Quade BJ, Nowak RA, Morton CC. HMGIC expression in human adult and fetal tissues and in uterine leiomyomata. *Genes Chromosomes Cancer* 1999; **25**(4)**:** 316-322.
46. Kazmierczak B, Meyer-Bolte K, Tran KH, Wockel W, Breightman I, Rosigkeit J *et al.* A high frequency of tumors with rearrangements of genes of the HMGI(Y)

family in a series of 191 pulmonary chondroid hamartomas. *Genes Chromosomes Cancer* 1999; **26**(2)**:** 125-133.
47. Wanschura S, Hennig Y, Deichert U, Schoenmakers EF, Van de Ven WJ, Bartnitzke S *et al.* Molecular-cytogenetic refinement of the 12q14-->q15 breakpoint region affected in uterine leiomyomas. *Cytogenet Cell Genet* 1995; **71**(2)**:** 131-135.
48. Kumar MS, Erkeland SJ, Pester RE, Chen CY, Ebert MS, Sharp PA *et al.* Suppression of non-small cell lung tumor development by the let-7 microRNA family. *Proc Natl Acad Sci U S A* 2008; **105**(10)**:** 3903-3908.
49. Lee YS, Dutta A. The tumor suppressor microRNA let-7 represses the HMGA2 oncogene. *Genes Dev* 2007; **21**(9)**:** 1025-1030.
50. Hebert C, Norris K, Scheper MA, Nikitakis N, Sauk JJ. High mobility group A2 is a target for miRNA-98 in head and neck squamous cell carcinoma. *Mol Cancer* 2007; **6:** 5.
51. Peng Y, Laser J, Shi G, Mittal K, Melamed J, Lee P *et al.* Antiproliferative effects by Let-7 repression of high-mobility group A2 in uterine leiomyoma. *Mol Cancer Res* 2008; **6**(4)**:** 663-673.
52. Liau SS, Rocha F, Matros E, Redston M, Whang E. High mobility group AT-hook 1 (HMGA1) is an independent prognostic factor and novel therapeutic target in pancreatic adenocarcinoma. *Cancer* 2008; **113**(2)**:** 302-314.
53. Crosthwaite SK. Circadian clocks and natural antisense RNA. *FEBS Lett* 2004; **567**(1)**:** 49-54.
54. Kumar M, Carmichael GG. Antisense RNA: function and fate of duplex RNA in cells of higher eukaryotes. *Microbiol Mol Biol Rev* 1998; **62**(4)**:** 1415-1434.

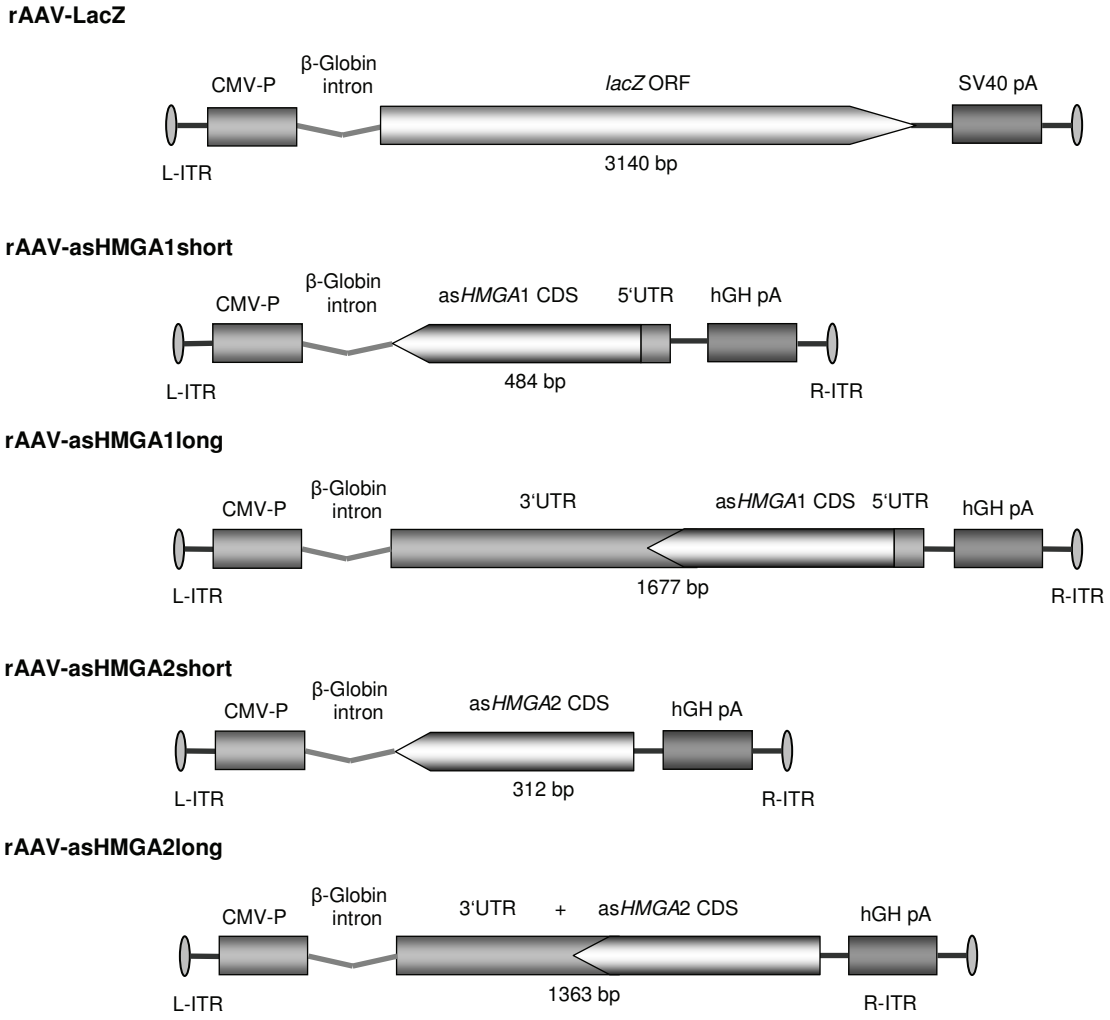

Figure 1 Schematic of recombinant AAV genomes encoding the *lacZ* ORF and anti-sense *HMGA1* and *HMGA2* RNA.

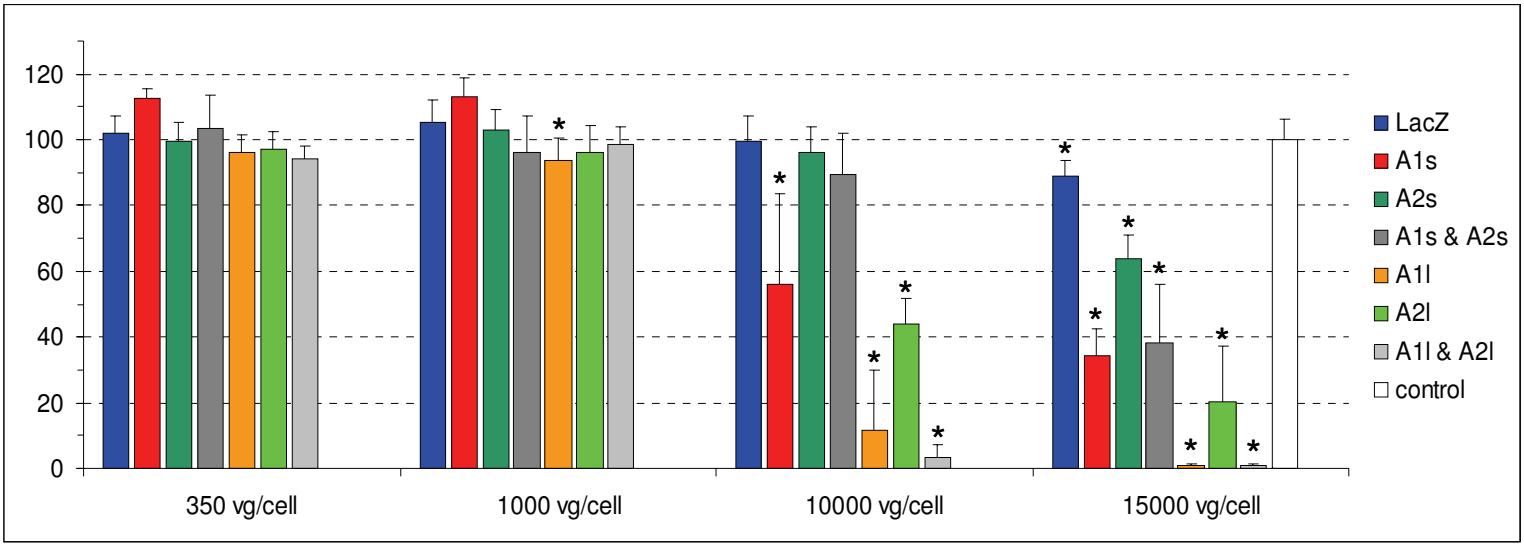

Figure 2 Inhibition of cell proliferation compared to the untreated control (colorimetric BrdU assay) by the addition of various recombinant AAV vectors at doses 350, 10001,000, 10.00010,000 and 15.00015,000 vg/cell (colored bars: LacZ: rAAV-LacZ, A1s: rAAV-asHMGA1 short, A2s: rAAV-asHMGA2 short, A1l: rAAV-asHMGA1 long and A2l: rAAV-asHMGA2 long; white bar: control, untreated CT1258 cells), $*P < 0.01$.

Supplementary Tables (one-way ANOVA statistics)

	Control	rAAV LacZ 350 vg/cell	rAAV LacZ 1000 vg/cell	rAAV LacZ 10.000 vg/cell	rAAV LacZ 15.000 vg/cell
Control					
rAAV LacZ 350 vg/cell	>0.01				
rAAV LacZ 1000 vg/cell	>0.01	>0.01			
rAAV LacZ 10.000 vg/cell	>0.01	>0.01	>0.01		
rAAV LacZ 15.000 vg/cell	<0.01	<0.01	<0.01	>0.01	

	Control	rAAV-asHMGA1 short 350 vg/cell	rAAV-asHMGA1 short 1000 vg/cell	rAAV-asHMGA1 short 10.000 vg/cell	rAAV-asHMGA1 short 15.000 vg/cell
Control					
rAAV-asHMGA1 short 350 vg/cell	>0.01				
rAAV-asHMGA1 short 1000 vg/cell	>0.01	>0.01			
rAAV-asHMGA1 short 10.000 vg/cell	>0.01	<0.01	<0.01		
rAAV-asHMGA1 short 15.000 vg/cell	>0.01	<0.01	<0.01	>0.01	

	Control	rAAV-as HMGA2 short 350 vg/cell	rAAV-as HMGA2 short 1000 vg/cell	rAAV-as HMGA2 short 10.000 vg/cell	rAAV-as HMGA2 short 15.000 vg/cell
Control					
rAAV-as HMGA2 short 350 vg/cell	>0.01				
rAAV-as HMGA2 short 1000 vg/cell	>0.01	>0.01			
rAAV-as HMGA2 short 10.000 vg/cell	>0.01	>0.01	>0.01		
rAAV-as HMGA2 short 15.000 vg/cell	<0.01	<0.01	<0.01	<0.01	

	Control	rAAV-as HMGA1/A2 short combination 350 vg/cell	rAAV-as HMGA1/A2 short combination 1000 vg/cell	rAAV-as HMGA1/A2 short combination 10.000 vg/cell	rAAV-as HMGA1/A2 short combination 15.000 vg/cell
Control					
rAAV-as HMGA1/A2 short combination 350 vg/cell	>0,01				
rAAV-as HMGA1/A2 short combination 1000 vg/cell	>0,01	>0,01			
rAAV-as HMGA1/A2 short combination 10.000 vg/cell	>0,01	>0,01	>0,01		
rAAV-as HMGA1/A2 short combination 15.000 vg/cell	<0,01	<0,01	<0,01	0,01	

	Control	rAAV-asHMGA1 long 350 vg/cell	rAAV-asHMGA1 long 1000 vg/cell	rAAV-asHMGA1 long 10.000 vg/cell	rAAV-asHMGA1 long 15.000 vg/cell
Control					
rAAV-asHMGA1 long 350 vg/cell	>0,01				
rAAV-asHMGA1 long 1000 vg/cell	>0,01	>0,01			
rAAV-asHMGA1 long 10.000 vg/cell	<0,01	<0,01	<0,01		
rAAV-asHMGA1 long 15.000 vg/cell	<0,01	<0,01	<0,01	<0,01	

	Control	rAAV-asHMGA2 long 350 vg/cell	rAAV-asHMGA2 long 1000 vg/cell	rAAV-asHMGA2 long 10.000 vg/cell	rAAV-asHMGA2 long 15.000 vg/cell
Control					
rAAV-asHMGA2 long 350 vg/cell	>0,01				
rAAV-asHMGA2 long 1000 vg/cell	>0,01	>0,01			
rAAV-asHMGA2 long 10.000 vg/cell	<0,01	<0,01	<0,01		
rAAV-asHMGA2 long 15.000 vg/cell	<0,01	<0,01	<0,01	<0,01	

	Control	rAAV-as HMGA1/A2 long combination 350 vg/cell	rAAV-as HMGA1/A2 long combination 1000 vg/cell	rAAV-as HMGA1/A2 long combination 10.000 vg/cell	rAAV-as HMGA1/A2 long combination 15.000 vg/cell
Control					
rAAV-as HMGA1/A2 long combination 350 vg/cell	>0,01				
rAAV-as HMGA1/A2 long combination 1000 vg/cell	>0,01	>0,01			
rAAV-as HMGA1/A2 long combination 10.000 vg/cell	<0,01	<0,01	>0,01		
rAAV-as HMGA1/A2 long combination 15.000 vg/cell	<0,01	<0,01	<0,01	>0,01	

VII

Co-transfection of plasmid DNA and laser-generated gold nanoparticles does not disturb the bioactivity of GFP-HMGB1 fusion protein.

Petersen S, Soller JT, Wagner S, Richter A, Bullerdiek J, Nolte I, Barcikowski S, Murua Escobar H.

Nanobiotechnology. 2009 Oct 24; 7(1): 6.

Eigenleistung:

- Koordinierung und Planung aller zellbiologischen Arbeiten
- Verfassen des Manuskripts zusammen mit S. Petersen und H. Murua Escobar

Journal of Nanobiotechnology

BioMed Central

Research

Open Access

Co-transfection of plasmid DNA and laser-generated gold nanoparticles does not disturb the bioactivity of GFP-HMGB1 fusion protein

Svea Petersen[†1], Jan T Soller[†2,3], Siegfried Wagner[2,3], Andreas Richter[3], Jörn Bullerdiek[2,3], Ingo Nolte[2], Stephan Barcikowski[*1] and Hugo Murua Escobar[2]

Address: [1]Laser Zentrum Hannover e.V., Hannover, Germany, [2]Small Animal Clinic and Research Cluster of Excellence "REBIRTH", University of Veterinary Medicine, Bischofsholer Damm 15, D-30173 Hannover, Germany and [3]Centre for Human Genetics, University of Bremen, Leobener Strasse ZHG, D-28359 Bremen, Germany

Email: Svea Petersen - s.petersen@lzh.de; Jan T Soller - jan.soller@tiho-hannover.de; Siegfried Wagner - Siegfrid.wagner@tiho-hannover.de; Andreas Richter - a.richter@uni-bremen.de; Jörn Bullerdiek - bullerd@uni-bremen.de; Ingo Nolte - ingo.nolte@tiho-hannover.de; Stephan Barcikowski* - s.barcikowski@lzh.de; Hugo Murua Escobar - hescobar@tiho-hannover.de

* Corresponding author †Equal contributors

Published: 24 October 2009

Journal of Nanobiotechnology 2009, **7**:6 doi:10.1186/1477-3155-7-6

Received: 27 March 2009
Accepted: 24 October 2009

This article is available from: http://www.jnanobiotechnology.com/content/7/1/6

Abstract

Ultrashort pulsed laser ablation in liquids represents a powerful tool for the generation of pure gold nanoparticles (AuNPs) avoiding chemical precursors and thereby making them especially interesting for biomedical applications. However, because of their electron accepting properties, laser-generated AuNPs might affect biochemical properties of biomolecules, which often adsorb onto the nanoparticles. We investigated possible effects of such laser-generated AuNPs on biological functionality of DNA molecules. We tested four differently sized and positively charged AuNPs by incubating them with recombinant eGFP-C1-HMGB1 DNA expression plasmids that code for eGFP fusion proteins and contain the canine architectural transcription factor HMGB1. We were able to show that successfully transfected mammalian cells are still able to synthesize and process the fusion proteins. Our observations revealed that incubation of AuNP with the plasmid DNA encoding the recombinant canine HMGB1 neither prevented the mediated uptake of the vector through the plasma membrane in presence of a transfection reagent nor had any effect on the transport of the synthesized fusion proteins to the nuclei. Biological activity of the recombinant GFP-HMGB1 fusion protein appears to have not been affected either, as a strong characteristic protein accumulation in the nucleus could be observed. We also discovered that transfection efficiencies depend on the size of AuNP. In conclusion, our data indicate that laser-generated AuNPs present a good alternative to chemically synthesized nanoparticles for use in biomedical applications.

Findings

Gold nanoparticles (AuNPs) are used widely for various biomedical applications including cell imaging [1], diagnostics [2], targeted drug delivery [3], and sensing [4]. Various methods have been established for AuNP generation. Many of these rely on several chemical reactions or gas

pyrolysis, showing the risk of impurities or agglomeration [5]. Laser ablation in liquids showed to be a powerful tool with many advantages, having almost no restriction in the choice of source material and the ability of yielding highly pure colloidal particles[6-11]. These pure AuNPs are characterised by their unique surface chemistry free of surfactants, a feature unattainable by other methods [12-14]. X-ray photoelectron spectroscopy of such AuNPs revealed the presence of the oxidation states Au^+ and Au^{3+} at the AuNP surface [15]. In previous studies we demonstrated that unmodified DNA oligonucleotides adsorb easily onto these positively charged nanoparticles [16,17], probably via amino- and keto-groups, which interact with the electron accepting surface of the generated AuNPs. However, these findings raised the possibility that more complex biomolecules could also be attracted and bound to such nanoparticles' surfaces, if incubated intentionally or unintentionally with colloidal laser-generated gold nanoparticles, even if no additional conjugation is envisaged. Such binding could have a strong effect on the properties of biomolecules and should be characterised with a view of their potential toxicity [18].

We therefore decided to analyse the possible effects of laser-generated AuNPs on DNA functionality. For this reason we incubated the charged particles with recombinant eGFP-C1-HMGB1 expression plasmids and subsequently transfected them into mammalian cells. As the HMGB1 protein is normally highly abundant in the cell nuclei, we were able to show that the treated expression plasmids are still functional and suitable for use as transcription matrix, because the transfected cells were still able to synthesize the fusion proteins, to process them and to transport them to their biofunctional destination. The effect of four differently sized nanoparticles on the activity of the eGFP-C1-HMGB1 plasmid was investigated by fluorescence microscopy. We additionally performed a binding assay to investigate structural effects on the plasmid due to AuNP co-incubation.

Nanoparticle generation

AuNPs were generated by laser ablation in water, as recently reported in detail [17]. Briefly, the beam of a femtosecond laser system (Spitfire Pro, Spectra-Physics), delivering 120 fs laser pulses at a wavelength of 800 nm, was focused with a 40 mm lens on a 99.99% pure gold target placed at the bottom of a Petri dish filled with 2 mL of bidistilled water. A pulse energy of 200 μJ at 5 kHz repetition rate was employed for 12 min. According to observations of Kabashin et al. [9] the focal position was lowered from one generation experiment to the other (0 mm, -2 mm, -4 mm relative to the focus in air) in order to obtain colloidal suspensions containing AuNPs with mean hydrodynamic diameters of d_h = 89 nm, d_h = 59 nm and d_h = 24 nm. The remaining small particles were removed by centrifugation at 15000 rpm for 10 min. To generate 14 nm AuNPs, laser ablation was carried out at a focal position of -4 mm, followed by a second irradiation for 5 min at 1 mJ with an Nd-YLF laser system (pulse length: 27 ns, 1047 nm, 5 kHz), as was described recently [19,20]. Characterization of nanoparticle suspensions was performed by dynamic light scattering using a Malvern Zetasizer and by UV-Vis spectroscopy using a Shimadzu 1650. The hydrodynamic number distributions and the average zeta potential of the colloids are shown in Figure 1. The zeta potential seems to be independent of the nanoparticle size, which might be explained by a similar surface charge density.

The particle mass concentration in the suspensions was determined by weighing the sediment after water evaporation.

Au-NP and eGFP-C1-HMGB1 vector in vitro *transfection assay*

The synthesised Au-NP suspensions were sterilized by filtration through a 0.2 μm filter device (Millex-GV Sterilizing Filter Unit, Millipore, Billerica, USA). Subsequently, 250 ng of each differently sized Au-NPs were incubated for 24 h at room temperature with 1 μg of recombinant plasmid eGFP-C1-HMGB1 in a total volume of 47 μl of ddH_2O. The time of co-incubation was intentionally kept that long as we aimed to investigate possible effects on the vector due to nanoparticle interferences. This was only possible as the circular double-stranded plasmid is not susceptible to rapid degenerative processes.

The recombinant plasmid encodes an eGFP-HMGB1 fusion protein. The HMGB1 coding sequence was derived from canine cDNA using PCR amplification (primer pair EcoR1_B15'CGGAATTCACCATGGGCAAAGGAGA3'/ KpnI_B1 (5'GCGGTACCTTATTCATCATCATC-3'). The obtained PCR products were separated on a 1.5% agarose gel, recovered with QIAquick Gel Extraction Kit (QIAGEN, Hilden, Germany), cloned into the pEGFP-C1 vector plasmid (BD Bioscience Clontech) and sequenced. Twelve hours prior to transfection, 3×10^5 cells from canine mammary cell line MTH53a were seeded into 12 multi well plates. The cells were grown at 37 °C and 5% CO_2 in medium 199 (Invitrogen, Karlsruhe, Germany) supplemented with 20% FCS, penicillin, and streptomycin. For transfection, 3 μl aliquots of Fugene HD (FHD) reagent (Roche, Mannheim, Germany) were added to 47 μl of different Au-NP/eGFP-C1-HMGB1 plasmid suspensions in a total volume of 50 μl and incubated for 15 min. The three control sample sets were: (i) 1 μg of eGFP-C1-HMGB1 DNA without nanoparticles, (ii) 250 ng of Au-NPs without any plasmid DNA, and (iii) a set of Au-NPs with DNA, but without the FHD.

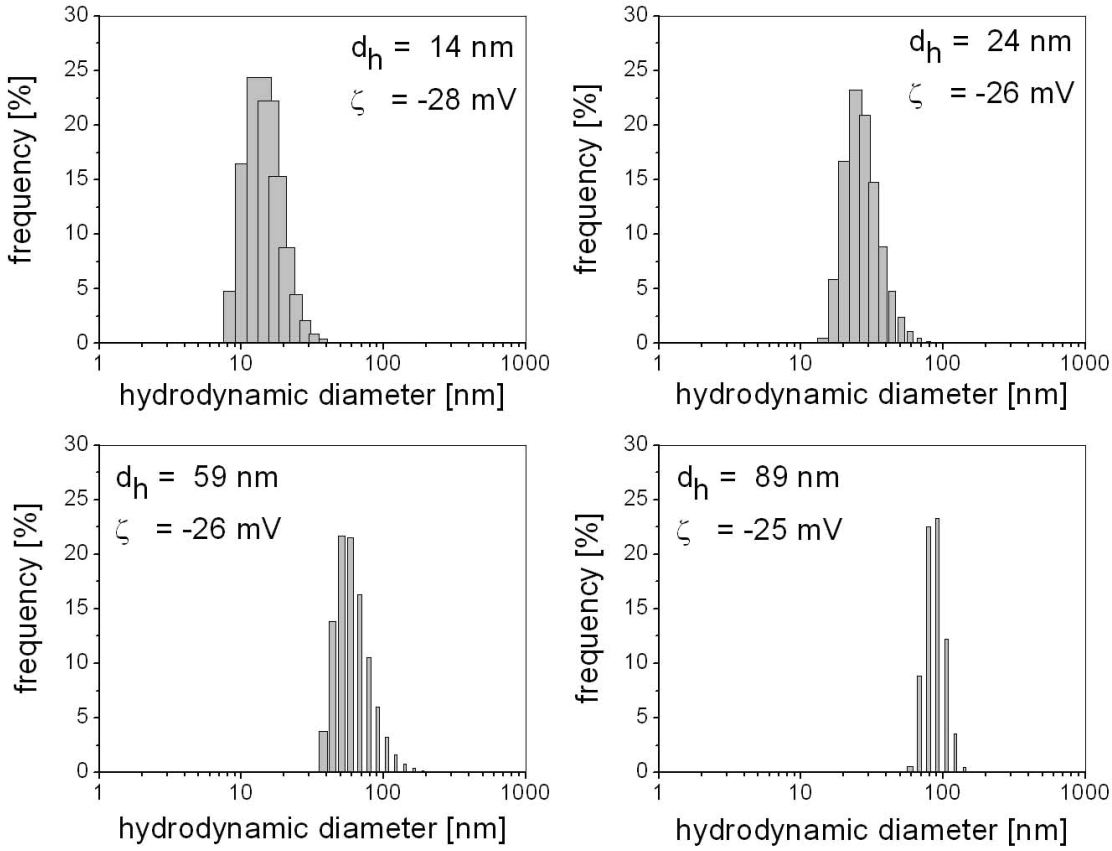

Figure 1

Size distribution and surface charge of laser generated gold nanoparticles. Gold nanoparticles (Au-NP) were generated by laser ablation in water using a femtosecond laser system (Spitfire Pro, Spectra-Physics) delivering 120 fs laser pulses at a wavelength of 800 nm (working pulse energy: 200 μJ per pulse, beam diameter: 4 mm). In order to generate four suspensions containing differently sized nanoparticles, the focal position was lowered from one generation experiment to the other (0 mm, -2 mm, -4 mm relative to the focus in air) resulting in the colloidal suspensions containing nanoparticles with mean hydrodynamic diameters of d_h = 89 nm, d_h = 59 nm and d_h = 24 nm. For the generation of 14 nm sized nanoparticles, laser ablation was carried out at a focal position of -4 mm and then reirradiated for 5 min at 1 mJ with an Nd-YLF laser system (pulse length: 27 ns, 1047 nm, 5 kHz). The hydrodynamic size distribution was analysed by Dynamic Light Scattering.

Following 15 min incubation at 23°C, the respective 50 μl transfection mixtures were added to cell cultures. The cells were incubated for 48 hours in medium 199 (20% FCS) at 37°C and 5% CO_2. The uptake of plasmid DNA and expression of the eGFP-C1-HMGB1 fusion protein were verified by fluorescence microscopy. All experiments were performed in quadruples.

Fluorescence microscopy

Transfected cells were washed with PBS, fixed in a 4% paraformaldehyde/PBS solution (pH 7.5) for 30 min at room temperature and washed again with PBS. Afterwards, the cells were incubated with 10 μl of mounting medium containing DAPI (4',6-diamidino-2-phenylindole) for fluorescent visualization of nucleic DNA (Vecta Laboratories, Burlingame, USA). Fluorescence microscopy was performed using the Carl Zeiss Axioskop 2 and images were recorded with the Axiovision Software. eGFP fluorescence was measured employing wavelength filter set 10 (Carl Zeiss MicroImaging, Göttingen, Germany), while DAPI fluorescence was measured employing wavelength filter set 2 (Figure 2A to 2M). Both fluorescence images were taken with a Zeiss 2-channel Axiocam MRm camera. Both images were then merged in a single image. Full colour images were taken with a Zeiss Axiocam HRc (Figure 2M and 2N). The uptake of plasmid DNA (efficiency of transfection) was estimated taking into account the quantity of cells within an ocular's visual field. Thus the estimation was done comparing the number of cells showing green fluorescence protein expression (green

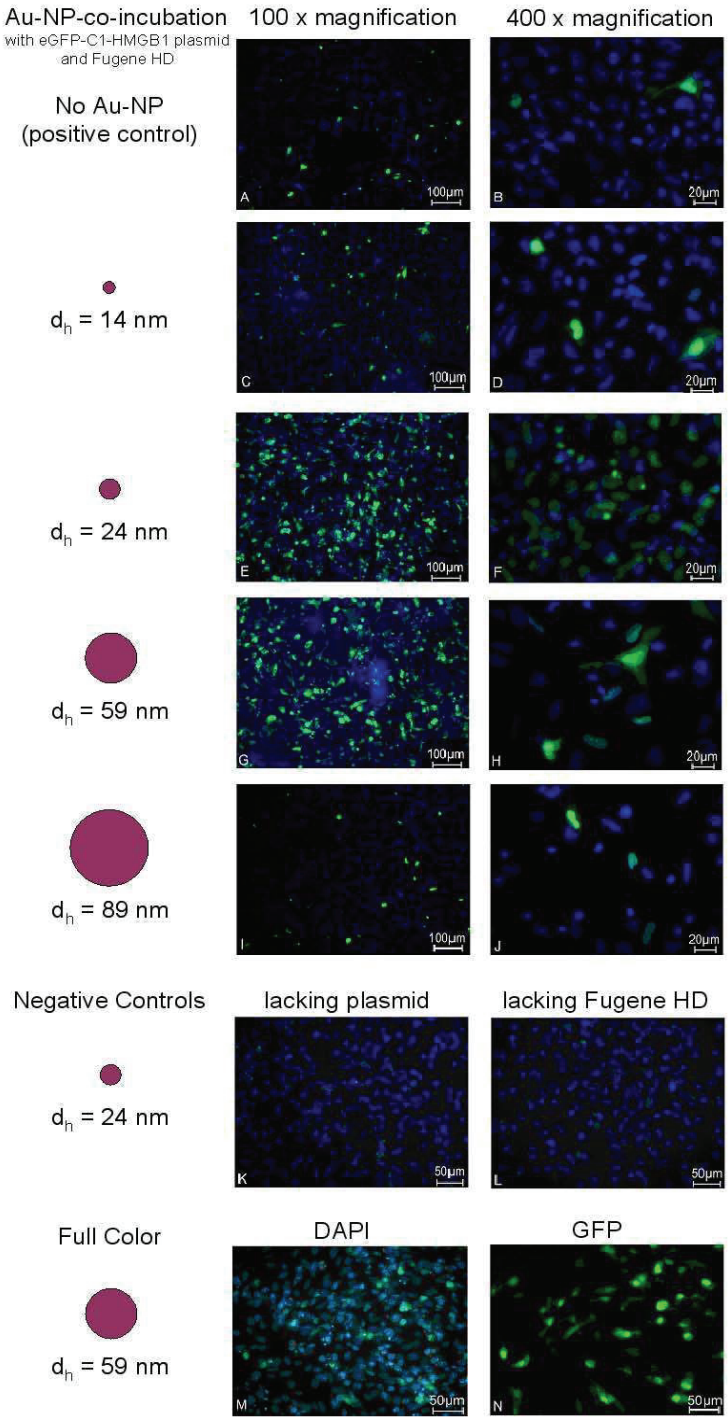

Figure 2

The effect of co-transfecting plasmid DNA and laser generated gold nanoparticles on the bioactivity of GFP-HMGB1 fusion protein. Images A to I (vertical) show a 100 fold magnification and B to J (vertical) a 400 fold magnification. Images A and B represent the positive control I: a transient transfection of MTH53a cells by Fugene HD reagent with the eGFP-C1-HMGB1 plasmid without Au-NP incubation. Cells in images C to J are treated like control I but include incubation of the plasmid with 14 nm sized Au-NP (C and D), 24 nm sized Au-NP (E and F), 59 nm sized nanoparticles (G and H) and 89 nm sized Au-NP (I and J), respectively. Image K and L represent the negative controls II and III. M and N are full color images of DAPI and GFP fluorescence.

Table 1: Summary of estimated transfection efficiencies

Size Au-NP (d_h)	Estimated Transfection Efficiency (%)	Figure
Positive controls	10 ± 2	A and B
14 nm	15 ± 5	C and D
24 nm	50 ± 5	E and F
59 nm	50 ± 10	G and H
89 nm	8 ± 3	I and J
Negative controls	-	K and L

Differently sized Au-NPs were incubated with plasmid DNA and transfected into the canine MTH53a cellline

staining) and cells showing blue DAPI fluorescence dye staining.

Co-transfection of plasmid DNA and laser-generated gold nanoparticles

As the HMGB1 protein is a transcription factor, it binds strongly to nuclear DNA. We therefore may assume that cell nuclei containing strong eGFP fluorescence represent successful functional transfection events. All cells transfected with AuNP-incubated plasmid DNA showed strong colocalised eGFP and DAPI staining (Figure 2), whilst the negative controls, cells treated with Au-NP and FHD (AuNP of d_h = 24 nm), showed no eGFP fluorescence (Figure 2K). We therefore conclude that co-incubation of AuNP with the plasmid DNA encoding the recombinant canine HMGB1 neither prevents the mediated uptake of the vector in presence of a transfection reagent nor has any visible effect on the transport and biological functionality of the synthesised fusion proteins.

By comparing fluorescence images of the cells co-incubated with the AuNPs of different sizes and to cells incubated without AuNPs, we were able to compare transfection efficiencies in each case. We estimate that the achieved efficiency of DNA transfection for the sample containing 14 nm AuNPs was approx. 15 ± 5% (Figure 2C and 2D).

The highest observed transfection efficiencies were achieved using 24 nm and 59 nm Au-NPs (50 ± 5% and 50 ± 10% respectively, see Figure 2E to 2H). The Au-NPs showed size dependent effects concerning the observed transfection efficiencies (see Table 1). Exemplarily, Au-NPs of a medium size (d_h: 24 and 59 nm) showed the highest effects. Thus, the observed GFP fluorescence of the respective fusion proteins was so intense that it even leaked into the DAPI channel (Fig 2M and 2N respectively for AuNP of d_h = 59 nm). Further negative control samples containing DNA- co-incubated AuNPs missing FHD, showed no recombinant protein expression, proving that our AuNPs did not act as transfection reagent themselves. (Figure 2L). The cell population seems to go along with transfection efficiency, as the observed seeding density was in all wells similar prior to transfection.

Shift assay

We performed binding experiments with plasmid DNA (eGFP-C1-HMGB1) and respective Au-NPs of different sizes and with various concentrations. We digested the co-incubated batches with a *NcoI* restriction enzyme (Fermentas, St Leon Rot, Germany) and separated the resulting DNA fragments in a 1.5% agarose gel. No significant shift alterations could be observed in the DNA mobility pattern. To ensure that this phenomenon is also valid in presence of proteins we added purified HMGB1 protein (Centre for Human Genetics, Bremen, Germany) to the

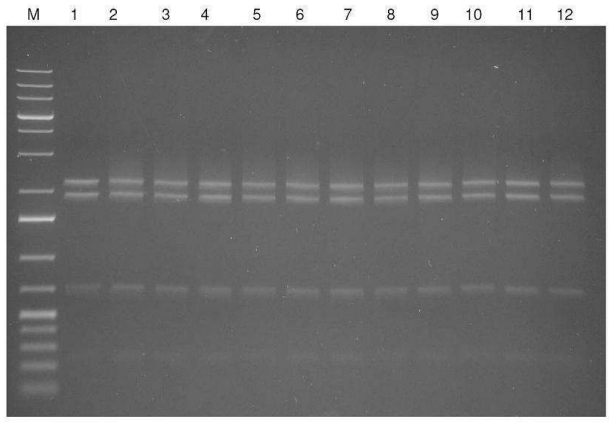

Figure 3
Au-NPs/DNA and HMGB1 protein mobility shift assay. **M**: GeneRuler 1 kb Plus (Fermentas), **lane 1**: 170 ng plasmid (NcoI digested); **lane 2**: 170 ng plasmid (NcoI digested) and 1.5 μg HMGB1; **lanes 3-6**: 170 ng plasmid 170 (NcoI digested) and 1.5 μg HMGB1 in 0.1 nM, 0.5 nM, 1.0 nM and 2.5 nM AuNPs suspensions, size d_h 24 nm; **lane 7**: 170 ng plasmid (NcoI) digested and 1.5 μg HMGB1 and 90 ng pure Au suspension, size d_h 24 nm; **lanes 8-11**: 170 ng plasmid (NcoI digested) and 1.5 μg HMGB1 in 0.1 nM, 0.5 nM, 1.0 nM and 2.5 nM AuNPs suspensions, size d_h 59 nm; **lane 12**: 170 ng plasmid (NcoI) digested and 1.5 μg HMGB1 and 50 ng pure Au suspension, size d_h 59 nm.

batches. Akin to the DNA mobility pattern of digested Plasmid DNA and HMGB1 without Au-NPs (lane 2, Figure 3) we could not detect any significant change in the shift pattern (see lanes 3 to 12, Figure 3). Consequently the DNA/Au-NPs complexes serve as substrates for the DNA-bindig protein HMGB1.

Conclusion

In conclusion, incubation of uncoated, positively charged AuNPs with a DNA plasmid that encodes recombinant eGFP-C1-HMGB1 fusion protein for 24 hours before cellular transfection does not seem to alter the protein expression and the protein functionality (DNA binding), while the presence of AuNPs seems to have a significantly positive effect on the transfection efficiencies. The observed effect was size-dependent: medium sized AuNPs enhanced transfection efficiency nearly 6 fold. These results support the hypothesis that laser-generated AuNPs present a good alternative to chemically synthesized nanoparticles and are especially suitable for biomedical applications.

Competing interests

The authors declare that they have no competing interests.

Authors' contributions

SP carried out the nanoparticle generation and partial drafting of the manuskript, JTS carried out the transfections, fluorescence microscopy analysis and partial drafting of the manuscript, SW performed cell culture and DNA preparation, AR generated the recombinant eGFP-C1-HMB1 plasmid, SB principal study design, manuscript drafting and supervision of nanoparticle work, HME principal design, partial manuscript drafting and supervision of molecular and cell biologic work. IN and JB participated in the conception design of the study. All authors read and approved the final manuscript.

Acknowledgements

The work was funded in part by the German Research Foundation within the excellence cluster REBIRTH.

References

1. Chen J, Saeki F, Wiley BJ, Chang H, Cobb MJ, Li ZY, Au L, Zhang H, Kimmey MB, Li X, Xia Y: *Nano Lett* 2005, **5:**473-477.
2. Chen J, Wiley B, Campbell D, Saeki F, Cahng L, Au L, Lee J, Li X, Xia Y: *Adv Mater* 2005, **17:**2255.
3. Yang PH, Sun X, Chiu JF, Sun H, Qing-Yu H: *Bioconjugate Chem* 2005, **16:**494-496.
4. Liu GL, Yin Y, Kunchakarra S, Mukherjee B, Gerion D, Jett SD, Bear DG, Gray JW, Alivisatos AP, Lee LP, Chen FF: *Nat Nanotechnol* 2006, **1:**47-52.
5. Dahl JA, Maddux BLS, Hutchison JE: *Chem Rev* 2007, **107:**2228-2269.
6. Mafuné F, Kohno J, Takeda Y, Kondow T, Sawabe H: *J Phys Chem B* 2000, **104:**9111-9117.
7. Mafuné F, Kohno J, Takeda Y, Kondow T: *J Phys Chem* 2001, **105:**9050-9056.
8. Dolgaev SI, Simakin AV, Voronov VV, Shafeev GA, Bozon-Verduraz F: *Appl Surf Sci* 2002, **186:**546-551.
9. Kabashin AV, Meunier M: *J Appl Phys* 2003, **94:**7941-7943.
10. Barcikowski S, Hahn A, Kabashin AV, Chichkov BN: *J Appl Phys A* 2007, **87:**47-55.
11. Barcikowski S, Menéndez-Manjón A, Chichkov B, Brikas M, Raèiukaitis G: *Appl Phys Lett* 2007, **91:**083113-1.
12. Sylvestre JP, Kabashin AV, Sacher E, Meunier M, Luong JHT: *J Am Chem Soc* 2004, **126:**7176-7177.
13. Sylvestre JP, Poulin S, Kabashin AV, Sacher E, Meunier M, Luong JHT: *J Phys Chem* 2004, **108:**16864-16869.
14. Kabashin AV, Meunier M, Kingston C, Luong JHT: *J Phys Chem B* 2003, **107:**4527-4531.
15. Sylvestre JP, Poulin S, Kabashin AV, Sacher E, Meunier M, Luong JHT: *Phys Chem B* 2004, **108:**16864-16869.
16. Petersen S, Jakobi J, Barcikowski S: *Appl Surf Sci* 2009, **255:**5435-5438.
17. Petersen S, Barcikowski S: *Adv. Funct. Mater.* 2009, **19:**1167-1172.
18. de Jong W, Borm PJA: *Journal of Nanomedicine* 2008, **3:**133-149.
19. Mafuné F, Kohno J, Takeda Y, Kondow TJ: *Phys Chem B* 2001, **105:**9050-9056.
20. Amendola V, Meneghetti M: *Phys Chem Chem Phys* 2009, **11:**3805-3821.

VIII

Cloning and characterization of the canine receptor for advanced glycation end products.

Murua Escobar H, Soller JT, Sterenczak KA, Sperveslage JD, Schlueter C, Burchardt B, Eberle N, Fork M, Nimzyk R, Winkler S, Nolte I, Bullerdiek J.

Gene. 2006 Mar 15; 369: 45-52.

Eigenleistung:

- Primerdesign und PCR, Klonierungen und Northern Blot
- *In silico* Analysen und Auswertungen
- Verfassen des Manuskripts zusammen mit H. Murua Escobar und J. Bullerdiek

Available online at www.sciencedirect.com
SCIENCE DIRECT
Gene 369 (2006) 45–52
GENE
SECTION
FUNCTIONAL GENOMICS
www.elsevier.com/locate/gene

Cloning and characterization of the canine receptor for advanced glycation end products

Hugo Murua Escobar [a,*,1], Jan T. Soller [a,b,1], Katharina A. Sterenczak [b], Jan D. Sperveslage [b], Claudia Schlueter [b], Birgit Burchardt [b], Nina Eberle [a], Melanie Fork [a], Rolf Nimzyk [b], Susanne Winkler [b], Ingo Nolte [a], Jörn Bullerdiek [b]

[a] *Small Animal Clinic, University of Veterinary Medicine, Bischofsholer Damm 15, D-30173 Hannover, Germany*
[b] *Centre for Human Genetics, University of Bremen, Leobener Strasse ZHG, D-28359 Bremen, Germany*

Received 2 August 2005; received in revised form 26 September 2005; accepted 11 October 2005
Available online 1 December 2005
Received by D.A. Tagle

Abstract

Metastasis is one of the major problems when dealing with malignant neoplasias. Accordingly, the finding of molecular targets, which can be addressed to reduce tumour metastasising, will have significant impact on the development of new therapeutic approaches. Recently, the receptor for advanced glycation end products (RAGE)–high mobility group B1 (HMGB1) protein complex has been shown to have significant influence on invasiveness, growth and motility of tumour cells, which are essential characteristics required for metastatic behaviour. A set of in vitro and in vivo approaches showed that blocking of this complex resulted in drastic suppression of tumour cell growth.

Due to the similarities of human and canine cancer the dog has joined the common rodent animal model for therapeutic and preclinical studies. However, complete characterisation of the protein complex is a precondition to a therapeutic approach based on the blocking of the RAGE–HMGB1 complex to spontaneously occurring tumours in dogs. We recently characterised the canine *HMGB1* gene and protein completely. Here we present the complete characterisation of the canine *RAGE* gene including its 1384 bp mRNA, the 1215 bp protein coding sequence, the 2835 bp genomic structure, chromosomal localisation, gene expression pattern, and its 404 amino acid protein. Furthermore we compared the CDS of six different canine breeds and screened them for single nucleotide polymorphisms.

Keywords: Receptor for advanced glycation end products; RAGE; HMGB1; Metastasis; *Canis familiaris*; Comparative genomics

Abbreviations: A, adenosine; aa, amino acid(s); AGE, advanced glycation end product(s); BAC, bacterial artificial chromosome; bp, base pair(s); BSA, bovine serum albumin; cDNA, DNA complementary to RNA; CDS, coding sequence(s); CFA, *Canis familiaris*; Ci, Curie; CD, carboxy-terminal domain; dCTP, deoxycytidine 5′-triphosphate; DNA, deoxy-ribonucleic acid; DNase, deoxyribonuclease; EC, extracellular; FISH, fluorescence in situ hybridisation; G, guanosine; GAPDH, glyceraldehyde-3-phosphate dehydrogenase; GTG, g-bands by trypsine using gimsa; HMG, high mobility group; HMGB1, high mobility group protein B1; HSA, Homo sapiens; I, inosine; Ig, immunoglobulin; kDa, kilo Dalton; M-MLV, Moloney murine leukemia virus; mRNA, messenger ribonucleic acid; NCBI, National Center for Biotechnology Information; ORF, open reading frame; ^{32}P, phosphorus 32 radioisotope; PHA, phytohemagglutinin; PCR, polymerase chain reaction; R, arginine; RACE, rapid amplification of cDNA ends; RAGE, receptor for advanced glycation end products; sRAGE, soluble RAGE variant(s); RNA, ribonucleic acid; SDS, sodium dodecyl sulfate; SNP, single nucleotide polymorphism; SSC, standard saline citrate; SSPE, sodium saline phosphate EDTA; TM, transmembrane domain; UTR, untranslated region; W, tryptophane.

* Corresponding author. Tel.: +49 511 856 7251; fax: +49 511 856 7686.
E-mail address: escobar@uni-bremen.de (H. Murua Escobar).

[1] H. Murua Escobar and J. T. Soller have contributed equally to this article.

0378-1119/$ - see front matter © 2005 Elsevier B.V. All rights reserved.
doi:10.1016/j.gene.2005.10.015

1. Introduction

The canine genome offers a wide field for genetic studies on various areas as e.g. phenotypic diversity, heredity and diseases including cancer. In terms of cancer, the canine model shows several advantages. First of all, the dog enjoys after the human the second best medical care of all species allowing a detailed surveillance of the cancer, progression, and therapy. The cancers seen in dogs are spontaneously developing as opposed to rodents with tumours being experimentally induced by carcinogen or transplanted to immunocompromised animals. Also, the canine cancers are more akin to human cancers than rodent tumours in terms of patient size and cell kinetics allowing better comparison of medical examinations as e.g. ultrasonography. It is generally believed that dogs develop cancer twice as frequently as humans, and it has been shown that the presentation, histology and biology of several canine cancers are similar to those in humans (Withrow and MacEwen, 1989, 2001; MacEwen, 1990). Most canine cancers progress more rapidly than their human counterparts permitting a better surveillance of the tumour state (Withrow and MacEwen, 2001). Additionally, dogs show similar characteristics of physiology and metabolism for most organ systems and drugs, which allows better comparability of modalities e.g. surgery, radiation, chemotherapy (Withrow and MacEwen, 2001), and new therapeutic approaches aimed at cancer treatment. At least a dozen distinct canine cancers are hypothesized to be appropriate models for their human counterparts (Patterson et al., 1982; Withrow and MacEwen, 1989; MacEwen, 1990; Knapp and Waters, 1997), among those osteosarcoma, breast carcinoma, oral melanomas, lung carcinomas and malignant non-Hodgkin's lymphomas (MacEwen, 1990).

Lately, the RAGE–HMGB1 protein complex has attracted significant interest in terms of metastasic behaviour of tumours. The receptor itself is a multiligand member of the immunoglobulin superfamily, which was shown to bind nonenzymatically glycated adducts, i.e. advanced glycation end products (AGE). It has been described to be involved in a variety of pathophysiological processes, e.g. immune/inflammatory disorders (Hofmann et al., 1999, 2002), Alzheimer's disease (Yan et al., 1997; Lue et al., 2001), abnormalities associated with diabetes, e.g. arteriosclerosis (Park et al., 1998) or impaired wound healing (Goova et al., 2001), and tumourigenesis (Taguchi et al., 2000; Huttunen et al., 2002). In terms of tumours and metastasis, the interaction with the extracellular ligand amphoterin, synonymously called HMGB1, was shown to have significant influence (Taguchi et al., 2000; Huttunen et al., 2002) by activating key cell signalling pathways such as MAP kinases and NF-κB (Taguchi et al., 2000). Taguchi et al. (2000) were able to show that blocking of this complex by using a soluble variant of the receptor lacking the cytosolic and transmembrane domains strongly inhibited the metastatic behaviour of glioma cells in terms of invasive growth, motility and migration. To establish a therapeutic approach based on blocking of the RAGE–HMGB1 protein complex in canine tumours as preclinical approach for human neoplasias, the knowledge of the canine protein complex is precondition. Previously we characterised the canine *HMGB1* gene and its protein (Murua Escobar et al., 2003). Here we present the complete characterisation of the canine *RAGE* gene including its mRNA, the genomic structure, chromosomal localisation, gene expression pattern, and its protein. Furthermore we compared the protein coding sequences (CDS) of six different canine breeds and screened them for single nucleotide polymorphisms (SNPs).

The complete characterisation of the canine RAGE–HMGB1 protein complex will serve as base for future clinical studies aimed at the development of blocking strategies to inhibit metastatic behaviour of canine and human tumours.

2. Methods and materials

2.1. Tissues

The tissues used in this study were provided by the Small Animal Clinic, University of Veterinary Medicine, Hannover, Germany. The breeds represented were Bernese Mountain Dog, Border Collie, Dachshund, Golden Retriever, Rottweiler, and Siberian Husky. From each breed up to three samples of lung tissue were taken and used for analyses.

2.2. Bacterial artificial chromosome (BAC) screening and fluorescence in situ hybridisation FISH

A canine genomic *RAGE* DNA probe was used for hybridisation of canine RPCI 81 BAC/PAC filter (BACPAC RESOURCES/Children's Hospital Oakland Research Institute, Oakland, USA). The 261 bp probe was generated by PCR with the primer set 480up and canisRlo623 (5′ AGGGACTCTTAGCTGGCACT 3′/5′ GAAGGTGGGGTGGGGAGCTC 3′) on genomic DNA prepared from a blood sample of a healthy dog. The obtained PCR product was separated on a 1.5% agarose gel, recovered with QIAEX II (QIAGEN, Hilden, Germany), cloned in pGEM–T-Easy vector system (Promega, Madison, USA) and sequenced for verification. The probe labelling was performed by random primed labelling (Roche Diagnostics, Mannheim, Germany) as described in the manufacturer's protocol with 250 ng probe and 250 μCi (α^{32}P)dCTP (GE Healthcare, Freiburg, Germany). Purification of the labelled probe was done using Sephadex G-50 Nick Columns (Amersham Pharmacia Biotech, Freiburg, Germany) and the probe was stored at −20 °C before use.

The filters were placed in a minimum volume of Church Buffer (0.15 mM bovine serum albumin (BSA), 1 mM EDTA, 0.5 M $NaHPO_4$, 7% SDS) and transferred into hybridisation bottles. The filters were prehybridised at 65 °C for 1 h in 25 ml Church Buffer. Hybridisation was performed at 65 °C overnight (16–18 h) in the same solution. All further steps were performed according to manufacturer's protocol. Signals were visualised using a STORM imager (Molecular Dynamics, Sunnyvale, USA).

Metaphase preparations were obtained from blood samples of different dogs. The samples were stimulated with phytohemagglutinin (PHA) and cultured for 96 h at 37 °C. After incubation for 2 h with colcemide (0.1 μg/ml), the lymphocytes

were harvested and slides were prepared according to routine procedures. Prior to FISH, chromosomes were stained using an adapted GTG-banding method. Chromosomal G-bands were identified according to Reimann et al. (1996). After recording the metaphases, the slides were destained in 70% ethanol for 15 min, air-dried and incubated at 60 °C overnight.

FISH was performed using the protocol of Fischer et al. (1996) with some modifications. BAC DNA was digoxigenin labelled (Dig-Nick-Translation-Kit, Roche Diagnostics, Mannheim, Germany). The hybridisation mixture contained 200 ng probe, 43.2 μg salmon sperm DNA, 800 ng sonicated dog DNA, 1× SSC, 1× SSPE, 50% formamide and 10% dextransulfate. The chromosomes were counterstained with propidiumiodide.

2.3. Genomic characterisation

For genomic characterization the canine *RAGE* gene was amplified by PCR using the screened BAC RP81339J10 (BACPAC RESOURCES/Children's Hospital Oakland Research Institute, Oakland, USA). A 1298 bp fragment spanning exon 1 to exon 6 was generated by the primer pair canisRup1/canisRlo623 (5′ ATGGCAGCAGGGGCGGCAGC 3′/5′ GAAGGTGGGGTGGGGAGCTC 3′) and an additional 1403 bp fragment spanning exon 6 to exon 11 was generated with pair cEx6up/3046lo (5′ CTCCCCACCCCACCTTCTCC 3′/5′ TCATGGCCCTGCTGCACCGCTCT 3′) including the respective introns. The obtained PCR products were separated on an 1.5% agarose gel, recovered with QIAEX II (QIAGEN, Hilden, Germany), cloned in pGEM–T-Easy vector system (Promega, Madison, USA) and sequenced for verification. The final genomic canine *RAGE* contig and the identity alignments were created with Lasergene software (DNAStar, Madison, USA) using various sequences from the NCBI database (GenBank accession nos.: D28769, AB036432, NM_001136, BC020669, M91211) and the following described cDNA (see Section 2.4).

2.4. cDNA characterisation

Total RNA was isolated from 50 mg canine lung tissue using TRIZOL LS (Invitrogen, Karlsruhe, Germany) following the manufacturer's protocol. To avoid genomic DNA contamination a *DNase* digest of each sample was performed using *RNase*-Free *DNase* Set (Qiagen, Hilden, Germany). cDNA was synthesised using 3′-RACE adaptor primer AP2 (AAGGATCCGTCGACATC(17)T), 5 μg total RNA, and SuperScript II (Invitrogen, Karlsruhe, Germany) reverse transcriptase according to the manufacturer's instructions. The PCRs for the molecular cloning of the cDNA were done using the primer pairs canisRup1/canisRlo623 (5′ ATGGCAGCAGGGGCGGCAGC 3′/5′ GAAGGTGGGGTGGGGAGCTC 3′), 480up/RAGElo1236 (5′ AGGGACTCTTAGCTGGCACT 3′/5′ TGTCTGTGGGCCCCTCAAGG 3′) and gene-specific primers cEx6up/cEx11up (5′ CTCCCCACCCCACCTTCTCC 3′/5′ GAATCAGTCAGAGGAGCCCGAGG 3′). 3′RACE PCR was done using the adaptor primer AP2 specified above. The primers were derived from human cDNA sequences (GenBank accession no. M91211). 5′RACE was performed using the primers 5′RACE Abridged Anchor Primer (5′ GGCCACGCGTCGACTAGTACGGGIIGGGIIGGGII 3′), Universal Amplification Primer (5′ CTACTACTACTAGGCCACGCGTCGACTAGTAC 3′), and the gene-specific primers RAGElo1236 and canisRlo623 determined as above according to the 5′RACE System for Rapid Amplifications of cDNA Ends by Invitrogen. The PCR products were separated on a 1.5% agarose gel, recovered with QIAEX II (QIAGEN, Hilden, Germany), cloned in pGEM–T-Easy vector system (Promega, Madison, USA) and sequenced. The cDNA contig and the identity alignments were created with Lasergene software (DNAStar, Madison, USA) and various sequences from the NCBI database (GenBank accession nos.: D28769, AB036432, NM_001136, BC020669, M91211).

2.5. CDS comparison between breeds

The CDSs were characterised for all breeds as described previously in Section 2.2. The contigs and the identity alignments were created using several sequences from the NCBI database (GenBank accession nos.: D28769 AB036432, NM_001136, BC020669, M91211). In case of single-nucleotide exchanges, the samples were sequenced again in both forward and reverse direction. Exchanges causing no amino acid (aa) substitution were not taken into account for further analyses. For all samples with aa substitutions, the initial PCR was repeated and the exchange verified by sequencing the product in both forward and reverse direction.

2.6. Protein sequences

The canine RAGE protein sequence was derived from the ORF (open reading frames) of the characterised cDNA sequence described previously in Section 2.4. The protein homology alignments were created with four sequences from the NCBI database (GenBank accession nos.: BAA89369, NP_776407, AAA42027, AAH61182).

2.7. Northern Blot and RT–PCR

Total RNA was isolated from canine liver, kidney, heart, testis, lung, muscle, pancreas and spleen tissue using RNeasy midi system (QIAGEN, Hilden, Germany). For Northern Blot hybridisation 30 μg of total RNA from each tissue sample was separated on a 1.2% denaturing agarose gel containing 0.65% formaldehyde. RNA was transferred onto Hybond–N^+ positive nylon membrane (Amersham Pharmacia Biotech, Freiburg, Germany) by capillary blot.

A 624 bp cDNA fragment derived from the canine *RAGE* sequence (exon 1/exon 5) served as a molecular probe for hybridisation. The probe was generated by PCR with the primer set canisRup1 and canisRlo623 (5′ ATGGCAGCAGGGGCGGCAGC 3′/5′ GAAGGTGGGGTGGGGAGCTC 3′) using the cloned cDNA described in Section 2.2. Probe labelling was performed by random primed labelling (Amersham Pharmacia Biotech, Freiburg, Germany) as described in the manufacturer's

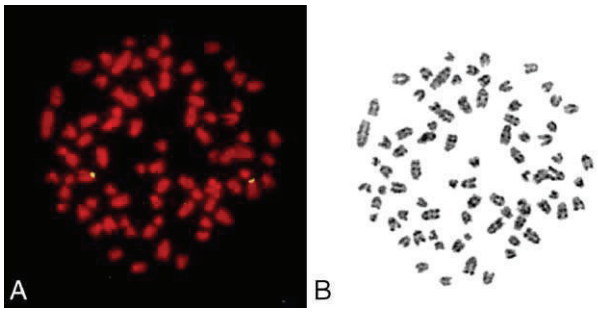

Fig. 1. An example of a metaphase spread after FISH with signals on both chromosomes 12 (A) and the same metaphase after GTG-banding (B).

protocol with 50 μCi (α^{32}P)dCTP (Amersham Pharmacia Biotech, Freiburg, Germany). Purification of the labelled probe was performed using Sephadex G-50 Nick Columns (Amersham Pharmacia Biotech, Freiburg, Germany) and the probe was stored at −20 °C before use.

Prehybridisation was carried out for 30 min and hybridisation overnight at 68 °C using the PERFECTHYB PLUS hybridisation solution (Sigma-Aldrich, Saint Louis, MO, USA). The membrane was washed for 5 min at room temperature in 2× SSC/0.1% SDS, and twice for 20 min at 68 °C in 0.5× SSC/0.1% SDS. Signals were visualised using a STORM phosphorimager (Molecular Dynamics, Sunnyvale, USA).

RT–PCR was performed using all isolated tissue cDNAs with primer pair cEx6up/3046lo (5′ CTCCCCACCCCACCTTCTCC 3′/5′ TCATGGCCCTGCTGCACCGCTCT 3′).

3. Results and discussion

The RAGE–HMGB1 protein complex has lately attracted significant interest of researchers working on cancer and other diseases. Several publications demonstrate the involvement of the RAGE receptor in a variety of pathophysiological processes, e.g. immune/inflammatory disorders (Hofmann et al., 1999, 2002), Alzheimer disease (Yan et al., 1997; Lue et al., 2001), abnormalities associated with diabetes, e.g. arteriosclerosis (Park et al., 1998) and impaired wound healing (Goova et al., 2001). It has been shown that the specific RAGE-related diseases are caused by binding of different specific ligands to the receptor (for reviews, see Schmidt et al., 2001; Huttunen and Rauvala, 2004). In terms of tumourigenesis and metastasis, the interaction with the extracellular ligand amphoterin, synonymously called HMGB1, was shown to have significant influence by activating key cell signalling MAP kinase pathways (Huttunen et al., 2002; Taguchi et al., 2000). A set of in vivo and in vitro experiments showed that blocking of this complex strongly inhibited the metastatic behaviour of cancer cells in terms of invasive growth, motility and migration (Taguchi et al., 2000). Furthermore, deregulation of the *RAGE* gene expression level was associated with prostate cancer (Simm et al., 2004), with malignant potential of colorectal cancer (Sasahira et al., 2005) and non-small-cell lung cancer (Bartling et al., 2005).

To establish a therapeutic approach based on blocking of the RAGE–HMGB1 protein complex in canine tumours as a preclinical approach for human neoplasias, the knowledge of the canine protein complex is preconditioned.

3.1. Chromosomal localisation

A canine *RAGE* genomic DNA probe was generated and used for screening of a canine BAC for localisation of the canine *RAGE* gene locus by FISH. The verified BAC 339-J10 was used for FISH experiments. Twelve well-spread metaphases were

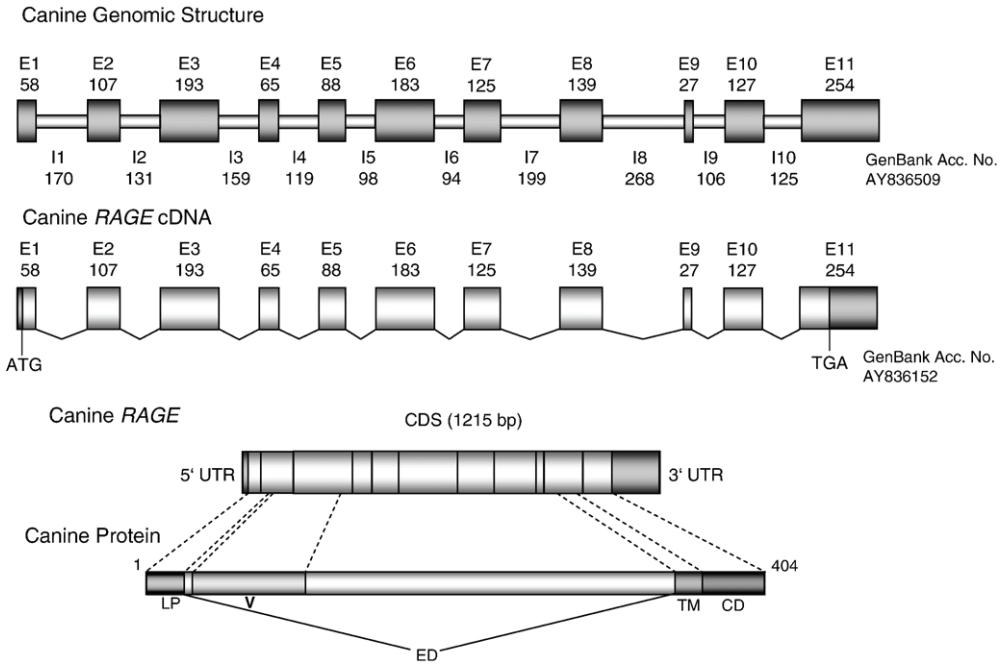

Fig. 2. Structure of the canine *RAGE* gene on genomic, cDNA and protein level.

examined for analyses, showing signals on both chromatides of both chromosomes CFA 12 (Fig. 1). The chromosomal localisation was done following the nomenclature established by Reimann et al. (1996). Presented synteny studies (Yang et al., 1999; Breen et al., 1999) showed that the canine CFA 12 shares homology to the human chromosome 6 where the *RAGE* gene is located at HSA 6p21.32. As far as we know, chromosomal aberrations affecting CFA 12 are not reported to be significantly associated with canine neoplasias.

3.2. Genomic structure

The genomic structure of the canine *RAGE* gene consists of eleven exons and ten introns. The complete canine gene spans 2835 bp. The exon/intron structure, size and the homologies to their human counterparts were analysed and defined (Fig. 2 and Table 1). The total identity to the corresponding human region shows 63.4%. In detail, the identities of the exons vary between 73.9% and 86.7% to their human counterpart, while the introns show identities between 43.4% and 71.0% (for details see Table 1). The genomic sequences were submitted to the NCBI database (GenBank accession no. AY836509).

Table 1
Detailed analysis of the *RAGE* gene elements and the RAGE protein

Element	Size in bp	Identity to human counterpart in % (D28769)
Total genomic gene	2835	63.4
Total cDNA	1384	80.9
5′UTR	18	100
CDS	1215	82.9
3′UTR	151	70.8
Detail exons/introns		
Exon 1	58	78.0
Intron 1	170	67.5
Exon 2	107	86.7
Intron 2	131	71.0
Exon 3	193	85.8
Intron 3	159	53.8
Exon 4	65	85.5
Intron 4	119	57.0
Exon 5	88	86.6
Intron 5	98	71.1
Exon 6	183	86.7
Intron 6	94	47.3
Exon 7	125	80.2
Intron 7	199	57.6
Exon 8	139	85.0
Intron 8	268	51.8
Exon 9	27	79.2
Intron 9	106	62.3
Exon 10	127	84.3
Intron 10	125	62.3
Exon 11	254	73.9
Protein	**Size in aa**	**Identity to human counterpart in % (BAA89369)**
Total protein	404	77.6
Total extracellular domain	318	78.2
Ig-type V domain	33	85.7
Transmebrane domain	19	78.9
Cytosolic tail	43	72.7

Identity comparison of the canine *RAGE* genomic elements, cDNA elements, and protein to their human counterparts.

3.3. The canine RAGE cDNA transcript

The complete canine *RAGE* cDNA consist of eleven exons spanning 1384 bp in total. The exon size varies between 27 bp to 254 bp composing all together a 5′UTR of 18 bp, a CDS of 1215 bp, and a 3′UTR of 151 bp (Fig. 2 and Table 1). Identity comparison to its human counterpart (GenBank accession no. D28769) revealed a total identity of 80.9% on nucleotide level varying in the exons from 73.9% (exon 11) to 86.7% (exon 2) (for details see Table 1). In humans several naturally occurring truncated *RAGE* transcripts have been described lacking the cytosolic and transmembrane domains named soluble *RAGE* variants (sRAGE) (Malherbe et al., 1999; Schlueter et al., 2003). These aberrant transcripts act as naturally occurring competitive inhibitors of the RAGE receptor taking effect on receptor efficiency. Detailed analysis of the aberrant transcript structure revealed the partial insertion of different genomic *RAGE* intron DNA fragments leading to the observed aberrant splicing products (Malherbe et al., 1999; Schlueter et al., 2003). In dogs, we could not detect corresponding aberrant splicing products using the experimental design developed previously in our group by Schlueter et al. (2003). However, the application of such soluble *RAGE* variants to block e.g. the HMGB1 protein drastically suppressed the growth of tumour cells in vitro and in vivo (for review see Huttunen et al., 2002). Treatment of mice with sRAGE completely suppressed diabetic atherosclerosis in a glycemia- and lipid-independent manner (Park et al., 1998). The total canine *RAGE* cDNA sequence was submitted to the NCBI database with GenBank accession no. AY836152 completing our previous submission of AY530943.

3.4. RAGE CDS comparison between different canine breeds

For six different canine breeds the protein coding sequences were characterised by amplification of a fragment spanning the CDS using the canine lung cDNA samples as template. Nucleotide exchanges causing no amino acid substitution were not taken into account in further analyses. The comparison of these six protein-coding sequences revealed one amino acid change. A Bernese Mountaindog sample showed a nucleotide transition from C (CGG) to T (TGG) at the first base of the CDS codon 364, leading to an aa replacement from arginine (R) to tryptophane (W). Possible PCR artefacts seem rather unlikely, since several clones were sequenced for verification. Polymorphisms causing mutations in the *RAGE* gene had been associated with various inflammatory diseases and diabetic syndromes such as rheumatoid arthritis, psoriasis, nephropathy, periodontitis, and microvascular diseases (Hudson et al., 1998, 2001; Kankova et al., 1999, 2001; Liu and Xiang, 1999; Poirier et al., 2001; Hofmann et al., 2002; Schmidt, 2002; Vasku et al., 2002). Considering the fact that canine breeds show breed-specific predispositions for various cancers and

other diseases, the detailed analyses of single breeds could be of significant value to unravel the disease associated mechanisms involved.

The CDS cDNA sequences of the six breeds were submitted to the NCBI database with GenBank accession nos. DQ125936, DQ125937, DQ125938, DQ125939, DQ125940, and DQ125941.

3.5. The canine RAGE protein

The canine RAGE protein sequence was deduced from the characterised cDNA sequence. The canine RAGE protein is a 404-amino-acid molecule with a calculated weight of 43 kDa (Fig. 1 and Table 1). Identity comparison of the canine molecule to its human counterpart (GenBank accession no. BAA89369) showed a total of 77.6% identity to the human protein including the described three extracellular (EC) immunoglobulin (Ig) type domains V, C, C′, the hydrophobic transmembrane domain (TM), and the highly charged cytosolic tail including acidic carboxy-terminal domain (CD) (Neeper et al., 1992). The total canine extracellular domain shows 78.2%, the transmembrane domain 78.9%, and the cytosolic tail 72.7% identity to their human counterparts, respectively. The RAGE immunoglobulin type V domain was identified as HMGB1 binding domain. The identity comparison of this domain between dog and human showed 85.7% with 10 amino acid exchanges (Fig. 3). Recently, the motive

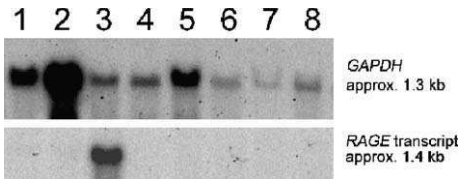

Fig. 4. Total RNA Northern blot showing 1.4 kb *RAGE* and 1.3 kb *GAPDH* transcripts. Lanes: (1) canine testis, (2) canine heart, (3) canine lung, (4) canine muscle, (5) canine kidney, (6) canine pancreas, (7) canine spleen, (8) canine liver.

of the human HMGB1 protein for binding the V domain of RAGE receptor was identified to consist of aa 150–183 including the HMG-Box-B and part of carboxy-terminal domain (Huttunen et al., 2002). We previously characterised the canine HMGB1 protein and comparison of the functional domains revealed that the canine amino acid sequence is identical to the human counterpart (Murua Escobar et al., 2003). Due to the high similarity of the canine and human RAGE–HMGB1 protein complexes in their interacting domains, therapeutic approaches applied in dogs could be more suitable in terms of transferability for the development of human therapies than approaches tested in other organisms.

Comparison of the canine RAGE protein with the described mouse (GenBank accession no. AAH61182), rat (GenBank accession no. AAA42027) and bovine (GenBank accession no.

```
   1                                                  50                                                 100
   ----------+----------+----------+----------+----------+----------+----------+----------+----------+----------
 1 MAAGAAAAAGAWVLVLSLWGAVVGDRNITARIGKPLVLNCRGAPKKPPQQLEWKLNTGRTEAWKVLSPQGG-PWDSVARVLPNGSLLLPAVGIQDEGTFRCRAT Canine
 1 MAAG--TAVGAWVLVLSLWGAVVGAQNITARIGEPLVLKCKGAPKKPPQRLEWKLNTGRTEAWKVLSPQGGGPWDSVARVLPNGSLFLPAVGIQDEGIFRCQAM Human
 1 MPAG--TAARAWVLVLALWGAVAGGQNITARIGEPLVLSCKGAPKKPPQQLEWKLNTGRTEAWKVLSPQGG-PWDSVARILPNGSLLLPATGIVDEGTFRCRAT Mouse
 1 MPTG--TVARAWVLVLALWGAVAGGQNITARIGEPLMLSCKGAPKKPTQKLEWKLNTGRTEAWKVLSPQGD-PWDSVARILPNGSLLLPAIGIVDEGTFRCRAT Rat
 1 MAAG--AVVGAWMLVLSLGGTVTGDQNITARIGKPLVLNCKGAPKKPPQQLEWKLNTGRTEAWKVLSPQGD-PWDSVARVLPNGSLLLPAVGIQDEGTFRCRAT Bovine
   105                                                155                                                205
   ----------+----------+----------+----------+----------+----------+----------+----------+----------+----------
104 SRNGKETRSTYQVRVYQIPGKPEIINPASELMAGVPSKVGTCVSEGGYPAGTLSWHWDGKPLIPDGKGVSVQEETRRHPETGLFTLQSELMVTPAQGGAPHPTF Canine
103 NRNGKETKSNYRVRVYQIPGKPEIVDSASELTAGVPNKVGTCVSEGSYPAGTLSWHLDGKPLVPNEKGVSVKEQTRRHPETGLFTLQSELMVTPARGGDPRPTF Human
102 NRRGKEVKSNYRVRVYQIPGKPEIVDPASELTASVPNKVGTCVSEGSYPAGTLSWHLDGKLLIPDGKETLVKEETRRHPETGLFTLRSELTVIPTQGG-THPTF Mouse
102 NRLGKEVKSNYRVRVYQIPGKPEIVNPASELTANVPNKVGTCVSEGSYPAGTLSWHLDGKPLIPDGKGTVVKEETRRHPETGLFTLRSELTVTPAQGG-TTPTY Rat
102 SRSGKETKSNYRVRVYQIPGKPEIVDPASELMAGVPNKVGTCVSEGGYPAGTLNWLLDGKTLIPDGKGVSVKEETKRHPKTGLFTLHSELMVTPARGGALHPTF Bovine
   210                                                250                                                300
   ----------+----------+----------+----------+----------+----------+----------+----------+----------+----------
209 SCSFSPGLPRRRALHAAPIQLNVW------ES-----VPL-EVQVMVEP-GGMLAPGGTVTLTCETPAQSSVQIHWIKDGMPLPLPPSPMLLSEVKPEDQGTYV Canine
208 SCSFSPGLPRHRALRTAPIQPRVW------EP-----VPLEEVQLVVEPEGGAVAPGGTVTLTCEVPAQPSPQIHWMKDGVPLPLPPSPVLILPEIGPQDQGTY Human
206 SCSFSLGLPRRRPLNTAPIQLRVR------EP-----GPPEGIQLLVEPEGGIVAPGGTVTLTCAISAQPPPQVHWIKDGAPLPLAPSPVLLLPEVGHEDEGTY Mouse
206 SCSFSLGLPRRRPLNTAPIQPRVR------EP-----LPPEGIQLLVEPEGGTVAPGGTVTLTCAISAQPPPQIHWIKDGTPLPLAPSPVLLLPEVGHEDEGIY Rat
207 SCSFTPGLPRRRALHTAPIQLRVWSEHRGGEGPNVDAVPLKEVQLVVEPEGGAVAPGGTVTLTCEAPAQPPPQIHWIKDGRPLPLPPGPMLLLPEVGPEDQGTY Bovine
   305                                                355                                                405
   ----------+----------+----------+----------+----------+----------+----------+----------+----------+----------
301 SCVAMHPSHGSQESRGVSV-VIETDKEGPTTGYVEGQGLGTVALALGILGGLGIAVLLIGAIMWRRR-QRQRQERKAPENQEEEEEERTELNQSEEPEAAESG Canine
302 SCVATHSSHGPQESRAVSISIIEPGEEGPTAGSVGGSGLGTLALALGILGGLGTAALLIGVILWQRR-QRRGEERKAPENQEEEEE--RAELNQSEEPEAGESS Human
300 SCVATHPSHGPQESPPVSIRVTETGDEGPAEGSVGESGLGTLALALGILGGLGVVALLVGAILWRKR-QPRREERKAPESQEDEEE--RAELNQSEEAEMPENG Mouse
300 SCVATHPSHGPQESPPVNIRVTETGDEGQAAGSVDGSGLGTLALALGILGGLGIAALLIGAILWRKR-QPRLEERKAPESQEDEEE--AELNQSEEAEMPENGR Rat
312 SCVATHPSHGPQESRAVSVTIIETGEEGTTAGSVEGPGLETLALTLGILGGLGTVALLIGVIVWHRRRQRKGQERKVPENQEEEEEE-RAELNQPEEPEAAESS Bovine
   410
   -------
404 AAGP | total canine aa 404
405 TGGP | total human  aa 404
403 AGGP | total murine aa 402
403 AGGP | total Rat    aa 402
416 TGGP | total bovine aa 416
```

Fig. 3. Comparison of the canine, human, mouse, rat, and bovine RAGE proteins. The amino acid differences are shown as bold letters.

NP_776407) molecules showed identities of 73.5%, 72.8% and 77.7%, respectively (Fig. 3).

The canine RAGE protein sequence was submitted to the NCBI database with GenBank accession no. AAX38183.

3.6. Canine RAGE expression analysis

To elucidate the expression patterns of the canine *RAGE* gene, a canine Northern blot was performed using RNA from canine liver, kidney, heart, testis, lung, muscle, pancreas and spleen tissue samples as well as RNA from different canine cell lines and hybridised with a ^{32}P-labelled canine RAGE cDNA probe. Except for the lung tissue showing a clear approx. 1.4 kb signal, none of the samples revealed a distinct signal. After stripping and rehybridisation with a canine GAPDH probe, all samples revealed signals corresponding to approx. 1.3 kb demonstrating intact RNA (Fig. 4). For verification, performed RT–PCR using the same RNA revealed, additionally to a clear lung signal, very weak signals in spleen and heart tissue (data not shown). These results are in accordance to the gene expression pattern seen in humans. However, as mentioned before, aberrant transcripts like those found in humans could not be detected by RT–PCR. Lately, deregulation of the *RAGE* gene had been associated with various cancers and diseases e.g. up-regulation of the gene has been shown to be associated with prostate cancer development, human heart dysfunction, and inhibition of liver regeneration (Simm et al., 2004; Cataldegirmen et al., 2005; Ishiguro et al., 2005), while down-regulation of the *RAGE* gene has been shown to support non-small-cell lung carcinomas (Bartling et al., 2005). Additionally, *RAGE* gene expression has been associated with malignant potential of colorectal adenomas (Sasahira et al., 2005). As far as we know, in canine neoplasias, no *RAGE* expression analyses have been carried out. Considering the mentioned characteristics of canine neoplasias as model for human cancer, expression analyses done in canine tumours could be of significant value to further elucidate the role of *RAGE* in tumour and disease development.

4. Conclusions

As reviewed lately by Khanna and Hunter (2005), the dog is significantly helping to reveal characteristics of human tumour biology especially of metastasis due to the described similarities of the naturally occurring malignancies in both species. Accordingly, the development of new therapeutic approaches in animal model systems will be facilitated by the ongoing characterisation of model species specific molecular targets. Especially in points of transferability, the newly gained knowledge will be of great value. Due to the significant role of the RAGE–HMGB1 protein complex in cancer metastasis and the described various other diseases, the complete characterisation of the canine RAGE–HMGB1 protein complex will serve as basis for future clinical studies.

References

Bartling, B., Hofmann, H.S., Weigle, B., Silber, R.E., Simm, A., 2005. Down-regulation of the receptor for advanced glycation end-products (RAGE) supports non-small cell lung carcinoma. Carcinogenesis 26 (2), 293–301.

Breen, M., Thomas, R., Binns, M.M., Carter, N.P., Langford, C.F., 1999. Reciprocal chromosome painting reveals detailed regions of conserved synteny between the karyotypes of the domestic dog (*Canis familiaris*) and human. Genomics 61, 145–155.

Cataldegirmen, G., et al., 2005. RAGE limits regeneration after massive liver injury by coordinated suppression of TNF-alpha and NF-kappaB. J. Exp. Med. 201 (3), 473–484.

Fischer, P., Holmes, N., Dickens, H., Thomas, R., Binns, M., Nacheva, E., 1996. The application of FISH techniques for physical mapping in the dog (*Canis familiaris*). Mamm. Genome 7, 37–41.

Goova, M.T., et al., 2001. Blockade of receptor for advanced glycation end-products restores effective wound healing in diabetic mice. Am. J. Pathol. 159, 513–525.

Hofmann, M.A., et al., 1999. RAGE mediates a novel proinflammatory axis: a central cell surface receptor for S100/calgranulin polypeptides. Cell 97, 889–901.

Hofmann, M.A., et al., 2002. RAGE and arthritis: the G82S polymorphism amplifies the inflammatory response. Genes Immun. 3, 123–135.

Hudson, B.I., Stickland, M.H., Grant, P.J., 1998. Identification of polymorphisms in the receptor for advanced glycation end products (*RAGE*) gene: prevalence in type 2 diabetes and ethnic groups. Diabetes 47, 1155–1157.

Hudson, B.I., Stickland, M.H., Futers, T.S., Grant, P.J., 2001. Effects of novel polymorphisms in the rage gene on transcriptional regulation and their association with diabetic retinopathy. Diabetes 50, 1505–1511.

Huttunen, H.J., Rauvala, H., 2004. Amphoterin as an extracellular regulator of cell motility: from discovery to disease. Intern. Med. 255 (3), 351–366.

Huttunen, H.J., Fages, C., Kuja-Panula, J., Ridley, A.J., Rauvala, H., 2002. Receptor for advanced glycation end products-binding COOH-terminal motif of amphoterin inhibits invasive migration and metastasis. Cancer Res. 62, 4805–4811.

Ishiguro, H., Nakaigawa, N., Miyoshi, Y., Fujinami, K., Kubota, Y., Uemura, H., 2005. Receptor for advanced glycation end products (RAGE) and its ligand, amphoterin are overexpressed and associated with prostate cancer development. Prostate 64 (1), 92–100 (Jun 15).

Kankova, K., Vasku, A., Hajek, D., Zahejsky, J., Vasku, V., 1999. Association of G82S polymorphism in the *RAGE* gene with skin complications in type 2 diabetes. Diabetes Care 22, 1745.

Kankova, K., et al., 2001. Polymorphisms 1704G/T and 2184A/G in the *RAGE* gene are associated with antioxidant status. Metabolism 50, 1152–1160.

Khanna, C., Hunter, K., 2005. Modeling metastasis in vivo. Carcinogenesis 26 (3), 513–523.

Knapp, D.W., Waters, D.J., 1997. Naturally occurring cancer in pet dogs: important models for developing improved cancer therapy for humans. Mol. Med. Today 3 (1), 8–11.

Liu, L., Xiang, K., 1999. RAGE Gly82Ser polymorphism in diabetic microangiopathy. Diabetes Care 22, 646.

Lue, L.F., et al., 2001. Involvement of microglial receptor for advanced glycation endproducts (RAGE) in Alzheimer's disease: identification of a cellular activation mechanism. Exp. Neurol. 171, 29–45.

MacEwen, E.G., 1990. Spontaneous tumours in dogs and cats: models for the study of cancer biology and treatment. Cancer Metastasis Rev. 9, 125–136.

Malherbe, P., et al., 1999. cDNA cloning of a novel secreted isoform of the human receptor for advanced glycation end products and characterization of cells co-expressing cell surface scavenger receptors and Swedish mutant amyloid precursor protein. Brain Res. Mol. Brain Res. 71, 159–170.

Murua Escobar, H., et al., 2003. Molecular characterization of the canine HMGB1. Cytogenet. Genome Res. 101 (1), 33–38.

Neeper, M., et al., 1992. Cloning and expression of a cell surface receptor for advanced glycosylation end products of proteins. J. Biol. Chem. 267, 14998–15004.

Park, L., et al., 1998. Suppression of accelerated diabetic atherosclerosis by the soluble receptor for advanced glycation endproducts. Nat. Med. 4, 1025–1031.

Patterson, D.F., Haskins, M.E., Jezyk, P.F., 1982. Models of human genetic disease in domestic animals. Adv. Hum. Genet. 12, 263–339.

Poirier, O., et al., 2001. Polymorphism screening of four genes encoding advanced glycation end-product putative receptors. Association study with nephropathy in type 1 diabetic patients. Diabetes 50, 1214–1218.

Reimann, N., et al., 1996. An extended nomenclature of the canine. Cytogenet. Cell Genet. 73, 140–144.

Sasahira, T., Akama, Y., Fujii, K., Kuniyasu, H., 2005. Expression of receptor for advanced glycation end products and HMGB1/amphoterin in colorectal adenomas. Virchows Arch. 446 (4), 411–415.

Schlueter, C., Hauke, S., Flohr, A.M., Rogalla, P., Bullerdiek, J., 2003. Tissue-specific expression patterns of the RAGE receptor and its soluble forms—a result of regulated alternative splicing? Biochim. Biophys. Acta 1630 (1), 1–6.

Schmidt, A.M., 2002. RAGE and arthritis: the G82S polymorphism amplifies the inflammatory response. Genes Immun. 3, 123–135.

Schmidt, A.M., Yan, S.D., Yan, S.F., Stern, D.M., 2001. The multiligand receptor RAGE as a progression factor amplifying immune and inflammatory responses. J. Clin. Invest. 108, 949–955.

Simm, A., Casselmann, C., Schubert, A., Hofmann, S., Reimann, A., Silber, R. E., 2004. Age associated changes of AGE-receptor expression: RAGE upregulation is associated with human heart dysfunction. Exp. Gerontol. 39 (3), 407–413.

Taguchi, A., et al., 2000. Blockade of RAGE–amphoterin signalling suppresses tumour growth and metastases. Nature 405, 354–360.

Vasku, V., et al., 2002. Gene polymorphisms (G82S, 1704G/T, 2184A/G and 2245G/A) of the receptor of advanced glycation end products (RAGE) in plaque psoriasis. Arch. Dermatol. Res. 294, 127–130 (JID-8000462).

Withrow, S.J., MacEwen, E.G., 1989. Clinical Veterinary Oncology. J.B. Lippincott, Co.

Withrow, S.J., MacEwen, E.G., 2001. Small Animal Clinical Oncology. W.B. Saunders Company.

Yan, S.D., et al., 1997. Amyloid-beta peptide-receptor for advanced glycation endproduct interaction elicits neuronal expression of macrophage-colony stimulating factor: a proinflammatory pathway in Alzheimer disease. Proc. Natl. Acad. Sci. U. S. A. 94, 5296–5301.

Yang, F., et al., 1999. A complete comparative chromosome map for the dog, red fox, and human and its integration with canine genetic maps. Genomics 62, 189–202.

IX

Cloning, characterisation, and comparative quantitative expression analyses of receptor for advanced glycation end products (*RAGE*) transcript forms.

Sterenczak KA, Willenbrock S, Barann M, Klemke M, Soller JT, Eberle N, Nolte I, Bullerdiek J, Murua Escobar H.

Gene. 2009 Apr 1; 434(1-2): 35-42.

Eigenleistung:

- *In silico* Analysen
- Bearbeitung der NCBI Datenbankeinträge

Gene 434 (2009) 35–42

Contents lists available at ScienceDirect

Gene

journal homepage: www.elsevier.com/locate/gene

Cloning, characterisation, and comparative quantitative expression analyses of receptor for advanced glycation end products (*RAGE*) transcript forms

Katharina A. Sterenczak [a,b], Saskia Willenbrock [a,b], Matthias Barann [b], Markus Klemke [b], Jan T. Soller [a,b], Nina Eberle [a], Ingo Nolte [a], Jörn Bullerdiek [a,b], Hugo Murua Escobar [a,b,*]

[a] *Small Animal Clinic and Research Cluster of Excellence "REBIRTH", University of Veterinary Medicine, Bischofsholer Damm 15, D-30173 Hannover, Germany*
[b] *Centre for Human Genetics, University of Bremen, Leobener Strasse ZHG, D-28359 Bremen, Germany*

ARTICLE INFO

Article history:
Received 25 April 2008
Received in revised form 16 July 2008
Accepted 31 October 2008
Available online 12 November 2008

Received by D.A. Tagle

Keywords:
Receptor for advanced glycation end products
RAGE
sRAGE
Tumour
Canis familiaris
Comparative genomics

ABSTRACT

RAGE is a member of the immunoglobulin superfamily of cell surface molecules playing key roles in pathophysiological processes, e.g. immune/inflammatory disorders, Alzheimer's disease, diabetic arteriosclerosis and tumourigenesis. In humans 19 naturally occurring *RAGE* splicing variants resulting in either N-terminally or C-terminally truncated proteins were identified and are lately discussed as mechanisms for receptor regulation. Accordingly, deregulation of sRAGE levels has been associated with several diseases e.g. Alzheimer's disease, Type 1 diabetes, and rheumatoid arthritis. Administration of recombinant sRAGE to animal models of cancer blocked tumour growth successfully. In spite of its obvious relationship to cancer and metastasis data focusing sRAGE deregulation and tumours is rare. In this study we screened a set of tumours, healthy tissues and various cancer cell lines for *RAGE* splicing variants and analysed their structure. Additionally, we analysed the ratio of the mainly found transcript variants using quantitative Real-Time PCR. In total we characterised 24 previously not described canine and 4 human RAGE splicing variants, analysed their structure, classified their characteristics, and derived their respective protein forms. Interestingly, the healthy and the neoplastic tissue samples showed in majority RAGE transcripts coding for the complete receptor and transcripts showing insertions of intron 1.

1. Introduction

The receptor for advanced glycation end products (RAGE) is a member of the immunoglobulin superfamily of cell surface molecules which binds nonenzymatically glycated adducts like advanced glycation end products (AGE). Acting as a multiligand receptor it has been described to interact with various ligands i.e. amphoterin also known as HMGB1 (Hori et al., 1995), amyloid beta (Yan et al., 1996), proteins of the S100/calgranulin family (Hofmann et al., 1999) and Mac-1 (Chavakis et al., 2003). The ligand-receptor-complexes regulate cell signalling pathways having influencing effect on cell growth and proliferation, i.e. p21ras, erk1/2 (p44/p42) MAP kinases, p38, SAPK/JNK Map kinases, rho GTPases, phosphoinostiol-3 kinase, NFkB, and cAMP response element binding protein (CREB) (Neeper et al., 1992; Yan et al., 1994; Lander et al., 1997; Deora et al., 1998; Hofmann et al., 1999; Huttunen et al., 1999; Kislinger et al., 1999; Huang et al., 2001; Huttunen et al., 2002b). In terms of pathophysiological processes RAGE has been described to be involved in various diseases including diabetic arteriosclerosis (Park et al., 1998; Cipollone et al., 2003), impaired wound healing (Goova et al., 2001), Alzheimer's disease (Yan et al., 1996; Lue et al., 2001, 2005), immune and inflammatory disorders (Hofmann et al., 1999; Schmidt et al., 2001; Hofmann et al., 2002; Chavakis et al., 2004) and various cancers (Taguchi et al., 2000; Huttunen et al., 2002a; Bartling et al., 2005; Bhawal et al., 2005; Ishiguro et al., 2005). In humans 19 naturally occurring *RAGE* splicing variants resulting in either N-terminally or C-terminally truncated proteins were identified and are currently discussed as mechanisms for receptor regulation (hRAGEsec (Malherbe et al., 1999), sRAGE1,

Abbreviations: aa, amino acid(s); Acc. No., Accession number; AGE, advanced glycation end product(s); bp, base pair(s); cAMP, cyclic adenosine monophosphate; CD, Cytosol domain; cDNA, DNA complementary to RNA; CDS, coding sequence(s); CFA, *Canis familiaris*; CREB, cAMP response element binding protein; DNA, deoxyribonucleic acid; DNase, deoxyribonuclease; EC, extracellular domain; ERK 1/2, extracellular signal-regulated kinase; esRAGE, endogenous secretory RAGE; gDNA, genomic DNA; GTPase, guanosine triphosphatase; HMG, high mobility group; HMGB1, high mobility group protein B1; JNK, C-Jun N-terminal kinase; kDa, kiloDalton; Mac-1, Macrophage-1 antigen; MAP, kinase mitogen activated protein kinase; M-MLV, Moloney murine leukemia virus; mRNA, messenger ribonucleic acid; NCBI, National Center for Biotechnology Information; NFκB, nuclear factor-kappa B; ORF, open reading frame; PCR, polymerase chain reaction; qRT-PCR, quantitative Real Time PCR; RAGE, receptor for advanced glycation end products; Ras, rat sarcoma virus; RNA, ribonucleic acid; RNase, ribonuclease; SAPK, stress-activated protein kinase; sRAGE, soluble RAGE variant (s); TM, transmembrane domain; UTR, untranslated region.

* Corresponding author. Small Animal Clinic and Research Cluster of Excellence "REBIRTH", University of Veterinary Medicine Hannover, Bischofsholer Damm 15, D-30173 Hanover, Germany. Fax: +49 511 856 7686.
E-mail address: hescobar@tiho-hannover.de (H.M. Escobar).

0378-1119/$ – see front matter © 2008 Elsevier B.V. All rights reserved.
doi:10.1016/j.gene.2008.10.027

sRAGE2, sRAGE3 (Schlueter et al., 2003), N-truncated and Secretory (Yonekura et al., 2003), Δ8-RAGE (Park et al., 2004), RageΔ, NtRAGEΔ and sRAGEΔ (Ding and Keller, 2005b), RAGE_v4-RAGE_v13 (Hudson et al., 2007). The function of these variants was unclear, but lately the described truncated RAGE protein variants were supposed to act as competitive inhibitors of the receptor either by ligand binding or displacing the full-length receptor in the membrane (Ding and Keller, 2005a; Geroldi et al., 2005). Deregulations of the naturally occurring protein isoforms are supposed to have significant effect on RAGE mediated diseases. Accordingly, deregulations of sRAGE levels have been associated with several diseases e.g. Alzheimer's disease (Emanuele et al., 2005), Type 1 diabetes (Challier et al., 2005; Forbes et al., 2005; Katakami et al., 2005; Miura et al., 2007), Type 2 diabetes (Nakamura et al., 2006; Tan et al., 2006; Yamagishi et al., 2006; Humpert et al., 2007), atherosclerosis (Falcone et al., 2005; Koyama et al., 2005), rheumatoid arthritis (Moser et al., 2005; Pullerits et al., 2005), essential hypertension (Geroldi et al., 2005), and renal disease (Kalousova et al., 2006). On the other hand Taguchi et al. (2000) were able to show that blocking of the binding of the RAGE ligand HMGB1 to the receptor, by using RAGE variants lacking the cytosolic or transmembrane domains, strongly inhibited the metastatic behaviour of glioma cells in terms of invasive growth, motility and migration. The data clearly showed that the application of soluble RAGE variants drastically suppressed the growth of tumour cells *in vitro* and *in vivo* (for review see Huttunen and Rauvala, 2004). In spite of its obvious relationship to cancer and metastasis data focusing soluble RAGE deregulations or structural aberrations and tumours is currently rare. Only recently Takeuchi et al. reported a correlation between esRAGE, RAGE, and HMGB1 and staging of chondrosarcomas classifying esRAGE expression as tumourmarker for malignancy (Takeuchi et al., 2007).

As reviewed lately by Khanna and Hunter (2005) the dog is significantly helping to reveal characteristics of human tumour biology especially of metastasis due to various similarities of the malignancies seen in both species. Generally, in the case of cancer, in dogs we find naturally spontaneously developing neoplasias which are more similar to human cancers than induced tumours used in rodent model systems in terms of presentation, histology and biology (Withrow and MacEwen, 1989, 2001; MacEwen, 1990). Additionally, dogs show similar characteristics of physiology and metabolism for most organ systems and drugs, which allows better comparability of modalities e.g. surgery, radiation, chemotherapy (Withrow and MacEwen, 2001), and new therapeutic approaches aimed at cancer treatment.

In this study we screened a set of 14 different canine tumours, healthy tissues and various canine and human cancer cell lines for *RAGE* splicing variants and analysed their structures. Additionally, we analysed the ratio of the mainly found transcript variants using quantitative and relative Real-Time PCR.

2. Methods and materials

2.1. Tissues and cell lines

The analysed canine healthy (lung, ovar, pancreas, skin, spleen, testis, thyroid) and tumour tissues (adenoma of pancreas, colon cancer, fibrosarcoma, histiocytoma, insulinoma, liver adenoma, malignant histiocytosis, malignant lymphoma, mamma tumour, mastocytoma, melanoma, splenic hemangiosarcoma, testis tumour, thyroid carcinoma, vaginal tumour) were provided by the Small Animal Clinic, University of Veterinary Medicine, Hanover, Germany. The canine cell lines CT1258 (prostate cancer), MTH53A (non neoplastic tissue of the mammary gland), MTH52C (malignant small-cell carcinoma of the mammary gland), and ZMTH3 (pleomorphic adenoma of the mammary gland) and the human cell lines Hela (cervical cancer), Li14 (lipoma), and MCF7 (breast cancer) which were used in this study, were provided by the Centre for Human Genetics, University of Bremen, Bremen, Germany.

2.2. RNA isolation and cDNA synthesis for transcript characterisation

The cultured cells were homogenized using QIAshredder spin columns (Qiagen, Hilden, Germany) while the used tissue samples were homogenized using the iron-beads QIAshredder homogenizer method (Qiagen, Hilden, Germany). Following, total RNA was isolated using the RNeasy Mini Kit according to the manufacturer's instructions (Qiagen, Hilden, Germany). To avoid genomic DNA contaminations, on-column DNase digestion with the RNase-Free DNase set (Qiagen, Hilden, Germany) was performed.

The respective total cDNA syntheses were performed using 5 μg total RNA of each sample, the adaptor poly dT primer AP2: AAG GAT CCG TCG ACA TC(17)T, and MMLV reverse transcriptase following the manufacturer's protocol (Invitrogen, Karlsruhe, Germany). The respective cDNA syntheses were performed several times during the experiments.

2.3. PCR reactions

All performed PCR reactions were designed to amplify products spanning from exon 1 to exon 11 of the canine or human *RAGE* mRNA, respectively. The PCR reactions using the total poly dT primed cDNAs of the canine cell lines and tissue samples were performed either with the primer pair 1 (up 5′GAA GCC TGG GAA GGA ACG ATG3′/lo 5′GAG AGC AAG GGG GAA GAA AAG3′) or pair 2 (up 5′CCT GGG TGC TGG TCC TCA GT3′/lo 5′TCA TGG CCC TGC TGC ACC GC TCT3′). The reactions using human templates were performed with the primer pair 5′CCT GGG TGC TGG TCC TCA GT3′ as upper primer and the primer 5′TCA AGG CCC TCC AGT ACT ACT TC3′ as lower primer for PCR reactions amplifying RAGE transcripts in human cell lines (Hela, Li14, MCF7).

The PCR reactions were performed with a “touch down” programme with the following conditions: initial denaturation at 95 °C for 5 min, followed by 10 cycles with 30 s denaturation at 95 °C, 1 min annealing by 70–60 °C with a decrease of 1 °C per cycle and an elongation at 72 °C for 1 min. The following 30 cycles were performed at 95 °C for 30 s, 60 °C for 1 min and 72 °C for 1 min, respectively.

2.4. Characterisation of RAGE transcript variants

The respective amplified PCR products were separated electrophoretically in 1.5% agarose gels and recovered using the QIAquick Gel Extraction Kit following the manufacturer's protocol (Qiagen, Hilden, Germany). The isolated fragments were cloned into the pGem-T-Easy vector system (Promega, Mannheim, Germany), transfected in thermocompetent DH5α *E. coli* cells, and verified by sequencing (MWG, Ebersberg, Germany). The received sequence data was analysed using Lasergene software (DNAStar, Madison, USA).The generated sequences were submitted to the NCBI database (GenBank accession nos: EU428788, EU428789, EU428790, EU428791, EU428792, EU428793, EU428794, EU428795, EU428796, EU428797, EU428798, EU428799, EU428800, EU428801, EU428802, EU428803, EU428804, EU428805, EU428806, EU428807, EU428808, EU428809, EU428810, EU428811, EU428812, EU428813, EU428814, EU428815, EU428816).The CDS and protein alignments were performed using various sequences from NCBI database (GenBank accession nos.: D28769, NM001048081; BAA89369, ABA18650).

2.5. Quantitative Real-time RT-PCR

2.5.1. RNA isolation and cDNA syntheses for qRT-PCR

Total RNAs from the homogenized cultured cells and tissue samples were isolated using the RNeasy Plus Mini Kit (Qiagen, Hilden,

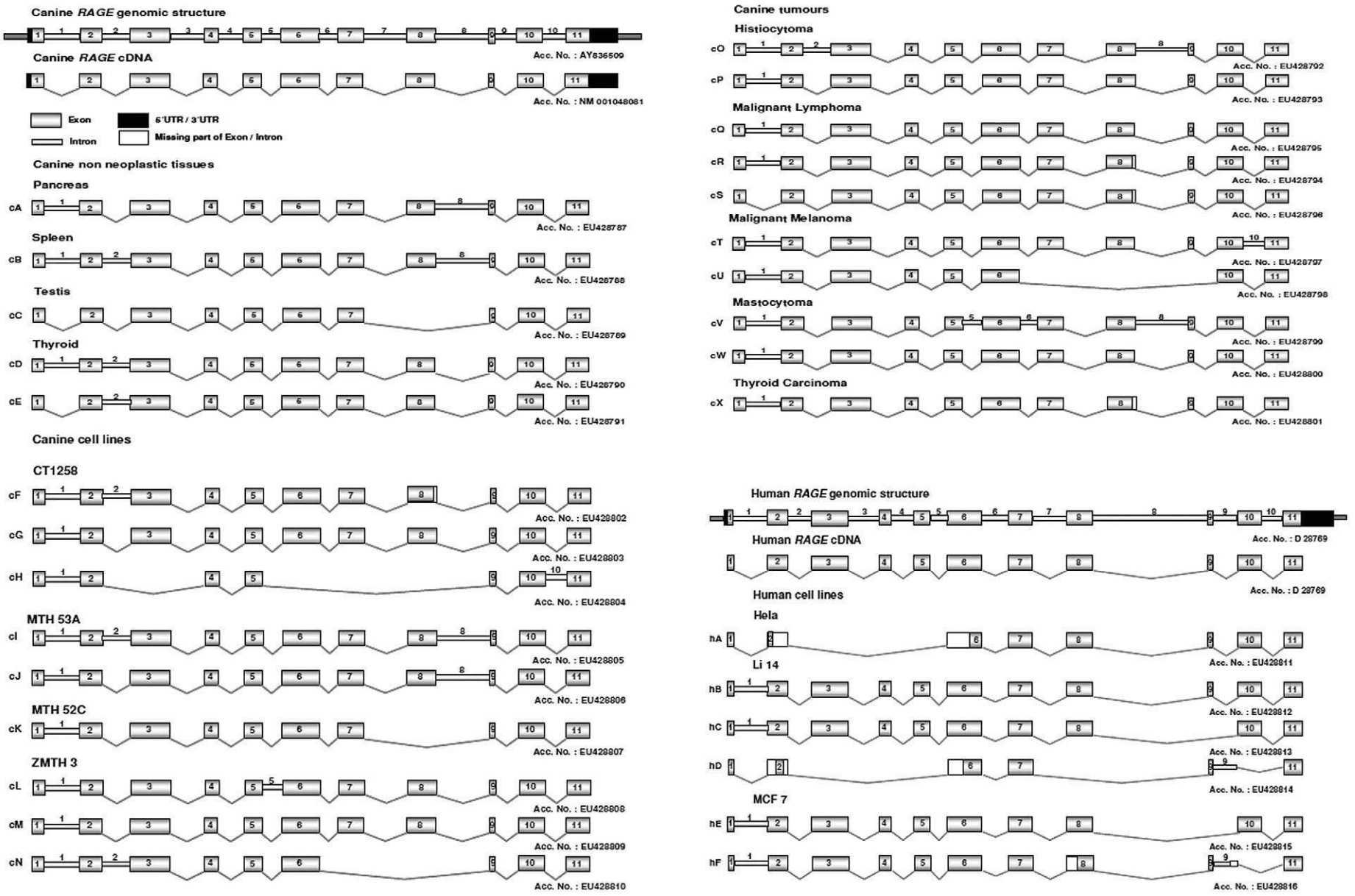

Fig. 1. *RAGE* transcript variants. Characterisation of *RAGE* transcript variants in canine non neoplastic tissues: pancreas, spleen, testis and thyroid (cA–cE), canine cell lines: CT1258, MTH 53A, MTH 52C and ZMTH3 (cF–cN), canine tumours: histiocytoma, malignant lymphoma, malignant melanoma, mastocytoma and thyroid carcinoma (cO–cX) and human cell lines: Hela, Li14 and MCF7 (hA–hF). The amplified PCR products range from the start codon in exon 1 till stop codon in exon 11. The RT PCR was performed with a poly dT primer. The transcript variants show different structural modifications like insertions of introns and deletions of both whole exons and parts of exons.

Table 1
Canine and human *RAGE* transcript variants

	Name (Fig. 1)	Structure insertion/deletion	Acc. No.	Putative protein (Fig. 2)/characteristic
Non neoplastic canine tissues				
Pancreas	cA	Insertion: intron1, intron 8	EU428787	J/non sense protein
Spleen	cB	Insertion: intron1, intron 2, intron 8	EU428788	I/non sense protein
Testis	cC	Deletion: exon 8	EU428789	A/soluble isoform, ligand binding
Thyroid	cD	Insertion: intron 1, intron 2	EU428790	C/membrane bound, no ligand binding
	cE	Insertion: intron 2	EU428791	F/membrane bound, no ligand binding
Canine cell lines				
CT1258	cF	Insertion: intron1, intron 2/deletion: 16 bp exon 8	EU428802	K/non sense protein
	cG	Insertion: intron 1	EU428803	E/membrane bound, no ligand binding
	cH	Insertion: intron 1/deletion: exon 3, exon 6, exon 7, exon 8	EU428804	No putative protein
MTH 53A	cI	Insertion: intron 1, intron 2, intron 8	EU428805	I/non sense protein
	cJ	Insertion: intron 1, intron 8	EU428806	J/non sense protein
MTH 52C	cK	Insertion: intron 1/deletion: exon 8	EU428807	M/non sense protein
ZMTH3	cL	Insertion: intron 1, intron 5	EU428808	D/membrane bound, no ligand binding
	cM	Insertion: intron 1	EU428809	E/membrane bound, no ligand binding
	cN	Insertion: intron 1, intron 2/deletion: exon 7, exon 8	EU428810	G/membrane bound, no ligand binding
Canine tumours				
Histiocytoma	cO	Insertion: intron 1, intron 2, intron 8	EU428792	I/non sense protein
	cP	Insertion: intron 1	EU428793	E/membrane bound, no ligand binding
Malignant lymphoma	cQ	Insertion: intron 1	EU428795	E/membrane bound, no ligand binding
	cR	Insertion: intron 1/deletion: 16 bp exon 8	EU428794	L/non sense protein
	cS	Deletion: 16 bp exon 8	EU428796	B/soluble isoform, ligand binding
Malignant melanoma	cT	Insertion: intron 1, intron 10	EU428797	No putative protein
	cU	Insertion: intron 1/Deletion: exon 7, exon 8, exon 9	EU428798	H/membrane bound, no ligand binding
Mastocytoma	cV	Insertion: intron1, intron 5, intron 6, intron 8	EU428799	No putative protein
	cW	Insertion: intron 1	EU428800	E/membrane bound, no ligand binding
Thyroid carcinoma	cX	Insertion: intron1/deletion: 16 bp exon 8	EU428801	L/non sense protein
Human cell lines				
Hela	hA	Deletion: 80 bp exon2, exon3, exon 4, exon 5, 120 bp exon6	EU428811	CC/membrane bound, no ligand binding
Li 14	hB	Insertion: intron 1	EU428812	AA/membrane bound, no ligand binding
	hC	Insertion: intron 1/deletion: exon 9	EU428812	BB/membrane bound, no ligand binding
	hD	Insertion: intron 9/deletion: 72 bp exon 2, exon 3, exon 4, exon 5	EU428814	No putative protein
MCF 7	hE	Insertion: intron 1/deletion: exon 9	EU428815	BB/membrane bound, no ligand binding
	hF	Insertion: intron 1, intron 9/deletion: 52 bp exon 8, 22 bp intron 9	EU428816	No putative protein

Detailed characterisation of the different respective *RAGE* transcript modifications and analyses of their derived protein isoforms.

Germany). This isolation method does not require an additional on column DNase digestion due to a direct removal of genomic DNA (gDNA) by a gDNA eliminating spin column.

The respective cDNA syntheses were performed using 250 ng total RNA of each sample, the gene specific lower primer 5′ TTCTGTCCGACCTGTGTTCAGCTT3′, and Quantiscript Reverse Transcriptase following the manufacturer's protocol (Qiagen, Hilden, Germany) with an integrated removal of genomic DNA contamination.

For absolute and relative quantification of the RAGE transcript levels RT-PCR amplifications were carried out using the Applied Biosystems 7300 Real-Time PCR System (Applied Biosystems, Darmstadt, Germany). 2 µl of each cDNA corresponding to 25 ng of total RNA was amplified in a total volume of 25 µl using universal PCR Mastermix (Applied Biosystems) with 600 nM of each primer (forward primer 1: 5′GTCTGTGGGGAGCAGTAGTAGG3′, forward primer 2: 5′TACTCCTCCACCATTGTCCCATCT3′, reverse primer: 5′ TTCTGTCCGACCTGTGTTCAGCTT3′) and 200 nM fluorogenic probe (5′ 6-FAM-AAGCCGCTGGTGCTCAACTGTA-TAMRA 3′). PCR conditions were as follows: 2 min at 50 °C and 10 min at 95 °C, followed by 45 cycles with 15 s at 95 °C and 1 min at 60 °C. All samples were measured in triplicate and for each run non-template controls and no reverse transcriptase reactions were included. Expression levels of RAGE mRNA transcripts were calculated using an amplicon-specific standard curve. For absolute quantification the transcript levels were normalised to total RNA concentration and expressed as copy number/250 ng total RNA. For relative quantification the healthy full length RAGE transcript was chosen as endogenous control. The calibrator sample was lung tissue to which all other samples were compared to determine the ratio of the relative expression level.

3. Results and discussion

3.1. Characterisation of RAGE transcript variants

In humans 19 naturally occurring *RAGE* splicing variants resulting in either N-terminally or C-terminally truncated proteins were identified and are just recently discussed as mechanisms for receptor regulation (hRAGEsec, sRAGE1, sRAGE2, sRAGE3, N-truncated and Secretory, Δ8-RAGE, RageΔ, NtRAGEΔ and sRAGEΔ, RAGE_v4 till RAGE_v13). The described truncated RAGE protein variants are discussed to act as competitive inhibitors of the receptor either by ligand binding or displacing the full-length receptor in the membrane. Deregulation of the naturally occurring protein isoforms is supposed to have significant effect on RAGE mediated diseases. Accordingly, deregulation of sRAGE levels has been associated with several diseases

Fig. 2. The canine RAGE CDS and protein structure. The different *RAGE* transcript variants characterised in canine non neoplastic tissues, cell lines, tumours and in human cell lines code for different putative protein structures: canine soluble RAGE protein isoforms with the ability to bind RAGE ligands without subsequent signalling in the cell (A, B), canine membrane bound RAGE isoforms without the competence of binding RAGE ligands (C–H), canine non sense RAGE protein isoforms (I–M) and human membrane bound RAGE protein isoforms (AA–CC).

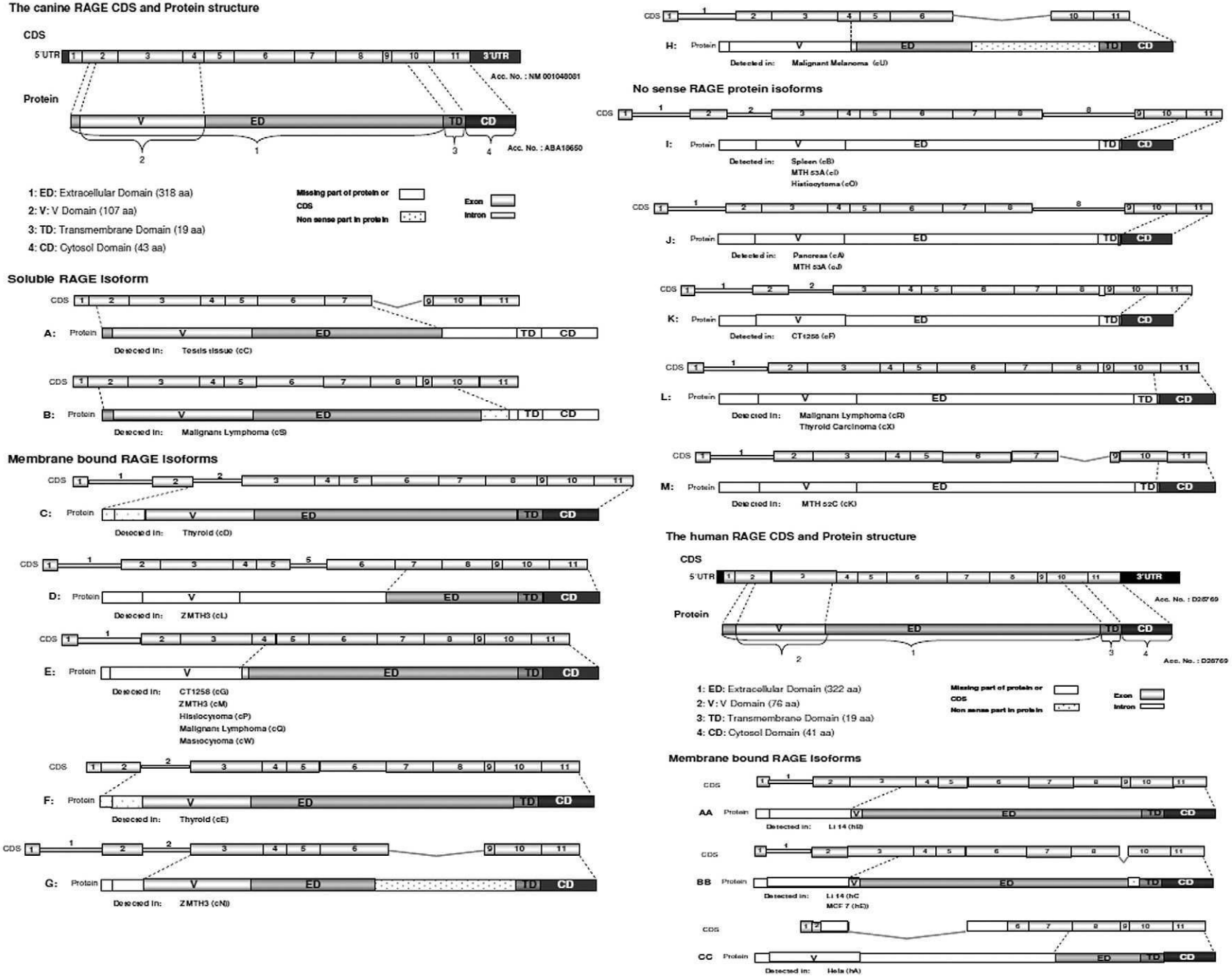
The canine RAGE CDS and Protein structure
CDS
5'UTR
3'UTR
Acc. No. : NM 001048081
Protein
V
ED
TD
CD
Acc. No. : ABA18650
1: ED: Extracellular Domain (318 aa)
2: V: V Domain (107 aa)
3: TD: Transmembrane Domain (19 aa)
4: CD: Cytosol Domain (43 aa)
Missing part of protein or CDS
Non sense part in protein
Exon
Intron
Soluble RAGE Isoform
A: Protein
Detected in: Testis tissue (cC)
B: Protein
Detected in: Malignant Lymphoma (cS)
Membrane bound RAGE Isoforms
C: Protein
Detected in: Thyroid (cD)
D: Protein
Detected in: ZMTH3 (cL)
E: Protein
Detected in: CT1258 (cG)
ZMTH3 (cM)
Histiocytoma (cP)
Malignant Lymphoma (cQ)
Mastocytoma (cW)
F: Protein
Detected in: Thyroid (cE)
G: Protein
Detected in: ZMTH3 (cN)
H: Protein
Detected in: Malignant Melanoma (cU)
No sense RAGE protein isoforms
I: Protein
Detected in: Spleen (cB)
MTH 53A (cI)
Histiocytoma (cO)
J: Protein
Detected in: Pancreas (cA)
MTH 53A (cJ)
K: Protein
Detected in: CT1258 (cF)
L: Protein
Detected in: Malignant Lymphoma (cR)
Thyroid Carcinoma (cX)
M: Protein
Detected in: MTH 52C (cK)
The human RAGE CDS and Protein structure
CDS
5'UTR
3'UTR
Acc. No. : D28769
Protein
V
ED
TD
CD
Acc. No. : D28769
1: ED: Extracellular Domain (322 aa)
2: V: V Domain (76 aa)
3: TD: Transmembrane Domain (19 aa)
4: CD: Cytosol Domain (41 aa)
Missing part of protein or CDS
Non sense part in protein
Exon
Intron
Membrane bound RAGE Isoforms
AA Protein
Detected in: LI 14 (hB)
BB Protein
Detected in: LI 14 (hC
MCF 7 (hE))
CC Protein
Detected in: Hela (hA)

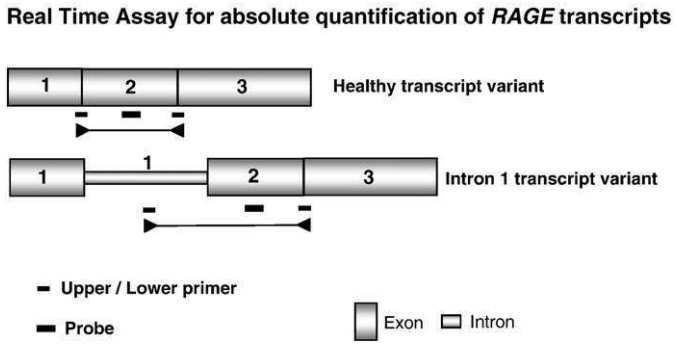

Fig. 3. Designed Real Time assay for absolute quantification of RAGE transcripts allowing differentiation of "healthy" and "intron 1" *RAGE* splicing variants. For the absolute quantification of healthy *RAGE* transcript the designed upper primer binds at the border of exon 1/exon 2, the probe anneals in exon 2 and the lower primer binds at the exon 2/exon 3 border avoiding measurement of genomic contaminations. The assay for measurement of the quantity of the intron 1 transcript variant consists of the same probe and lower primer like the healthy transcript detection, and the upper primer anneals in intron 1. Due to the upper and lower primer, transcripts which bear intron 1 but no genomic contaminations will be detected.

e.g. Alzheimer's disease, Type 1 diabetes, Type 2 diabetes, atherosclerosis, rheumatoid arthritis, essential hypertension, and renal disease. On the other hand blocking of the binding of the RAGE ligand HMGB1 to the receptor by using RAGE variants lacking the cytosolic or transmembrane domains, strongly inhibited the metastatic behaviour of glioma cells in terms of invasive growth, motility and migration (Taguchi et al., 2000). A recent study based on immunohistologic analyses reports a correlation of esRAGE and staging of chondrosarcomas classifying RAGE expression as tumourmarker for malignancy (Takeuchi et al., 2007).

In the herein screened canine 17 neoplastic and seven healthy tissue samples as well as the four canine and 3 human cell lines we found in total 24 canine and 6 human transcripts coding for 16 structural different canine and 5 different human forms. Fourteen of these found canine and four human forms were previously not described for any other species (Fig. 1, Table 1). In detail the transcripts detected in healthy tissues are characterised by various combinations of insertions of intron 1, 2 and 8 and by an observed deletion of the exon 8 (Figs. 1cA–cE). In canine cell lines the following events could be detected: various combinations of insertions of the introns 1, 2, 5, 8 and 10, a 16 bp partial deletion of exon 8, and complete deletions of the exons 3, 6, 7 and 8 (Figs. 1cF–cN). The neoplastic samples showed several insertions of introns 1, 2, 5, 6, 8 and 10, the partial 16 bp deletion of exon 8, and finally deletions of exons 7, 8 and 9 (Figs. 1cO–cX). The human cell lines showed insertion of intron 1, partial large deletions of parts of the exons 2, 6, and 8, compete deletions of the exons: 3, 4, 5, 8, and 9, and finally insertion of intron 9 with an additional deletion of parts of intron 9 (Figs. 1hA–hF).

These different transcript variants can be roughly classified into two groups. One group of splicing variants coding for full length *RAGE* transcripts or soluble *RAGE* variants which code for protein forms capable to bind extracellular ligands, and the other group showing various insertions of introns and alternative splicing of exons leading to mutated protein forms (Fig. 1,Fig. 2, Table 1). The recurrent remarkable modification in the latter group is the insertion of intron 1. This modification is seen in transcripts found in healthy tissues as well as in the cell lines and neoplastic samples. Depending on further modifications of the seen transcripts respective protein isoforms would result, missing the V — domain required for ligand binding or result in nonsense proteins (Fig. 2). Previously Yonekura et al. found a similar variant showing an insertion of intron 1 in a sample of human endothelial cells and pericytes (Yonekura et al., 2003). However, this reports the existence of these transcripts for the first time in neoplastic samples and cell lines.

3.2. Quantitative Real-Time PCR analyses

Following the assumption that the transcripts showing the intron 1 insertion are lost as competitive inhibitors we decided to quantify the ratio between these variants and variants coding for proteins capable to bind RAGE ligands in neoplastic canine samples providing naturally occurring tumour material. The designed assay discriminates genomic DNA detection, due to the position of the chosen primers (Fig. 3). The comparative quantification showed a diverse pattern (Table 2) in the analysed samples. Generally, in all screened tissue samples and cell lines, an expression of both forms could be detected varying from $1.38*10^3$ (mastocytoma) to $6.53*10^8$ (lung) transcripts for the normal splicing variant and $1.3*10^3$ (mastocytoma) to $1.88*10^6$ (lung) transcripts for the "intron 1" variant. In the screened healthy tissues the variant coding for a functional complete or soluble RAGE variant is significantly higher expressed in lung, testis and thyroid tissue showing in absolute numbers $6.53*10^8$, $6.27*10^5$ and $1.02*10^7$ more "healthy" transcripts than their respective "intron 1" variants. The pattern seen in the 17 tumour tissue samples and cell lines is quite different. The majority of samples showed a higher presence of the "intron 1" variant with the exception of a mastocytoma, which shows a similar level of both variants ($1.3*10^3$ "intron 1" to $1.38*10^3$ "healthy") and a testis tumour, which as only neoplastic sample showed a higher expression "healthy" variant (Table 2). In absolute numbers the "intron 1" variant outnumbers in the "healthy" variant 15 of the neoplastic samples with a range of 15 to 17 transcripts. The screened four cell lines showed uniformly a higher level of the intron 1 variant varying from $5.38*10^4$ to $9.17*10^4$.

However, as lately discussed by Hudson et al. (2007), the wide diversity of seen RAGE transcripts and the obvious relationship of RAGE to several pathologic findings arise many new questions. The

Table 2
Absolute Real Time quantification transcript numbers of "healthy" and "intron 1" *RAGE* transcript variants in canine healthy tissues, neoplastic samples and cell lines

	Copy no./250 ng total RNA	
	Healthy transcript	Intron 1 transcript
Non neoplastic canine tissues		
Lung	$6.53*10^8$	$1.88*10^6$
Ovar	$6.9*10^3$	$7.36*10^4$
Pancreas	$2.6*10^4$	$3.08*10^5$
Skin	$1.9*10^3$	$1.1*10^4$
Spleen	$7.1*10^3$	$8.26*10^4$
Testis	$6.27*10^5$	$5.6*10^4$
Thyroid	$1.02*10^7$	$1.9*10^5$
Canine cell lines		
CT1258	$2.98*10^3$	$5.38*10^4$
MTH 53A	$4.68*10^3$	$6.77*10^4$
MTH 52C	$9.3*10^3$	$9.17*10^4$
ZMTH3	$6.83*10^3$	$8.8*10^4$
Canine tumours		
Adenoma of pancreas	$4.26*10^3$	$5.5*10^4$
Colon cancer	$5.66*10^3$	$6.19*10^4$
Fibrosarcoma	$4.7*10^3$	$7.67*10^4$
Histiocytoma	$1.46*10^4$	$1.47*10^5$
Insulinoma	$1.7*10^4$	$2.6*10^5$
Liver adenoma	$3.9*10^3$	$2.9*10^4$
Malignant histiocytosis	$9.52*10^3$	$8.34*10^4$
Malignant lymphoma	$1.18*10^4$	$1.49*10^5$
Malignant lymphoma	$7.6*10^3$	$8.62*10^4$
Malignant lymphoma	$1.2*10^4$	$2.1*10^5$
Mammatumour	$1.5*10^4$	$5.29*10^4$
Mastocytoma	$1.38*10^3$	$1.3*10^3$
Melanoma	$4.77*10^3$	$4.14*10^4$
Splenic hemangiosarcoma	$2.17*10^4$	$1.07*10^5$
Testis tumour	$7.84*10^5$	$2.11*10^5$
Thyroid carcinoma	$5.16*10^4$	$1.53*10^5$
Vaginal tumour	$1.13*10^4$	$1.5*10^5$

growing understanding of its biology combined with the accessibility of an adequate animal model – like the dog providing naturally occurring neoplastic samples – will be of great value to elucidate the pathologic events with RAGE involvement. The here newly described 24 canine and 4 human RAGE splicing variants as well as their respective derived protein forms will further help to understand the diversity of RAGE biology. The comparative quantitative Real-Time PCR analyses of both major *RAGE* transcript classes represent a first approach to analyse, if deregulation/structural aberrations of *RAGE* can be detected at RNA level and play a role in RAGE mediated pathologic events. Anyway, further studies will be needed, to confirm at protein level the qPCR data. We tested the commercially availed RAGE antibodies for detection of recombinant canine protein but got unspecific results. This may be due to the fact that the identity of the canine RAGE protein to its human is just 77.6% (Murua Escobar et al., 2006).

However, studies done with human neoplasias using the herein generated data as basis should be a promising approach to answer the remaining questions.

Acknowledgment

This work was funded by the German Research Foundation (DFG) within the SFB/TransRegio 37.

References

Bartling, B., Hofmann, H.S., Weigle, B., Silber, R.E., Simm, A., 2005. Down-regulation of the receptor for advanced glycation end-products (RAGE) supports non-small cell lung carcinoma. Carcinogenesis 26, 293–301.

Bhawal, U.K., et al., 2005. Association of expression of receptor for advanced glycation end products and invasive activity of oral squamous cell carcinoma. Oncology 69, 246–255.

Challier, M., Jacqueminet, S., Benabdesselam, O., Grimaldi, A., Beaudeux, J.L., 2005. Increased serum concentrations of soluble receptor for advanced glycation endproducts in patients with type 1 diabetes. Clin. Chem. 51, 1749–1750.

Chavakis, T., Bierhaus, A., Al-Fakhri, N., Schneider, D., Witte, S., Linn, T., et al., 2003. The pattern recognition receptor (RAGE) is a counterreceptor for leukocyte integrins: a novel pathway for inflammatory cell recruitment. J. Exp. Med. 198, 1507–1515.

Chavakis, T., Bierhaus, A., Nawroth, P.P., 2004. RAGE (receptor for advanced glycation end products): a central player in the inflammatory response. Microbes Infect. 6, 1219–1225.

Cipollone, F., et al., 2003. The receptor RAGE as a progression factor amplifying arachidonate-dependent inflammatory and proteolytic response in human atherosclerotic plaques: role of glycemic control. Circulation 108, 1070–1077.

Deora, A.A., Win, T., Vanhaesebroeck, B., Lander, H.M., 1998. A redox-triggered ras-effector interaction. Recruitment of phosphatidylinositol 3′-kinase to Ras by redox stress. J. Biol. Chem. 273, 29923–29928.

Ding, Q., Keller, J.N., 2005a. Evaluation of rage isoforms, ligands, and signaling in the brain. Biochim. Biophys. Acta 1746, 18–27.

Ding, Q., Keller, J.N., 2005b. Splice variants of the receptor for advanced glycosylation end products (RAGE) in human brain. Neurosci. Lett. 373, 67–72.

Emanuele, E., et al., 2005. Circulating levels of soluble receptor for advanced glycation end products in Alzheimer disease and vascular dementia. Arch. Neurol. 62, 1734–1736.

Falcone, C., et al., 2005. Plasma levels of soluble receptor for advanced glycation end products and coronary artery disease in nondiabetic men. Arterioscler. Thromb. Vasc. Biol. 25, 1032–1037.

Forbes, J.M., et al., 2005. Modulation of soluble receptor for advanced glycation end products by angiotensin-converting enzyme-1 inhibition in diabetic nephropathy. J. Am. Soc. Nephrol. 16, 2363–2372.

Geroldi, D., et al., 2005. Decreased plasma levels of soluble receptor for advanced glycation end-products in patients with essential hypertension. J. Hypertens. 23, 1725–1729.

Goova, M.T., et al., 2001. Blockade of receptor for advanced glycation end-products restores effective wound healing in diabetic mice. Am. J. Pathol. 159, 513–525.

Hofmann, M.A., et al., 1999. RAGE mediates a novel proinflammatory axis: a central cell surface receptor for S100/calgranulin polypeptides. Cell 97, 889–901.

Hofmann, M.A., et al., 2002. RAGE and arthritis: the G82S polymorphism amplifies the inflammatory response. Genes Immun. 3, 123–135.

Hori, O., et al., 1995. The receptor for advanced glycation end products (RAGE) is a cellular binding site for amphoterin. Mediation of neurite outgrowth and co-expression of rage and amphoterin in the developing nervous system. J. Biol. Chem. 270, 25752–25761.

Huang, J.S., Guh, J.Y., Chen, H.C., Hung, W.C., Lai, Y.H., Chuang, L.Y., 2001. Role of receptor for advanced glycation end-product (RAGE) and the JAK/STAT-signaling pathway in AGE-induced collagen production in NRK-49F cells. J. Cell Biochem. 81, 102–113.

Hudson, B.I., Carter, A.M., Harja, E., Kalea, A.Z., Arriero, M., Yang, H., et al., 2007. Identification, classification, and expression of RAGE gene splice variants. FASEB J. 22 (5), 1572–1580.

Humpert, P.M., et al., 2007. Soluble RAGE but not endogenous secretory RAGE is associated with albuminuria in patients with type 2 diabetes. Cardiovasc. Diabetol. 6, 9.

Huttunen, H.J., Rauvala, H., 2004. Amphoterin as an extracellular regulator of cell motility: from discovery to disease. J. Intern. Med. 255, 351–366.

Huttunen, H.J., Fages, C., Rauvala, H., 1999. Receptor for advanced glycation end products (RAGE)-mediated neurite outgrowth and activation of NF-kappaB require the cytoplasmic domain of the receptor but different downstream signaling pathways. J. Biol. Chem. 274, 19919–19924.

Huttunen, H.J., Fages, C., Kuja-Panula, J., Ridley, A.J., Rauvala, H., 2002a. Receptor for advanced glycation end products-binding COOH-terminal motif of amphoterin inhibits invasive migration and metastasis. Cancer Res. 62, 4805–4811.

Huttunen, H.J., Kuja-Panula, J., Rauvala, H., 2002b. Receptor for advanced glycation end products (RAGE) signaling induces CREB-dependent chromogranin expression during neuronal differentiation. J. Biol. Chem. 277, 38635–38646.

Ishiguro, H., Nakaigawa, N., Miyoshi, Y., Fujinami, K., Kubota, Y., Uemura, H., 2005. Receptor for advanced glycation end products (RAGE) and its ligand, amphoterin are overexpressed and associated with prostate cancer development. Prostate 64, 92–100.

Kalousova, M., et al., 2006. Soluble receptor for advanced glycation end products in patients with decreased renal function. Am. J. Kidney Dis. 47, 406–411.

Katakami, N., et al., 2005. Decreased endogenous secretory advanced glycation end product receptor in type 1 diabetic patients: its possible association with diabetic vascular complications. Diabetes Care 28, 2716–2721.

Khanna, C., Hunter, K., 2005. Modeling metastasis in vivo. Carcinogenesis 26, 513–523.

Kislinger, T., et al., 1999. N(epsilon)-(carboxymethyl)lysine adducts of proteins are ligands for receptor for advanced glycation end products that activate cell signaling pathways and modulate gene expression. J. Biol. Chem. 274, 31740–31749.

Koyama, H., et al., 2005. Plasma level of endogenous secretory RAGE is associated with components of the metabolic syndrome and atherosclerosis. Arterioscler. Thromb. Vasc. Biol. 25, 2587–2593.

Lander, H.M., Tauras, J.M., Ogiste, J.S., Hori, O., Moss, R.A., Schmidt, A.M., 1997. Activation of the receptor for advanced glycation end products triggers a p21(ras)-dependent mitogen-activated protein kinase pathway regulated by oxidant stress. J. Biol. Chem. 272, 17810–17814.

Lue, L.F., et al., 2001. Involvement of microglial receptor for advanced glycation endproducts (RAGE) in Alzheimer's disease: identification of a cellular activation mechanism. Exp. Neurol. 171, 29–45.

Lue, L.F., Yan, S.D., Stern, D.M., Walker, D.G., 2005. Preventing activation of receptor for advanced glycation endproducts in Alzheimer's disease. Curr. Drug Targets CNS Neurol. Disord. 4, 249–266.

MacEwen, E.G., 1990. Spontaneous tumours in dogs and cats: models for the study of cancer biology and treatment. Cancer Metastasis Rev. 9, 125–136.

Malherbe, P., et al., 1999. cDNA cloning of a novel secreted isoform of the human receptor for advanced glycation end products and characterization of cells co-expressing cell-surface scavenger receptors and Swedish mutant amyloid precursor protein. Brain Res. Mol. Brain Res. 71, 159–170.

Miura, J., et al., 2007. Endogenous secretory receptor for advanced glycation end-products levels are correlated with serum pentosidine and CML in patients with type 1 diabetes. Arterioscler. Thromb. Vasc. Biol. 27, 253–254.

Moser, B., Hudson, B.I., Schmidt, A.M., 2005. Soluble RAGE: a hot new biomarker for the hot joint? Arthritis Res. Ther. 7, 142–144.

Murua Escobar, H., et al., 2006. Cloning and characterization of the canine receptor for advanced glycation end products. Gene 369, 45–52.

Nakamura, K., et al., 2006. Elevation of soluble form of receptor for advanced glycation end products (sRAGE) in diabetic subjects with coronary artery disease. Diabetes Metab. Res. Rev.

Neeper, M., et al., 1992. Cloning and expression of a cell surface receptor for advanced glycosylation end products of proteins. J. Biol. Chem. 267, 14998–15004.

Park, L., et al., 1998. Suppression of accelerated diabetic atherosclerosis by the soluble receptor for advanced glycation endproducts. Nat. Med. 4, 1025–1031.

Park, I.H., et al., 2004. Expression of a novel secreted splice variant of the receptor for advanced glycation end products (RAGE) in human brain astrocytes and peripheral blood mononuclear cells. Mol. Immunol. 40, 1203–1211.

Pullerits, R., Bokarewa, M., Dahlberg, L., Tarkowski, A., 2005. Decreased levels of soluble receptor for advanced glycation end products in patients with rheumatoid arthritis indicating deficient inflammatory control. Arthritis Res. Ther. 7, 817–824.

Schlueter, C., Hauke, S., Flohr, A.M., Rogalla, P., Bullerdiek, J., 2003. Tissue-specific expression patterns of the RAGE receptor and its soluble forms—a result of regulated alternative splicing? Biochim. Biophys. Acta 1630, 1–6.

Schmidt, A.M., Yan, S.D., Yan, S.F., Stern, D.M., 2001. The multiligand receptor RAGE as a progression factor amplifying immune and inflammatory responses. J. Clin. Invest. 108, 949–955.

Taguchi, A., et al., 2000. Blockade of RAGE-amphoterin signalling suppresses tumour growth and metastases. Nature 405, 354–360.

Takeuchi, A., et al., 2007. Endogenous secretory receptor for advanced glycation endproducts as a novel prognostic marker in chondrosarcoma. Cancer 109, 2532–2540.

Tan, K.C.B., et al., 2006. Association between serum levels of soluble receptor for advanced glycation end products and circulating advanced glycation end products in type 2 diabetes. Diabetologia 49, 2756–2762.

Withrow, S.J., MacEwen, E.G., 1989. Clinical Veterinary Oncology. J.B. Lippincott, Co.

Withrow, S.J., MacEwen, E.G., 2001. Small Animal Clinical Oncology. W.B. Saunders Company.

Yamagishi, S., et al., 2006. Positive association between serum levels of advanced glycation end products and the soluble form of receptor for advanced glycation end products in nondiabetic subjects. Metabolism 55, 1227–1231.
Yan, S.D., et al., 1994. Enhanced cellular oxidant stress by the interaction of advanced glycation end products with their receptors/binding proteins. J. Biol. Chem. 269, 9889–9897.
Yan, S.D., et al., 1996. RAGE and amyloid-beta peptide neurotoxicity in Alzheimer's disease. Nature 382, 685–691.
Yonekura, H., et al., 2003. Novel splice variants of the receptor for advanced glycation end-products expressed in human vascular endothelial cells and pericytes, and their putative roles in diabetes-induced vascular injury. Biochem. J. 370, 1097–1109.

X

Cytokine genes single nucleotide polymorphism (SNP) screening analyses in canine malignant histiocytosis.

Soller JT, Murua Escobar H, Janssen M, Fork M, Bullerdiek J, Nolte I.

J Hered. 2007; 98(5): 485-90.

Eigenleistung:

- Koordinierung und Planung aller Arbeiten
- PCR-Screening und *in silico* Analysen
- Verfassen des Manuskripts mit I. Nolte

ANTICANCER RESEARCH *26*: xxx-xxx (2006)

No: **7182-S**
Please mark the appropriate section for this paper
☐ Experimental
☐ Clinical
☐ Epidemiological

Cytokine Single Nucleotide Polymorphism (SNP) Screening Analyses in Canine Malignant Histiocytosis

JAN THIES SOLLER[1,2], HUGO MURUA ESCOBAR[1,2], MIRIAM JANSSEN[1], MELANI FORK[2], JÖRN BULLERDIEK[1] and INGO NOLTE[2]

1Centre for Human Genetics, University of Bremen, Bremen;
2Small Animal Clinics, University of Veterinary Medicine Hanover, Hanover, Germany

Abstract. *In humans, malignant histiocytosis is a tumour-like disease characterised by increasing proliferation of macrophages and reinforced degradation of erythrocytes. High progression of this disease leads to an unfavourable prognosis for the patients, most of them children up to the age of three years. Histological and cytological findings have proposed an important role of aberrant expression of cytokines in histiocytosis. Due to the fact that Bernese Mountain Dogs (BMD) show a predisposition for spontaneously developing malignant histiocytosis, these dogs could possibly be used as a genetic model organism to elucidate the mechanisms of human malignant histiocytosis. Canine cytokine cDNA transcripts of TNFα, Interleukin-1-α (IL-1α) and Interleukin-1-beta (IL-1β) were screened for single nucleotide polymorphisms (SNPs). SNP screening in canine cytokine transcripts for malignant histiocytosis has not been carried out before. Total RNA was isolated from tissue samples from lung, spleen, testis, and skin of 17 different dogs (seven BMDs, one Collie and one West Highland Terrier). The corresponding cytokine cDNAs were amplified, sequenced and then screened for SNPs. The resulting effects on the protein sequence were analysed. Several BMDs and the West Highland Terrier showed SNPs in the coding sequences which led to missense mutations within the protein sequences of TNF α, IL1α and IL1β.*

Malignant histiocytosis (MH) and Langerhans cell histiocytosis (LCH) are neoplastic diseases which often spontaneously manifest in histiocytes also called Langerhans cells. These histiocytes rapidly change their behaviour to proliferate like metastases with undetermined pathogenesis and heterogeneous diagnostic findings (1).

Due to aberrant immune response, these histiocytes, normally present in lung, liver, spleen, bones, brain, lymph nodes, skin and other epithelia, transform into highly mobile and infiltrating macrophages, which affect many different organs forming neoplasms with an enhancement of phagocytosis of erythrocytes. The clinical spectrum of this disease is wide with variable degrees of malignancy. However, histopathological findings of granulomas organised in clusters are uniform within the involved tissues (1, 2). The progressive course of histiocytosis is characterised by fast spreading symptoms and unfavourable prognosis, and is particularly often lethal in infants and children. Histiocytosis is not referred to as cancer by definition, although manifestations of this disease behave like tumour diseases, *e.g.* metastasising and an aggressive invasiveness of growth. Histiocytosis is defined as a disorder of the immune system with vague understanding of aetiology and pathogenesis (1).

As abundantly described in the literature, in many cases dogs and humans share the genetic pathways for the development of neoplastic diseases (3-5). Dogs can be used as an animal model to unravel the mechanisms of malignant histiocytosis as well as LCH. Most clinical and pathological features of canine histiocytosis resemble those of Langerhans cell histiocytosis in humans. In particular, there is a breeding predisposition for this disease observed in Bernesese Mountain Dogs (BMD) (6-8). During the malignant histiocytosis disease, LCH cells and T cells produce large quantities of cytokines, raising a cytokine "storm" (9). Screening for single nucleotide polymorphism (SNP) within the nucleotide sequence of the responsible genes could be an instrument for revealing the cause of the disease. Cytokine genes are abundantly expressed in histiocytes and have been proposed to play a major role in pathogenesis. Due to the fact that the pro-inflammatory cytokines IL-1 (IL-1α and IL-1β) and the tumour necrosis factor- α (TNFα) are described to play a major role as

Correspondence to: Prof. Dr. J. Bullerdiek, Centre for Human Genetics, University of Bremen, Leobener Strasse ZHG, 28359 Bremen, Germany. Tel: +49-421-218 4239, Fax: +49-421-218 4239, e-mail: bullerd@uni-bremen.de

Key Words: Canis familiaris, Bernese Mountain Dog (BMD), malignant histiocytosis, single nucleotide polymorphism, cytokine genes.

Table I. *Detected SNPs and insertion in screened cytokine coding sequences.*

Transcript	Exon	Sample (tissue)	Codon	Substitution	Amino acid exchange
TNFα	4	2 (lung)	206	GAT → GGT	Asp → Gly
IL-1α	3	2 (lung)	23	TTC → TCC	Ser → Pro
	4	2 (lung)	47	TGC → CGC	Cys → Arg
IL-1α Exon 5 del	4	9 (skin)	43	CTT → CCT	Leu → Pro
IL-1β	5	5 (liver)	113	GAT → GGT	Asp → Gly
	5	1 (liver)	124	CAG → AAG	Gln → Lys
	7	4 (liver)	228	TCT → CCT	Ser → Pro
	7	4 (liver)	234	TAC → CAC	Tyr → His

autocrine growth factors in many oncogenic malignancies (2, 10-12), it is interesting to focus on gene expression and SNP screening. Additionally, IL-1α/β were also described to be involved in the regulation of the immune system, fever proteins and inflammationary processes (9, 13).

In order to clarify whether SNPs in canine cytokine transcripts exist, *TNFα* and *IL-1α* and *IL-1β* cDNAs derived from various tissues of dog breeds both with and without a known predisposition for the development of MH were screened. Cytokine cDNAs were derived from healthy lung, skin, liver, spleen and testis tissues from different breeds including BMDs, West Highland Terriers and Collies.

Materials and Methods

Spleen, lung, liver, skin and testis tissue from BMDs, Collies and West Highland Terriers were provided by the Small Animal Clinic, University of Veterinary Medicine, Hanover, Germany. Canine cytokine cDNA transcripts were screened and synthesised by total RNA from 17 different individuals (15 BMDs, one Collie and one West Highland Terrier).

Total RNA was isolated using the RNeasy Mini Kit (QIAGEN, Hilden, Germany) protocol for animal tissues and proteinase K digestion. *RNase*-Free *DNase* Set was used for preventing genomic DNA contamination by *DNase* I digestion of the total RNA. For cDNA 3'-RACE synthesis up to 5 μg of total RNA was set as template for reverse transcription (SuperScript II RT, Invitrogen) using AP2 poly-T adaptor primer (AAGGATCCGTCGACATCT$_{17}$). The adjacent RT-PCRs for cytokine cDNA screening were carried out with the following primer pairs. *TNFα*: primer pair TNFaUP / TNFaLO (5'AGCCCCTCTCAGAAGCAGAC'3 / 5'GTCATCGGG GTCTCACATCC'3). *IL-1B*: primer pair ILbUP / ILbLO (5'TTCAGGTTTCTAAAGCAGCCAT'3 / 5'TTAGCAGTGAT TTAGGGAAGGC'3). IL-1A: primer pair ILaUP / ILaLO (5'ACAAAAGGCGAAGTAGTCTG'3 / 5'TGTTAGTGTCGGT TCCATTAG'3). A 1.5 % agarose gel electrophoresis was performed to separate the PCR products, the fragments were recovered with the QIAquick Gel Extraction Kit (QIAGEN, Hilden, Germany). The PCR products were cloned in the pGEM-T Easy Vector System (Promega, Madison, WI, USA) and sequenced in forward and reverse direction for verification (MWG-Biotech AG, Ebersberg, Germany). The protein sequences were deduced by in silico analyses. Identity comparison of the proteins and respective cDNA contigs were done by Lasergene software (DNAStar, Madison, USA) and miscellaneous canine and human cytokine sequences from the NCBI database (accession numbers AY423389, AF047011, AF322077, AF322078, NM_001037971).

Results

Of the 17 individuals screened, eight cytokine transcripts showed nucleotide substitutions leading to amino acid exchanges within the deduced proteins of TNFα, IL-1α and IL-1β (Table I). SNPs causing no amino acid exchange were not taken into account for further analysis.

A BMD lung sample showed one nucleotide substitution affecting *TNFα* exon 4 codon 113 (GAT → GGT, Asp → Gly).

For *IL-1α*, the complete canine IL-1α coding sequence and the sequence for the alternative *IL-1α Exon 5 del* splice variant were amplified (14). The complete *IL-1α* coding sequence of one lung sample (BMD) showed substitutions in exon 2 codon 23 (TTC → TCC, Ser → Pro) and exon 4 codon 47 (TGC → CGC, Cys → Arg). One substitution was found in the *IL-1α Exon 5 del* splice variant transcript in a skin sample (West Highland Terrier). The transcript showed one nucleotide substitution in exon 4 codon 43 (CTT → CCT, Leu → Pro).

Three *IL-1β* transcripts derived from liver samples showed nucleotide substitution in the canine exons. Two samples (BMD) each showed one nucleotide substitution in the coding sequence of exon 5, affecting codon 113 (GAT → GGT, Asp → Gly) and codon 124 (CAG → AAG, Gln → Lys), respectively. One sample (BMD) showed two substitutions each in exon 7 codon 228 (TCT → CCT, Ser → Pro) and codon 234 (TAC → CAC, Tyr → His).

Discussion

Cytokines are considered to play a major role in the pathogenesis of malignant histiocytosis. In the present study, we focused on SNPs in the canine coding sequences of the cytokines *TNFα*, *IL-1α* and *IL1-β*, causing amino acid exchanges in the deduced protein sequences. With the exception of two samples (West Highland Terrier and

Collie), all samples were taken from BMDs, known to be frequently affected by malignant histiocytosis.

IL-1α and *IL-1β* both belong to the same gene family of *Interleukin-1* and are translated as precursor proteins with a molecular weight of 31 kD. They are expressed in various cell types *e.g.* activated monocytes, macrophages and lymphocytes. The processing of proIL-1α and proIL-1β by cellular proteases results in a mature form of the protein of approximately 17 kD. Both proteins induce cell signalling pathways upon binding with a membrane-bound receptor IL-1R1, including the NFκB inducing kinase (NIK) and three distinct MAP kinase cascades (13, 15). These switched pathways activate different transcription factors, *e.g.* NFκB, AP1 and CREB for regulation of immediate early genes vital to inflammatory and immune responses (13). Intracellular proIL-α is fully active and is cleaved by Ca^{2+}-dependent membrane associated cysteine proteases called calpains. ProIL-α is cleaved to IL-1α propiece and mature IL-1α, which is released to the extra cellular compartment (15, 16).

The *IL-1α* transcript (BMD sample 2 / lung tissue) in the present study revealed two amino acid exchanges at position 23 and 47 within the deduced protein sequence of the IL1-1α propiece. At position 23, the polar amino acid serine was substituted by unpolar proline. At position 47, the polar amino acid cysteine was exchanged with positively-charged arginine. Cysteines are able to form disulfide bridges, which are often modified by methylation. Both 32 kD proIL-1α and the 16kD IL-1α propiece are able to bind to nuclear DNA. ProIL-1α is commonly found in the cytoplasm and after myristoylation it binds to the membrane (17).

An SNP in the *IL-1α Exon 5 del* splice variant from skin (Western Highland Terrier sample 9) showed one amino acid exchange at position 43 within the deduced protein isoform IL-1α. Unpolar leucine is substituted to unpolar proline. Due to deletion of exon 5, the calpain cleavage site is lacking and calpain is unable to cleave the mature protein. These splice variant transcripts were mainly detected in macrophages and synovial membrane tissue of dogs, cats and pigs at various expression levels (14).

Pro IL-β remains in the cytoplasm until it is cleaved by the cysteine proteinase interleukin 1β converting enzyme (ICE) to the 16kD IL-1β propiece and the biologically active 17 kD mature IL-1β protein. Either proteins can be myristoylated and are able to be bound to the cell membrane or to be transported out of the cell (14, 15). In the *IL-1β* transcript (BSH sample 1), one SNP showed an amino acid substitution in the deduced canine mature IL-1β sequence. At position, 124 glutamine was substituted by lysine within a β-strand motif of the protein (18-20). At position 228 and 234, two SNPs (BSH sample 4) caused two amino acid exchanges in the deduced canine mature IL-1β also within a β strand motif. At position 228, serine was exchanged with proline and at position 234 tyrosine was exchanged with histidine. Regarding the tyrosine exchange at position 234 the motif asparagine-tryptophan-tyrosine is highly conserved in different species, *e.g.* human, mouse, rat, cattle and rabbit. However side-directed mutagenesis in this peptide motif of human IL-1β changing the tyrosine residue (Tyr 237) to phenylalanine did not affect the protein binding affinity to its receptor (19).

At position 113, one SNP (BSH sample 5) led to an amino acid exchange in the deduced propiece IL-1β protein. Position 113 covers the last amino acid in the sequence. Hydrophilic aspartic acid is exchanged with unpolar glycine. The aspartic acid – alanine side (canine amino acid position 113 - 114) was determined to be cleaved by cysteine proteinase interleukin β converting enzyme (ICE). Interestingly, all SNPs in the IL-1β transcripts were exclusively detected in liver samples.

The pleiotropic cytokine TNFα is primarily secreted by stimulated macrophages. It additionally acts as a potent pyrogen when stimulated by IL-1. Further on, it plays an important role in abundant cellular signal transduction processes during immune response and inflammation. It can induce cell death in certain tumour cells. TNFα exists in two forms: a soluble form of 157 amino acids (17 kD), cleaved at amino acid position 76 and 77 by ADAM17 and as a type II membrane protein of 233 amino acids (26 kD) (21). One SNP in the canine TNFα transcript (BSH sample 2 / lung tissue) led to an amino acid exchange in the deduced membrane binding region of TNFα. At position 206, the amino acid aspartic acid was exchanged with glycine.

SNPs within the promoter and or enhancer region of the cytokine genes IL-1 α/β and TNFα, which play an important role in the development of diseases *e.g.* cancer, Alzheimer disease, sepsis and rheumatoid arthritis, were described (22-24). For malignant histiocytosis, the data regarding SNP screening in canine cytokine transcripts is currently scarce. Our results showed several SNPs within the cytokine coding sequence of mRNA isolated from BMD tissue samples. These SNPs led to missense mutations causing changes of amino acid sequences within the deduced protein. Due to the fact that the BMDs show a genetic predisposition for malignant histiocytosis, these dogs could be used to elucidate the genetic mechanisms of malignant histiocytosis and to elucidate in further studies if the found SNPs play a role in the pathogenesis of this disease.

Acknowledgements

This research was supported by a grant of the Gesellschaft zur Förderung Kynologischer Forschung e.V., Bonn, Germany.

References

1 Tazi A, Soler P and Hance AJ: Adult pulmonary Langerhans' cell histiocytosis. Thorax *55(5)*: 405-416, 2000.

2 Kannourakis G and Abbas A: The role of cytokines in the pathogenesis of Langerhans cell histiocytosis. Br J Cancer Suppl *23*: S37-40, 1994.

3 Ostrander EA, Galibert F and Patterson DF: Canine genetics comes of age. Trends Genet *16(3)*: 117-124, 2000.

4 Ostrander EA and Kruglyak L: Unleashing the canine genome. Genome Res *10(9)*: 1271-1274, 2000.

5 Patterson DF: Companion animal medicine in the age of medical genetics. J Vet Intern Med *14(1)*: 1-9, 2000.

6 Ramsey IK, McKay JS, Rudorf H and Dobson JM: Malignant histiocytosis in three Bernese mountain dogs. Vet Rec *138(18)*: 440-444, 1996.

7 Nolte I and Nolte M: Praxis der Onkologie bei Hund und Katze. Stuttgard, Enke Verlag, pp. 143-144, 2000.

8 Affolter VK and Moore PF: Localized and disseminated histiocytic sarcoma of dendritic cell origin in dogs. Vet Pathol *39(1)*: 74-83, 2002.

9 Egeler RM, Favara BE, van Meurs M, Laman JD and Claassen E: Differential *in situ* cytokine profiles of Langerhans-like cells and T cells in Langerhans cell histiocytosis: abundant expression of cytokines relevant to disease and treatment. Blood *94(12)*: 4195-4201, 1999.

10 Tazi A, Moreau J, Bergeron A, Dominique S, Hance AJ and Soler P: Evidence that Langerhans cells in adult pulmonary Langerhans cell histiocytosis are mature dendritic cells: importance of the cytokine microenvironment. J Immunol *163(6)*: 3511-3515, 1999.

11 Arico M and Danesino C: Langerhans' cell histiocytosis: is there a role for genetics? Haematologica *86(10)*: 1009-1014, 2001.

12 Arico M: Langerhans cell histiocytosis: Too many cytokines, not enough gene regulation? Pediatr Blood Cancer 2006.

13 Stylianou E and Saklatvala J: Interleukin-1. Int J Biochem Cell Biol *30(10)*: 1075-1079, 1998.

14 Straubinger AF, Viveiros MM and Straubinger RK: Identification of two transcripts of canine, feline, and porcine interleukin-1 alpha. Gene *236(2)*: 273-280, 1999.

15 Dinarello CA: Biologic basis for interleukin-1 in disease. Blood *87(6)*: 2095-2147, 1996.

16 Kobayashi Y, Yamamoto K, Saido T, Kawasaki H, Oppenheim JJ and Matsushima K: Identification of calcium-activated neutral protease as a processing enzyme of human interleukin 1 alpha. Proc Natl Acad Sci USA *87(14)*: 5548-5552, 1990.

17 Stevenson FT, Bursten SL, Fanton C, Locksley RM and Lovett DH: The 31-kDa precursor of interleukin 1 alpha is myristoylated on specific lysines within the 16-kDa N-terminal propiece. Proc Natl Acad Sci USA *90(15)*: 7245-7249, 1993.

18 Priestle JP, Schar HP, Grutter MG: Crystal structure of the cytokine interleukin-1 beta. Embo J *7(2)*: 339-343, 1988.

19 Priestle JP, Schar HP and Grutter MG: Crystallographic refinement of interleukin 1 beta at 2.0 A resolution. Proc Natl Acad Sci USA *86(24)*: 9667-9671, 1989.

20 Eisenberg SP, Brewer MT, Verderber E, Heimdal P, Brandhuber BJ and Thompson RC: Interleukin 1 receptor antagonist is a member of the interleukin 1 gene family: evolution of a cytokine control mechanism. Proc Natl Acad Sci USA *88(12)*: 5232-5236, 1991.

21 Beutler B and Cerami A: The biology of cachectin/TNF – a primary mediator of the host response. Annu Rev Immunol *7*: 625-655, 1989.

22 Dennis RA, Trappe TA, Simpson P, Carroll C, Huang BE, Nagarajan R, Bearden E, Gurley C, Duff GW, Evans WJ, Kornman K and Peterson CA: Interleukin-1 polymorphisms are associated with the inflammatory response in human muscle to acute resistance exercise. J Physiol *560(Pt 3)*: 617-626, 2004.

23 Zienolddiny S, Ryberg D, Maggini V, Skaug V, Canzian F and Haugen A: Polymorphisms of the interleukin-1 beta gene are associated with increased risk of non-small cell lung cancer. Int J Cancer *109(3)*: 353-356, 2004.

24 Correa PA, Gomez LM, Cadena J and Anaya JM: Autoimmunity and tuberculosis. Opposite association with TNF polymorphism. J Rheumatol *32(2)*: 219-224, 2005.

Received May 11, 2006
Accepted June 28, 2006

XI

Comparison of the human and canine cytokines IL-1 (α/β) and TNF-α to orthologous other mammalians.

Soller JT, Murua Escobar H, Willenbrock S, Janssen M, Eberle N, Bullerdiek J, Nolte I.

J Hered. 2007; 98(5): 485-90.

Eigenleistung:

- Koordinierung und Planung aller Arbeiten
- *In silico* Analysen und grafische Auswertung
- Verfassen des Manuskripts mit I. Nolte

Journal of Heredity 2007:98(5):485–490
doi:10.1093/jhered/esm025
Advance Access publication June 15, 2007

Comparison of the Human and Canine Cytokines *IL-1*(α/β) and *TNF*-α to Orthologous Other Mammalians

Jan T. Soller, Hugo Murua-Escobar, Saskia Willenbrock, Miriam Janssen, Nina Eberle, Jörn Bullerdiek, and Ingo Nolte

From the Small Animal Clinic, University of Veterinary Medicine, Bischofsholer Damm 15, 30137 Hanover, Germany (Soller, Escobar, Willenbrock, Eberle, and Nolte); and the Centre for Human Genetics, University of Bremen, Leobener Strasse ZHG, 28359 Bremen, Germany (Soller, Escobar, Willenbrock, Janssen, and Bullerdiek).

Address correspondence to Dr. I. Nolte at the address above, or e-mail: inolte@klt.tiho-hannover.de.

Abstract

The cytokines interleukin-1 (IL-1α and IL-1β) and the tumor necrosis factor-α (TNF-α) both play a major role in the initiation and regulation of inflammation and immunity responses. Polymorphisms within the gene sequences of these cytokines *IL-1* and *TNF*-α have been proposed to play an important role in the pathogenesis of certain diseases. Affecting nearly every organ, various diseases, including some cancers, are described to be associated with an increased level of IL-1 and TNF-α proteins, for example, solid tumors, hematologic malignancies, malignant histiocytosis, autoimmune disorders, Alzheimer's disease, Parkinson's disease, sepsis, and rheumatoid arthritis. Regarding genetic backgrounds and pathways, numerous canine diseases show close similarities to their human counterparts. As a genetic model, the dog could be used to unravel the genetic mechanisms, for example, in particular the predispositions, the development, and progression of cancer and metabolic diseases. The identity comparison of gene and protein sequences of different species could be used to elucidate the structure and function of the genes and proteins by identifying the evolutionary conserved regions and domains. Herein we analyzed in detail the mRNA and protein structures and identities of the present known mammalian (human, canine, murine, rat, ovine, equine, feline, porcine, and bovine) *TNF*-α, *IL*-1α, and *IL-1*β mRNAs and proteins. Additionally, based on the canine genome sequence, we derived in silico the complete mRNA structures of the *IL-1*α and *IL-1*β mRNAs.

The cytokines interleukin-1 (IL-1α and IL-1β) and tumor necrosis factor-α (TNF-α) are primarily secreted by monocytes and macrophages and act as potent multifunctional cytokines in abundant signal transduction processes during immune response and inflammation, acting as proinflammatory proteins. These cytokines bind to cell-surface receptors inducing the activation of different transcription factors, for example, AP1, CREB, and NF-κB for regulation of immediate early genes. In detail, IL-1α and IL-1β will bind to membrane-bound receptor IL-1RI, whereas 2 distinct receptors TNF-R55 and TNF-R60 exist for TNF-α. Although both receptors for IL-1α and TNF-α are structurally unrelated, they operate both in a similar biological manner (Brockhaus et al. 1990; Eisenberg et al. 1991; Dinarello 1996).

In particular, NFκB-dependent signaling pathways play a key role for inflammatory responses caused by injury and infection stimuli. In mammals, 5 NF-κB proteins, RelA, RelB, c-Rel, NF-κB1, and NF-κB2 were described, which form homo- and heterodimer complexes in the cytoplasm. NF-κB proteins are inactivated by binding the inhibitory protein IκB. IL-1 and TNF-α are able to trigger phosphorylation and ubiquitinylation pathways to degrade the IκB protein having a releasing effect for NF-κB and thus inducing the transcription of several genes in the nucleus (for review see Beutler and Cerami 1989; Stylianou and Saklatvala 1998; Alberts et al. 2002).

*IL-1*α and *IL-1*β both belong to the same gene family of *Interleukin-1* and are translated as precursor proteins with a molecular weight of 31 kDa. The processing of the isoforms of proIL-1α and proIL-1β by cellular proteases results in a mature form of the protein of approximately 17 kDa (Dinarello 1996).

Intracellular proIL-1α is fully active and cleaved by Ca^{2+}-dependent membrane-associated cysteine proteases called calpains to IL-1α propiece (16 kDa), which then is able to bind to nuclear DNA, and to mature IL-1α, which is released to the extracellular compartment (Kobayashi et al. 1990; Dinarello 1996). IL-1α shows significant antitumor activity

on solid tumor cells in vitro and in vivo (Braunschweiger et al. 1988). It also has an effect on bone marrow cells to produce colony-stimulating factors (Bagby et al. 1986).

ProIL-β remains in the cytoplasm until it is cleaved by the cysteine proteinase IL-1β–converting enzyme to the IL-1β propiece (16 kDa) and the biologically active 17-kDa mature IL-1β protein. Either protein is able to bind the cell membrane or to be transported out of the cell (Dinarello 1996).

The TNF-α protein exists in 2 forms: a soluble form of 157 amino acids (aa) (17 kDa) cleaved at aa position 76 and 77 by ADAM17 and as a membrane-bound form of 233 aa (26 kDa). Additionally, it acts as a potent pyrogen when stimulated by IL-1. Also TNF-α can induce cell death of certain tumor cells (Beutler and Cerami 1989).

The human nucleotide sequences of the *IL-1*α and *IL-1*β genes contain 6 introns and 7 exons. The genes are located on HSA 2q14 (Furutani et al. 1986; Webb et al. 1986; Modi et al. 1988; Lafage et al. 1989). In humans, the *TNF*-α gene consists of 3 introns and 4 exons and spans approximately 3 kb and was mapped on HSA 6p21 (Nedwin et al. 1985; Spies et al. 1986).

Cytokines are considered to play a major role in the pathogenesis of several diseases.

Polymorphisms within the promoter and/or enhancer regions within the gene sequences of *IL-1*α/β and *TNF*-α are proposed to play a role in the development and pathogenesis of Alzheimer's disease and Parkinson's disease (Nicoll et al. 2000; McGeer PL and McGeer EG 2001; Mattila et al. 2002), as well as nonsmall cell lung cancer (Zienolddiny et al. 2004), tuberculosis (Correa et al. 2005), sepsis, and rheumatoid arthritis (Cox et al. 1999; Ruuls and Sedgwick 1999). Also the production of large quantities of IL-1 and TNF-α cytokines in T-cells are expected to be responsible for the development and progression of certain autoimmune and tumor diseases like in human the Langerhans' cell histiocytosis and the canine malignant histiocytosis (Ramsey et al. 1996; Egeler et al. 1999; Tazi et al. 2000; Affolter and Moore 2002; Arico 2006).

Some human and canine diseases show similarities, concerning the dysfunction of regulation of the immune system and inflammatory processes and the genetic pathways for the development of neoplastic diseases, for example, malignant histiocytosis (Ramsey et al. 1996; Affolter and Moore 2002). Comparative analyses of canine cytokine genes to the known gene information of other mammalians could be used to clarify the mechanisms of etiology and pathogenesis. The knowledge gained by the species comparison could help to evaluate the different species as appropriate models for research studies opening new aspects for experimental and therapeutic approaches.

In Figure 1A and B, the *IL-1*α, *IL-1*β, and *TNF*-α mRNA sequences of 7 mammalians currently present at the National Center for Biological Information (NCBI) database (October 2006) are shown in detail (including the present information on the coding sequences (CDS), 5′ untranslated regions [UTRs] and 3′UTRs). Additionally, we derived in silico the complete structures of the *IL-1*α and *IL-1*β mRNAs using the released canine genome sequence (Lindblad-Toh et al. 2005).

For CDS and protein identity analyses, we used the described sequences from human, dog, mouse, cat, pig, cattle, rat, horse, and sheep and deduced, if necessary, the corresponding parts for analysis. The in silico analysis were done using LASERGENE software programs (DNASTAR, Madison, WI).

The first publications of human and murine *IL-1*α gene sequences (NM_000575, NM_010554) were done at the middle of the 1980s. The human CDS is composed of 816 bp and 813 bp for the murine sequence (Furutani et al. 1985; Lomedico et al. 1984; March et al. 1985). Straubinger et al. characterized the canine (798 bp) and feline (813 bp) CDS and parts of 3′UTR for the *IL-1*α mRNAs (NM_001003157, AF047012) spanning exon 2–7, respectively. Two different splice variant transcripts of canine, feline, and porcine *IL-1*α were described to be found in total RNA from lipopolysaccharide-stimulated lung macrophages. One transcript was identified as a new mRNA splice variant of canine *IL-1*α missing the 175 bp of exon 5 (Straubinger et al. 1999). Due to the deletion of exon 5, the calpain cleavage site is lacking, and calpain is unable to cleave the precursor protein to the mature protein. In previous studies aimed at a single-nucleotide polymorphism screening analysis in canine cytokine mRNA transcripts of *IL-1*(α/β) and *TNF*-α, we cloned the *IL-1*α mRNAs adding new information on the 5′UTR (complete exon 1 and parts of exon 2) and additional parts for the 3′UTR (Soller et al. 2006). We also found both splice variants *IL-1a* (DQ923806) and the splice variant bearing the exon 5 deletion (EF068230): We analyzed them in detail and submitted them to the NCBI database completing the known information due to the fact that the sequences describing the splice variant were not submitted to the databases by the respective author. The genetic structure and organization of all compared *IL-1a* cytokines are highly conserved among the different mammalians. The detailed sequence comparisons (Figure 1A) showed that all cytokine transcripts of the different species with exception of the feline and ovine sequences are composed of equal number of 7 exons. The ovine and feline exceptions are the missing of the sequence information coding for exon 1, probably due to the transcripts have not been completely characterized up to date.

The identities of the canine *IL-1*α CDS (NM_001003157) to the CDS sequences of other species vary between mouse CDS (NM_008361) 43.9%, rat CDS (D00403) 69.3%, human CDS (NM_000575) 79.6%, horse CDS (U92480) 84.8%, and cat CDS (AF047012) 88.8% (Table 1). Respectively. the identities of the canine IL-1α protein sequence (ABJ51907) to the protein sequences of the other species vary between mouse protein (NP_034684) 57.1%, rat protein (BAA00306) 59.6%, human protein (NP_000566) 68.5%, horse protein (AAC39255) 79.3%, and cat protein (AAC03067) 82.7% (Table 1).

The IL-1α proteins of all mammalians show strong conservation of the predicted calpain cleavage site (-KP**RS**V-), located between the arginine residue at position 108 and the serine residue at position 109 of the canine protein. The average IL-1α protein size of the described mammalians is about 270 aa. The protein size range about 266 aa (dog,

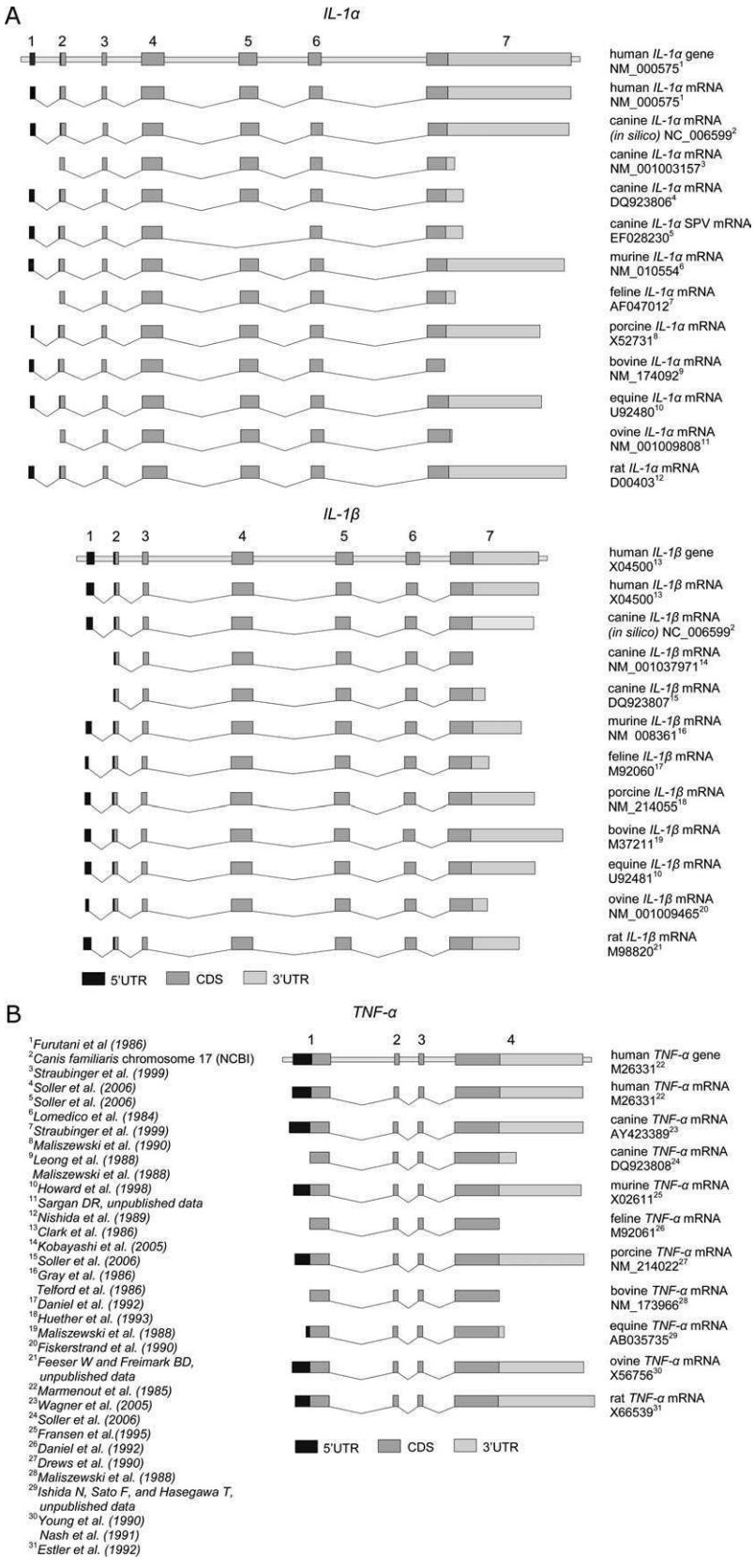

Figure 1. **(A)** Species comparison of *IL-1*(α/β) transcripts. The introns are scaled down by factor 0.4. **(B)** Species comparison of *TNF*-α transcripts.

Table 1. Cytokines IL-1 and TNF-α identity comparison (CDS and protein) of various species to canine transcripts and proteins; size in base pairs (bp) and amino acids (aa), and listed accession numbers

	Identity (%) to *Canis. familiaris*	
IL-1α	CDS 798 bp (DQ923806)	Protein 266 aa (ABJ51907)
Human (*Homo sapiens*) (NM_000575/NP_000566)	79.6 (816 bp)	68.5 (272 aa)
Mouse (*Mus musculus*) (NM_000575/NP_000566)	43.9 (813 bp)	57.1 (271 aa)
Cat (*Felis catus*) (AF047012/AAC03067)	88.8 (813 bp)	82.7 (271 aa)
Pig (*Sus scrofa*) (X52731/CAA36945)	81.8 (813 bp)	73.2 (271 aa)
Cattle (*Bos Taurus*) (NM_174092/NP_776517)	81.2 (807 bp)	75.1 (269 aa)
Horse (*Equus caballus*) (U92480/AAC39255)	84.8 (813 bp)	79.3 (268 aa)
Sheep (*Ovis aries*) (NM_001009808/NP_001009808)	81.0 (807 bp)	75.1 (266 aa)
Rat (*Rattus norvegicus*) (D00403/BAA00306)	69.3 (813 bp)	59.1 (268 aa)
IL-1β	CDS 801 bp (DQ923807)	Protein 267 aa (ABJ51908)
Human (*Homo sapiens*) (X04500/CAA28185)	76.4 (810 bp)	62.8 (270 aa)
Mouse (*Mus musculus*) (NM_008361/NP_032387)	71.7 (810 bp)	58.3 (270 aa)
Cat (*Felis catus*) (M92060/AAA30814)	83.8 (804 bp)	74.0 (268 aa)
Pig (*Sus scrofa*) (NM_214055/NP_999220)	76.3 (804 bp)	64.7 (268 aa)
Cattle (*Bos Taurus*) (M37211/AAA30584)	76.5 (801 bp)	62.5 (267 aa)
Horse (*Equus caballus*) (U92481/AAC39256)	79.5 (806 bp)	67.3 (266 aa)
Sheep (*Ovis aries*) (NM_001009465/NP_001009465)	75.5 (800 bp)	61.4 (261 aa)
Rat (*Rattus norvegicus*) (M98820/AAA41426)	70.3 (806 bp)	58.0 (263 aa)
TNF-α	CDS 702 bp (AY423389)	Protein 234 aa (AAR27885)
Human (*Homo sapiens*) (M26331/AAA36758)	90.8 (702 bp)	91.0 (234 aa)
Mouse (*Mus musculus*) (X02611/CAA26457)	80.4 (708 bp)	78.2 (236 aa)
Cat (*Felis catus*) (M92061/AAA30818)	93.3 (702 bp)	94.4 (234 aa)
Pig (*Sus scrofa*) (NM_214022/NP_999187)	85.5 (699 bp)	85.5 (233 aa)
Cattle (*Bos Taurus*) (NM_173966/NP_776391)	83.4 (705 bp)	78.7 (235 aa)
Horse (*Equus caballus*) (AB035735/BAA349)	89.3 (705 bp)	87.7 (233 aa)
Sheep (*Ovis aries*) (NM_001024860/NP_001020031)	83.9 (705 bp)	79.1 (233 aa)
Rat (*Rattus norvegicus*) (X66539/CAA47146)	79.7 (708 bp)	77.0 (234 aa)

sheep), 268 aa (horse, rat), 269 aa (cattle) to 271 aa (mouse, cat, pig), and 272 aa (human).

Correspondingly, the human (BC_008678) and the murine *IL-1*β (NM_008361) CDS and protein sequences (Auron et al. 1984; Gray et al. 1986; Telford et al. 1986) were analyzed by identity comparison and evaluated with the canine, feline, porcine, bovine, equine, ant rat sequences.

As described for *IL-1*α, we cloned the canine *IL-1*β mRNA, analyzed it in detail, and submitted it to the NCBI database adding new information on the 3′UTR to the present data. As shown in Figure 1A, again the genetic structure and organization of all compared *IL-1*β cytokine transcripts are highly conserved among the different analyzed mammalians. The detailed sequence data comparison (Figure 1A) showed that all analyzed mammalian cytokine transcripts, with the exception of the cloned canine sequences (NM_001037971 and DQ923807), are composed of equal number of 7 exons. The canine sequences (NM_001037971 and DQ923807) are missing the sequence information for the 5′UTR (exon 1) that have not been completely cloned until now. Taking into account the in silico-derived structure of the canine *IL-1*β (Figure 1A), the dog shows also 7 exons with a highly conserved structure to the compared species.

The CDS identities of the canine *IL-1*β (NM_001037971, DQ923807) to the sequences of the other mammalians vary between mouse CDS (NM_008361) 71.7%, human CDS (BC_008678) 76.4%, horse CDS (U92481) 79.3%, and cat CDS (M92060) 83.8% (Table 1). The identities of the canine IL-1β protein to the protein sequences of the other mammalians vary between mouse (NP_032387) 58.3%, human protein (CAA28185) 62.8%, horse protein (AAC39256) 67.3%, and cat protein (AAA30814) 74.0% (Table 1).

In the canine IL-1β protein, a β-strand motif at aa residue position 232–240 (-PNWYISTSQ-) is highly conserved in the other described mammalians human, mouse, rat, cat, pig, sheep, horse, and cattle. The IL-1β protein sizes of the different species vary between 267 aa (cattle, dog) and 270 aa (human).

The genetic structure and organization of all compared *TNF*-α cytokine transcripts are also highly conserved among the different species. The detailed sequence comparisons (Figure 1B) showed that all *TNF*-α transcripts of the different species are composed of 4 exons. All described sequences, with the exception of feline (M92061), bovine (NM_173966), and equine cDNAs (BAA88349), show the full mRNA sequences including the CDS, 5′UTR, and 3′UTRs. The feline, bovine, and equine sequences exceptions are the missing of the sequence information coding for the 5′UTRs and 3′UTRs, surely due to the missing complete characterization of the respective mRNA transcripts.

The highest identity values among the analyzed cytokines show the CDS and proteins of TNF-α. The canine CDS for

TNF-α (AY423389) shows identities from mouse CDS (X02611) 80.4%, sheep CDS (NM_001024860) 83.9%, pig CDS 85.5% (NM_214022), to human CDS 90.8% (M26331), and cat CDS 93.3% (M92061) (Table 1). Respectively, the identities of the canine TNF-α protein sequence (AAR27885) to the protein sequences of the other species vary between mouse protein (CAA26457) 78.2%, sheep protein (NP_001020031) 79.1%, pig protein (NP_999187) 85.5%, human protein (AAA36758) 91.0%, and cat protein (AAA30818) 94.4%. The TNF-α protein sizes vary between 233 aa (pig and sheep), 234 aa (human, dog, cat and rat) to 235 aa (cattle), and 236 aa (mouse).

The overall described cytokine identity values (Table 1) of the analyzed CDS and the derived proteins show a wide variance from 43.9% to 93.43% among the CDS and from 57.1% to 94.4% for the analyzed proteins.

The described mammalian cytokine transcript and protein comparison data emphasizes the relevance of structural comparative analysis of genes and proteins for the development of therapeutic strategies aimed at the development of therapeutic approaches targeting canine disorders. The observed overall cytokine identities are variable among the different species analyzed. In particular, the performed protein alignments of the cytokines IL-1 and TNF-α showed highly conserved protein regions and domains of the compared elements among the mammalian species. In spite of the observed high variability in terms of nucleotide sequence identity, the structure of the analyzed genes is highly conservative.

The described properties of the cytokine genes IL-1 and TNF-α and their described role in the development of tumor and metabolic diseases offer various possibilities for new approaches and applications and also for existing therapy concepts. The highly conserved structure of the cytokine proteins seen in mammalians allows knowledge transfer of already established experimental data and approaches from one mammalian species to another due to the fact that essential protein properties are comparable. It is to expect that future therapeutic approaches targeting cytokine-mediated diseases in humans and dogs will benefit from each other.

Acknowledgments

This research was supported by a grant of the Gesellschaft zur Förderung Kynologischer Forschung.

References

Affolter VK, Moore PF. 2002. Localized and disseminated histiocytic sarcoma of dendritic cell origin in dogs. Vet Pathol. 39:74–83.

Alberts B, Johnson A, Lewis J, Raff M, Roberts K, Walter P. 2002. Molecular biology of the cell. 4th ed. New York: Garland Science.

Arico M. 2006. Langerhans cell histiocytosis: too many cytokines, not enough gene regulation? Pediatr Blood Cancer. 47:118–119.

Auron PE, Webb AC, Rosenwasser LJ, Mucci SF, Rich A, Wolff SM, Dinarello CA. 1984. Nucleotide sequence of human monocyte interleukin 1 precursor cDNA. Proc Natl Acad Sci USA. 81:7907–7911.

Bagby GC Jr, Dinarello CA, Wallace P, Wagner C, Hefeneider S, McCall E. 1986. Interleukin 1 stimulates granulocyte macrophage colony-stimulating activity release by vascular endothelial cells. J Clin Invest. 78:1316–1323.

Beutler B, Cerami A. 1989. The biology of cachectin/TNF—a primary mediator of the host response. Annu Rev Immunol. 7:625–655.

Braunschweiger PG, Johnson CS, Kumar N, Ord V, Furmanski P. 1988. Antitumor effects of recombinant human interleukin 1 alpha in RIF-1 and Panc02 solid tumors. Cancer Res. 48:6011–6016.

Brockhaus M, Schoenfeld HJ, Schlaeger EJ, Hunziker W, Lesslauer W, Loetscher H. 1990. Identification of two types of tumor necrosis factor receptors on human cell lines by monoclonal antibodies. Proc Natl Acad Sci USA. 87:3127–3131.

Clark BD, Collins KL, Gandy MS, Webb AC, Auron PE. 1986. Genomic sequence for human prointerleukin 1 beta: possible evolution from a reverse transcribed prointerleukin 1 alpha gene. Nucleic Acids Res. 14: 7897–7914.

Correa PA, Gomez LM, Cadena J, Anaya JM. 2005. Autoimmunity and tuberculosis. Opposite association with TNF polymorphism. J Rheumatol. 32:219–224.

Cox A, Camp NJ, Cannings C, di Giovine FS, Dale M, Worthington J, John S, Ollier WER, Silman AJ, Duff GW. 1999. Combined sib-TDT and TDT provide evidence for linkage of the interleukin-1 gene cluster to erosive rheumatoid arthritis. Hum Mol Genet. 8:1707–1713.

Daniel SL, Legendre AM, Moore RN, Rouse BT. 1993. Isolation and functional studies on feline bone marrow derived macrophages. Vet Immunol Immunopathol. 36:107–122.

Dinarello CA. 1996. Biologic basis for interleukin-1 in disease. Blood. 87:2095–2147.

Drews RT, Coffee BW, Prestwood AK, McGraw RA. 1990. Gene sequence of porcine tumor necrosis factor alpha. Nucleic Acids Res. 18:5564.

Egeler RM, Favara BE, van Meurs M, Laman JD, Claassen E. 1999. Differential in situ cytokine profiles of Langerhans-like cells and T cells in Langerhans cell histiocytosis: abundant expression of cytokines relevant to disease and treatment. Blood. 94:4195–4201.

Eisenberg SP, Brewer MT, Verderber E, Heimdal P, Brandhuber BJ, Thompson RC. 1991. Interleukin 1 receptor antagonist is a member of the interleukin 1 gene family: evolution of a cytokine control mechanism. Proc Natl Acad Sci USA. 88:5232–5236.

Estler HC, Grewe M, Gaussling R, Pavlovic M, Decker K. 1992. Rat tumor necrosis factor-alpha. Transcription in rat Kupffer cells and in vitro post-translational processing based on a PCR-derived cDNA. Biol Chem Hoppe Seyler. 373:271–281.

Fiskerstrand C, Sargan D. 1990. Nucleotide sequence of ovine interleukin-1 beta. Nucleic Acids Res. 18:7165.

Fransen L, Muller R, Marmenout A, Tavernier J, Van der Heyden J, Kawashima E, Chollet A, Tizard R, Van Heuverswyn H, Van Vliet A, et al. 1985. Molecular cloning of mouse tumour necrosis factor cDNA and its eukaryotic expression. Nucleic Acids Res. 13:4417–4429.

Furutani Y, Notake M, Yamayoshi M, Yamagishi J, Nomura H, Ohue M, Furuta R, Fukui T, Yamada M, Nakamura S. 1985. Cloning and characterization of the cDNAs for human and rabbit interleukin-1 precursor. Nucleic Acids Res. 13:5869–5882.

Furutani Y, Notake M, Fukui T, Ohue M, Nomura H, Yamada M, Nakamura S. 1986. Complete nucleotide sequence of the gene for human interleukin 1 alpha. Nucleic Acids Res 14:3167–3179.

Gray PW, Glaister D, Chen E, Goeddel DV, Pennica D. 1986. Two interleukin 1 genes in the mouse: cloning and expression of the cDNA for murine interleukin 1 beta. J Immunol. 137:3644–3648.

Howard RD, McIlwraith CW, Trotter GW, Nyborg JK. 1998. Cloning of equine interleukin 1 alpha and equine interleukin 1 beta and determination of their full-length cDNA sequences. Am J Vet Res. 59:704–711.

Huether MJ, Lin G, Smith DM, Murtaugh MP, Molitor TW. 1993. Cloning, sequencing and regulation of an mRNA encoding porcine interleukin-1 beta. Gene. 129:285–289.

Kobayashi S, Baba H, Uchida K, Shimada S, Negoro K, Takeno K, Yayama T, Yamada S, Yoshizawa H. 2005. Localization and changes of intraneural inflammatory cytokines and inducible-nitric oxide induced by mechanical compression. J Orthop Res. 23:771–778.

Kobayashi Y, Yamamoto K, Saido T, Kawasaki H, Oppenheim JJ, Matsushima K. 1990. Identification of calcium-activated neutral protease as a processing enzyme of human interleukin 1 alpha. Proc Natl Acad Sci USA. 87:5548–5552.

Lafage M, Maroc N, Dubreuil P, de Waal Malefijt R, Pebusque MJ, Carcassonne Y, Mannoni P. 1989. The human interleukin-1 alpha gene is located on the long arm of chromosome 2 at band q13. Blood 73:104–107.

Leong SR, Flaggs GM, Lawman M, Gray PW. 1988. The nucleotide sequence for the cDNA of bovine interleukin-1 beta. Nucleic Acids Res. 16:9054.

Lindblad-Toh K, Wade CM, Mikkelsen TS, Karlsson EK, Jaffe DB, Kamal M, Clamp M, Chang JL, Kulbokas EJ III, Zody MC, et al. 2005. Genome sequence, comparative analysis and haplotype structure of the domestic dog. Nature. 438:803–819.

Lomedico PT, Gubler U, Hellmann CP, Dukovich M, Giri JG, Pan YC, Collier K, Semionow R, Chua AO, Mizel SB. 1984. Cloning and expression of murine interleukin-1 cDNA in Escherichia coli. Nature. 312:458–462.

Maliszewski CR, Baker PE, Schoenborn MA, Davis BS, Cosman D, Gillis S, Cerretti DP. 1988. Cloning, sequence and expression of bovine interleukin 1 alpha and interleukin 1 beta complementary DNAs. Mol Immunol. 25: 429–437.

Maliszewski CR, Renshaw BR, Schoenborn MA, Urban JF Jr, Baker PE. 1990. Porcine IL-1 alpha cDNA nucleotide sequence. Nucleic Acids Res. 18:4282.

Marmenout A, Fransen L, Tavernier J, Van der Heyden J, Tizard R, Kawashima E, Shaw A, Johnson MJ, Semon D, Muller R, et al. 1985. Molecular cloning and expression of human tumor necrosis factor and comparison with mouse tumor necrosis factor. Eur J Biochem. 152:515–522.

March CJ, Mosley B, Larsen A, Cerretti DP, Braedt G, Price V, Gillis S, Henney CS, Kronheim SR, Grabstein K, et al. 1985. Cloning, sequence and expression of two distinct human interleukin-1 complementary DNAs. Nature. 315:641–647.

Mattila KM, Rinne JO, Lehtimaki T, Roytta M, Ahonen JP, Hurme M. 2002. Association of an interleukin 1B gene polymorphism (-511) with Parkinson's disease in Finnish patients. J Med Genet. 39:400–402.

McGeer PL, McGeer EG. 2001. Polymorphisms in inflammatory genes and the risk of Alzheimer disease. Arch Neurol. 58:1790–1792.

Modi WS, Masuda A, Yamada M, Oppenheim JJ, Matsushima K, O'Brien SJ. 1988. Chromosomal localization of the human interleukin 1 alpha (IL-1 alpha) gene. Genomics 2:310–314.

Nash AD, Barcham GJ, Brandon MR, Andrews AE. 1991. Molecular cloning, expression and characterization of ovine TNF alpha. Immunol Cell Biol. 69:273–283.

Nedwin GE, Naylor SL, Sakaguchi AY, Smith D, Jarrett-Nedwin J, Pennica D, Goeddel DV, Gray PW. 1985. Human lymphotoxin and tumor necrosis factor genes: structure, homology and chromosomal localization. Nucleic Acids Res. 13:6361–6373.

Nicoll JA, Mrak RE, Graham DI, Stewart J, Wilcock G, MacGowan S, Esiri MM, Murray LS, Dewar D, Love S, et al. 2000. Association of interleukin-1 gene polymorphisms with Alzheimer's disease. Ann Neurol. 47:365–368.

Nishida T, Nishino N, Takano M, Sekiguchi Y, Kawai K, Mizuno K, Nakai S, Masui Y, Hirai Y. 1989. Molecular cloning and expression of rat interleukin-1 alpha cDNA. J Biochem. 105:351–357.

Ramsey IK, McKay JS, Rudorf H, Dobson JM. 1996. Malignant histiocytosis in three Bernese mountain dogs. Vet Rec. 138:440–444.

Ruuls SR, Sedgwick JD. 1999. Unlinking tumor necrosis factor biology from the major histocompatibility complex: lessons from human genetics and animal models. Am J Hum Genet. 65:294–301.

Soller JT, Murua Escobar H, Janssen M, Fork M, Bullerdiek J, Nolte I. 2006. Cytokine genes single nucleotide polymorphism (SNP) screening analyses in canine malignant histiocytosis. Anticancer Res. 26:3417–3420.

Spies T, Morton CC, Nedospasov SA, Fiers W, Pious D, Strominger JL. 1986. Genes for the tumor necrosis factors alpha and beta are linked to the human major histocompatibility complex. Proc Natl Acad Sci USA. 83:8699–8702.

Straubinger AF, Viveiros MM, Straubinger RK. 1999. Identification of two transcripts of canine, feline, and porcine interleukin-1 alpha. Gene 236: 273–280.

Stylianou E, Saklatvala J. 1998. Interleukin-1. Int J Biochem Cell Biol. 30: 1075–1079.

Tazi A, Soler P, Hance AJ. 2000. Adult pulmonary Langerhans' cell histiocytosis. Thorax. 55:405–416.

Telford JL, Macchia G, Massone A, Carinci V, Palla E, Melli M. 1986. The murine interleukin 1 beta gene: structure and evolution. Nucleic Acids Res. 14:9955–9963.

Wagner JL, Palti Y, DiDario D, Faraco J. 2005. Sequence of the canine major histocompatibility complex region containing non-classical class I genes. Tissue Antigens. 65:549–555.

Webb AC, Collins KL, Auron PE, Eddy RL, Nakai H, Byers MG, Haley LL, Henry WM, Shows TB. 1986. Interleukin-1 gene (IL1) assigned to long arm of human chromosome 2. Lymphokine Res 5:77–85.

Young AJ, Hay JB, Chan JY. 1990. Primary structure of ovine tumor necrosis factor alpha cDNA. Nucleic Acids Res. 18:6723.

Zienolddiny S, Ryberg D, Maggini V, Skaug V, Canzian F, Haugen A. 2004. Polymorphisms of the interleukin-1 beta gene are associated with increased risk of non-small cell lung cancer. Int J Cancer. 109:353–356.

This paper was delivered at the 3rd International Conference on the Advances in Canine and Feline Genomics, School of Veterinary Medicine, University of California, Davis, CA, August 3–5, 2006.

Corresponding Editor: Steven Hannah

XII

A domain of the thyroid adenoma associated gene (*THADA*) conserved invertebrates becomes destroyed by chromosomal rearrangements observed in thyroid adenomas.

Drieschner N, Kerschling S, Soller JT, Rippe V, Belge G, Bullerdiek J, Nimzyk R.

Gene. 2007 Nov 15; 403(1-2): 110-7.

Eigenleistung:

- Sammlung der Proben, RNA-Isolierung
- cDNA Synthese

Available online at www.sciencedirect.com
ScienceDirect
Gene 403 (2007) 110–117
GENE
www.elsevier.com/locate/gene

A domain of the thyroid adenoma associated gene (*THADA*) conserved in vertebrates becomes destroyed by chromosomal rearrangements observed in thyroid adenomas

Norbert Drieschner [a], Svenja Kerschling [a], Jan T. Soller [a,b], Volkhard Rippe [a], Gazanfer Belge [a], Jörn Bullerdiek [a,*], Rolf Nimzyk [a]

[a] *Center for Human Genetics, University of Bremen, Leobenerstr./ZHG, D-28359 Bremen, Germany*
[b] *Small Animal Clinic, University of Veterinary Medicine, Bischofsholer Damm 15, D-30173 Hanover, Germany*

Received 16 May 2007; received in revised form 25 June 2007; accepted 25 June 2007
Available online 7 August 2007
Received by A. Bernardi

Abstract

THADA, mapping to chromosomal band 2p21 is target gene of specific chromosomal rearrangements observed in thyroid benign tumors. Thus, it is one of the most common gene targets in chromosomal rearrangements in benign epithelial tumors. Nevertheless, nothing is known about the function of its protein. Therefore, we have analyzed the genetic structure of *THADA* homologous genes in selected vertebrates (*Canis familiaris*, *Chlorocebus aethiops*, *Gallus gallus*, and *Mus musculus*), which are not characterized up to now. The coding sequences of the mRNA of these species have been sequenced and analyzed revealing similarities to ARM repeat structures which indicates an involvement in protein–protein interactions. Using multiple alignments we identified the most conserved part of the protein (aa 1033–1415 *Homo sapiens*) with an identity of 70.5% between the most different organisms implying a putative important functional domain. The truncations observed in human thyroid adenomas disrupt this conserved domain of the protein indicating a loss of function of THADA contributing to the development of the follicular neoplasias of the thyroid.

Keywords: THADA; ARM repeat; Chromosomal rearrangement; Adenoma; Thyroid; Conserved domain

1. Introduction

The thyroid adenoma associated gene (*THADA*) first has been described as the target gene of chromosomal 2p21 rearrangements in benign thyroid lesions (Rippe et al., 2003). For benign thyroid lesions including hyperplasias and follicular thyroid adenomas 2p21 rearrangements are beneath rearrangements of chromosomal region 19q13.4 and trisomy 7 the third frequent cytogenetic subgroup (Bondeson et al., 1989; Teyssier et al., 1990; Dal Cin et al., 1992; Belge et al., 1994, 1998; Bol et al., 1999). 3′-RACE analysis on two cell lines derived from benign thyroid lesions with 2p21-translocations revealed fusion genes involving *THADA* (*THADA-FUS3p* and *THADA-FUS7p*). The breakpoints of chromosomal band 2p21 in these cell lines are located within intron 28 of *THADA*. In both fusion genes *THADA* ends after exon 28 followed by ectopic non-coding sequences derived from the translocation partners (Rippe et al.,

Abbreviations: aa, amino acid(s); A, adenosine; BLAST, basic local alignment search tool; bp, base pair(s); CDD, conserved domain database; cDNA, DNA complementary to RNA; CDS, coding sequence(s); COG, cluster of orthologous groups of proteins; CV1, cell line deriving from fibroblasts of *Chlorocebus aethiops*; dNTP(s), deoxyribonucleoside triphosphate(s); EBI, European bioinformatics institute; FISH, fluorescence in situ hybridization; G, guanine; kb, kilo base(s); HMM, hidden Markov model; Mb, mega base(s); M-MLV, Moloney murine leukaemia virus; mRNA, messenger ribonucleic acid; NCBI, National Center for Biotechnology Information; NIH3T3, cell line deriving from embryonic fibroblasts of *Mus musculus*; PPARγ, Peroxisome proliferator-activated gene gamma; Probcons, Probabilistic Consistency-based Multiple Alignment of Amino Acid Sequences; RNA, ribonucleic acid; SCOP, Structural classification of proteins; T, thymidine; *THADA*, Thyroid adenoma associated gene; THADA-FUS3p, Thyroid adenoma associated fusion gene 3p; *THADA-FUS7p*, Thyroid adenoma associated fusion gene 7p; UTR, untranslated region(s).

* Corresponding author. Tel./fax: +49 421 218 4239.
E-mail address: bullerd@uni-bremen.de (J. Bullerdiek).

0378-1119/$ - see front matter © 2007 Elsevier B.V. All rights reserved.
doi:10.1016/j.gene.2007.06.029

2003). In *THADA-FUS3p* the ectopic sequences are derived from an intronic region of the *peroxisome proliferator-activated gene gamma* (*PPARγ*). A functional *THADA/PPARγ* fusion was excluded because the fused sequences were in reverse orientation to the genomic *PPARγ* orientation (Drieschner et al., 2006). It was thus concluded that the truncation of the gene rather than its fusion to coding sequences is the critical event in benign thyroid tumors with *THADA* rearrangements (Rippe et al., 2003; Drieschner et al., 2006).

As for the possible function of THADA there is only one databank entry indicating that THADA is involved in the death receptor pathway (Puduvalli VK and Ridgeway L, Gene Bank reference note). Accordingly, the truncation of THADA and its loss of the C-terminus may lead to an altered apoptosis induction facilitating the development and/or the proliferation of benign thyroid lesions (Rippe et al., 2003).

THADA has a genomic size of about 365 kb. So far, two transcript variants (GeneBank accession nos. NM_022065 and NM_198554) have been described. The cDNA of transcript variant 1 (NM_022065) contains 38 exons with a size of 6090 bp. Transcript variant 2 comprises 36 exons with a size of 5900 bp (GeneBank accession no. NM_198554). To date for other species (e.g. *Pan troglodytes*, *Mus musculus*, and *Rattus norvegicus*) only predicted cDNA and/or mRNA sequences are accessible from databases.

The ORF of transcript variant 1 of human *THADA* has a length of 5862 bp hypothetically coding for 1953 amino acids. There is so far no homology to other human proteins or domains described and only one uncharacterized conserved domain COG5543 (Cluster of Orthologous Groups NCBI (Tatusov et al., 2003)) has been found in databases.

In this work, the *THADA* cDNA sequences of four different species (*Canis familiaris*, *Chlorocebus aethiops*, *Gallus gallus*, and *M. musculus*) have been analyzed and the genomic structures of *THADA* have been described. Based on these results the mRNA sequences as well as the protein sequences of the different species were compared in order to identify similar regions and possible conserved domains.

2. Materials and methods

2.1. Tissue samples and cell lines

For RNA isolation fresh-frozen tissue samples of liver and myocardium (*G. gallus*) and of the testis (*C. familiaris*) were used. The tissue samples were obtained commercially (*G. gallus*) and from the Small Animal Clinic (University of Veterinary Medicine, Hanover, Germany) (*C. familiaris*), respectively. For *C. aethiops* a cell line (CV1) derived from fibroblasts of the kidney and for *M. musculus* a cell line (NIH3T3) derived from embryonic fibroblasts were used for RNA isolation.

2.2. Fluorescence in situ hybridization (FISH)

For analysis of chromosomal localisation of *THADA* in *C. aethiops* fluorescence in situ hybridization on the cell line CV1 was performed. Cell culture of the cell line and karyotyping of Giemsa-banded metaphases were performed as previously described for pleomorphic adenomas of the parotid gland (Bullerdiek et al., 1987). For FISH analyses human BAC clones (RP11-1069E24 (GeneBank accession nos. AQ694385 and AQ703756) and RP11-183F15 (GeneBank accession no. AC092838)) (RZPD, Heidelberg, Germany) located within human *THADA* were used. FISH analyses were performed after GTG banding of the same metaphase spreads. Treatment of metaphases and subsequent FISH experiments were performed as described previously (Kievits et al., 1990). For FISH studies, BAC DNA was labeled with dig-11-dUTP by nick translation (Roche Diagnostics, Mannheim, Germany). For FISH experiments the labeled BAC DNA was pooled (concentration: 3 ng/µl). Post-hybridization was performed at 42 °C in 0.1× SSC for 5 min. Detection was performed with anti-dig-fluorescein fab-fragments (Roche Diagnostics, Mannheim, Germany). Chromosomes were counterstained with DAPI (0.025 mg/ml). For the cell line CV1, 10 metaphases were examined. Slides were analyzed on a Zeiss Axiophot fluorescence microscope using an FITC and DAPI filter set. Metaphases were recorded with the Power Gene Karyotyping System (Applied Imaging, Newcastle, UK).

2.3. RNA isolation and cDNA synthesis

The RNeasy Mini Kit (QIAGEN, Hilden, Germany) was used for the extraction and purification of total RNA from the fresh–frozen tissue samples (*G. gallus* and *C. familiaris*). Prior to the RNA isolation the tissue samples were homogenized with a tissue lyser (QIAGEN, Hilden, Germany). Total RNA was isolated from the cell lines (CV1 and NIH3T3) using the Trizol reagent (Invitrogen, Karlsruhe, Germany).

cDNA synthesis was performed with 5 µg total RNA using the M-MLV reverse transcriptase (Invitrogen, Karlsruhe, Germany).

2.4. Oligonucleotides and RT-PCR

Primers were designed using Lasergene primer select (DNAStar) and Vector NTI (Invitrogen). Up to nine PCR primer pairs were selected covering the whole CDS of the predicted *THADA* cDNA sequence of each organism. The fragment lengths of the primer pairs varied between 200 bp and 1800 bp. RT-PCR was performed with the Taq-DNA Polymerase (Invitrogen, Karlsruhe, Germany). Optimal annealing temperatures were detected by gradient RT-PCR (55 °C–65 °C) with a Mastercycler Gradient (Eppendorf, Hamburg, Germany) for each primer pair and organism. 1 µl of cDNA was used as template in a total reaction volume of 50 µl containing 0.2 mM of each primer, the reaction buffer supplied by manufacturer (Invitrogen, Karlsruhe, Germany), 0.2 mM dNTPs, 1.5 mM $MgCl_2$, and 2.5 U Taq DNA polymerase (Invitrogen, Karlsruhe, Germany). After 3 min initial denaturation at 95 °C 35 cycles of 60 s at 95 °C, 90 s at optimized annealing temperature (55 °C–65 °C) and 60 s at 72 °C followed by a final extension at 72 °C for 10 min. were performed in a Mastercylcer Gradient (Eppendorf, Hamburg, Germany).

2.5. Purification and determination of yield of RT-PCR products

RT-PCR fragments were isolated and purified with the Gel Extraction Kit (QIAGEN, Hilden, Germany). Quantification of the purified DNA was done by dot blot. A dilution series of the purified DNA was dotted on an agarose gel (1%) and stained with ethidiumbromide. The concentration was estimated by comparing the intensities of the dots of the purified DNA and a standardized dilution series of the 1 kb Plus DNA ladder (Invitrogen, Karlsruhe, Germany).

2.6. Determination of gene sequences

The sequence analysis of the mRNA and chromosomal assignment of the human *THADA* gene have been described previously (Rippe et al., 2003). According to the human *THADA* gene sequence the genomic structures of the homolog *THADA* genes in the examined organisms have been predicted aligning the human *THADA* sequence (GeneBank accession nos. NM_022065 and NP_071348) with the available genomic sequences (*C. familiaris*, *G. gallus*, and *M. musculus*). For this purpose Spidey (Lander et al., 2001), BLAST (Altschul et al., 1997), and Perl (www.perl.org) with Bioperl Modules (Stajich et al., 2002) have been used for sequence assembly and identification of splicing sites. If no similarities were detectable or splice sites have been missed manual corrections have been done. For all species described mRNA sequences have been included in the analyses.

20 ng/100 bp of purified DNA was used for DNA sequencing (MWG Biotech, Ebersberg, Germany). Each PCR fragment was sequenced in both directions using the corresponding PCR-primers. The sequencing chromatograms were corrected manually using the ChomasLite software (http://www.technelysium.com.au/). Clustering of the sequences has been done with the help of the Vector NTI Software ContigExpress (Vector NTI, Invitrogen).

2.7. Bioinformatics

The genomic organisation of the different *THADA* genes were determined by aligning the cDNA sequences with the available genomic sequences using Spidey with the option to use large intron sizes (Lander et al., 2001). Comparative interspecies sequence alignments were performed by the European Bioinformatics Institute (EBI) online tool, clustalw (http://www.ebi.ac.uk/clustalw/) (Higgins, 1994), PROBCONS (http://probcons.stanford.edu/), and AlignX (Vector NTI, Invitrogen). Protein pattern, profiles, and motives have been searched using the EBI tool InterProScan an integrated documentation resource for protein families, domains, and sites (http://www.ebi.ac.uk/) and HHpred using Homology detection by Hidden Markov Model — Hidden Markov Model comparison (http://toolkit.tuebingen.mpg.de/).

3. Results

3.1. Gene prediction and primer design

For primer design the *THADA* genes or *THADA* homologous sequences, respectively, of the analyzed organisms (*C. familiaris*, *C. aethiops*, *G. gallus*, and *M. musculus*) have been determined with bioinformatic tools. The human *THADA* mRNA and amino acid sequences (GeneBank accession nos. NM_022065, NP_071348) were split into sequences corresponding to single exons of the human gene. The conserved sequences AG and GT indicating the splice sites have been added to the nucleotide sequences. For alignments with the mouse, dog, and chicken genomic sequences in which the *THADA* genes have been detected (GenBank accession nos. NT_039649, NW_876251, NW_001471679) bl2seq blastn and tblastn programs have been used (Tatusova and Madden, 1999)). Perl and Bioperl Modules (Stajich et al., 2002) in combination with the program BLAST (Altschul et al., 1997) and Spidey have been used for sequence assembly and identification of splicing sites. The predicted sequences which were nearly identical to the later determined sequences (data not shown) served as template for the primer design. For the analysis of the African green monkey human *THADA* specific primers have been used. The primer pairs were constructed spanning 200 to 1800 bp and the produced PCR products were overlapping for optimal sequencing and contig building.

3.2. Genomic organisation of the THADA homologous genes from C. familiaris, C. aethiops, G. gallus, and M. musculus

The predicted mRNA sequences from *C. familiaris*, *G. gallus*, and *M. musculus* have been used for primer design. Therefore, the lengths of the deduced mRNA sequences and the

Table 1
Genomic, mRNA and protein sequence organisation of the THADA genes from *Canis familiaris*, *Chlorocebus aethiops*, *Gallus gallus*, *Homo sapiens* and *Mus musculus*

	Homo sapiens	*Mus musculus*	*Canis familiaris*	*Chlorocebus aethiops* [a]	*Gallus gallus*
Chromosome	2	17	10	14	3
Genomic length	365186 bp	274170 bp	326318 bp	–	152400 bp [b]
Number of exons	38	38	38	–	38
Sequenced mRNA	6.090 bp	5.914 bp	5.976 bp	5.899 bp	6.501 bp
Open reading frame	5.862 bp	5.817 bp	5.847 bp	5.862 bp	5.793 bp
Protein length	1.954 aa	1.939 aa	1.949 aa	1.954 aa	1.931 aa

[a] Genomic sequences of *Chlorocebus aethiops* not available.
[b] The genomic contig (GeneBank accession no. NW_001471679) of *Gallus gallus* chromosome 3 contains parts in this region which are not fully determined. This result should be treated as preliminary.

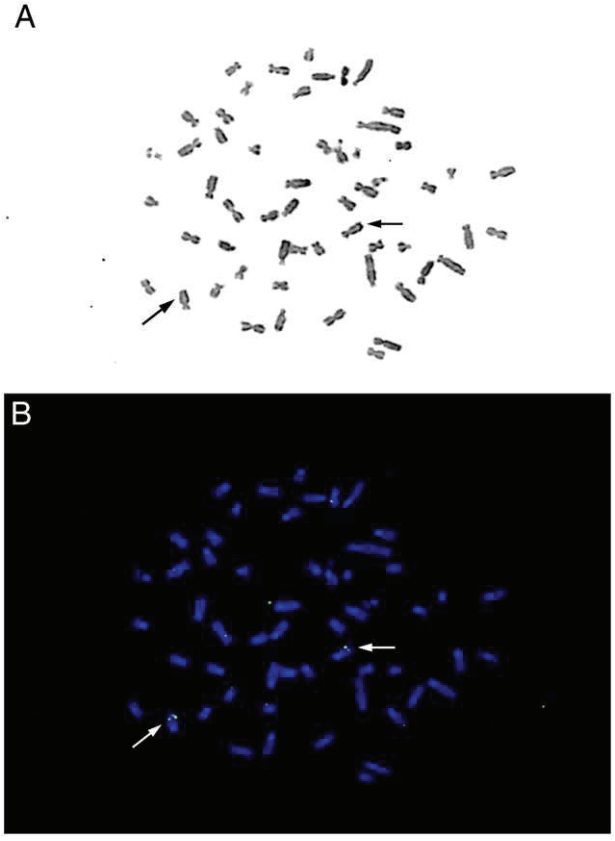

Fig. 1. Chromosomal localisation of *THADA* in *Chlorocebus aethiops*. A metaphase of the cell line CV1 after GTG banding (A) and the same metaphase after FISH with human *THADA* BAC clones (B). Arrows indicating signals on the long arms of both chromosomes 14 of *Chlorocebus aethiops*.

corresponding genomic regions depend on this design. Parts of the 5′ and 3′ untranslated regions have not been determined. Nevertheless, in all cases the predicted coding regions have been sequenced including ATG translational initiation codons and stop codons. The mRNA sequences of the analyzed organisms (Table 1) were submitted to GenBank (Benson et al., 2006) under accession numbers EF222204 (*C. familiaris*), EF222205 (*C. aethiops*), F222206 (*G. gallus*), and EF222207 (*M. musculus*). The genomic size of *THADA* in human is 365.186 bp. The *THADA* homologous sequences of the organisms analyzed herein are spanning shorter genomic regions compared to the human *THADA* gene (Table 1). For *C. aethiops* no genomic sequences of the corresponding region are available. Fluorescence in situ hybridization (FISH) analysis with human BAC clones containing *THADA* confirms the localisation on the long arm of *C. aethiops* chromosome 14 (Fig. 1).

3.3. Identification and characterization of the open reading frame

All deduced mRNA sequences of *THADA* from *C. familiaris*, *C. aethiops*, *G. gallus*, and *M. musculus* are containing only one reasonable open reading frame (Table 1). To determine the position of the start codon a sequence analysis of a 100 bp region containing the putative start codon has been performed by multiple alignments of the *C. familiaris*, *G. gallus*, *Homo sapiens*, and *M. musculus* mRNAs. The overall nucleotide similarity calculated by an AlignX (Invitrogen) multiple alignment is 13.7% upstream the predicted start codon and 58.8% within the first 50 bp of the coding region indicating the translation start at this ATG. Furthermore a Kozak sequence is strongly indicating the translation start. The most important positions at position −3 (A) and position +4 (G) (Kozak, 2002) with respect to the predicted translation initiation codon ATG were found to be conserved in all analyzed organisms.

The physical properties of the deduced proteins resemble the human THADA. The lengths of the proteins range between 1930 aa (*G. gallus*) and 1953 aa (*C. aethiops*) which is the same as in humans (Table 1). Thus, the molecular weight is between 216,601 Da (*G. gallus*) and 219,595 Da (*Homo sapiens*), respectively.

3.4. Sequence comparison

Using PROBCONS (Do et al., 2005) for the alignment and AlignX (Vector NTI, Invitrogen) for calculation of the similarity the determined mRNA and protein sequences have been aligned and the similarity has been calculated. The similarities between the human THADA and the THADA proteins of the other organisms correspond to the evolutionary relationship between these organisms. The African green monkey as the nearest relative has the highest similarity to the human (97.1% nucleotide similarity of the coding region and 95.9% amino acid similarity). The chicken as the only non-mammalian organism has the lowest similarity, i.e. 64.7% nucleotide similarity of the coding region and 64.9% amino acid similarity (Table 2).

3.5. Identification of conserved domains

The predicted THADA protein sequences from *C. familiaris*, *C. aethiops*, *G. gallus*, *M. musculus*, and the human sequence have been aligned with PROBCONS (Do et al., 2005) in a multiple sequence alignment. For visualisation of the similarity and identification of conserved regions a similarity plot has been calculated (AlignX similarity plot) (Fig. 2). The region with the highest similarity is found from position 1043–1425 in the

Table 2
Similarity comparison of the open reading frame and deduced protein sequences from *Canis familiaris*, *Chlorocebus aethiops, Gallus gallus,* and *Mus musculus* (GeneBank accession nos. ABQ10598, ABQ10599, ABQ10600, and ABQ10601) to the human mRNA transcript of THADA (GeneBank accession no. NM_022065) and the human THADA protein (GeneBank accession no. NP_071348)

Organism	Similarity to THADA *Homo sapiens*	
	ORF/CDS (%)	Protein (%)
Chlorocebus aethiops	97.1	95.9
Canis familiaris	86.7	83.1
Mus musculus	81.1	78.2
Gallus gallus	64.7	57.2

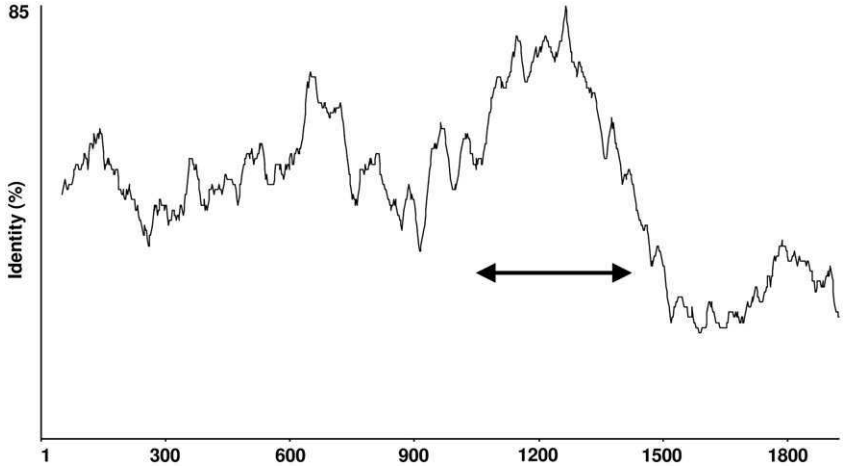

Fig. 2. Similarity plot of the THADA protein from *Canis familiaris*, *Chlorocebus aethiops*, *Gallus gallus*, *Homo sapiens*, and *Mus musculus*. For the sake of visualisation clarity only identical positions in all organisms are included. A window size of 100 aa has been used, therefore the first and last positions are not shown. The most conserved part, position 1043–1425, is marked by an arrow.

multiple alignment corresponding to region 1033–1415 in humans with an identity calculation of 70.4% and the similarity including conserved amino acid changes being 78.6%. The overall similarity of the THADA proteins is calculated to 48.6% identical amino acids and including conserved amino acid changes to 60.9%. Another shorter segment (position 586–705 in humans) is highly similar, 72.5% identity and 78.3% similarity including conserved amino acid substitutions. The lowest similarity is seen in the carboxy terminal part of the protein from position 1491 to 1953 in humans with 27.5% identical positions and 41.9% if conserved substitutions are included.

3.6. Domain and motif assignment

The deduced THADA protein sequences were compared with different domain and motif databases by the help of EBI InterProScan tool and NCBI Conserved Domain Database (CDD) to gather more information regarding the function of THADA. The conserved domain search of the NCBI CDD yields one domain with the identifier COG5543 (COG = Clusters of orthologous groups of proteins). The COG5543 is a cluster of 3 hypothetical proteins from different fungi (GeneBank accession nos. NP_588532, NP_597091, Q03496)

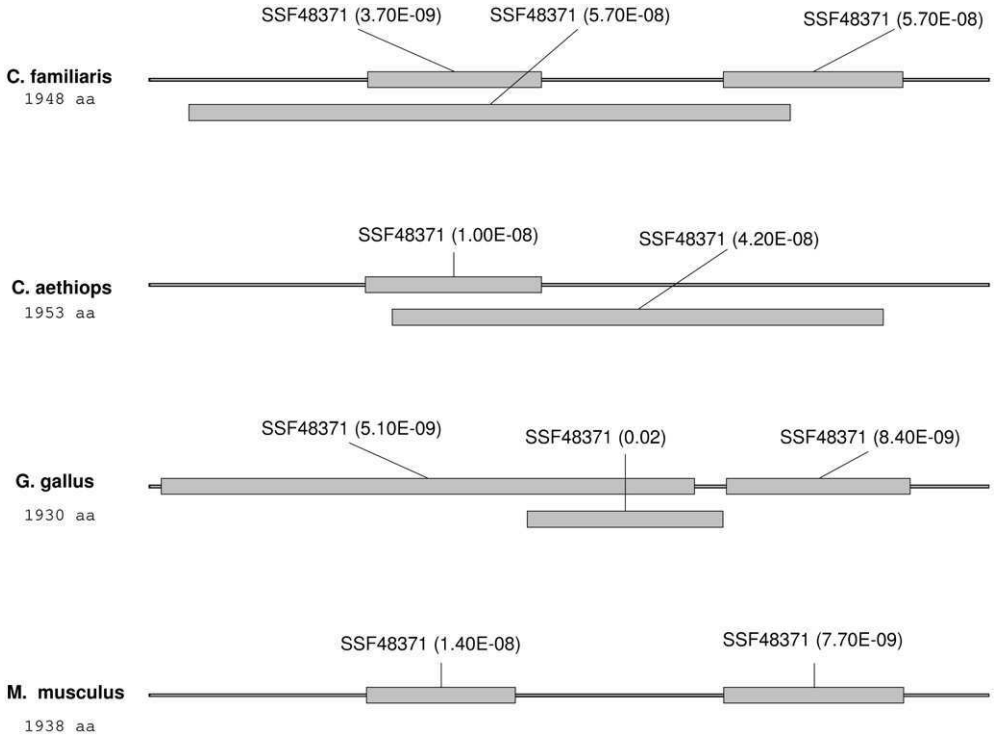

Fig. 3. Similarities to the superfamily of ARM repeat structures (SSF48371) detected in the THADA protein from *Canis familiaris*, *Chlorocebus aethiops*, *Gallus gallus* and *Mus musculus*.

without functional assignment. This conserved multi domain cluster COG5543 has a length of 1400 aa. The alignment to the conserved cluster is localised in the most conserved region of the protein (see Identification of conserved domains) from approx. aa 1025 to aa 1425 in the different THADA proteins with an expect value around 2e−40. In mouse and chicken another part of the THADA protein shows similarities to this cluster with a lower significance (mouse THADA pos 394–902, e-value 0.00002 and chicken THADA position 396–837, e-value 0.00009).

The InterProScan reveals in the THADA proteins from all analyzed organisms significant assignments to the superfamily ARM repeat (SSF48371) of the Superfamily database of profile Hidden Markov Models (HMMs) (Gough et al., 2001) (Fig. 3). The Superfamily database is based of the SCOP (Structural Classification of Proteins) database which provides a description of structural and evolutionary relationships of proteins with known structure (Murzin et al., 1995). The ARM repeat superfamily summarizes different right-handed superhelices of helices like Armadillo repeat, HEAT repeat, and clathrin associated domains. Similarities with low significance (e-value from 17 to 0.055) to HEAT domains have been found repeatedly, from 5 in the human, dog, and green monkey to 8 in the chicken THADA using the Pfam database (Finn et al., 2006) (data not shown).

The HHpred server of the Max Planck Institute for Developmental Biology for remote protein homology detection and structure prediction has been used for aligning the previously described PROBSCON multiple alignment of THADA from *C. familiaris*, *C. aethiops*, *G. gallus*, *Homo sapiens*, and *M. musculus* with Hidden Markov Models from different databases of protein domains like InterPro, SCOP, Superfamily and COG. The HHpred software is an implementation of pair wise comparisons of profile Hidden Markov Models (HMM) (Soding et al., 2005). The HMM of the COG5543 cluster found with a PSI-BLAST in the CDD Database "aligns" using the HHpred software with an e-value of 0 to the HMM of the THADA multiple alignment (position 394–1749). If the Superfamily database was used in the HHpred scan different models of the superfamily ARM repeat SSF48371 aligning with lower significance (e-values 16–8600) to the multiple alignment of THADA (position 35–1756). Using HMMs calculated by HHpred from entries of the Protein Data Bank (PDB) (Berman et al., 2000) and the SCOP database the best matches to THADA are CAND1 (e-value 0.00025) and different importin proteins (e-value 0.11–10). CAND1 and importins are proteins containing ARM repeat related structures.

4. Discussion

The human *THADA* gene is the target gene of rearrangements involving chromosomal region 2p21 in thyroid neoplasias (Rippe et al., 2003). These rearrangements constitute one of the most frequent specific chromosomal rearrangements in human epithelial tumors at all and lead to fusion genes in which the 3′ part of *THADA* is truncated. Up to now there is no further information regarding the function of the protein and the possible molecular background of the cell transformation resulting from that chromosomal rearrangement (Rippe et al., 2003). Hypothetically the truncated form of the protein may lead to an altered apoptosis induction due to the possible involvement in the death receptor pathway (Rippe et al., 2003). In the present study the orthologeous *THADA* mRNA sequences of the vertebrates *C. familiaris*, *C. aethiops*, *G. gallus*, and *M. musculus* have been determined and characterized to gather more information regarding the function of the *THADA* gene and its role in the development of human thyroid neoplasias.

The size of the mRNA, the protein size, and the genomic organisation of *THADA* is conserved among humans and the other species analyzed. Furthermore the genomic organisation of *THADA* in all analyzed organisms is very similar to the genomic organisation of the *THADA* gene in humans. All homologous *THADA* genes have the same number of 38 exons corresponding to the genomic organisation of the human *THADA* gene (Table 1). The start codons are localised always in the second exon and the stop codon in the last exon. With the exception of exons 1, 2, and 38 containing the 5′ and 3′ untranslated regions all exons have a very similar size and 23 exons are even identical in length. All exon/intron boundaries are conforming to the AG/GT rule for acceptor and donor of splicing sites (Madhani and Guthrie, 1994). Thus, the different genomic sizes of *THADA* in the analyzed organisms are due to distinct length of the intronic sequences. The chromosomal expansion of the genes (*Homo sapiens* 365186 bp, *C. familiaris* 326318 bp, *M. musculus* 274,170 bp, and *G. gallus* approx. 152,400 bp) corresponds roughly – with the exception of mouse and dog, which differ in length only slightly – to the total length of the genome of the analyzed organisms (3000 Mb in humans, 2400 Mb in the dog, 2500 Mb in the mouse, and 1200 Mb in the chicken; estimated genome lengths according to NCBI genome database). This observation is in accordance to the general findings by (Deutsch and Long, 1999) that the lengths of the introns correspond with the size of the whole genome.

Neither the structures nor the sequences of the deduced proteins of THADA were confirmed with biochemical techniques. This study was aimed at the characterization of the coding region and the determination of the start codon for further expression studies. The longest putative open reading frames have been predicted as coding regions. Similarity in length (>1930 aa in all analyzed organisms) and sequence make this assumption highly reasonable. The first ATG translational initiation codon of the open reading frame is seen as start codon. The analysis of the region surrounding the predicted start position revealed a high similarity of the sequence beginning with the position −3 (A) in all organisms whereas the 5′ untranslated region is showing less similarity. This is in concordance with the observation that sequences of 5′-UTRs as well as 3′-UTRs are less conserved compared to coding regions (Pesole et al., 2000). Furthermore, the positions at −3 (A) and +4 (G) to the predicted ATG translation initiation codon meet the criteria for a Kozak sequence (Kozak, 2002). Thus, it is highly probable that this ATG codon is the initial start codon for protein synthesis.

The protein size of all analyzed organisms lies in between 1931 aa (*G. gallus*) and 1954 aa (*C. aethiops* and *Homo sapiens*). Interestingly only 5% (513) of 24,264 annotated human proteins (NCBI RefSeq database; (Pruitt et al., 2005)) exceed the human THADA size.

The multiple alignment of the THADA protein sequences serves to identify conserved domains in THADA. In the region from approximately 1033–1415 aa in human THADA the sequence similarity in the PROBCONS multiple alignment shows the highest regional similarity with an identity calculation of 70.5% and including conserved amino acid substitutions of 78.6%. Furthermore, there are two parts within this region with a size of 21 aa and 23 aa that are identical in all species analyzed. In the same region similarities to the uncharacterized conserved domain COG5543 of the NCBI Conserved Domain Database have been detected. This conserved part of the protein could be a functional important region of THADA as conserved domains correspond in most cases to functional regions (Bornberg-Bauer et al., 2005).

Interestingly, the truncation at the position 1352 of THADA observed in the previously described fusion genes in human benign thyroid lesions (Rippe et al., 2003) is located in the middle of the conserved part of THADA. Thus, it seems that this part harbours a domain with important function and in thyroid adenomas this function is destroyed. Also, it cannot be excluded that the c-terminal part of THADA beginning with position 1491 in humans showing the lowest similarity of 27.5% identity could have structural important functions and maybe the truncation results in an overall rearrangement of the protein.

The similarities to the superfamily domain ARM repeat (SSF48371) a domain of the Superfamily database (Gough et al., 2001) and the HHpred alignments (Soding et al., 2005), which are used for more remote homology detection, are helpful to gather more information regarding the function of THADA. The Superfamily database is based of the SCOP (Structural Classification of Proteins) database and superfamilies are families of proteins, that have low sequence identities but whose structures and, in many cases, functional features suggest that they have a common evolutionary origin (Murzin et al., 1995). The superfamily ARM repeat summarizes repeated domains like Armadillo repeats and HEAT repeats which contain tandem copies of a degenerate protein sequence motif that forms right-handed superhelices of helices. This repeated structure creates a surface for protein–protein interaction (Coates, 2003). The HEAT domains are detected repeatedly with low significance in the human THADA and as well as in the predicted THADA homologous proteins herein analyzed. The ARM repeats like the here mentioned Armadillo repeat and HEAT repeat are difficult to detect because of low constraints of sequence conservation (Andrade et al., 2001). Armadillo repeats were found among others in plakoglobin, β-cathenin, the nuclear import factor α-importin, and the tumor suppressor adenomatous polyposis coli (Andrade et al., 2001). HEAT domains are present in importins β1, β2, and proteins related to the clathrin-associated adaptor complex. Members of these proteins are also detected in the HHpred scan. The best alignment is to CAND1/TIP120 cullin-associated neddylation-dissociated protein 1. This protein is binding to cullin-RING-ligases, which regulate diverse cellular functions such as cell cycle progression and cytokine signalling by ubiquitinating key regulatory proteins (Min et al., 2005). With lower significance similarities to importins which are involved in the protein transport through nuclear pore complexes are found. All proteins with similarities to THADA share the ARM repeats which are involved in protein–protein interactions. The Gene Ontology (Ashburner et al., 2000) term "protein binding (GO:0005515)" commonly refer to different protein binding activities like, among others, the death receptor activities.

With these new findings, similarities to protein–protein binding proteins with receptor activities and the possible structure with ARM repeats, the conserved and expressed in *Homo sapiens*, *C. familiaris*, *C. aethiops*, *G. gallus*, and *M. musculus* THADA appears to be involved in protein binding activity as e.g. found in proteins belonging to the death receptor pathway. This, indicating a function as receptor with protein–protein interaction, corroborates our theory of THADA involvement in the death receptor pathway. In thyroid adenomas with 2p21 rearrangements (Rippe et al., 2003) the truncation results in a disruption of the most conserved part of the protein which seems to be a functional important domain.

References

Altschul, S.F., Madden, T.L., Schaffer, A.A., Zhang, J., Zhang, Z., Miller, W., Lipman, D.J., 1997. Gapped BLAST and PSI-BLAST: a new generation of protein database search programs. Nucleic Acids Res. 25, 3389–3402.

Andrade, M.A., Perez-Iratxeta, C., Ponting, C.P., 2001. Protein repeats: structures, functions, and evolution. J. Struct. Biol. 134, 117–131.

Ashburner, M., et al., 2000. Gene ontology: tool for the unification of biology. The gene ontology consortium. Nat. Genet. 25, 25–29.

Belge, G., Thode, B., Rippe, V., Bartnitzke, S., Bullerdiek, J., 1994. A characteristic sequence of trisomies starting with trisomy 7 in benign thyroid tumors. Hum. Genet. 94, 198–202.

Belge, G., Roque, L., Soares, J., Bruckmann, S., Thode, B., Fonseca, E., Clode, A., Bartnitzke, S., Castedo, S., Bullerdiek, J., 1998. Cytogenetic investigations of 340 thyroid hyperplasias and adenomas revealing correlations between cytogenetic findings and histology. Cancer Genet. Cytogenet. 101, 42–48.

Benson, D.A., Karsch-Mizrachi, I., Lipman, D.J., Ostell, J., Wheeler, D.L., 2006. GenBank. Nucleic Acids Res. 34, D16–D20.

Berman, H.M., Westbrook, J., Feng, Z., Gilliland, G., Bhat, T.N., Weissig, H., Shindyalov, I.N., Bourne, P.E., 2000. The protein data bank. Nucleic Acids Res. 28, 235–242.

Bol, S., Belge, G., Thode, B., Bartnitzke, S., Bullerdiek, J., 1999. Structural abnormalities of chromosome 2 in benign thyroid tumors. Three new cases and review of the literature. Cancer Genet. Cytogenet. 114, 75–77.

Bondeson, L., Bengtsson, A., Bondeson, A.G., Dahlenfors, R., Grimelius, L., Wedell, B., Mark, J., 1989. Chromosome studies in thyroid neoplasia. Cancer 64, 680–685.

Bornberg-Bauer, E., Beaussart, F., Kummerfeld, S.K., Teichmann, S.A., Weiner 3rd, J., 2005. The evolution of domain arrangements in proteins and interaction networks. Cell. Mol. Life Sci. 62, 435–445.

Bullerdiek, J., Boschen, C., Bartnitzke, S., 1987. Aberrations of chromosome 8 in mixed salivary gland tumors—cytogenetic findings on seven cases. Cancer Genet. Cytogenet. 24, 205–212.

Coates, J.C., 2003. Armadillo repeat proteins: beyond the animal kingdom. Trends Cell Biol. 13, 463–471.

Dal Cin, P., Sneyers, W., Aly, M.S., Segers, A., Ostijn, F., Van Damme, B., Van Den Berghe, H., 1992. Involvement of 19q13 in follicular thyroid adenoma. Cancer Genet. Cytogenet. 60, 99–101.

Deutsch, M., Long, M., 1999. Intron–exon structures of eukaryotic model organisms. Nucleic Acids Res. 27, 3219–3228.

Do, C.B., Mahabhashyam, M.S., Brudno, M., Batzoglou, S., 2005. ProbCons: probabilistic consistency-based multiple sequence alignment. Genome Res. 15, 330–340.

Drieschner, N., Belge, G., Rippe, V., Meiboom, M., Loeschke, S., Bullerdiek, J., 2006. Evidence for a 3p25 breakpoint hot spot region in thyroid tumors of follicular origin. Thyroid 16, 1091–1096.

Finn, R.D., Mistry, J., Schuster-Bockler, B., Griffiths-Jones, S., Hollich, V., Lassmann, T., Moxon, S., Marshall, M., Khanna, A., Durbin, R., Eddy, S.R., Sonnhammer, E.L., Bateman, A., 2006. Pfam: clans, web tools and services. Nucleic Acids Res. 34, D247–D251.

Gough, J., Karplus, K., Hughey, R., Chothia, C., 2001. Assignment of homology to genome sequences using a library of hidden Markov models that represent all proteins of known structure. J. Mol. Biol. 313, 903–919.

Higgins, D.G., 1994. CLUSTAL V: multiple alignment of DNA and protein sequences. Methods Mol. Biol. 25, 307–318.

Kievits, T., Dauwerse, J.G., Wiegant, J., Devilee, P., Breuning, M.H., Cornelisse, C.J., van Ommen, G.J., Pearson, P.L., 1990. Rapid subchromosomal localization of cosmids by nonradioactive in situ hybridization. Cytogenet. Cell Genet. 53, 134–136.

Kozak, M., 2002. Pushing the limits of the scanning mechanism for initiation of translation. Gene 299, 1–34.

Lander, E.S., et al., 2001. Initial sequencing and analysis of the human genome. Nature 409, 860–921.

Madhani, H.D., Guthrie, C., 1994. Dynamic RNA–RNA interactions in the spliceosome. Annu. Rev. Genet. 28, 1–26.

Min, K.W., Kwon, M.J., Park, H.S., Park, Y., Yoon, S.K., Yoon, J.B., 2005. CAND1 enhances deneddylation of CUL1 by COP9 signalosome. Biochem. Biophys. Res. Commun. 334, 867–874.

Murzin, A.G., Brenner, S.E., Hubbard, T., Chothia, C., 1995. SCOP: a structural classification of proteins database for the investigation of sequences and structures. J. Mol. Biol. 247, 536–540.

Pesole, G., Grillo, G., Larizza, A., Liuni, S., 2000. The untranslated regions of eukaryotic mRNAs: structure, function, evolution and bioinformatic tools for their analysis. Brief. Bioinform. 1, 236–249.

Pruitt, K.D., Tatusova, T., Maglott, D.R., 2005. NCBI Reference Sequence (RefSeq): a curated non-redundant sequence database of genomes, transcripts and proteins. Nucleic Acids Res. 33, D501–D504.

Rippe, V., Drieschner, N., Meiboom, M., Escobar, H.M., Bonk, U., Belge, G., Bullerdiek, J., 2003. Identification of a gene rearranged by 2p21 aberrations in thyroid adenomas. Oncogene 22, 6111–6114.

Soding, J., Biegert, A., Lupas, A.N., 2005. The HHpred interactive server for protein homology detection and structure prediction. Nucleic Acids Res. 33, W244–W248.

Stajich, J.E., et al., 2002. The Bioperl toolkit: Perl modules for the life sciences. Genome Res. 12, 1611–1618.

Tatusov, R.L., et al., 2003. The COG database: an updated version includes eukaryotes. BMC Bioinformatics 4, 41.

Tatusova, T.A., Madden, T.L., 1999. BLAST 2 Sequences, a new tool for comparing protein and nucleotide sequences. FEMS Microbiol Lett 174, 247–250.

Teyssier, J.R., Liautaud-Roger, F., Ferre, D., Patey, M., Dufer, J., 1990. Chromosomal changes in thyroid tumors. Relation with DNA content, karyotypic features, and clinical data. Cancer Genet. Cytogenet. 50, 249–263.

XIII

Chromosomal assignment of canine *THADA* gene to CFA 10q25.

Soller JT, Beuing C, Murua Escobar H, Winkler S, Reimann-Berg N, Drieschner N, Dolf G, Schelling C, Nolte I, Bullerdiek J.

Mol Cytogenet. 2008 Jun 3; 1(1): 11.

Eigenleistung:

- Koordinierung und Planung aller Arbeiten
- Etablierung der PCRs für das BAC Screening, *in silico* Analysen
- Verfassen des Manuskripts mit C. Beuing und J. Bullerdiek

Molecular Cytogenetics

BioMed Central

Short report

Open Access

Chromosomal assignment of canine *THADA* gene to CFA 10q25

Jan T Soller[†1,2], Claudia Beuing[†2], Hugo Murua Escobar*[1,2], Susanne Winkler[1], Nicola Reimann-Berg[1], Norbert Drieschner[1], Gaudenz Dolf[3], Claude Schelling[4], Ingo Nolte[2] and Jörn Bullerdiek[1,2]

Address: [1]Centre for Human Genetics, University of Bremen, Leobener Straße ZHG, 28359 Bremen, Germany, [2]Small Animal Clinic and Research Cluster of Excellence "REBIRTH", University of Veterinary Medicine Hanover, Bischofsholer Damm 15, 30173 Hannover, Germany, [3]Institute of Genetics, Vetsuisse Faculty, University of Berne, Bremgartenstrasse 109a, PO Box 8466, 3001 Bern, Switzerland and [4]Department of Animal Science, Swiss Federal Institute of Technology Zurich, Vetsuisse-Faculty Zurich, University of Zurich, Winterthurerstrasse 204, 8057 Zürich, Switzerland

Email: Jan T Soller - soller@uni-bremen.de; Claudia Beuing - claudia.beuing@tiho-hannover.de; Hugo Murua Escobar* - escobar@uni-bremen.de; Susanne Winkler - winklers@uni-bremen.de; Nicola Reimann-Berg - nicola.reimann-berg@uni-bremen.de; Norbert Drieschner - norbert.drieschner@uni-bremen.de; Gaudenz Dolf - dolf.gaudenz@itz.unibe.ch; Claude Schelling - claude.schelling@inw.agrl.ethz.ch; Ingo Nolte - inolte@klt.tiho-hannover.de; Jörn Bullerdiek - bullerd@uni-bremen.de

* Corresponding author †Equal contributors

Published: 3 June 2008

Molecular Cytogenetics 2008, **1**:11 doi:10.1186/1755-8166-1-11

Received: 13 March 2008
Accepted: 3 June 2008

This article is available from: http://www.molecularcytogenetics.org/content/1/1/11

Abstract

Background: Chromosomal translocations affecting the chromosome 2p21 cluster in a 450 kb breakpoint region are frequently observed in human benign thyroid adenomas. *THADA* (thyroid adenoma associated) was identified as the affected gene within this breakpoint region. In contrast to man tumours of the thyroid gland of dogs (*Canis lupus familiaris*) constitute mainly as follicular cell carcinomas, with malignant thyroid tumours being more frequent than benign thyroid adenomas. In order to elucidate if the *THADA* gene is also a target of chromosomal rearrangements in thyroid adenomas of the dog we have physically mapped the canine *THADA* gene to canine chromosome 10.

A PCR was established to screen a canine genome library for a BAC clone containing the gene sequence of canine *THADA*. Further PCR reactions were done using the identified BAC clone as a template in order to verify the corresponding PCR product by sequencing.

Canine whole blood was incubated with colcemid in order to arrest the cultured cells in metaphases. The verified BAC DNA was digoxigenin labeled and used as a probe in fluorescence *in situ* hybridization (FISH). Ten well spread metaphases were examined indicating a signal on canine chromosome 10 on both chromatids. A detailed fine mapping was performed indicating the canine *THADA* gene locus on the q-arm of chromosome 10.

Results: The canine *THADA* gene locus was mapped on chromosome 10q25. Our mapping results obtained in this study following the previously described nomenclature for the canine karyotype.

Conclusion: We analysed whether the *THADA* gene locus is a hotspot of canine chromosomal rearrangements in canine neoplastic lesions of the thyroid and in addition might play a role as a candidate gene for a possible malignant transformation of canine thyroid adenomas. Although the available cytogenetic data of canine thyroid adenomas are still insufficient the chromosomal region to which the canine *THADA* has been mapped seems to be no hotspot of chromosomal aberrations seen in canine thyroid adenomas.

Background

In human thyroid adenomas chromosomal translocations involving the regions 19q13 and 2p21 have frequently been described [1,2]. Chromosomal aberrations showing 2p21 rearrangements belong to the most common abnormalities in benign epithelial tumours with an observed frequency of 10% [3]. Recently, a gene named *THADA* (thyroid adenoma associated) [GenBank: NM_022065] which is directly affected by this cytogenetic rearrangement, could be identified within the 2p21 breakpoint region [3].

In terms of animal cancer models, the dog has lately been attracting significant interest due to the fact that the malignancies of humans and dogs show various similarities [4]. Among the striking arguments for the dog as an animal model for man are spontaneous appearance of the tumours, comparable histological variance, similar cancer types and similar biological behaviour of the observed neoplasias, including metastasis [5-7].

In man the majority of tumours affecting the thyroid gland are benign, whereas in dogs the situation is quite different. Thyroid carcinomas are rare in the human population, the overall incidence is <1% [8,9]. A total of 1.2% of all canine tumours affects the thyroid gland with thyroid carcinomas occurring more frequently than adenomas [9,10]. Carcinomas of follicular origin are the most common form of canine thyroid neoplasias [11].

In order to elucidate whether human genes which are involved in the pathogenesis of benign thyroid adenomas could play a role as orthologous candidate genes for a possible malignant transformation of thyroid tumours in dogs, we have mapped the canine *THADA* gene and analysed if the canine gene locus is involved in cytogenetic rearrangements.

Methods

BAC library screening

A PCR reaction for PCR-based screening of the *Canis familiaris* DogBAC library [12] (Institute of Animal Genetics, Nutrition and Housing, University of Berne, Berne, Switzerland) for a BAC clone containing *THADA* was established using canine genomic DNA derived from blood. The primers T1: 5'GCATTTTTCGATTGTCATAAC'3 and T2: 5'TCAGCCAAAACTAGATAACAC'3 were designed using the predicted canine *THADA* gene sequence of canine chromosome 10, [GeneBank: NC_006592]. PCR parameters were: 95°C for 5 min, followed by 35 cycles of 95°C 30 sec, 55°C 30 sec, 72°C 30 sec, and a final elongation of 72°C for 10 min. The corresponding 601 bp PCR product was cloned into the pGEM-T Easy vector system (Promega) and verified by sequencing. The obtained canine sequence contained the 97 bp of exon 2 with a 92% similarity to human exon 2 of *THADA* [GenBank: NM_022065]. The sequence was submitted to the NCBI database [GenBank DQ836130]. The DNA contigs and alignments were done with Lasergene software (DNAstar, Madison, USA) and various sequences from the NCBI database [GeneBank: AC_000045, NM_022065].

For verification and secondary screening a semi-nested PCR reaction was established, using the T1 primer and a nested primer T1B (5'TCAGTACTATTGGCATTTGGAG'3) generating a 147 bp amplicon. A positive BAC clone (DogBAC library ID S011P24K05RE) was identified and verified by PCR. The obtained PCR products were cloned into the pGEM-T Easy vector system (Promega) and verified by sequencing. The verified clone was used as probe for following FISH experiments.

Slide Preparation

1 ml of canine whole blood was incubated for 72 h in Chromosome Medium B (Biochrom). Subsequently, colcemide (0.1 μg/ml) (Biochrom) was added for 2 hours. The cells were centrifuged at 135 × g for 10 min and incubated for 20 min in 0.05 M KCl. Finally, the cells were fixed overnight with methanol/glacial acetic acid. This suspension was dropped on ice-cold slides and dried for at least 7 days at 37°C. The chromosomes were stained by GTG banding for karyotype description. Prior to use in FISH investigations, the slides were destained with 70% ethanol.

Fluorescence in situ hybridization

BAC-DNA was digoxigenin labeled (Dig-Nick-Translation-Kit, Roche). The hybridization mixture contained 200 ng probe, 40 ng ssDNA, 600 ng sonicated dog DNA, 2 × SSC, 2 × SSPE, 50% formamide and 10% dextran sulfate. 50 μl of this mixture were applied to each slide and the cover slips were sealed with rubber cement. Probe and chromosomes were denatured at 75°C on an Eppendorf thermocycler gradient, using the in situ adapter. Afterwards, the slides were incubated in a moist chamber at 37°C over night. Cover slips were carefully removed and the slides were incubated in 0.1 × SSC at 61°C and 1 × PBS at RT. Slides were then covered with 100 μl NFDM for 20 min. at 37°C in a moist chamber. For signal detection 100 μl NFDM containing 3 μg of anti-digoxigenin-rhodamine, fab fragments (Roche) were added to each slide and again incubated for 20 min at 37°C in a moist chamber, followed by washes with 1 × PBS, 3 × 3 min at RT. Slides were air dried before chromosome staining was performed with 25 μl of Vectashield mounting medium with DAPI (Vector Laboratories).

Ten well spread metaphases were examined indicating a signal on canine chromosome 10 on both chromatids of both chromosomes of canine chromosome 10 (Fig. 1).

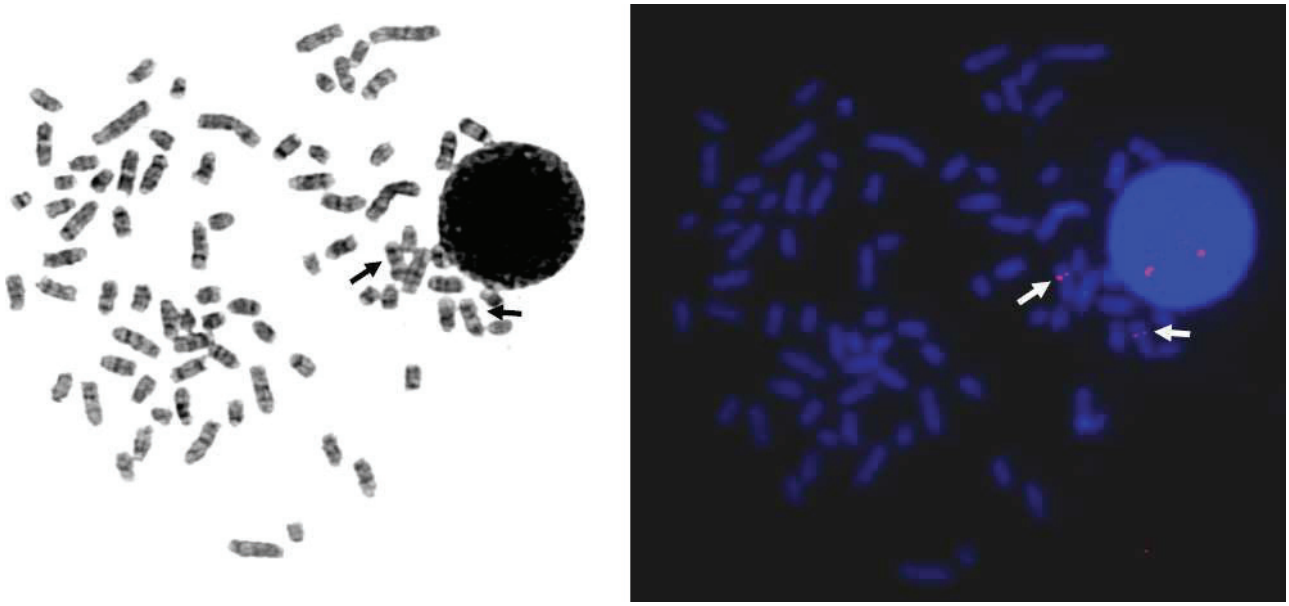

Figure 1
FISH mapping of canine THADA. Metaphase spread after fluorescence *in situ* hybridisation with signals on CFA 10q25 (right) of both chromosomes, the same metaphase after GTG-banding (left).

The determination of chromosomes followed the nomenclature of the canine karyotype as described previously [13].

Results and Discussion

In humans 10% of all chromosomal rearrangements in benign thyroid tumours involve a 450 kb breakpoint region on 2p21 [14]. These 2p21 rearrangements are the most commonly detected cytogenetic aberrations in benign thyroid adenomas. Within the mentioned breakpoint region the *THADA* gene was identified as a target gene for translocation events. *THADA* transcripts fused downstream to ectopic sequences of human chromosome 3 and 7 have been detected in thyroid adenoma cell lines S325/TSV40 and S533/TSV40 [3] (Centre for Human Genetics, University of Bremen, Bremen, Germany). The loss of parts of the *THADA* coding sequence is proposed to play a major role in the pathogenesis of these lesions affecting the thyroid gland due to the truncation of the gene and its deduced protein sequence [3,15]. Rippe et al. (2003) proposed an involvement of THADA in a death receptor pathway and characterized the human *THADA*. The mRNA of *THADA* contains 6090 bp (ORF 5862 bp) and 38 exons and encodes a hypothetical protein of 1954 amino acids.

The UCSC genome browser on Dog May 2005 [16] assembly showed the canine *THADA* chromosomal location on CFA 10 at region 48,883,266 to 49,209,580 and the gene encompasses a sequence of 326,315 bp. The genome browser also described that the canine *THADA* region is highly conserved between the homologous gene locations of man, mouse and rat. Particularly the *THADA* region seems to be more evolutionarily conserved between man and dog than in rodents. In detail NCBI Blast analyses [17] were performed in order to show similarities between various mammalian and avian *THADA* nucleotide sequences from the NCBI databases. The similarities of the canine *THADA* [GenBank: EF222204] coding sequence (CDS) to the CDS of other species vary between human CDS [GenBank: NM_022065] 87%, mouse CDS 80% [GenBank: EF222207], rat predicted CDS 80% [GenBank XM_001060686.1] and chicken 69% [Genbank EF222206]. Respectively the similarities of the canine proposed THADA protein sequence to the deduced protein sequence of other species vary between human protein 83% [GenBank: NP_071348], mouse protein 75% [GenBank: ABQ10601], rat predicted protein 76% [XP_233829] and chicken protein 59% [GenBank: NP_001103529]. Also all deducted mammalian and avian THADA proposed protein sequence have in common one highly conserved domain termed COG5543 [CDD: 35102], the clusters of orthologous groups protein motif with yet unknown function, identified by the NCBI Conserved Domain Database (CDD) [18].

The mapping of *THADA* to canine chromosome 10 shows that the chromosomal region to which the canine *THADA* has been mapped is not a hotspot of chromosomal aberrations seen in canine thyroid adenomas. Previous case

reports of canine thyroid adenomas showed either a trisomy of chromosome 18 as a sole cytogenetic abnormality [19], or a rather complex karyotype of chromosomal fusions [20]. However, the available cytogenetic data of canine thyroid adenomas are still insufficient.

In 1999, reciprocal chromosome painting probes were established for a comparative chromosome map between human, red fox and dog showing the hybridisation pattern of canine probes onto human chromosomes [21,22]. Corresponding to the data obtained by the painting probes conserved syntheny exists between canine chromosome 10 and the human chromosomes 2, 12, and 22. Our mapping result obtained in this study is in accordance with the described homology of the canine and human chromosomes allowing a fine mapping of the *THADA* gene locus on canine chromosome 10q25 (Fig 1.) which corresponds to the 2p21 region of the p-arm of human chromosome 2.

Conclusion

In dogs malignant thyroid carcinomas occur more often than adenomas but interestingly no cytogenetic reports of canine thyroid carcinomas have been published until now (NCBI, Pubmed 2008). In order to elucidate whether canine *THADA* could be a candidate gene for a possible malignant transformation of canine thyroid adenomas further cytogenetic studies of the tumours could be of significant value.

Competing interests

The authors declare that they have no competing interests.

Authors' contributions

JTS and CB carried out the molecular genetic studies, established the PCR condition, performed the *in silico* analyses and drafted the manuscript, SW and ND carried out the FISH, SW and NRB determined the gene locus and performed the fine-mapping following the nomenclature of the canine karyotype, GD and CS screened the DogBAC library for a BAC clone containing gene of interest, HME, IN and JB conceived the study, participated in the experimental design and coordination, and helped to draft the manuscript. All authors read and approved the final manuscript.

References

1. Bartnitzke S, Herrmann ME, Lobeck H, Zuschneid W, Neuhaus P, Bullerdiek J: **Cytogenetic findings on eight follicular thyroid adenomas including one with a t(10;19).** *Cancer genetics and cytogenetics* 1989, **39(1):**65-68.
2. Belge G, Roque L, Soares J, Bruckmann S, Thode B, Fonseca E, Clode A, Bartnitzke S, Castedo S, Bullerdiek J: **Cytogenetic investigations of 340 thyroid hyperplasias and adenomas revealing correlations between cytogenetic findings and histology.** *Cancer Genet Cytogenet* 1998, **101(1):**42-48.
3. Rippe V, Drieschner N, Meiboom M, Murua Escobar H, Bonk U, Belge G, Bullerdiek J: **Identification of a gene rearranged by 2p21 aberrations in thyroid adenomas.** *Oncogene* 2003, **22(38):**6111-6114.
4. Khanna C, Hunter K: **Modeling metastasis in vivo.** *Carcinogenesis* 2005, **26(3):**513-523.
5. Hahn KA, Bravo L, Adams WH, Frazier DL: **Naturally occurring tumors in dogs as comparative models for cancer therapy research.** In *Vivo* 1994, **8(1):**133-143.
6. Ostrander EA, Galibert F, Patterson DF: **Canine genetics comes of age.** *Trends Genet* 2000, **16(3):**117-124.
7. Ostrander EA, Wayne RK: **The canine genome.** *Genome Res* 2005, **15(12):**1706-1716.
8. Pacini F, Schlumberger M, Dralle H, Elisei R, Smit JW, Wiersinga W: **European consensus for the management of patients with differentiated thyroid carcinoma of the follicular epithelium.** *European journal of endocrinology / European Federation of Endocrine Societies* 2006, **154(6):**787-803.
9. Harari J, Patterson JS, Rosenthal RC: **Clinical and pathologic features of thyroid tumors in 26 dogs.** *Journal of the American Veterinary Medical Association* 1986, **188(10):**1160-1164.
10. Klein MK, Powers BE, Withrow SJ, Curtis CR, Straw RC, Ogilvie GK, Dickinson KL, Cooper MF, Baier M: **Treatment of thyroid carcinoma in dogs by surgical resection alone: 20 cases (1981-1989).** *Journal of the American Veterinary Medical Association* 1995, **206(7):**1007-1009.
11. Ramos-Vara JA, Miller MA, Johnson GC, Pace LW: **Immunohistochemical detection of thyroid transcription factor-1, thyroglobulin, and calcitonin in canine normal, hyperplastic, and neoplastic thyroid gland.** *Vet Pathol* 2002, **39(4):**480-487.
12. Schelling C, Schläpfer J, Billaut A, Guziewicz K, Gmür A, Katmann I, Pineroli B, Colomb B, Rickli O, Wittwer C, Piasecka A, Dolf G: **Construction of a canine artificial chromosome library for screening with PCR.** *Journal of Animal Breeding and Genetics* 2002, **119(6):**400-401.
13. Reimann N, Bartnitzke S, Bullerdiek J, Schmitz U, Rogalla P, Nolte I, Ronne M: **An extended nomenclature of the canine karyotype.** *Cytogenet Cell Genet* 1996, **73(1-2):**140-144.
14. Bol S, Belge G, Rippe V, Bullerdiek J: **Molecular cytogenetic investigations define a subgroup of thyroid adenomas with 2p21 breakpoints clustered to a region of less than 450 kb.** *Cytogenet Cell Genet* 2001, **95(3-4):**189-191.
15. Drieschner N, Belge G, Rippe V, Meiboom M, Loeschke S, Bullerdiek J: **Evidence for a 3p25 breakpoint hot spot region in thyroid tumors of follicular origin.** *Thyroid* 2006, **16(11):**1091-1096.
16. **Dog (Canis familiaris) Genome Browser Gateway** [http://genome.ucsc.edu/cgi-bin/hgGateway]
17. **Basic Local Alignment Search Tool** [http://www.ncbi.nlm.nih.gov/blast/Blast.cgi]
18. **NCBI Conserved Domain Database** [http://www.ncbi.nlm.nih.gov/Structure/cdd/cdd.shtml]
19. Reimann N, Nolte I, Bonk U, Werner M, Bullerdiek J, Bartnitzke S: **Trisomy 18 in a canine thyroid adenoma.** *Cancer Genet Cytogenet* 1996, **90(2):**154-156.
20. Mayr B, Schleger W, Loupal G, Burtscher H: **Characterisation of complex karyotype changes in a canine thyroid adenoma.** *Research in veterinary science* 1991, **50(3):**298-300.
21. Breen M, Thomas R, Binns MM, Carter NP, Langford CF: **Reciprocal chromosome painting reveals detailed regions of conserved synteny between the karyotypes of the domestic dog (Canis familiaris) and human.** *Genomics* 1999, **61(2):**145-155.
22. Yang F, O'Brien PC, Milne BS, Graphodatsky AS, Solanky N, Trifonov V, Rens W, Sargan D, Ferguson-Smith MA: **A complete comparative chromosome map for the dog, red fox, and human and its integration with canine genetic maps.** *Genomics* 1999, **62(2):**189-202.